



Norwegian University of
Science and Technology

System integration of large scale offshore wind power

Guillaume Verez

Master of Science in Energy and Environment

Submission date: January 2011

Supervisor: Terje Gjengedal, ELKRAFT

Problem Description

The European Commission proposal for 20% renewable energy by 2020 paves the way for a massive expansion of wind energy and a new energy future for Europe. To reach the goal wind energy is a key technology and large scale integration is required both onshore and offshore. This represents heavy challenges to the power system requiring new ways of designing and operating the system. Especially large scale offshore wind power will require attention to new focus areas. The wind may be more stable offshore, but there will be less geographical smoothing effect, so wind variations will still be a key issue. Power transmission and grid connection represent other main challenges for realisation of large scale wind power, and especially for offshore wind farms.

The scope of the project is defined as how to find an efficient and secure design and operation of the overall system when large scale offshore wind power is integrated.

Assignment given: 05. September 2010
Supervisor: Terje Gjengedal, ELKRAFT

PREFACE

The work of this thesis was performed in the Department of Electrical Power Engineering at the Norwegian University of Science and Technology (NTNU) in collaboration with Statnett, the Norwegian transmission system operator. It ends my two years studies in Norway in order to complete a Master in Energy and Environment.

I would like to thank Terje Gjengedal, who is SVP-R&D director for Statnett and my supervisor, for giving me the opportunity to do this thesis. As a professor in NTNU, his course entitled Wind power in the Norwegian energy system, gave me the motivation to focus my studies on wind power and to do my Master Thesis in this field.

Trond Toftevaag, researcher for SINTEF Energy Research and professor at NTNU, has giving me a very precious help for my work and I am grateful for spending so much time with me even though he is not my supervisor. His help regarded translation of the grid model from different software and transmission problems.

I would like to thank the other researchers in SINTEF who worked with Professor Toftevaag and gave me some advice regarding transmission in HVAC and HVDC as long as help with programming and translating files.

My thanks go to Sachin and Mahesh from India who were my two office workmates. We had a lot of discussion and exchange regarding our master works. Mahesh particularly helped me with the simulation tool.

My Erasmus and Norwegian roommates are to be thanked for making my stay enjoyable. I met a lot of people during those two years and I will never forget this foreign experience.

I would like to thank Helen, my girlfriend, for being supportive regarding my studies abroad since she lives in France. My family helped me getting installed in Norway and supported me all along and I am thankful to them.

Finally, I would like to thank my friend Jennifer who is completing a doctoral thesis in France and who helped me with the page setting of my work.

ABSTRACT

Electricity generation, along with motor vehicles, is one of the biggest sources of pollution for the planet. Renewable energies are not able to replace massively polluting power plants but they can at least alleviate for it. Biomass and hydro power are the main source of renewable energy but wind power is developing to high extent, increasing by 30% its installed capacity every year in the world. Norway is increasing its wind power production since every hydro power areas are already used. The shallow Norwegian waters along with the increase of energy demand leads to offshore wind project.

The aim of this thesis is to study the integration of large scale offshore wind farms into the grid. The biggest offshore wind farm is currently installed in the United Kingdom (Thanet) and its capacity is 300 MW. The wind farm studied here has a capacity of 1000 MW. HVAC and HVDC transmission are investigated in order to connect the wind farm to Norway. Case faults are performed in order to study the system stability. The connection points are located in the most populated areas of Norway, where there is a real need for new power plants: Sørlandet and Vestlandet.

Statnett is the Norwegian transmission system operator and thus the focus was made on the connection with power flow and stability analysis and not on the full description of the wind farm. For simulations, Statnett is mainly using PSS[®]E (Power System Simulator) from Siemens but as much of the help was providing by SINTEF, the largest independent research organisation in Scandinavia, it was more convenient to use their tool: SIMPOW from STRI AB.

TABLE OF CONTENTS

TABLE OF CONTENTS	1
TABLE OF FIGURES.....	6
INTRODUCTION	9
1 OFFSHORE WIND ENERGY	10
1.1 HISTORY OF OFFSHORE WIND GENERATION	10
1.2 STATE OF OFFSHORE WIND GENERATION	10
1.3 INSTALLATION OF OFFSHORE WIND TURBINES	12
1.4 WIND POWER IN THE NORDIC GRID	14
1.4.1 GENERATION IN THE NORDIC GRID.....	14
1.4.2 IMPACT OF LARGE SCALE WIND POWER ON POWER SYSTEM OPERATION	15
1.5 WIND POWER IN NORWAY.....	17
1.5.1 POWER EXCHANGE IN NORWAY	17
1.5.2 THE GRID CODE	17
1.5.3 ONSHORE WIND POWER.....	20
1.5.4 OFFSHORE WIND POWER.....	22
2 TECHNOLOGIES INVOLVED	24
2.1 WIND TURBINES' DESIGN	24
STALL	24
PITCH	25
YAW	25
2.2 OPTIMISATION.....	26
2.2.1 BETZ' LAW.....	26
2.2.2 TIP SPEED RATIO.....	27
2.3 WIND TURBINES' GENERATORS	27
2.3.1 TYPE A: FIXED SPEED	28
2.3.2 TYPE B: LIMITED VARIABLE SPEED.....	28
2.3.3 TYPE C: VARIABLE SPEED WITH DFIG	29
2.3.4 TYPE D: VARIABLE SPEED WITH FULL-SCALE FREQUENCY CONVERTER.....	30
3 STABILITY IN WIND POWER SYSTEMS	31
4 TRANSMISSION TECHNOLOGIES.....	33
4.1 HISTORY OF DC TRANSMISSION	33
4.2 HVAC CONFIGURATION	34

4.3	HVDC CONFIGURATION	35
4.4	COMPARISON BETWEEN AC AND DC LINES	37
4.4.1	ECONOMIC COMPARISON OF AC AND DC LINES	37
4.4.2	TECHNICAL COMPARISON OF AC AND DC LINES.....	37
4.5	SUBMARINE POWER CABLES.....	38
4.5.1	REQUIREMENTS.....	38
4.5.2	CONSTRUCTION OF DC CABLES	38
4.5.3	MASS-IMPREGNATED CABLES	39
4.5.4	LOW-, MEDIUM-, AND HIGH-PRESSURE GAS FILLED CABLES.....	40
4.5.5	CROSS-LINKED POLYETHYLENE CABLES.....	40
4.5.6	PAPER-INSULATED OIL-FILLED CABLES.....	41
4.6	TRANSMISSION SYSTEMS	42
4.6.1	HVAC TRANSMISSION.....	42
4.6.2	LINE-COMMUTATED CONVERTER BASED HVDC TRANSMISSION	44
4.6.3	VOLTAGE SOURCE CONVERTER BASED HVDC TRANSMISSION	48
4.7	TRANSMISSION SYSTEMS COMPARISON.....	51
4.7.1	TECHNICAL COMPARISON	51
4.7.2	ECONOMICAL COMPARISON	53
4.7.3	COMPARISON BETWEEN VSC AND LCC BASED HVDC	54
5	SIMULATION MODELS	55
5.1	SIMULATION TOOL	55
5.2	GRID MODEL.....	55
5.2.1	GENROU GENERATOR MODEL	58
5.2.2	GENSAL GENERATOR MODEL.....	60
5.2.3	EXCITERS AND STABILIZERS	61
5.2.4	POWER LINES.....	64
5.3	WIND FARM MODEL.....	66
5.4	HVAC CONFIGURATION	71
5.5	HVDC CONFIGURATION.....	74
6	LOAD FLOW	77
6.1	INITIAL POWER FLOW.....	77
6.2	CONNECTING THE WIND FARM.....	78
6.3	POWER FLOW ON BUS 5600	79
6.4	POWER FLOW ON BUS 6000	84

7	DYNAMIC SIMULATIONS	88
7.1	THREE-PHASE FAULT AND CRITICAL CLEARING TIME	88
7.2	CASE FAULTS.....	90
7.3	CASE 1: HVAC - 3PSG ON 5600 FOR 185 ms.....	91
7.4	CASE 2: HVAC - 3PSG ON 5600 FOR 50 ms.....	96
7.5	CASE 3: HVAC - 3PSG ON 5600 FOR 5 ms.....	100
7.6	CASE 4: HVAC - 3PSG ON 6000 FOR 50 ms.....	103
7.6	CASE 5: HVAC – STOP OF PRODUCTION OF 6100.....	106
7.7	CASE 6: HVAC – DISCONNECTION OF A LINE.....	110
7.8	CASE 7: HVDC – 3PSG ON 5600 FOR 185 ms.....	113
7.9	CASE 8: HVDC – STOP OF PRODUCTION OF 6100	115
8	DISCUSSION	117
9	CONCLUSION AND FUTURE WORK.....	118
	REFERENCES	120
	APPENDIX	123
	APPENDIX A: DEFAULT CP CURVES OF THE FPCWT.....	124
	APPENDIX B: HVAC OPTPOW FILE	130
	APPENDIX C: HVAC DYNPOW FILE.....	139
	APPENDIX D: HVDC OPTPOW FILE.....	149
	APPENDIX E: HVDC DYNPOW FILE.....	156
	APPENDIX F: INITIAL POWER FLOW	164

TABLE OF FIGURES

Figure 1	Installed capacity: cumulative share by country (end 2009) in MW (3)	11
Figure 2	Share of consented offshore wind capacity per country (3)	11
Figure 3	Share of offshore wind capacity under construction (3).....	11
Figure 4	Characteristics of the marine environments.....	12
Figure 5	Beatrice Project	13
Figure 6	Different foundations designs	13
Figure 7	Nordic Grid (10).....	15
Figure 8	Aggregated wind production curve for Western Denmark (9)	16
Figure 9	Mean absolute error as % of capacity (Finland, 2004) (9)	16
Figure 10	Total power exchange in MWh/h	17
Figure 11	Frequency controlled actions in the Nordel system (12).....	18
Figure 12	Voltage dip profile due to a fault (12)	19
Figure 13	Wind map for Norway (13)	20
Figure 14	Annual Norwegian production of wind power (15)	21
Figure 15	Installed Norwegian wind power (15).....	21
Figure 16	Offshore production costs (16).....	22
Figure 17	Distribution of costs for an onshore and offshore wind farm (16)	23
Figure 18	Sectional view of a wind turbine (18).....	24
Figure 19	Power curve: pitch versus stall	25
Figure 20	Upstream and downstream wind (19)	26
Figure 21	Tip speed.....	27
Figure 22	Fixed speed wind turbine	28
Figure 23	Limited variable speed wind turbine	28
Figure 24	Variable speed wind turbines with DFIG	29
Figure 25	Variable speed wind turbine with full-scale frequency converter.....	30
Figure 26	Classification of power system stability (23)	31
Figure 27	English Electric mercury arc valves at the Manitoba Hydro Radisson Converter Station	33
Figure 28	Electrical system for a large AC wind park	34
Figure 29	The electrical system for an AC/DC wind park.....	35
Figure 30	Electrical system for a large DC wind park with two DC transformer steps.....	36
Figure 31	DC electrical system with series connected wind turbines	36
Figure 32	Mass-impregnated cable construction.....	40
Figure 33	Cross-linked polyethylene cable	41
Figure 34	Basic configuration of a 600 MW wind farm with a HVAC solution	43
Figure 35	Thyristors valves stacks at the Manitoba Hydro Radisson Converter Station	44
Figure 36	Thyristor circuit model.....	44
Figure 37	12-pulse HVDC LCC transmission line	45
Figure 38	Monopolar LCC based HVDC (43)	46
Figure 39	Bipolar LCC based HVDC (43)	46
Figure 40	Multiterminal LCC based HVDC (43)	47
Figure 41	LCC converter station.....	47
Figure 42	IGBT circuit model.....	48

Figure 43	1200 A, 3300 V IGBT module (IGBTs and free-wheeling diodes).....	48
Figure 44	VSC based HVDC transmission system.....	49
Figure 45	Active and reactive power operating range for VSCs	49
Figure 46	VSC based HVDC converter station.....	50
Figure 47	600 MW wind farm connected with VSC based HVDC.....	50
Figure 48	Loss against cable length comparison	51
Figure 49	Choice of transmission technology depending on distance and capacity.....	53
Figure 50	Grid model	56
Figure 51	Grid model power flow.....	57
Figure 52	SIMPOW turbine model ST2	59
Figure 53	SIMPOW governor model SG3.....	59
Figure 54	PSS®E turbine and generator model IEESGO	59
Figure 55	SIMPOW turbine model HYTUR.....	60
Figure 56	SIMPOW governor model HYGOV	60
Figure 57	PSS®E turbine and generator model HYGOV	61
Figure 58	SIMPOW exciter model ST3	61
Figure 59	PSS®E exciter model SCRX	62
Figure 60	SIMPOW exciter model BBC1	62
Figure 61	PSS®E exciter model SCRX.....	62
Figure 62	SIMPOW exciter model IEEEEX2	63
Figure 63	PSS®E exciter model IEEEET2.....	63
Figure 64	SIMPOW stabilizer model STAB2A.....	64
Figure 65	PSS®E stabilizer model STAB2A.....	64
Figure 66	SIMPOW line types	65
Figure 67	Full Power Converter Wind Turbine model	66
Figure 68	Initial speed drop	69
Figure 69	Initial torque drop.....	69
Figure 70	Initial torque change.....	70
Figure 71	HVAC configuration.....	71
Figure 72	PI-link model	71
Figure 73	Symmetrical SVC with proportional-integral regulator	73
Figure 74	HVDC configuration	74
Figure 75	ABB HVDC Light Open Model Version 1.1.6	75
Figure 76	Location of busses 5600 and 6000.....	78
Figure 77	Power flow around bus 5600 without a wind farm connected	79
Figure 78	Power flow around bus 5600 with a wind farm connected in HVAC	80
Figure 79	Power flow around bus 5600 with a wind farm connected in HVDC	81
Figure 80	Areas in the Norwegian grid model.....	82
Figure 81	Power flow around bus 6000 without a wind farm connected.....	84
Figure 82	Power flow around bus 6000 with a wind farm connected in HVAC	85
Figure 83	Power flow around bus 6000 with a wind farm connected in HVDC	85
Figure 84	Classical model of a synchronous generator	88
Figure 85	Equivalent circuit during the fault	88
Figure 86	Power-angle characteristics.....	89
Figure 87	Case1: Voltage on bus 1000.....	91

Figure 88	Case 1: Voltages on busses 1003 and 5600	92
Figure 89	Case 1: Reactive power of the SVC	92
Figure 90	Case 1: Mechanical power of the FPCWT	93
Figure 91	Case 1: Speed of the FPCWT	94
Figure 92	Case 1: Active power transfer from offshore to onshore	94
Figure 93	Case 1: Reactive power transfer from offshore to onshore	95
Figure 94	Case 2: Voltage on bus 1000.....	96
Figure 95	Case 2: Voltages on busses 1003 and 5600	96
Figure 96	Case 2: Reactive power at the SVC	97
Figure 97	Case 2: Mechanical power of the FPCWT	97
Figure 98	Case 2: Active power transfer from offshore to onshore.....	98
Figure 99	Case 2: Reactive power transfer from offshore to onshore	99
Figure 100	Case 2: Speed of the FPCWT.....	99
Figure 101	Case 3: Voltage on bus 1000.....	100
Figure 102	Case 3: Voltages on busses 1003 and 5600	100
Figure 103	Case 3: Reactive power at the SVC	101
Figure 104	Case 3: Active power transfer between the offshore and onshore busses	102
Figure 105	Case 3: Reactive power transfer between the offshore and onshore busses.....	102
Figure 106	Case 4: Voltage on bus 1000.....	103
Figure 107	Case 4: Voltages on busses 1003 and 6000	104
Figure 108	Case 4: Reactive power at the SVC	104
Figure 109	Case 4: Active power transfer between offshore and onshore.....	105
Figure 110	Case 4: Reactive power transfer between offshore and onshore.....	105
Figure 111	Case 5: Voltage on bus 1000.....	106
Figure 112	Case 5: Voltage on bus 3300.....	107
Figure 113	Case 5: Voltage on busses 1003 and 5600	107
Figure 114	Case 5: Mechanical power of the FPCWT	108
Figure 115	Case 5: Active power transfer between the offshore and onshore busses	109
Figure 116	Case 5: Reactive power transfer between the offshore and onshore busses.....	109
Figure 117	Case 6: Voltages on busses 1003 and 5600	110
Figure 118	Case 6: Reactive power at the SVC	111
Figure 119	Case 6: Active power exchange between the offshore and onshore busses	111
Figure 120	Case 6: Reactive power exchange between the offshore and onshore busses	112
Figure 121	Case 7: Voltage on the FPCWT bus.....	113
Figure 122	Case 7: Voltage on busses 1003 and 5600	113
Figure 123	Case 7: Reactive power at the SVC	114
Figure 124	Case 7: Active power transfer in the DC lines	114
Figure 125	Case 8: DC power on grid-side PWM converter	115
Figure 126	Case 8: DC power on FPCWT-side PWM converter.....	115
Figure 127	Case 8: Voltages on the offshore and onshore busses.....	116
Figure 128	Case 8: Reactive power at the SVC	116

INTRODUCTION

Wind energy is widely used nowadays in Europe and especially in Denmark where it represents more than 20% of the total production. In Norway, wind power gained a lot of interests in the last decade and now reaches an annual production above 3 TWh. However, suitable onshore sites for large wind parks (over 1000 MW) are already exploited or can't be exploited.

Europe is one of the best areas in the world for the implementation of offshore wind farms since the maritime part is made of relatively shallow waters. Winds are strong and stable in the Baltic and North Sea and thus offshore implementation of wind farms is seen as the development of many future wind farm projects. It is such that offshore wind power could represent 10% of the electric production of European Union in 2020.

Offshore sites can be found in the South and West of Norway but most of the fjord area is protected from industrial infrastructures. Modern wind farms are installed in shallow waters, at depth up to 50 meters but for example, the most promising places in Norway are at water depths from 30 to 150 meters. Thus, the development of large scale offshore wind farm is limited by the development of the necessary foundations.

Three main types of transmission technologies are available on the market for offshore connexion of wind parks: High Voltage Alternating Current (HVAC) and High Voltage Direct Current (HVDC). HVAC is the easiest way to make this connexion and it is very well-known. However, the reactive power capability of AC cables has shown its limits and HVDC tends to replace most of offshore connexions. Line-Commutated Converter (LCC) based HVDC equips most of HVDC transmissions but Self commutating converters are also the next step, with Voltage-Source Converters (VSC) already replacing LCC. VSC stations are smaller and thus for high amount of power, it is much easier to install offshore.

This thesis was made in regard of integration of large scale offshore wind farms. Firstly, offshore wind energy is studied in order to show the state of the art in this field. Then, the different types of transmission are compared to each other. The simulation model is thus constructed based on the knowledge acquired previously. Finally, the model is simulated with different configurations and different case faults in order to understand the system stability. SIMPOW from STRI AB is the simulation tool used.

1 OFFSHORE WIND ENERGY

1.1 HISTORY OF OFFSHORE WIND GENERATION

The first use of a wind as a source of power generation was in 1888 in Cleveland, Ohio. The 12 kW produced out of a windmill were the premises to the development of large scale wind power generation in 1991. That year, the German Strom-Einspeise-Gesetz, a law regarding energy demand, required the use of renewable energy sources to feed into their grids. This law led to the development of wind parks in Germany (1).

The history of offshore wind generation begins in 1986 with the world's first wind farm construction in Denmark. Sixteen turbines of 55 kW each produced energy to a city of 4000 inhabitants. Through the late 1990, this development paved the way to new projects in Scandinavia.

1.2 STATE OF OFFSHORE WIND GENERATION

Offshore wind power is a very promising branch of renewable energies. Its potential for development is huge since offshore winds are strong and steady. This potential is not fully exploited because offshore wind farms require high technologies, even though massive research and development are in progress. Offshore wind power could represent 10% of the electric production of European Union in 2020 (2).

Europe is one of the best areas in the world for the implementation of offshore wind farms since the maritime part is made of relatively shallow waters. The North Sea and the Baltic Sea are the most promising places in terms of depth and strong wind potential. Moreover, those areas are located closed to European megalopolis, the most densely populated and energy consuming place of the continent. Even though offshore winds are stronger and steadier than onshore winds, the tariff is higher than with onshore wind farms as linking and investment costs are higher. As an example, according to the decree of November 17, 2008, French tariff is 13 c€/kWh for the ten first years and between 3 and 13 c€/kWh the ten next years. In Germany, it is 15 c€/kWh and Portugal 23 c€/kWh.

The installed capacity of offshore wind turbines by the end of year 2009 is represented on Figure 1. The United Kingdom owns 900 MW and is leading the production of offshore wind power. The amount of installed offshore wind turbines is small compared to onshore wind farms but as Figure 2 shows, over 3 700 MW are under construction in Europe, especially in the United Kingdom, Germany and Belgium. This is due to the fact that the offshore wind energy market is new and many researches are still in progress. Figure 3 illustrates the share of consented offshore wind capacity per country and shows the trend followed by European countries regarding offshore projects. Germany consents over 8 500 MW and a total of 16 GW is consented over Europe (3).

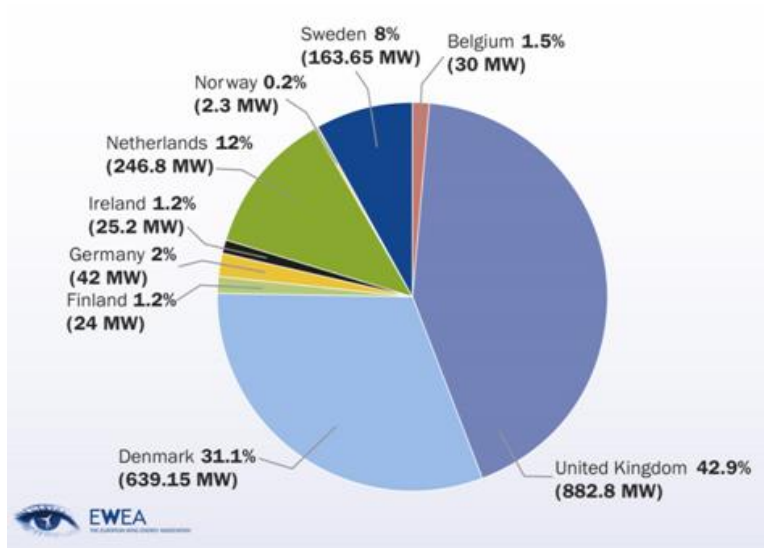


Figure 1 Installed capacity: cumulative share by country (end 2009) in MW (3)

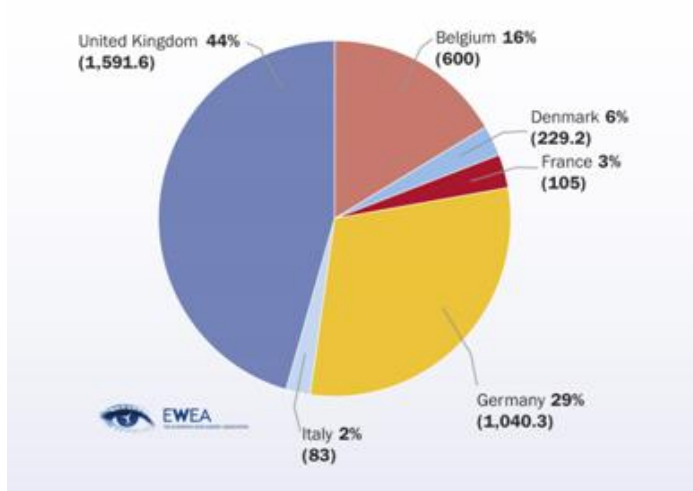


Figure 3 Share of offshore wind capacity under construction (3)

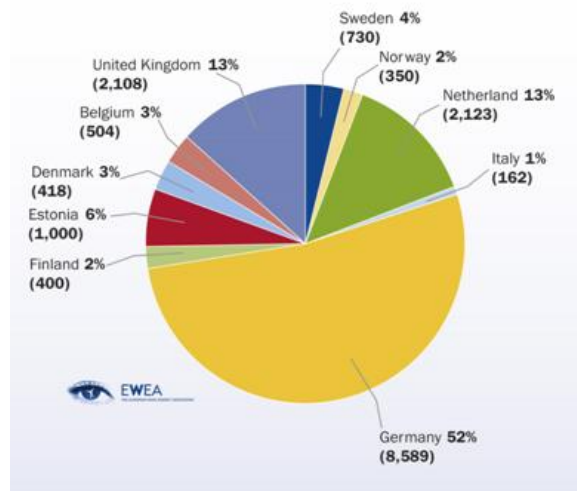


Figure 2 Share of consented offshore wind capacity per country (3)

By the end of 2009, 32 offshore wind farms were operational in ten countries: United Kingdom, Denmark, Netherland, Sweden, Germany, Belgium, Ireland, Finland, Norway and Italy. The total amount of installed power is 1400 MW and the production is 11 TWh. The biggest sites are installed in Denmark and are called Horns Rev 1 and Horns Rev 2. They own respectively 80 and 91 wind turbines, which represents 160 MW and 209 MW.

Even though offshore wind turbines are working on the same principle than onshore ones and are built from almost the same materials, their foundations are different. They can be built out of metal or concrete and it depends on the depth and characteristics of the sea bed. Actual offshore wind turbines can only be installed at a maximum depth of 30 meters. Offshore wind turbines have a higher power rating (5 MW) compared to onshore turbines (3 MW).

Wind turbines are often classified as noisy and ugly by the population. Thus, the offshore implementation is alleviating for those problems. However, the installation of wind turbines must

take into account the environment where it is placed: the marine life and underwater flora but also seabirds. Moreover, it can also impact human activities such as fishing, sand extraction, maritime traffic and tourism.

1.3 INSTALLATION OF OFFSHORE WIND TURBINES

Modern wind farms are installed in shallow waters, at depth up to 50 meters but for example, the most promising places in Norway are at water depths from 30 to 150 meters. There are several research and development projects in progress today, regarding the design of the foundations of wind turbines in order to achieve better depths. Offshore oil platforms use tripod and jack support structures, up to 70 meters deep but these must be scaled in size and costs to fit offshore wind turbines (4).

Figure 4 illustrates the characteristics of the marine environments researchers have to study in order to design floating platforms for offshore wind turbines (5). Those characteristics also have to be taken into account by other offshore wind turbines designs. Wind quality is important and weather conditions have to be taken account for the design of the turbine. The sea bed where the turbine lies has to be studied also regarding earth movement.

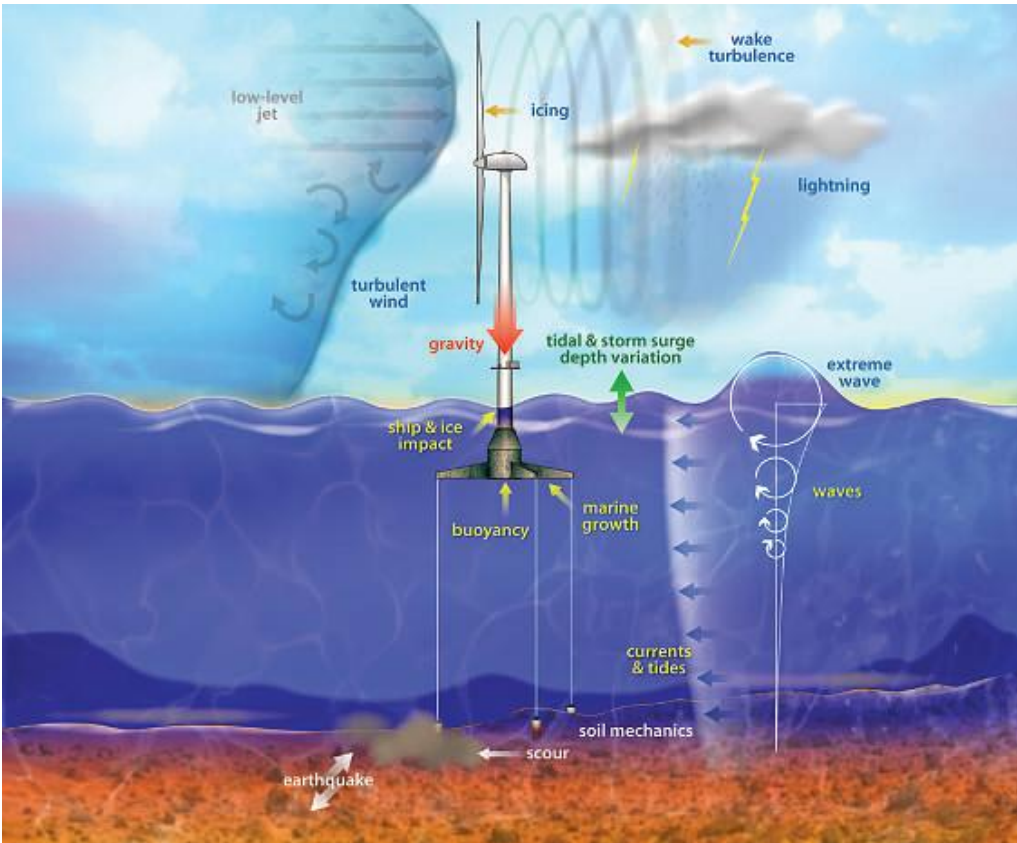


Figure 4 Characteristics of the marine environments

OWEC Tower AS has developed through its projects called Beatrice and Alpha Ventus that the Jacket Quattropod is a proven design. Substructures, along with the tower, account for 25% of the

total cost of an offshore wind turbine. The jack support is suitable for moderate to deep water (6). The Beatrice project is shown on Figure 5. Many projects like this are in progress nowadays and the aim for companies is to be able to install turbines at deeper places.



Figure 5 Beatrice Project

There are various foundations designs available on the market and they depend on the sea bed where the turbine is placed. They are depicted in Figure 6 (7). The monopile foundation is a simple construction consisting of a steel pile with a diameter of about 4 meters that is driven 10 to 20 meters into the seabed. Erosion is normally not a problem with this type of foundation. Such an installation costs between 1.7 M NOK and 2.3 M NOK (215 000€ to 286 000€). The cost is proportional to the size of the foundation, which depends on the place where it is installed. In the North Sea, the wave size determines the dimension whereas in the Baltic Sea, the pack ice pressure is determining it (8). Concrete foundations are more expensive than steel ones because for water depths of more than 10 meters, concrete foundations tend to become prohibitively heavy to install. The tripod foundation relies on light weight and cost efficient three-legged steel jackets. This type of foundation is suitable for deeper installation and is not suitable for water depth above 7 meters. The price is roughly the same than for a monopile foundation. Suction bucket is mostly used on sand sea beds whereas tripod foundations can be used on a rocky sea bed.

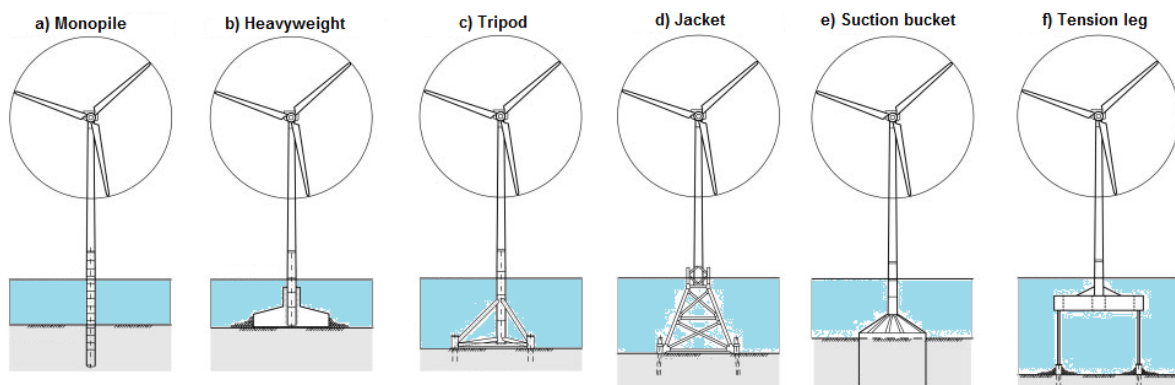


Figure 6 Different foundations designs

1.4 WIND POWER IN THE NORDIC GRID

1.4.1 GENERATION IN THE NORDIC GRID

Over 5 000 MW of cumulated onshore and offshore wind power plants are currently installed in the Nordic Grid. Denmark is the major producer and Sweden is the second but is producing much less out of wind power. Norway and Finland are generating little power from wind power since Norway owns many hydroelectric dam and Finland is using coal and nuclear power plants. Table 1 shows the part of wind power generation in GWh in the Nordic Grid (Denmark, Sweden, Finland and Norway) (9).

Table 1 Part of wind power generation in the Nordic Grid

Country	Total generation (GWh)	Wind power generation (GWh)	Percentage of wind power generation
Denmark	34 648	6 977	20.14%
Sweden	146 021	1 995	1.37%
Finland	74 137	262	0.35%
Norway	142 727	917	0.64%

Table 2 represents the wind generation volumes in the Nordic Grid. The details of registered wind power installed (MW) and the energy delivered (TWh) in 2009 is computed. The table contains also the estimated goals for 2020. A total of 5 300 MW of wind power plants were installed in 2009 for Denmark, Sweden, Finland and Norway and the goal for 2020 is 17 700 MW, which represents an increase of 334%. This increase in wind power generation is the consequence of the European wide climate policy and is achievable thanks to renewable support systems. There are a large number of projects in the Nordic region and the capacity of generation proposed by projects largely exceeds the planned estimations.

Norway's goal for 2010 has been 3 TWh but it was not achieved. The estimate of 12 TWh for 2020 seems to be on the same level as the Swedish estimate, due to a green certificate market with Sweden. Though, such a fast development is achievable since it already occurred in Germany and Spain.

Table 2 Wind generation volumes in the Nordic Grid (2009 and 2020) (9)

Country	Installed/delivered in 2009 (MW/TWh)	Estimated in 2020 (MW/TWh)
Denmark	3273/9	5635/14
Sweden	1448/2.52	4550/12.5
Finland	147/0.3	2500/6
Norway	431/1	5000/12
Total	5300/13	17700/44.5

1.4.2 IMPACT OF LARGE SCALE WIND POWER ON POWER SYSTEM OPERATION

The main challenges a Transmission System Operator (TSO) has to face concerning system operation with an important contribution from wind generation are:

- To balance the production and the consumption acknowledging the variability of wind
- To manage the various technical features of wind power generation such as the amount of rotating mass, the voltage support and the short-circuit capacity

To address these challenges, improvements in forecasting and the extensive use of flexible generation units and loads are done. The full Nordic grid is featured by the company Nordel and is shown in Figure 7 (10).



Figure 7 Nordic Grid (10)

An example from the wind production curve for Western Denmark, shown in Figure 8, is relevant to represent the challenge of the variability of wind. Due to its location between the North Sea and the Baltic Sea, and due to its shape, Denmark has one of the highest wind penetrations in the world. Depending on the wind conditions, the output power for Western Denmark can vary from 200 MW to 1 600 MW. Thus a deviation in the wind forecast of +/- 1m/s can result in +/- 320MW.

The production level of wind power largely varies and hence induces uncertainties into the operation for the TSO. Wind power production when the wind production is high would be easy to forecast but for speeds over 25m/s, wind turbines are shut down for safety reasons. As result, within a few hours, the production can change from full to null.

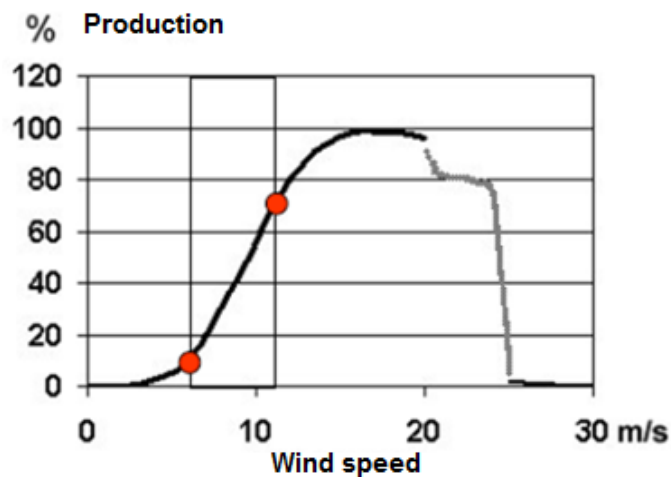


Figure 8 Aggregated wind production curve for Western Denmark (9)

Fluctuations in wind power production due to meteorological variations, such as low and high speed winds, are smoothed out over large areas. This allows higher predictability and thus production for the TSO. It is important to consider the geographical spreading of wind farms in the Nordic area since it contributes to the mitigation of the variations of wind power as it can be seen in Figure 9. The prediction error for a single site is higher than for the aggregated output of four sites with a maximum distance of 380 km between them.

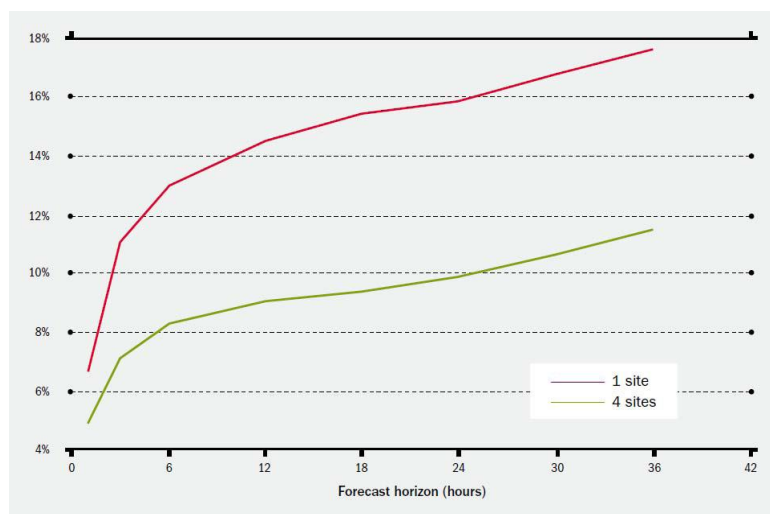


Figure 9 Mean absolute error as % of capacity (Finland, 2004) (9)

1.5 WIND POWER IN NORWAY

1.5.1 POWER EXCHANGE IN NORWAY

The Norwegian electric network is connected to the ones of Sweden, Finland, Russia, Denmark and the Netherlands. The connection between Norway and Denmark is the HVDC transmission system of Cross-Skagerrak. As the main source of energy in Norway is hydropower, energy is supplied to Norway during dry years, and is supplied to Denmark during years with sufficient precipitations. Moreover, this link serves as an energy supply in case of emergency (loss of generation in one country). Cross-Skagerrak went in service in 1977 and was updated to Cross-Skagerrak 3 in 1993, and Cross-Skagerrak 4 is in research. The current state is a 500 MW - 350 kV monopole and the maximum power transfer capability is 1050 MW (11).

The connection between Norway and the Netherlands is NorNed and is a monopolar HVDC link of 700 MW, 450 kV. It is the longest submarine power cable in the world and was in operation in 2008. It benefits to the Netherlands since the importation of energy from Norway is a source of renewable energy, considering hydro power and wind power.

Norway mainly exports electricity, especially during the summer since dams are generally full and there is no need for extensive lighting and heating. Winters are tough in Norway and especially the previous one in 2009-2010. Figure 10 represents the importation and exportations of energy over the last three years in MWh/h and the winter of 2009-2010 shows a lot of importation from Norway.

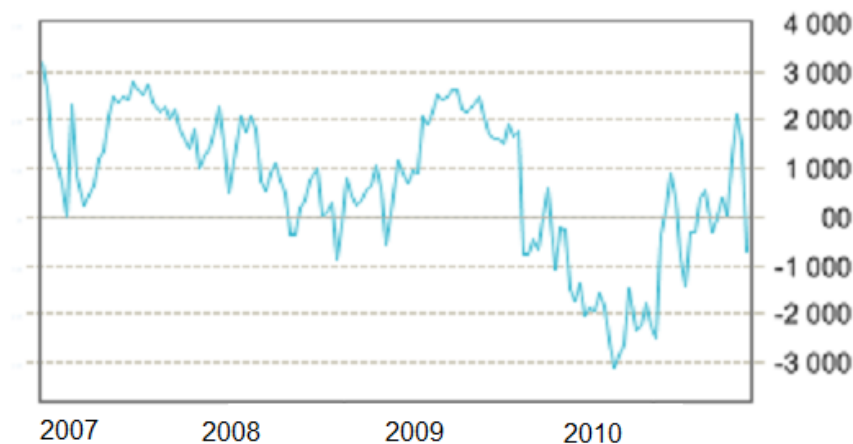


Figure 10 Total power exchange in MWh/h

1.5.2 THE GRID CODE

Norway is part of the Nordic grid and thus has to follow the rules of the Nordic Grid Code. The aim of this code proposed by Nordel is to harmonise the rules that govern the national grid companies of Norway, Sweden, Finland and Denmark. It concerns the transmission system operators (TSO) and it is made of general provisions for cooperation, a planning code, an operational code, a connection code and a data exchange code. Interconnections between Nordic countries date back from 1912 between Sweden and Denmark, and thus there is a long tradition of cooperation in the field of power exchange between the four countries. Those countries depend on each other and

contribute to the improvement of renewable energy. For example Norway is the best area for hydropower and Denmark for wind power. Thus, they can develop in their way since they can count on each other's power resources. More stable sources of energy such as thermal plants exist in Denmark, Sweden and Finland. Figure 11 (12) illustrates the frequency control and regulating reserves used by Nordel to keep the balance in the grid.

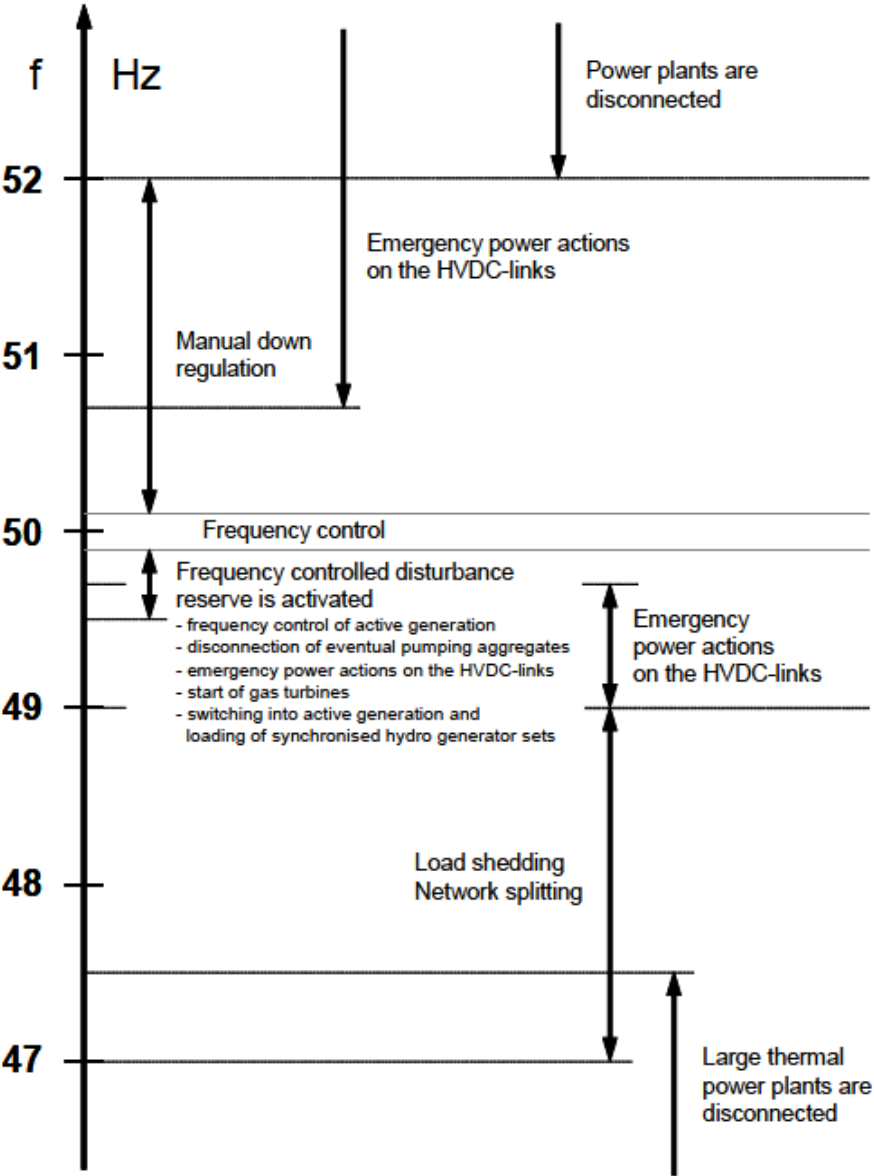


Figure 11 Frequency controlled actions in the Nordel system (12)

The requirements that are given by Nordel regarding wind generation are:

- **Active power control.** An adjustable upper limit to the active power production from the wind farm must be set. This limit should be made possible to control in the range of 20% to 100% of the wind farm's rated power. Ramping control of active power production, fast down regulation and frequency control must be possible. The details of the frequency control depend on the TSO. The grid frequency can't be lower than 47.5 Hz and higher than 53 Hz.
- **Reactive power control.** It must be done continuously and automatically. The wind plants must be able to perform this control by controlling the voltage at the connection point.
- **Operation during grid disturbances.** Wind turbines must be able to stay connected to the system after dimensioning of a fault in the grid. They can also disconnect if the voltage is too low.

If the voltage in the connection point is zero, the fault duration is set to 250 ms. The voltage at the wind turbine generator terminals is higher in case of a fault because of the transformer and the network impedance. Figure 12 (12) shows the voltage dip profile a wind power plant must be able to withstand without disconnecting from the grid.

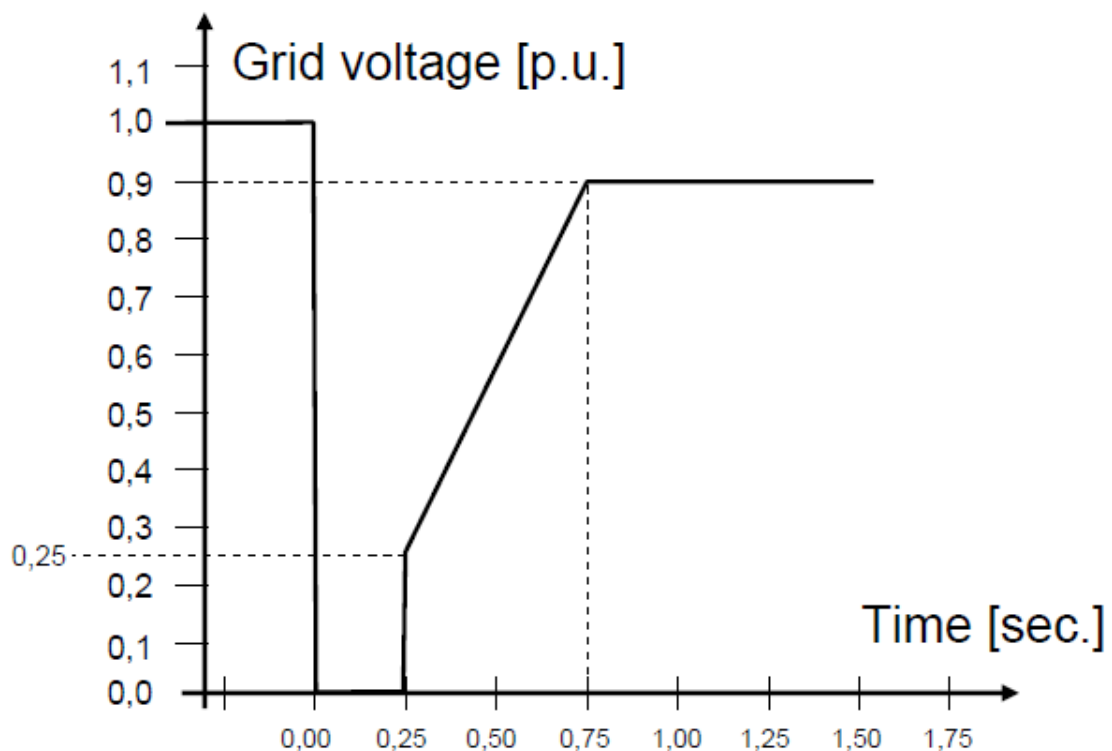


Figure 12 Voltage dip profile due to a fault (12)

1.5.3 ONSHORE WIND POWER

The wind map for Norway is shown in Figure 13 (13). It represents the annual mean wind speed in land and offshore. The highest wind speed areas are located offshore but some regions in the South offer acceptable wind conditions. Moreover, Norway owns many islands where the wind blows almost as high as offshore wind park sites. For example, the island of Smøla, located on the western coast closed to Trondheim, offers a profitable site where Statkraft installed 68 turbines for a total capacity of 150 MW (14).

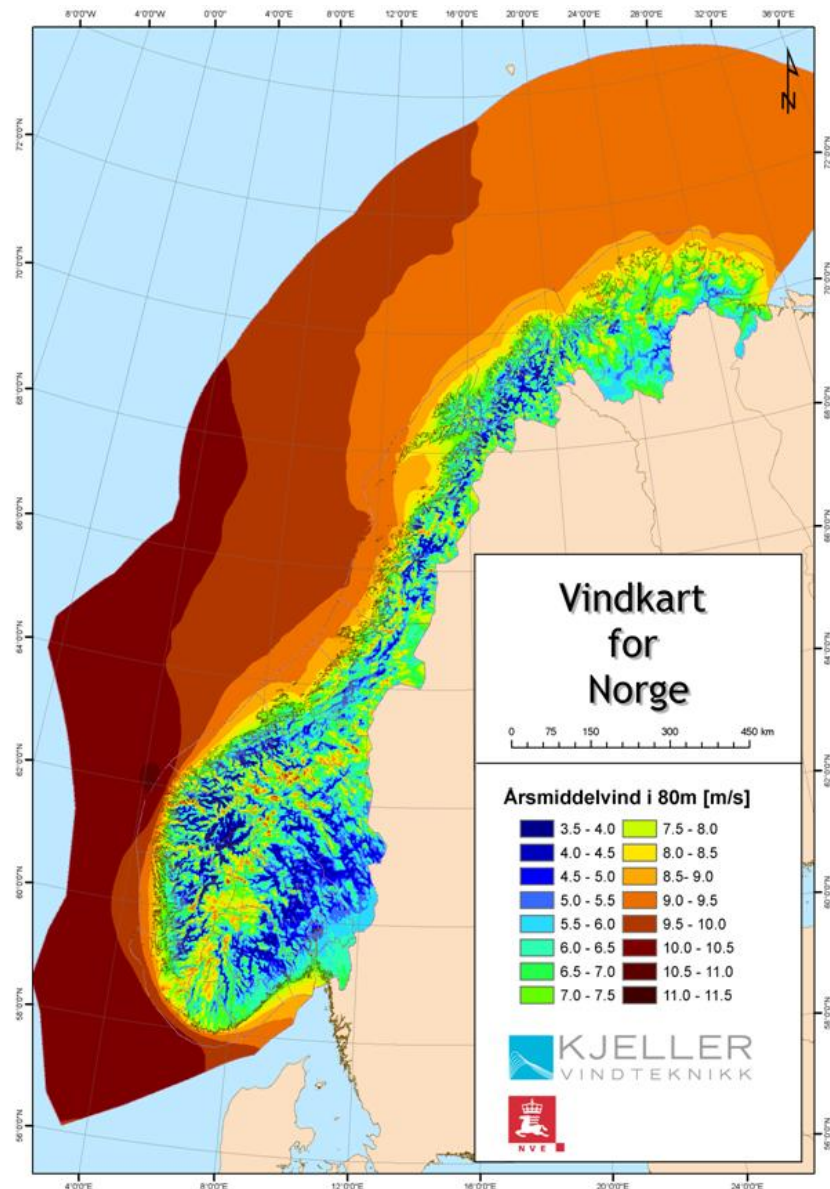


Figure 13 Wind map for Norway (13)

Even though wind power has played a modest role in Norwegian production, some wind studies and small turbines were installed from the late 1980's. In 1997, the interest grew up and as can be seen from Figure 14 (15), the annual production from wind power gained a lot more importance in the Norwegian grid. At the end of 2007, the annual production was closed to 1 TWh, based on power plant owners' estimations. Those numbers will keep increasing, since new licenses are given every year to build additional turbines.

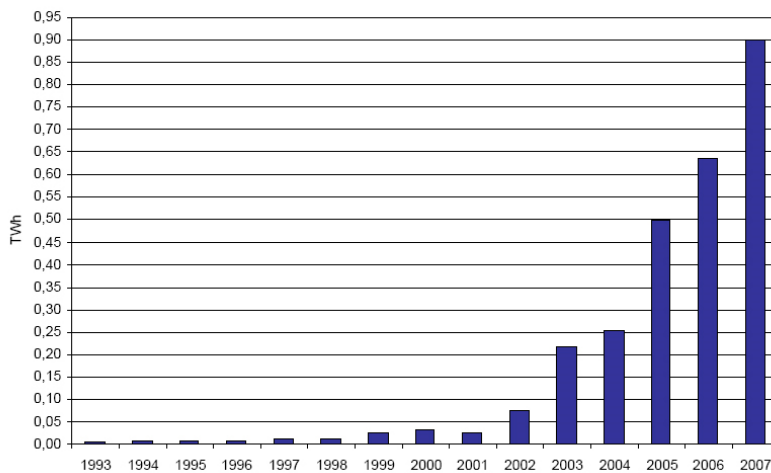


Figure 14 Annual Norwegian production of wind power (15)

Figure 15 (15) shows the size of the Norwegian wind power park that was installed over the years. The Norwegian goal of 3 TWh for 2010 represents approximately 1 000 MW. This goal is realistic since in 2008, plans were reported from the Norwegian Water Resources and Energy Directorate (NVE) and that involved 1 800 MW (under construction and already existing) for that year. The development of wind power in Norway is largely determined by the budgetary authorities because wind power is not yet profitable and therefore depends on public support.

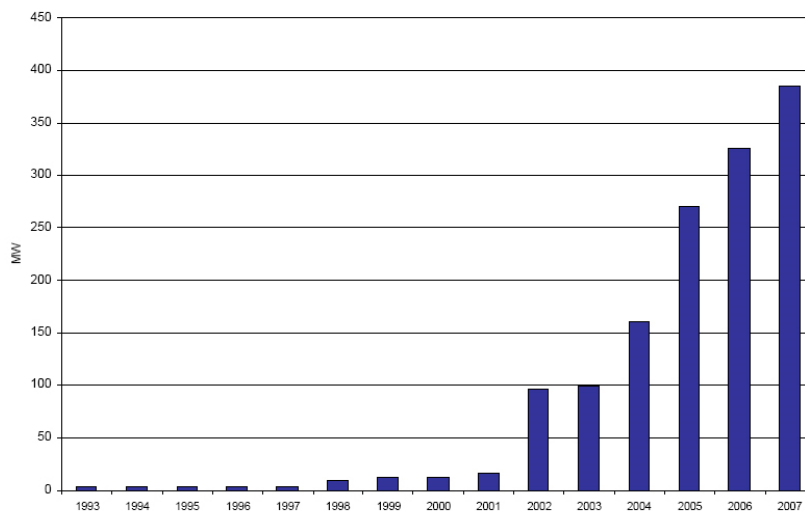


Figure 15 Installed Norwegian wind power (15)

1.5.4 OFFSHORE WIND POWER

In shallow regions, where the depth does not exceed 20 meters, the estimated potential for offshore wind generation is 6 000 to 30 000 MW. This amount depends on the minimal distance from the plant to the land which can be 1 km to 10 km. Moreover, areas protected from substructures installations are also taken into account. In fact, only a portion of the estimation can be made practical, if specific costs for installation and characteristics of the environment are accounted.

During the past years, wind generation industry suffered from an increase in installation costs. It is due to unusual tight market situation where the demand for offshore wind energy is not followed by a corresponding increase in production capacity for wind turbines. Moreover, high steel costs is also making it worst. However, it is estimated that prices will begin to decrease from 2010. Figure 16 (16) shows this trend (1 øre = 0.00125 €).

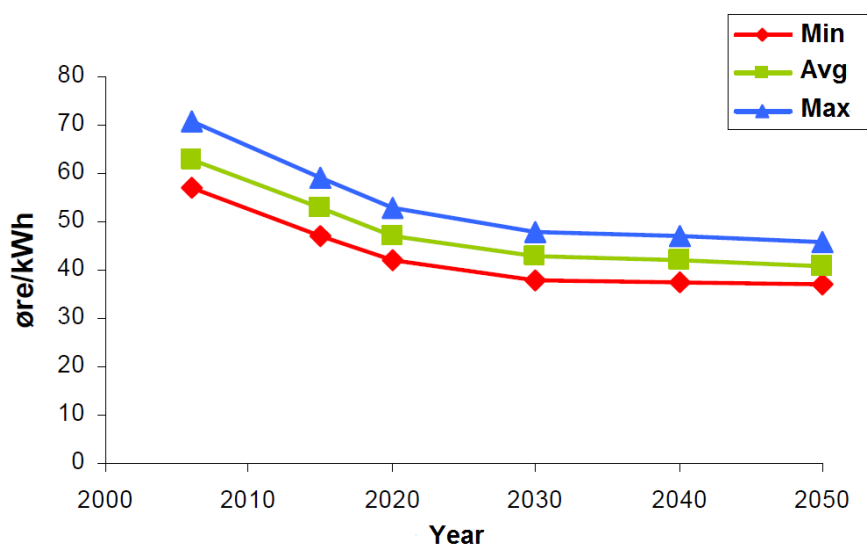


Figure 16 Offshore production costs (16)

Costs of offshore and onshore wind farm installations are different on many points. For an onshore wind farm, 67% to 75% of the farm is the turbine cost, but this is not applicable to an offshore farm. Depending on the sources, the costs of offshore wind farms are different and it can be explained by the fact that each project is different and depends on the site where it is installed. However, Figure 17 (16) tries to show how the costs are split inside the whole farm (1 kr = 0.125 €). Connection to existing networks is not registered. The turbine is cheaper for an offshore park, but the foundations and the installation are much more expensive, since it requires maritime skills.

In Norway, wind conditions off the coast are satisfactory except in the fjord areas (South West). The further from the coast, the better the wind conditions but the depth sometimes becomes a problem as soon as far as 50 km from the shore. For such a distance, the wind blows at an average 11-12 m/s, which is slightly slower than that of the best areas of Norway where the terrain is such that there is acceleration effect. However, the maritime wind is less turbulent and therefore easier to exploit. As a result, the wind is generally not a limiting factor for the installation of offshore wind farms, except in the fjord areas.

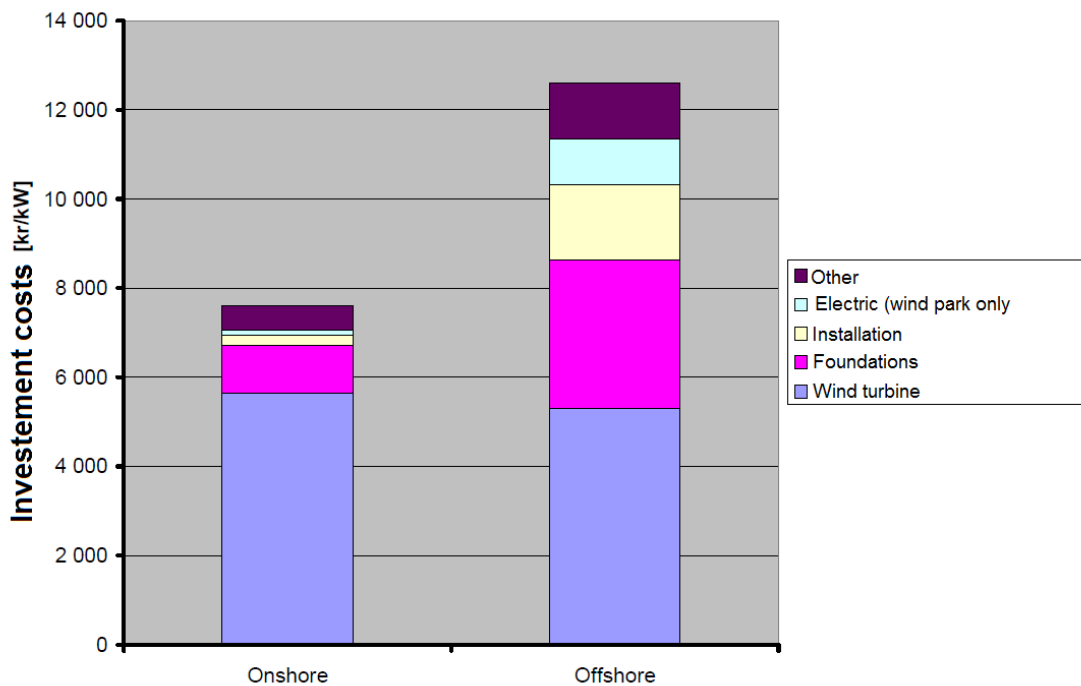


Figure 17 Distribution of costs for an onshore and offshore wind farm (16)

As Figure 13 illustrates, the wind energy resources of Norway are among the best available in Europe but the seas off the Norwegian coast are generally very deep. This is a consequence of the Norwegian Trench. Even though Norway as a long coastline, the possibilities of offshore wind installations are compromised, making it much different from its European neighbours benefiting from the large shallow water areas of the North Sea and the Baltic Sea. Moreover, there are many area restrictions. The coastal traffic and fishing in Norway are important and wind turbines can be spaced by 1 km inside a wind farm (16), which implies sea lanes right through the farm. Moreover, national parks, plants and animal conservation areas and UNESCO's World Heritage places limits further offshore wind power development.

2 TECHNOLOGIES INVOLVED

2.1 WIND TURBINES' DESIGN

Nowadays, the most common design for wind turbines is the Horizontal Axis Wind Turbine (HAWT). Its axis of rotation is parallel to the ground. HAWT are classified according to the orientation of the rotor (upwind or downwind), the design of the hub (rigid or teetering), the control of the rotor (pitch and stall), the number of blades and the alignment of the blades towards the wind (free yaw or active yaw) (17). Figure 18 is a sectional view of the hub of a Siemens wind turbine SWT-2.3-82 VS and shows the typical elements of a wind turbine (18).

1. Spinner
2. Spinner bracket
3. Blade
4. Pitch bearing
5. Rotor hub
6. Main bearing
7. Main shaft
8. Gearbox
9. Brake disc
10. Coupling
11. Service crane
12. Generator
13. Meteorological sensors
14. Yaw gear
15. Yaw ring
16. Tower
17. Nacelle bedplate
18. Canopy
19. Oil filter
20. Generator fan
21. Oil cooler

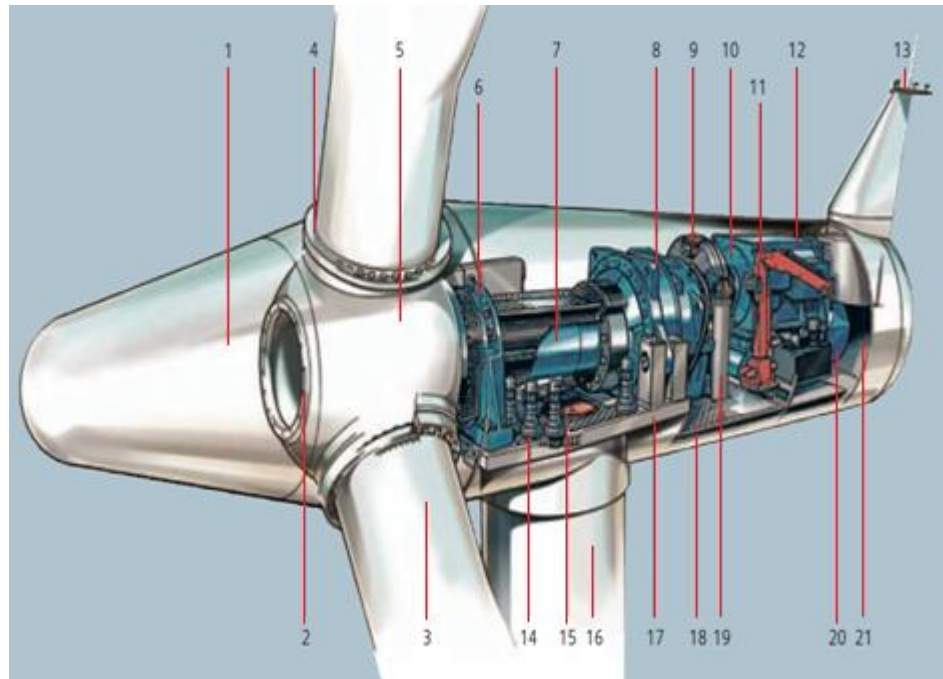


Figure 18 Sectional view of a wind turbine (18)

There are several options for controlling aerodynamically the power output of the wind turbine. They all result in different changes in the design of the turbine.

STALL

The stall is a passive torque regulation, determined by the turbine's aerodynamic properties. Aerodynamic lifts occur at high angle of attack from the blade of the turbine and the aim of the stall is to reduce the high torque induced. The rotor speed of the generator needs to be controlled separately for this power control and connecting an induction generator directly to the grid is the most common solution. The blades of the turbine are simply connected to the hub, without a pitch bearing as shown in Figure 18. The drive train has to be designed to contain the torques encountered during high wind speeds.

PITCH

The pitch is an active torque regulation, made through the pitching of the rotor blades. It is applied for both optimization and power output limitation. Turbines equipped with variable pitch systems have their blades that can rotate around their long axis, which results in changing the pitch angle. Thus, the angle of attack is changed and the torque produced can be controlled. Pitch provides more control than stall but the hub of the turbine needs more elements such as pitch bearings and pitch actuation systems. When only the outer part of blades is pitched, the system is called partial span pitch control.

A power curve is a plot used to understand the relationship between power and wind speed. Cut-in speed (approx. 3-5 m/s) and cut-out speed (approx. 25 m/s) are the operating limits of the turbine.

Figure 19 is the power curve for pitch-controlled and a stall-controlled wind turbine. The curve for pitch-controlled is the ideal power curve since the energy capture is maximized and the power quality is ensured. Operation above the rated speed (approx. 15 m/s) is the power regulation is efficient. On the contrary, the stall-controlled turbine is not able to match the ideal power curve and can only operate at maximum efficiency at one wind speed. Thus, the power regulation is poor.

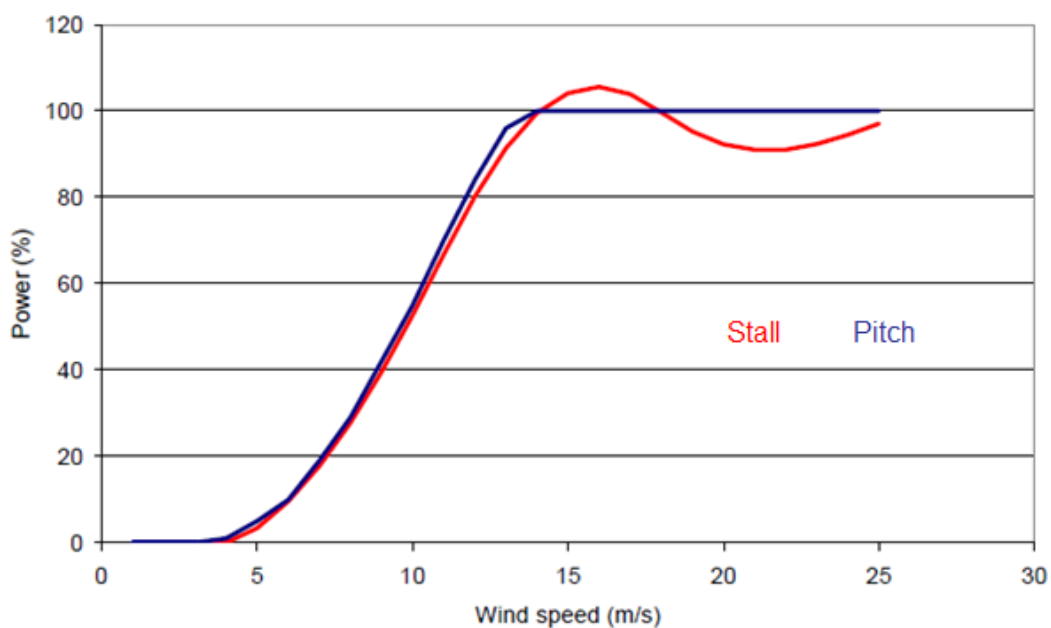


Figure 19 Power curve: pitch versus stall

YAW

During high winds, yaw control allows the rotor to turn away from the wind and results in a reduced power output. The yaw ring is shown in Figure 18 and the system must be resistant to high wind forces.

2.2 OPTIMISATION

2.2.1 BETZ' LAW

Albert Betz, a German physicist developed a theory in 1919 that induced that the maximum possible energy that could be derived by a wind turbine is limited to 59.3% of the kinetic energy in wind. The theoretical calculations imply perfect and thus unreachable assumptions in reality. Thus the Betz coefficient (C_p) appears as a limit and even the best modern turbines can only operate at efficiencies substantially below the Betz limit. Typical values for a 3-bladed turbine is $C_p = 0.5$ (19).

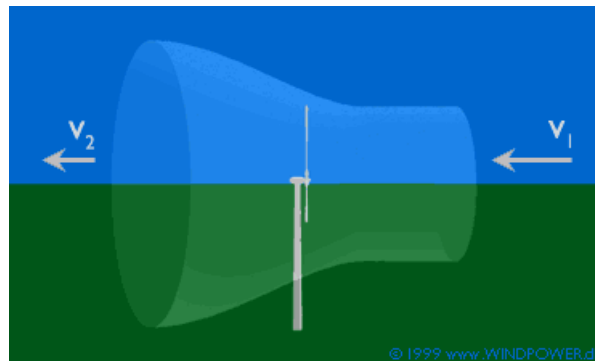


Figure 20 Upstream and downstream wind (19)

The maximum theoretical efficiency is calculated out of a thin rotor imagined to be replaced by a disc that withdraws energy from the fluid passing through it. The application of conservation of mass gives the force exerted on the wind by the rotor:

$$F = \rho \cdot S \cdot v \cdot (v_1 - v_2)$$

Where ρ is the fluid density, S the area of the turbine, v the speed at the fluid power device, and v_1 and v_2 respectively the speed upstream and downstream.

The turbine power can be expressed by the following equation:

$$P = \frac{dE}{dt} = F \cdot \frac{dx}{dt} = F \cdot v = \rho \cdot S \cdot v^2 \cdot (v_1 - v_2)$$

The wind velocity of the rotor may be taken as the average of the upstream and downstream velocities. Thus:

$$v = \frac{1}{2} \cdot (v_1 + v_2)$$

By differentiating the expression for power based on kinetic energy, the maximum is achieved when

$$\frac{v_2}{v_1} = \frac{1}{3}$$

Hence, the power is given by the following equation, where $C_p = \frac{16}{27}$:

$$P_{wind} = \frac{1}{2} \cdot C_p \cdot \rho_{air} \cdot S_{rotor} \cdot v_{wind}^3$$

2.2.2 TIP SPEED RATIO



Figure 21 Tip speed

The tip speed ratio is the ratio between the rotational speed of the tip of the blade, called tip speed, and the velocity of the wind. On one hand, if the rotor of the wind turbine turns too slow, most of the wind will pass undisturbed through the gap between the blades. On the other hand, if the rotor turns too fast, the blades will appear like a solid wall to the wind. Thus, there is a trade-off to extract as much power as possible from the wind (20).

$$\begin{aligned} \text{Tip speed} &= U = \omega \cdot R \\ \text{Tip speed ratio} &= \lambda = \frac{\omega \cdot R}{v} \end{aligned}$$

The optimum tip speed ratio for the maximum power output is $\lambda_{max} = \frac{4\pi}{n}$, where n is the number of blades.

2.3 WIND TURBINES' GENERATORS

Generators for offshore and onshore wind turbines are similar. There are four types of generation principles: fixed speed, limited variable speed, variable speed with doubly-fed induction generators (DFIG) and variable speed with full-scale frequency converter. These configurations will be discussed and they show that wind turbines have gradually upgraded over the last 25 years from simple constant speed turbines to fully variable speed systems, with active output control.

In constant speed turbines, the speed is given by the electrical grid frequency and the turbine is not operating at its peak efficiency. Though, it is a cost effective and robust configuration. Variable speed systems use power electronic converters. It enables an optimisation of the performance by reducing the mechanical loading and delivering active control. Until the late 1990s, constant speed wind turbines were the most used ones and still represent 30% of the installed turbines (21).

Wind turbine concepts are classified by type of generator, power electronics and methods of power control into four types: A, B, C and D.

2.3.1 TYPE A: FIXED SPEED

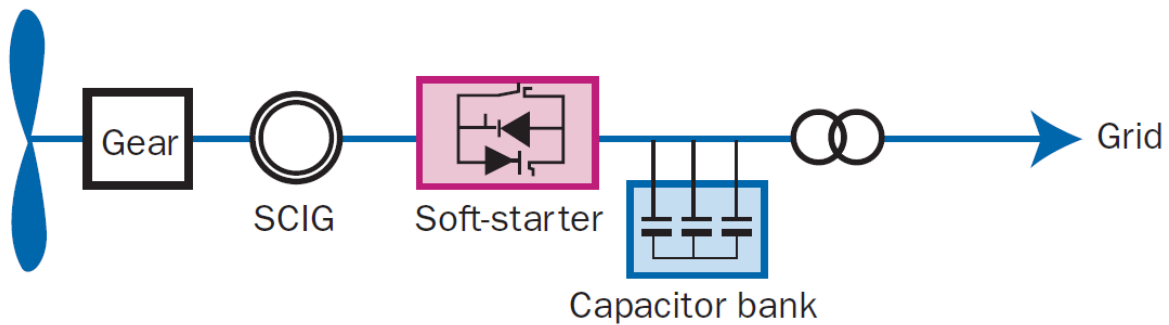


Figure 22 Fixed speed wind turbine

A schematic representation of a fixed speed wind turbine is shown in Figure 22. The generator is a squirrel cage induction generator (SCIG). The turbine drives the rotor of the generator, and the stator is directly connected to the grid. This is the simplest model. As the name suggest, the rotation speed is constant, but it can slightly change between 1% and 2%. There are two versions of the fixed speed turbine: a single speed and a double speed version. The double speed configuration allows improved performance and lower noise disturbance at low speed compared to the single speed configuration.

The aerodynamic control that exists on this type of turbine is passive stall and thus there are few active control options, except connection and disconnection of the turbine. However, a rotor angle control can be installed, and is called *pitch-control* or *active stall* (22).

The main manufacturers of type A wind turbines are Suzlon, Siemens Bonus, Ecotècnia and Nordex. They have been used since the 80s and still represent 30% of the market share.

2.3.2 TYPE B: LIMITED VARIABLE SPEED

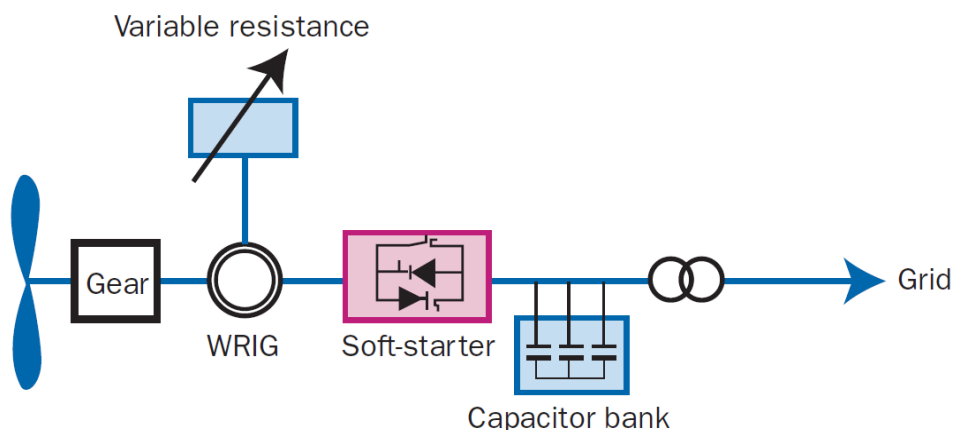


Figure 23 Limited variable speed wind turbine

Limited variable speed wind turbines use wound-rotor induction generators (WRIG). The main difference with the previous type of turbines is the variable resistance that changes the generator's rotor current and thus the speed. Power electronics play an important role since they control the rotor electrical resistance. The variation in speed is not total and is limited to +/- 10% . However, it can maximise the power quality and reduce the mechanical loading of the components of the turbine (21).

There are limitations to pitch control with regard to actuator speed and performance. Additional achievements can be done by variable speed control such as a further optimization of efficiency. Moreover, wind turbines can't store energy but thanks to variable speed control, the energy of the rotor inertia can be exploited as short-term energy storage. Variable speed control enables faster and more precise control. Implementation of variable speed control is achieved with type B, C and D (22).

The main manufacturer is Vestas. They have been mostly used in the 80s and the 90s, and they represent 10% of the market share today.

2.3.3 TYPE C: VARIABLE SPEED WITH DFIG

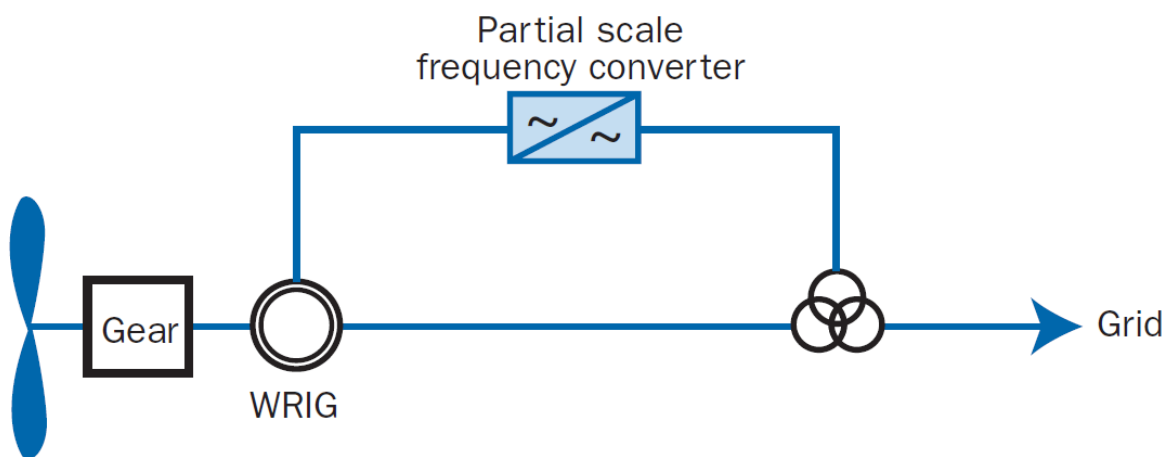


Figure 24 Variable speed wind turbines with DFIG

Induction machines draw high starting currents, up to 8 times the nominal current, but grid codes demand low inrush currents. DFIGs have an inrush current lower than nominal (22).

The variable speed with DFIG is the most popular system and represents 45% of the market share today. Its popularity comes from the fact that this type of wind turbines combines the advantages of type A and B, with improved power electronics. The DFIG that is usually used is the wound-rotor doubly-fed induction generator. The partial scale frequency converter is a back-to-back voltage source converter (VSC) that is connected to the rotor of the WRIG and to the grid. The VSC

controls the excitation of the machine in order to match the frequency of the rotor and the frequency of grid.

The use of power electronics allows a control of the active and the reactive power produced by the turbine. There is thus an active voltage control. Only 40% of the output power of the machine passes through the partial scale frequency converter and the rest goes directly into the grid. As a result, the speed variation that is possible to achieve with type C turbines is +/- 40% of the synchronous speed.

The main manufacturers are General Electric, Repower, Ingetur, Suzlon, Gamesa, Ecotènia, Vestas and Nordex.

2.3.4 TYPE D: VARIABLE SPEED WITH FULL-SCALE FREQUENCY CONVERTER

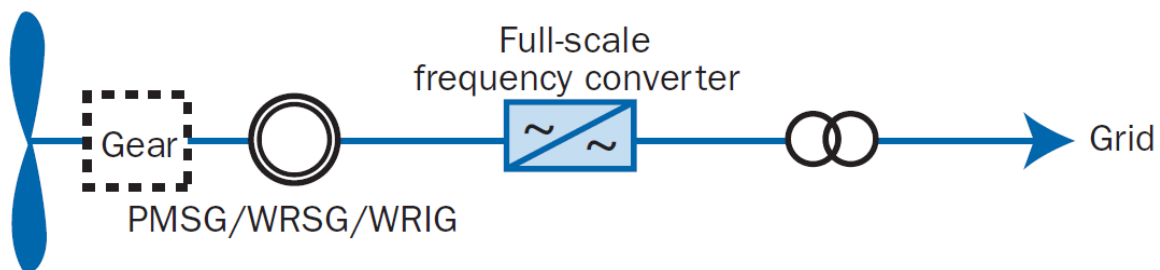


Figure 25 Variable speed wind turbine with full-scale frequency converter

Type D wind turbines are similar to type C, on the exception that the frequency converter is completely decoupling the generator from the grid. Thus, the turbine's generator can run at a wider range of operating speeds than type C turbines. Moreover, the range of reactive power and voltage control capacities is also increased.

Many types of generators can be used: permanent magnet synchronous generators (PMSG), wound-rotor synchronous generators (WRSG), wound-rotor induction generators (WRIG) and also squirrel cage induction generators.

The main manufacturers are Jeumont, Mtorres, Enercon, Multibrid (Areva), General Electric, Leitner, Made, Zephyros, Winwind and Siemens. Type D turbines represent 15% of the market share.

3 STABILITY IN WIND POWER SYSTEMS

The Institute of Electrical and Electronics Engineers (IEEE) and the International Council on Large Electric Systems (CIGRE) have proposed a definition of power system stability (23):

Power system stability is the ability of an electric power system, for a given initial operating condition, to regain a state of operating equilibrium after being subjected to a physical disturbance, with most system variables bounded so that practically the entire system remains intact.

Even though power stability is a single problem, there can be various types of instabilities a system can undergo. In order to perform practical analysis of stability problems, it is necessary to classify power system stability. Stability can be classified depending on the physical nature of the mode of instability, on the size of the disturbance, the time taken to reach stability after a fault, etc. Figure 26 shows the classification proposed by IEEE and CIGRE (23).

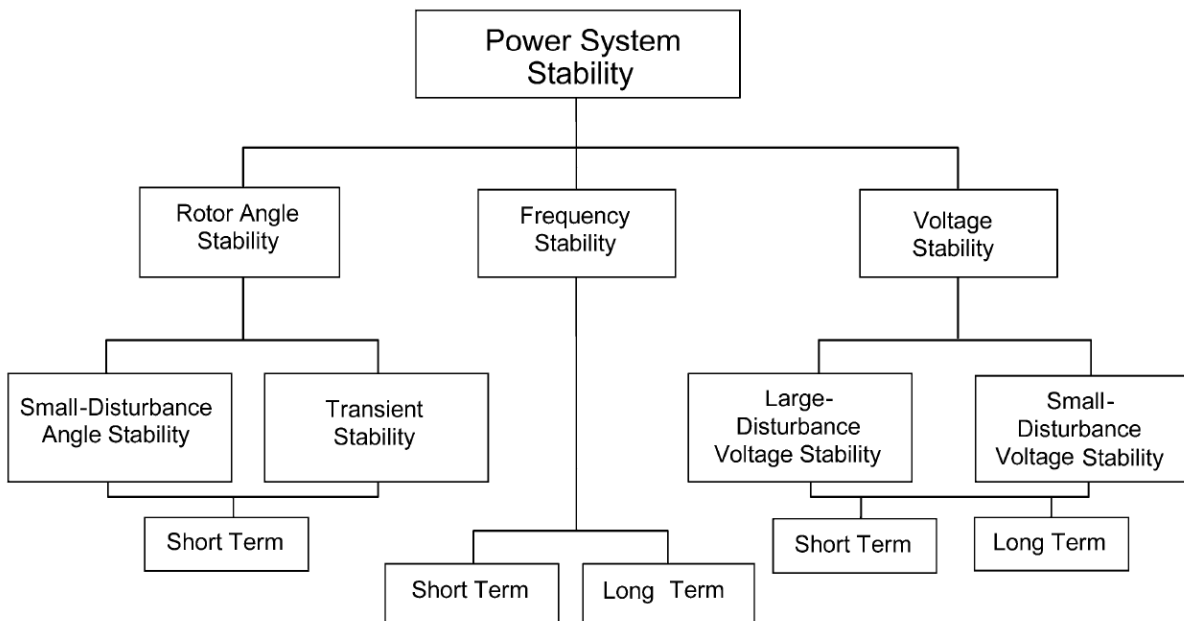


Figure 26 Classification of power system stability (23)

In an interconnected system, rotor angle stability is the ability to remain in synchronism after a fault, for a synchronous machine. Frequency stability refers to the power system being able to maintain a constant frequency when an imbalance between the generation and the load occurs. Voltage stability is the ability to maintain a steady voltage at each bus of the system after a disturbance.

The world's total wind power capacity by the end of 2010 was approximately 200 GW. It represents 19 000 TWh of energy production, and thus 2.2% of the world's production (24). Wind power is becoming more and more competitive and a number of researches are currently in progress regarding large scale integration of wind power into the grid. It involves power system stability and thus concerns network reinforcement and reserve requirements. The main parameters that need to be investigated are the fluctuations of wind power, the location of wind resources, the generator technologies and their control.

Wind power is different from conventional power stations. Firstly, wind resources are located at specific locations, onshore or offshore, and require specific power systems optimized for the transportation of energy. Secondly, wind turbines' generators are not conventional synchronous machines and are more complex, especially in their control due to fluctuation of wind resources. Thirdly, wind farms are generally connected to subtransmission or distribution voltage levels and not to transmission levels as conventional power stations (25).

Transient stability is a phenomenon that has to be investigated. Even though wind speed variations are slow compared to transient stability time frames (from one to ten seconds), those variations have an indirect influence on transient stability. High amount of wind power than can especially be found offshore require high spinning reserve and thus add inertia to the system, which has an influence on transient stability.

It has been shown (25) that the location of wind parks can have a large impact on transient stability. In high wind speed regions, the power flow can be changed to such an extent that the critical fault clearing times can be reduced and that it might be necessary to install new lines. Fixed-speed induction machines have a negative impact on dynamic voltage stability but variable speed induction generators are able to improve transient stability margins, especially when upgraded with low voltage ride-through and reactive current boost. Moreover, the connection of wind farms to subtransmission or distribution voltage levels also has a negative impact on transient stability because high reactive losses can occur.

Voltage stability is another phenomenon that needs to be looked at. Regarding large scale wind farms, the amount of wind power can be increased thanks to Static Var Compensators (SVC) which provides extra reactive power supply. It thus increases the voltage stability limit, proportionally to the active power that can be produced out of the wind farm. Even though voltage control and reactive power compensation helps on the damping of the oscillation modes of the system, it can have both positive and negative impact on the entire system (26).

4 TRANSMISSION TECHNOLOGIES

In order to transmit bulk electrical power, three phase alternating current and high-voltage direct current are used. Since the energy lost in a transmission line is proportional to the square of the current, transmission lines operate at high voltages. For a given power output of a generation system, a higher voltage means a lower current and thus lower losses in the wires used. This power lost can also be reduced by increasing the diameter of the cable, and thus reducing the resistance. However, bigger cables means higher costs.

4.1 HISTORY OF DC TRANSMISSION

Electricity supply dates back from 1883 in the West End of London where the *Grosvenor Gallery Company* started to deliver electricity to the neighbour houses, linking the entire system with overhead lines across the roofs of houses (27). In the late 1880s, the War of the Currents happened between the defenders of Tom Edison's Direct Current (DC) and Nicolas Tesla and George Westinghouse's Alternating Current (AC). In 1887, Tesla filed for polyphase AC motors and power transmission (transformers, transmission lines, etc.) patents which Westinghouse found to be the solution to long-distance power transmission. The War ended at the Columbian Exposition on May 1, 1893 where a hundred thousand incandescent lamps were lighted the surrounding buildings thanks to AC generation (28). From that point, more than 80% of the US electrical devices ordered were AC systems. However, DC transmission was not forgotten and engineers understood that higher voltage levels were necessary. DC installations up to 1500 V in Chelsea in 1889 and Lambeth in 1896 were performed.



Figure 27 English Electric mercury arc valves at the Manitoba Hydro Radisson Converter Station

HVDC was firstly made possible in 1889 by the *Societa Acquadotto de Ferrari-Gallieri*, under the direction of Pr. Thury, in Italy. The installation was 121 km long and was able to transmit 630 kW at 14 kV (29). Other installations based on Thury's continuous current system were performed later, up to 100 kV in the 1930s but the required machinery was not efficient and required high maintenance.

The introduction of mercury arc valves to convert high-voltage or high-current alternating current into direct current became of interest for power transmission at that time. The fully static mercury arc valve was used industrially from 1954 and started the modern HVDC era. That year, on the Swedish east coast, the HVDC Gotland link was the first fully static commercial HVDC transmission. It could transfer 20 MW at 100 kV over a submarine distance of 98 km. From 1975, Line-Commutated Converters (LCC) replaced mercury arc valves with thyristor valves. At the beginning of the 21st Century, force commutated converters are believed to replace LCC systems, such as Capacitor Commutative Converters (CCC). Self commutating converters are also the next step, with Voltage-Source Converters (VSC) already replacing LCC.

4.2 HVAC CONFIGURATION

High voltage alternating current is mostly used in transmission systems, with three phase lines. The current produced out of the generator is directly transmitted to the grid via a transformer unit if there is the need for a stepping up or down. The power transmission and operation is achievable in both directions. However, AC lines produce large amount of reactive power and thus require reactive compensation units.

For HVAC transmission, the use of 3-cores cables is preferred to single-core cables since 3-cores cables require the installation of only two cables compared to four cables for single-core ones. In case of external damage of one cable, it is necessary to achieve a reasonable security of supply by adding an additional cable. Though, 3-cores cables are not able to meet with major cable installations ratings and then one-core cables are necessary. AC submarine cable systems can be constructed with three-core cables where all three insulated conductors are stranded into a single cable. For larger transmission power, the AC systems comprise three single-core cables, each containing only one insulated conductor. A fourth spare cable is often added.

In order to connect a large offshore wind farm to a grid with HVAC, the system shown in Figure 28 is the most common (30). This configuration presents a local wind park grid at lower voltage level (20-30 kV) than the transmission line. This local grid is connected to a transformer before the transmission system. This HVAC configuration requires and the installation of an offshore platform for the transformer and the switch gear.

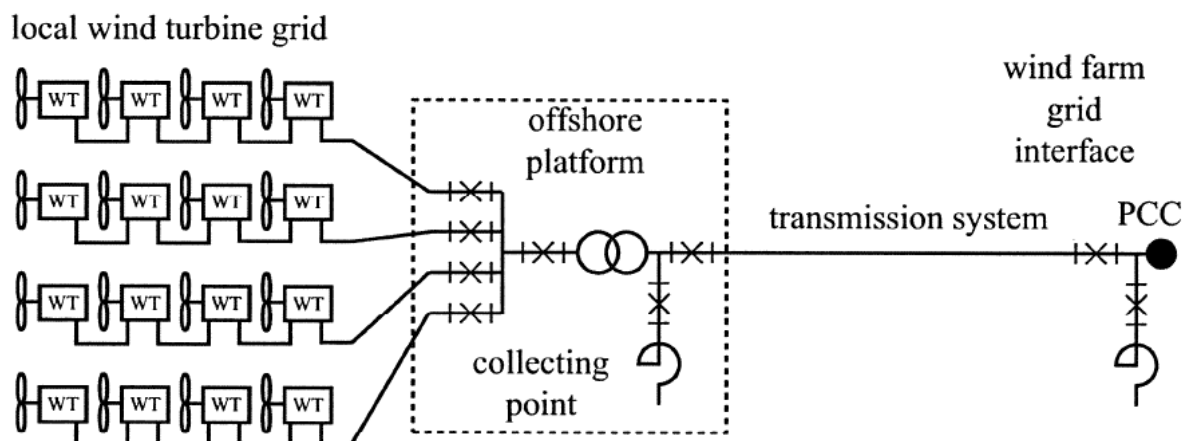


Figure 28 Electrical system for a large AC wind park

The voltage control is ensured by Automatic Voltage Regulators (AVR) in case of wind turbine equipped with synchronous generators. Otherwise, switched capacitor banks, mechanically or thyristor based, are more common than AVRs. The use of converter based power electronics can be made internally as a part of wind turbines' power conversion system. It can also be used externally, as separate solutions within the wind farm transformer station, at the point of common connection, such as Static Var Compensators (SVC) and Static Synchronous Compensators (STATCOM) (31).

4.3 HVDC CONFIGURATION

Submarine transmission cables have a high capacitance that results in a high charging current in AC transmission. Capacitance is proportional to length and thus there is a maximum acceptable length from which the charging current is equal to the thermal current rating of the cable, resulting in no capability for active power. Moreover, the voltage also has an influence on the charging current which results in reducing the maximum length when increasing the rated voltage. Expansive shunt reactors placed at intervals along the cable can overcome this effect but this is not practicable for submarine use. DC cables also encounter a charging current but only during switching on or off and thus, this current has no effect on the continuous current rating of the system (32).

As a result, there is no length limitation to be applied to DC transmission and as a result, this type of transmission is preferred over AC transmission in our study. Moreover, a minimum of two cables is necessary for DC transmission whereas three cables are necessary for AC transmission which is a reduction in cost on cables for DC transmission. This transmission can consist of one polarity cable carrying full circuit power or two cables, one with a positive polarity and the other negative, each carrying half circuit power.

Figure 29 shows an AC/DC wind park. In this system the AC transmission has been replaced with a DC transmission compared to the HVAC solution proposed in Figure 28. This configuration is not present in many existing offshore farms but is proposed in many modern farm projects when the transmission distance is long or when the AC grid to which the farm is connected is weak (30). The local AC system is independent where both the frequency and the voltage are completely controllable thanks to the offshore converter station. Such a configuration can be used for a collective variable speed system of all wind turbines that are in the wind farm. The main benefit is that the aerodynamic and electrical efficiency can be increased.

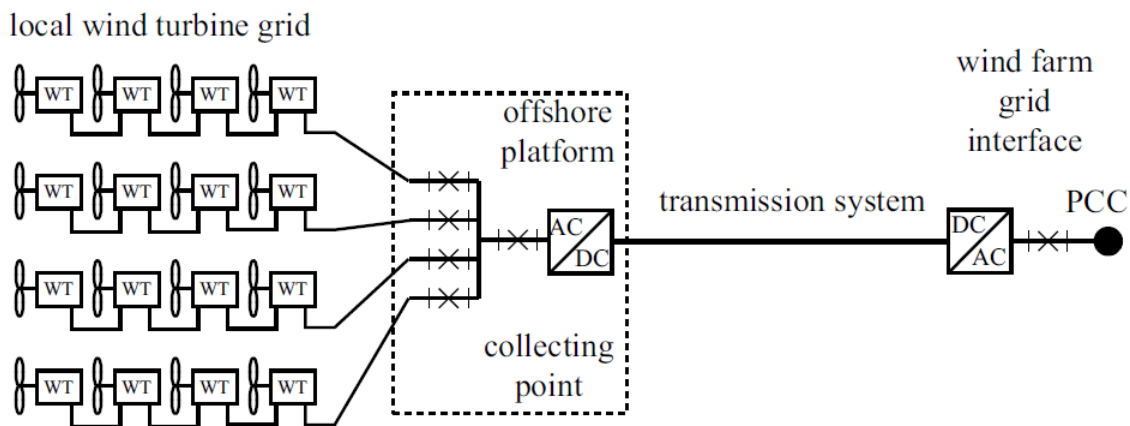


Figure 29 The electrical system for an AC/DC wind park

In Figure 29 appear only one cable for the transmission system but there is in fact a bipolar configuration installed, one for the positive pole and one for the negative pole, referred to as one cable. In case of a large DC wind park, the configuration differs from the large AC park because it requires one or two transformation steps in order to increase the voltage output of the wind turbines to a suitable transmission voltage level. Generally, if the DC output voltage of the wind turbines is over 20 kV, only one transformation step is necessary, but in case of a typical lower voltage, such as 5

kV, two steps are needed. Figure 30 shows a large wind farm that includes two DC transformer steps. As voltage levels are low, the entire wind farm is divided into several smaller clusters connected one by one to the first transformation step. The high voltage side of the first transformer is connected to the second transformation step.

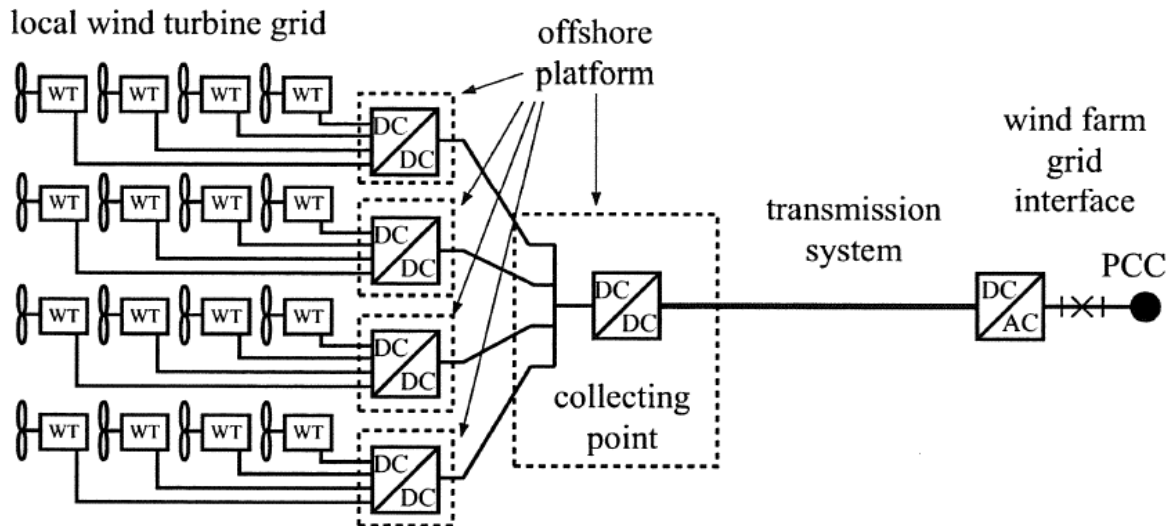


Figure 30 Electrical system for a large DC wind park with two DC transformer steps

A DC electrical system with series connected wind turbines is presented in Figure 31. The size of such a wind farm can be large but it does not necessarily imply large DC transformers and offshore platforms. There is however an electrical insulation provided by the local DC/DC transformer for safety reasons. Despite the huge benefit of not having a large transformer, the DC/DC converters need to have the capability to operate towards HVDC at their terminals. If a single wind turbine does not feed out energy and thus fails to hold its output voltage, the other turbines must compensate for this lack and thus increase their output voltage.

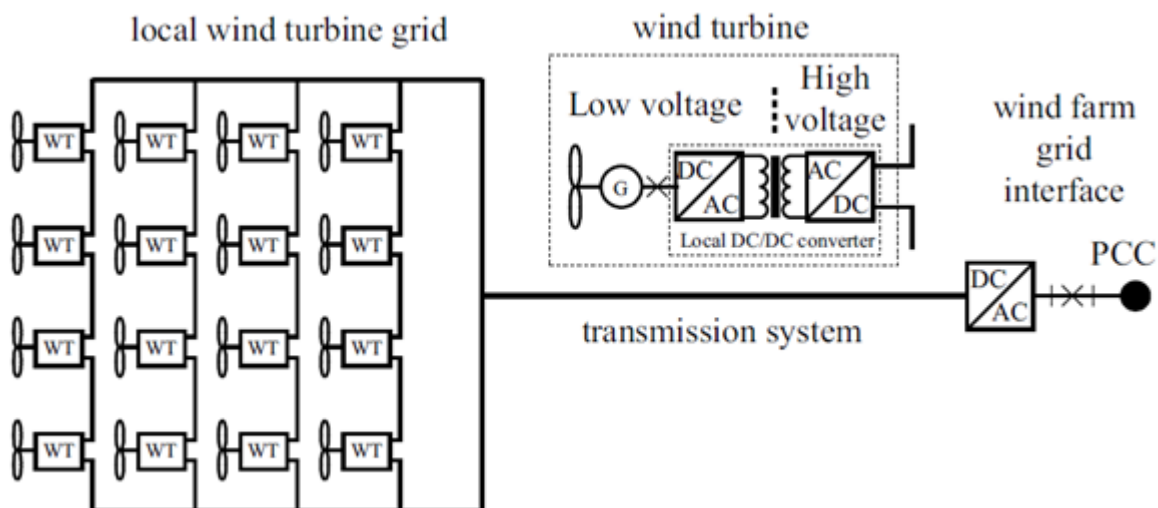


Figure 31 DC electrical system with series connected wind turbines

4.4 COMPARISON BETWEEN AC AND DC LINES

4.4.1 ECONOMIC COMPARISON OF AC AND DC LINES

A simple economic comparison can be carried out with these considerations (33):

- The same power is transmitted by a three-phase AC line and a bipolar DC line
- The DC voltage is equal to the AC peak voltage ($U_{dc} = \sqrt{2} * U_{ac}$)
- The DC current in every pole is equal to the RMS AC current in each three-phase conductor

$$P_{ac} = 3 * U_{ac} * I_{ac} * \cos(\varphi)$$
$$P_{dc} = 2 * U_{dc} * I_{dc}$$

The ratio between the DC and AC power is then:

$$\frac{P_{dc}}{P_{ac}} = \frac{2 * U_{dc} * I_{dc}}{3 * U_{ac} * I_{ac} * \cos(\varphi)} = \frac{2 * \sqrt{2} * U_{ac} * I_{ac}}{3 * U_{ac} * I_{ac} * \cos(\varphi)} = \frac{2 * \sqrt{2}}{3 * \cos(\varphi)}$$

This ratio is equal to 1 when $\cos(\varphi)$ is equal to 0.945. A bipolar DC line that has the same voltage as the peak phase-to-ground voltage of a three-phase AC line is able to transport the same power, with the same current. However, the DC line requires only two conductors of the same size as the AC line which requires three conductors. Moreover, a DC line leads to a reduction from 25 to 35% of ohmic losses compared to an AC line over the same distance for the same power. This comparison does not include shunts, transformers and substations costs.

4.4.2 TECHNICAL COMPARISON OF AC AND DC LINES

The advantages of DC lines towards AC lines when operating isolated are (33):

- lower power losses
- lower switching overvoltages
- no problem of stability as the interconnected systems do not operate in synchronism
- great ability to interconnect systems of different frequencies thanks to back-to-back converter stations
- reduced levels of short-circuit powers

The disadvantages of DC lines towards AC lines are caused by the lack of simple voltage transformation into DC voltages and its contrary:

- DC lines can't supply loads directly. Converter stations are needed and are usually expensive
- DC transmission can't compete economically with AC transmission regarding intermediate substations to supply consumers
- Converter stations for DC transmission require a high reactive power reaching 60% of the active power in order to supply the commutation equipment.

4.5 SUBMARINE POWER CABLES

4.5.1 REQUIREMENTS

AC and DC submarine cables used for power transmission have to fulfil the requirements listed below. Those requirements are more or less relevant depending on the water depth and the length of the cable route (32):

- 1) The cable must have a high electrical factor of safety since maintenance underwater is complicated and expensive.
- 2) The cable should be designed to reduce transmission losses.
- 3) The cable should preferably be laid into the sea while the entire length is joined together with flexible joints during the manufacture or prior to the underwater fitting. There should not be any need to insert joints while at sea.
- 4) The cable must withstand the high bending under tension, the twisting and the coiling that can occur during the manufacture and the installation.
- 5) The cable must withstand the external water pressure at any part of its route.
- 6) The cable's armour must be sufficiently robust to resist impact damage and severance of the cable if fouled by a ship's anchor or fishing gear.
- 7) The cable must be reasonably torque balanced to avoid uncontrolled twisting during the underwater installation.
- 8) The cable's weight must be sufficient to allow as few movements as possible due to tidal currents since this would cause abrasion and fatigue damage to the cable.
- 9) The cable must be adequately protected from all corrosion hazards.
- 10) All cable components must have adequate flexural fatigue life.
- 11) All paper insulated and some polymeric insulated cables are required to be watertight along their complete lengths.

4.5.2 CONSTRUCTION OF DC CABLES

The conductor

DC lines do not suffer from skin and proximity effects (32). As a result, thinner conductors can be used. The use of DC results in lower conductor losses. Copper conductors are suitable for medium voltage and high voltage. They offer a better conduction and better thermal properties compared to other materials but they are also more expensive. Aluminium is more convenient for

low voltage applications. It is lighter and cheaper but the losses are higher. Moreover, it requires a larger cross-section area compared to copper, and it corrodes more easily. The conductor of DC cables can be up to 2000 mm².

The semiconductor screen

Its aim is to protect the cable. There are two screens, one placed directly on the cable's core, which is the inner screen, and the other placed on the cable's outer shell, which is the outer screen. It is generally made of polyethylene materials which have a high percent of black carbon. Partial discharges are due to space charges accumulations and thus damage the insulation. Semiconductor screens have a large resistivity because of their poor dielectric properties and thus the electric field is not able to penetrate the insulation part.

The insulation

The insulation part of the cable insulates it electrically from the environment where it lies. DC cables can be operated at higher electrical stresses than AC cables. The stress in a DC cable is governed by the insulation's resistivity and by its geometry. The resistivity is expressed by the equation: $\rho = \rho_0 e^{-\alpha\theta} e^{-\beta E}$ where ρ_0 is the resistivity at reference temperature, θ is the difference in temperature between the actual and reference temperatures, α is the temperature coefficient of electrical resistivity, β is the stress coefficient of electrical resistivity and E is the electrical stress in the insulation.

The optimal configuration for a DC cable would imply a constant insulation resistivity, as less sensitive as possible to electrical field and temperature changes. It would also require minimal thermal resistivity, small capacity of storing space charges and high DC breakdown strength insensitive to temperature rise.

4.5.3 MASS-IMPREGNATED CABLES

These cables can transmit up to 1000 MW per cable in a 600 kV DC system and thus 2000 MW at bipolar operation (34). Mass-impregnated cables have been used since 1895 in medium voltage AC transmission applications. Nowadays, it is mainly used in HVDC for large power transfer and for such high DC voltages as 600 kV, there is no alternative than those cables (35). The current longest distance achieved is the NorNed submarine power cable between Norway and the Netherlands which is 580 km.

Mass-impregnated paper insulation cables do not need oil-feeding system. The insulation part is made of oil impregnated paper, with high density (1 kg/dm³) in order to obtain the best dielectric strength. Different types of papers are used such as semi-conducting carbon-black paper for the conductor screen and carbon-black paper combined with metal-laminated paper for the insulation screen. With high-viscosity compounds in the cable, the length can be infinite, since external pressurization stations aren't needed.

This type of cable is not suitable for HVAC transmission since under repeated partial discharges due to AC current, paper disintegration and breakdown can happen. Regarding environmental aspects, mass-impregnated cables do not leak oil when they are damaged, which thus preserves the area where it is placed in case of injuries.

The construction of the cable is shown in Figure 32 (36):

- 1 - Conductor (key-stone type)
- 2 - Conductor shielding
- 3 - Insulation (oil impregnated paper)
- 4 - Insulation shielding
- 5 - Lead sheath
- 6 - Plastic jacket
- 7 - Tape armour
- 8 - Optical fiber (option)
- 9 - Steel wire armour
- 10 - Serving



Figure 32 Mass-impregnated cable construction

4.5.4 LOW-, MEDIUM-, AND HIGH-PRESSURE GAS FILLED CABLES

The first gas filled cable installation was made in 1938. Low-pressure gas filled cable systems are in the range of 10 kV to 40 kV and operating with a gas pressure between 10 to 15 pounds per square inch. Medium pressure systems are in the range of 40 kV to 69 kV with pressures between 24 and 40 pounds per square inch. High pressure systems are in the range of 69 kV to 138 kV with pressures between 150 and 200 pounds per square inch (37).

The construction is similar to solid type paper-insulated cables but longitudinal gas feed channels are created in order to perform a uniform gas-pressure maintenance and control. During operation of the cable, the heat dilates the oil and the surplus of oil is forced to go out of the cable. Thus, oil tanks are used to maintain a satisfying amount of oil the cable.

The main advantages of this type of cable is that it is simple, economical and of small size. However, as the cable is under oil pressure, it has to be reinforced, which induces an additional weight compared to Mass Impregnated cables. Moreover, as the oil is flowing inside the cable, the length of the cable is limited to short distances, which does not make it practical for offshore wind installations. Even though the cable is of a small size, oil tanks that permit the constant oil pressure are bulky and not easy to install.

4.5.5 CROSS-LINKED POLYETHYLENE CABLES

Cross-Linked Polyethylene (XLPE) cables have been used since 1973 for submarine transmission. The cross-linking of polyethylene allows much more stability of the material at higher temperature. It does not melt, but it is however destroyed by pyrolysis above 300°C. The temperature it usually stands is 90°C and the short-circuit temperatures can go above 200°C (35).

XLPE cables are lighter than paper insulating cable since they require less insulation material. XLPE cables also have interesting mechanical properties. They have a higher mechanical resistance and bending capabilities which is the reason why they don't require maintenance. Moreover, as there is no oil circulation as in gas-filled cables, there is no need for oil tanks or many joints along the cable.

XLPE cables suffer from moisture ingress into the insulation and an impermeable moisture barrier must be provided to the cable. Applying a lead alloy sheath to the cable prevents moisture and also helps the cable's stabilization when placed underwater. This water sensitivity was a real problem to the expansion of XLPE cables because water-trees could be initiated and cause electric breakdown. Triple-extrusion and dry curing tubes are now provided to the cables by manufacturers to avoid any water-treeing problem.

The most important parameter of the cable is the dielectric strength but the value depends on the manufacturers, the material used, the temperature, the sample preparation and more. Thus it is not possible to obtain a fixed value. Among others benefits, XLPE submarine cables are maintenance free, have low electrical losses and are environmentally friendly.

Joints are a limiting factor for the use of XLPE cables in submarine applications. This is the only option for linking pieces of cables together along the cable route. Joints have been made possible up to 345 kV but generally, manufacturers try to deliver the cable as a simple piece, which restricts the available cable length. However, submarine cable for lower AC ratings such as 170 kV can be produced for distances over 50 km. For example, ABB produced XLPE-insulated AC cables for system requirements of 420 kV and 1000 MVA (34). Figure 33 shows a single-core XLPE cable. Its design is similar to the one of mass-impregnated cables.



Figure 33 Cross-linked polyethylene cable

Three-core cables are available for very long length of more than 50 km and single-core cables are rated up to 500 kV but for limited lengths.

4.5.6 PAPER-INSULATED OIL-FILLED CABLES

This type of cables are filled with low viscosity oil and are known under various abbreviations such as Low-Pressure Oil-Filled cables (LPOF), Self-Contained Fluid-Filled cables (SCFF) and Self-Contained Oil-Filled cables (SCOF). High pressure cables are not used for submarine power transmission. The paper used in this type of cables has a lower density (0.7 kg/dm^3) than Mass-Impregnated cables (1 kg/dm^3).

The insulation is achieved with thin paper since it has a higher dielectric strength than thicker one (35). However, this strength relies on the pressure applied to oil inside the cable by external stations. As the pressure is not the same at the centre of the cable route and at both ends of the cable, it is necessary to provide the cable with large enough oil channels. For single core cables, the oil channel is located in the conductor centre and the voltage rating can be over 150 kV. As external pressurization stations are required, the cable length is small (30-60 km).

This type of cable tends to disappear to Mass-Impregnated cables which are more conventional. Yet, the paper insulation of oil-filled cables can be improved with reinforced polymeric films and voltage ratings have been achieved up to 800 kV in AC transmission.

4.6 TRANSMISSION SYSTEMS

In order to connect an offshore wind farm to the shore, three different transmission technologies are mostly used. HVAC transmission is the most common nowadays since the majority of offshore wind farms are of a relatively small size compared to onshore ones and because distances are not far from the shore. However, the offshore wind market is leading towards bigger power and implementations further away from the coast. HVDC is thus a necessity and LLC-HVDC and VSC-HVDC are also presented.

4.6.1 HVAC TRANSMISSION

As investigated previously, a typical HVAC transmission consists of:

- An offshore AC collector system that includes, in the case of a large offshore wind project, a transformer unit with reactive power compensators
- Single- or Three-core cross-linked polyethylene cables (XLPE)
- An onshore substation including a static VAR compensator (SVC)

Some parameters have to be taken into account before deciding to investigate HVAC for a project. High inductance means more voltage drop and thus it is important to choose the cross-section area of the cable wisely (38). The larger the cross-section, the lower the inductance but the bigger the cable and thus the cost.

The capacitance plays also an important role in the determination of having an HVAC transmission system since it sets the technical and economical limit of the cable length (39). Capacitance is responsible for charging current flowing in the cable route. This current is not desirable but the cable has to carry it along with the useful current. It results in a lower load capability for the cable. A longer cable means a higher capacitance and thus higher charging current. The capacitance itself can also create overvoltages, high harmonic currents and resonance effects. As a result, special circuit breakers can be necessary for the system.

The real power losses also limit the HVAC line length. Four losses of this kind occur in the cable: the dielectric losses (small), the Joule's law losses in the conductor (large), the Joule's law losses in the metallic shield (one third of the conductor losses) and the Joule's law losses in the steel wire armour (one half of the conductor losses) (39).

AC connections undergo a major matter that is the reactive power control. The reactive power transfer into the transmission cables needs to be compensated depending on the load. The compensation is maximal at no load, and is then approximately halved during rated operation (40). Figure 34 illustrates a basic configuration of a 600 MW wind farm with a HVAC solution. The compensation is shown as separated in two. The fixed compensation is the smaller and can be placed on offshore substations. The controlled compensation is placed onshore, to maintain the voltage within a range of rated values. Moreover, the wind generators also provide some reactive power and

voltage control. At the onshore grid connection point, SVCs are used to balance the reactive power and to control the voltage. Moreover, centrally placed SVC can improve the behaviour of any wind turbine generator model during and after faults. Thus SCV at the offshore substation is necessary in most cases.

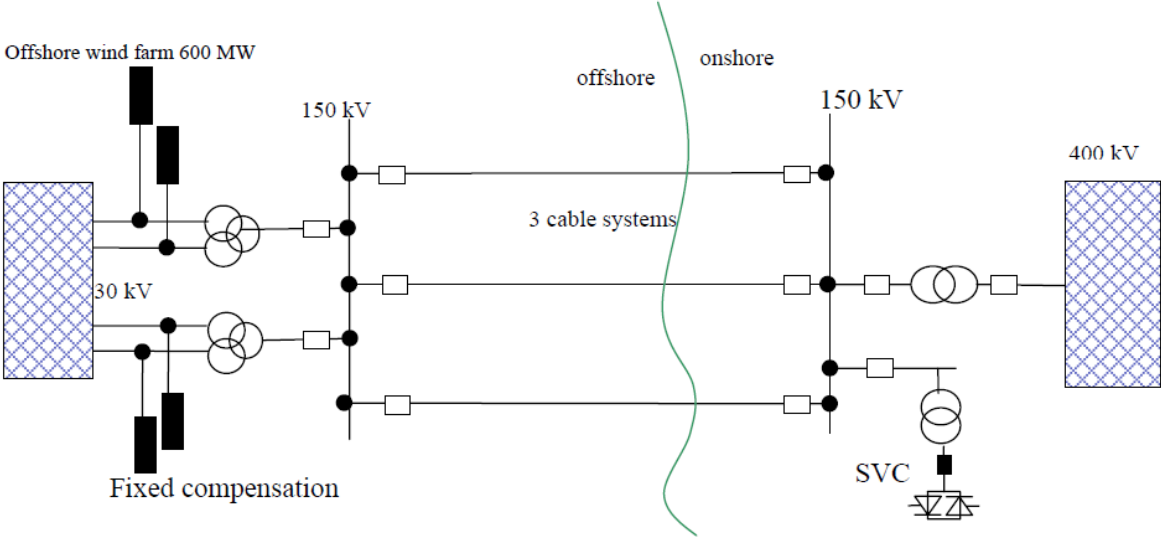


Figure 34 Basic configuration of a 600 MW wind farm with a HVAC solution

Nowadays, the maximum rating of HVAC submarine cables is approximately 200 MW per three-phase cable at a voltage rating of 150 to 170 kV, accounting for compensation at both ends of the cable and a maximum cable length of 200 km (41). Thus, in order to study a large wind farm of 1000 MW with HVAC, five cables would be required to connect the farm to the grid. Rated voltage up to 275 kV are possible (34) but for shorter distances, with powers of 400 MW. Under same conditions, a 230 kV cable can transmit 350 MW over 100 km with 4.3% of losses, and 300 MW over 200 km with 7.3% of losses. However, researches are on the way for higher ratings, such as 400 kV cable transmitting 1200 MVA over 100 km.

4.6.2 LINE-COMMUTATED CONVERTER BASED HVDC TRANSMISSION

LCC based HVDC has been used since 1954 as a transmission technology for bulk power over long distances and for system interconnection. However, it has never been used for offshore wind power applications. The reason is that it can only transfer power between two active grids, and thus an auxiliary start-up system is required in order to connect an offshore wind farm to the grid (42).

A typical LCC based HVDC system comprises transformers, thyristor-based power converters, AC and DC filters, a DC current filtering reactance and capacitors (or STATCOM) for reactive power compensation at each end of the DC cable. Thyristor valves are used and it requires a synchronous voltage source in order to operate. The building block that is most commonly used is a three-phase full-wave bridge. This bridge is a 6-pulse bridge and thus has 6 controlled switching elements which are thyristor valves. Each valve comprises a number of series-connected thyristors, depending on the voltage rating.

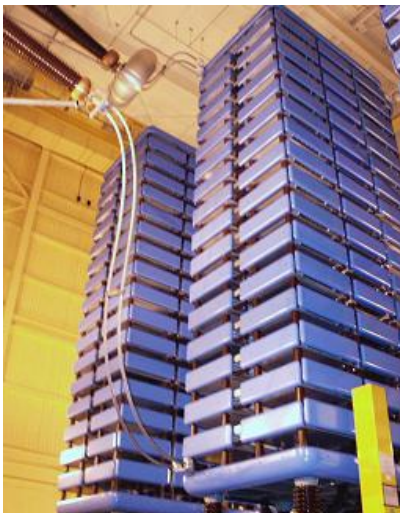


Figure 35 Thyristors valves stacks at the Manitoba Hydro Radisson Converter Station

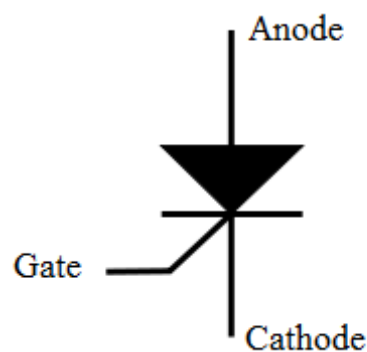


Figure 36 Thyristor circuit model

12-pulse operation can be used when two 6-pulse bridges are connected in series when phase-displaced by 30 degrees. This operation mode is convenient to increase the DC voltage and suppress some of the AC current and DC voltage harmonics. This phase-displacement is achieved by using a transformer with a wye-connected secondary for one bridge and a delta-connected secondary for the other bridge. Figure 37 shows this configuration. 12-pulse conversion gives two independent DC circuits that are capable to transmit half of the capacity.

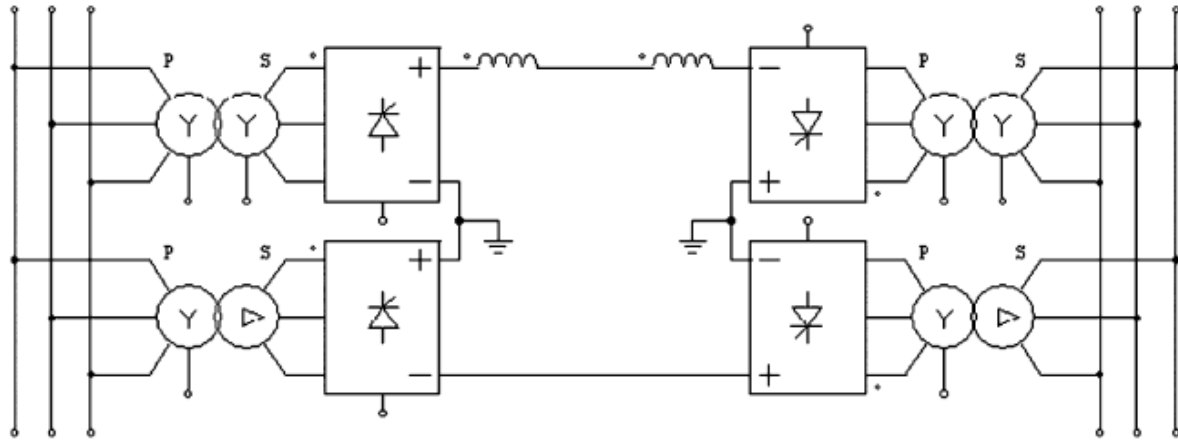


Figure 37 12-pulse HVDC LCC transmission line

The transformers are placed at substations at each end of the cables, in order to raise the voltage to the transmission line requirements. It provides also electric isolation for the AC and the DC circuit and it must include tapping for the system control.

The thyristors are the core of the inverters and rectifiers used in the LCC based HVDC transmission system. They are made with silicon wafers of 125 mm with voltage ratings of 8kV and DC currents of 4 kA (42). Thyristors operate at switching frequencies of 50-60 Hz with power losses of 1 or 2 % (42) depending on the transmission system. As a result, the total conversion efficiency using the two converters at each end of the cable (AC - DC - AC) is between 97 and 98% (41). The higher the efficiency, the higher the cost of the installation. Line-Commutated Current Source Converters can only operate with the AC current lagging the voltage. As a result, reactive power is needed for the conversion process (43) by the thyristors. Moreover, the control characteristics of the system are affected by the reactance of the cable and by the reactance of the transformers. Thus, constant extinction angle control is also required.

The AC and DC filters are needed in order to alleviate for the low-order harmonics in the line currents, generated by the thyristors. They also provide reactive power that is required by the thyristors. The DC current filtering reactance also helps reducing the undesirable harmonics and it allows uninterrupted operation during minimum load.

Different arrangements of the converters are possible depending on the system that needs to be connected to the grid. The most common is the monopolar configuration shown in Figure 38. The monopole with ground return is the easiest and thus most feasible configuration for long distances. As there is only one cable, the costs are reduced as low as possible. Electrodes are used in order to return the current into the ground or the sea. This causes troubles if metallic objects are on the cable route, such as underwater oil or gas pipes. The monopole with metallic return is based on the same principle but the earth is guaranteed by a low voltage DC cable. It suppresses the undesirable behaviour of the ground return, but increases the total cost.

If the capacity of the system becomes too high, a bipolar configuration can be used. This is the combination of two monopolar systems, one with a positive polarity and the other one with a negative polarity. Figure 39 shows two bipolar configurations and the series connection of bipolar converters.

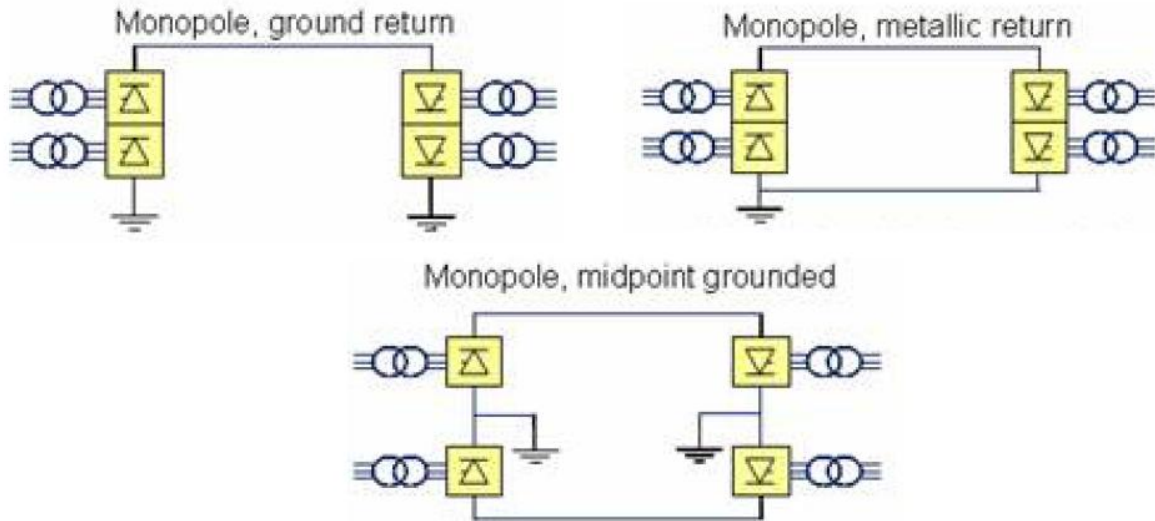


Figure 38 Monopolar LCC based HVDC (43)

The bipole with ground return offers safety to the system in case of fault. If a fault occurs on one line, the current of the second line will return by the ground. In case of such a fault with a bipole with metallic return, the current of the second line will return by the metallic return patch. Half of the power can still be transmitted by the operating line during the clearing of the fault. The configuration with ground return is achieved with electrodes based on the same principle than the monopolar configuration. In case electrodes shall not be used, the metallic return is a suitable option but it is more expensive, due to the additional cables allocated for the return.

Bipolar configuration with series-connected converters is used for high power transmission in HVDC, for voltages between 500 kV and 800 kV (43). The series connection is made to increase the availability of power in case of a defective converter or of a default of insulation.

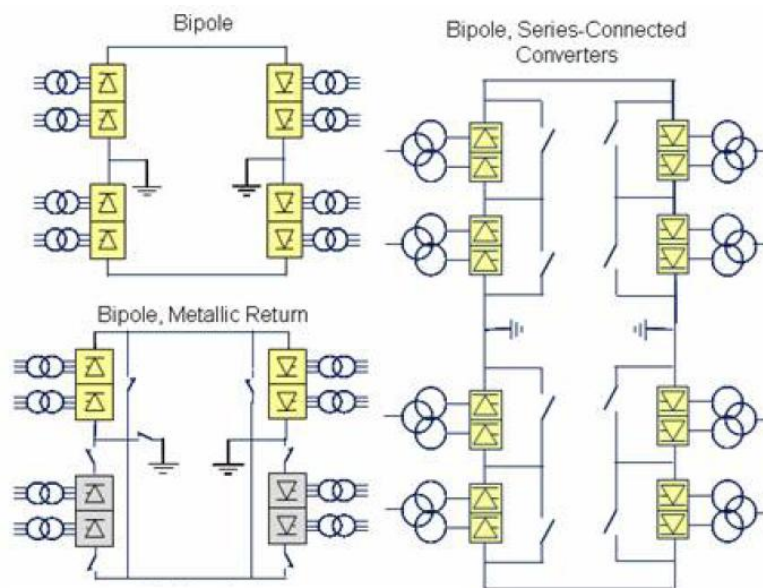


Figure 39 Bipolar LCC based HVDC (43)

Figure 40 shows a multiterminal configuration. It is used when the connection of three or more AC systems is necessary.

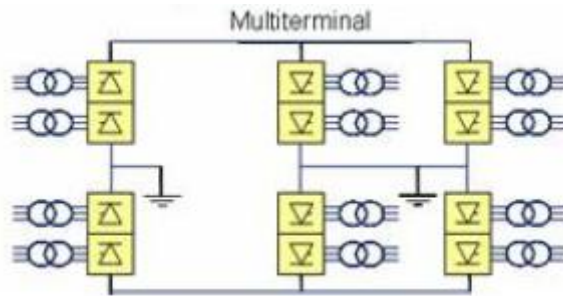


Figure 40 Multiterminal LCC based HVDC (43)

A conventional HVDC converter station with Current Source Converters (CSC), which is the same than LCC based HVDC, is drawn in Figure 41. Such stations can be large. The one shown in Figure 41 is a 600 MW station and the size is 200 x 120 x 22 meters. Offshore substations are smaller but yet it requires a lot of space and real infrastructures.

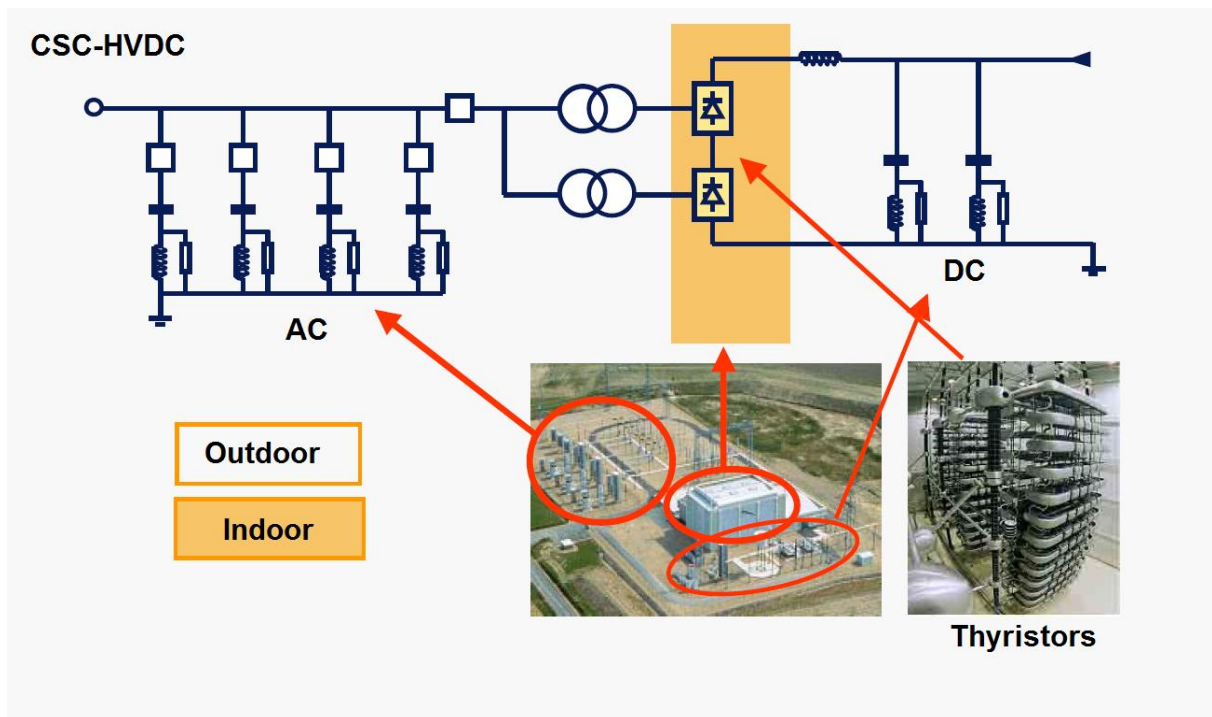


Figure 41 LCC converter station

4.6.3 VOLTAGE SOURCE CONVERTER BASED HVDC TRANSMISSION

VSC based HVDC is a brand new technology that results from major improvements in power electronics. It relies on the use of Insulated-Gate Bipolar Transistors (IGBTs). VSC based HVDC is called HVDC Light by the power technology company ABB, and HVDC Plus by Siemens. As Table 3 shows (41) (40), by the end of 2005, few operational offshore implementations were using VSC transmission technology but it is gaining a large interest in future projects.

Table 3 VSC based HVDC existing systems (2005)

Project	Country	Distance (km)	Rating (MVA)	Start operation	Main motive
Gotland Light	Sweden	70	60	1999	Infeed wind power
Direct Link	Australia	65	3x60	2000	Power trading
Tjæreborg	Denmark	4	8	2000	Infeed wind power
Eagle Pass	USA	Btb	36	2000	AC voltage control
Cross Sound	USA	40	330	2002	Power trading
Murray link	Australia	180	200	2002	Power trading
Troll A	Norway	67	2x41	2005	Power to platform

A VSC transmission system consists of an AC based collector system inside the offshore wind farm, an offshore and an onshore substation with VSCs, AC and DC filters and a DC current filtering reactance. It does not differ compared to LCC based HVDC except on the VSC converters. Figure 42 shows a high power IGBT module. Figure 43 shows its circuit model.



Figure 43 1200 A, 3300 V IGBT module (IGBTs and free-wheeling diodes)



Figure 42 IGBT circuit model

IGBTs are electronic switches that combine and take benefits of the command simplicity of Field-Effect Transistors (FET) and low conduction losses of Bipolar Junction Transistors (BJT). IGBTs in VSC based HVDC operate at high frequency in the range of 1 to 2 kHz. As a result, losses are higher, in the range of 4 to 5 %. As the frequency is higher, there is lower harmonic distortion compared to LCC based HVDC. Thus, the use of filters is reduced. The topology of VSCs is based on the use of two cables since it is generally not connected to the ground. Figure 44 shows a VSC based HVDC transmission system that is connected to the ground.

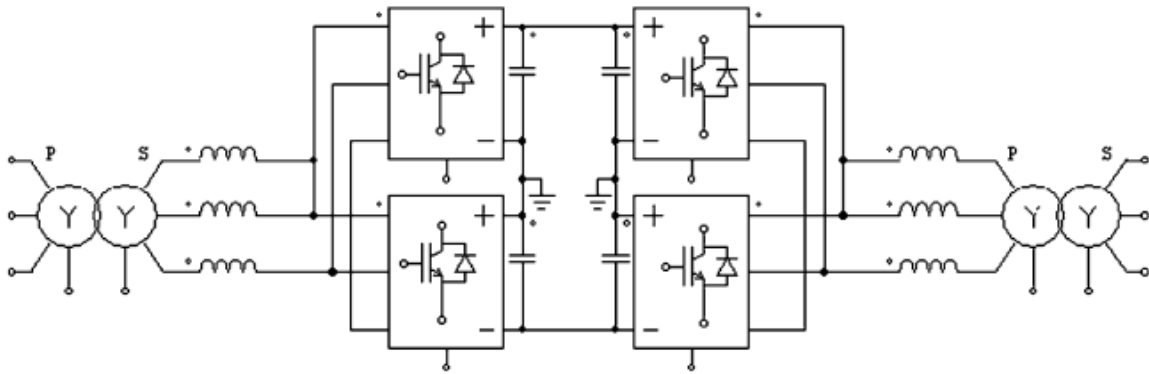


Figure 44 VSC based HVDC transmission system

The transformers onshore and offshore adapt their voltage level to the transmission line requirements while VSCs make the AC/DC conversion.

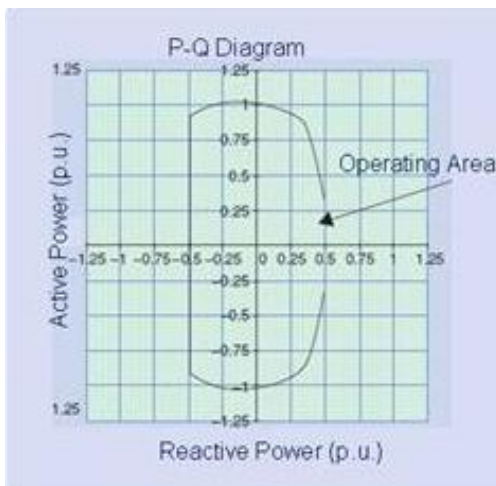


Figure 45 Active and reactive power operating range for VSCs

VSC based HVDC systems allow the active and reactive power supply to be controlled independently of each other at each end of the line (42). Thus, power transmission can be controlled with high flexibility. On the one hand, reactive power can be supplied at the offshore station for the Wind Turbine Generators, and it can also be supplied at the onshore stations to regulate the voltage. On the other hand, active power can be used to control the grid frequency, in case it is weak. Figure 45 shows the active and reactive power operating range of a VSC based HVDC system.

VSCs can start up against a nonloaded network because the current inside the converters can be switched off and thus active commutation voltage is not required. When the onshore grid has collapsed, the system can start by itself. The VSCs synthesize a balanced set of three phase voltages like a virtual synchronous generator (43).

A HVDC converter station with Voltage Source Converters is shown in Figure 46. This station has almost the same power rating than the one shown for the LCC based HVDC system, 550 MW instead of 600 MW, but the size is reduced by half. It only does 120 x 50 x 11 meters. Thus, offshore stations are more compact and take less space, and thus are less expensive. However, from now (41), the rating per converter is only 300 to 350 MW with cable ratings of 150 kV, 500 MW. Thus, for higher power transfers than 300 MW, several converter stations have to be connected. Figure 47 shows a 600 MW wind farm using two VSC.

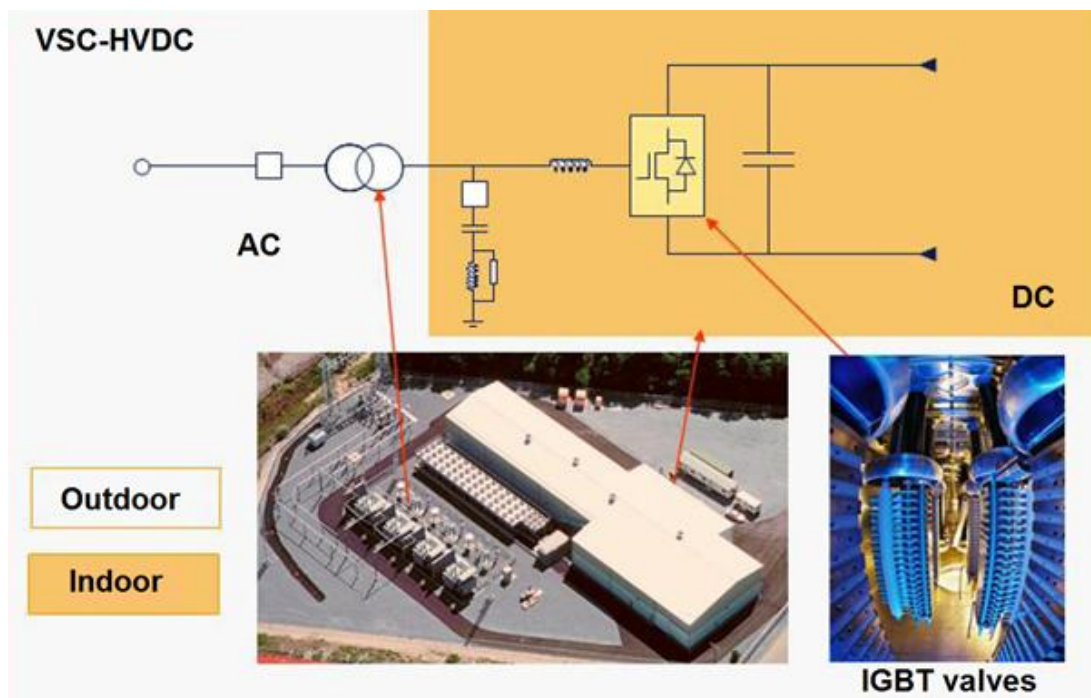


Figure 46 VSC based HVDC converter station

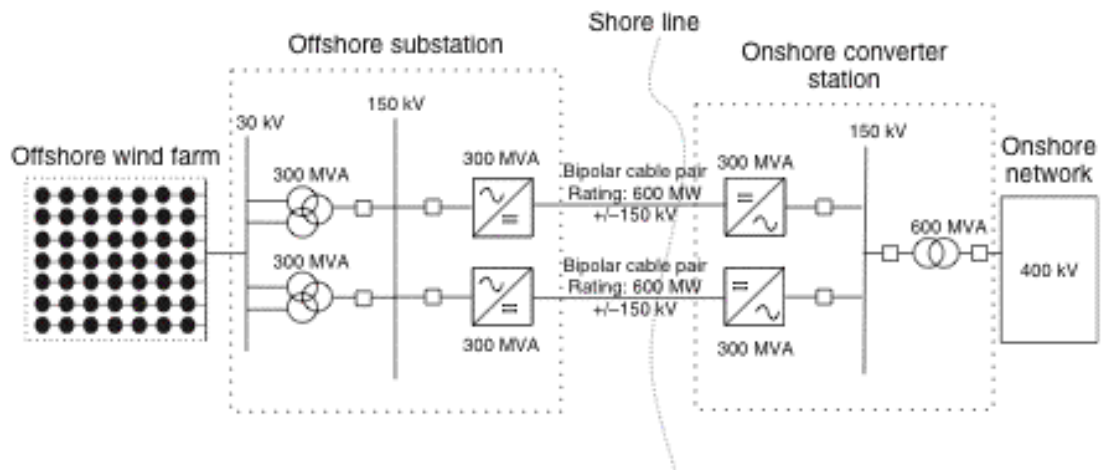


Figure 47 600 MW wind farm connected with VSC based HVDC

4.7 TRANSMISSION SYSTEMS COMPARISON

4.7.1 TECHNICAL COMPARISON

As presented before, the maximum rating of three-phase AC cables is 200 MW for a maximum distance of 200 km with a voltage level of 150-170 kV. For distances of less than 100 km, this rating can be improved to 350 MW at 245 kV. For VSC based HVDC, the rating of bipolar cables is 600 MW for any distance at a voltage level of 150 kV. However, converter stations are not able to transfer that amount of power, and their maximum rating is 350 MW. Thus, in order to use the full 600 MW cable, two converter stations are needed. Research is on the way for 500 MW converter stations (41). LCC based HVDC cables are limited to 1000 MW even though cable and converter ratings are not limiting factors. Table 4 (41) shows the number of cables required for different configurations. A higher number of cables imply higher costs but also better reliability. For VSC based HVDC, the power rating of the converter station is specified.

Table 4 Number of cables required for different configurations

Capacity (MW)	HVAC	LCC based HVDC		VSC based HVDC	
		150 kV, bipolar	450 kV, monopolar	150 kV, 300 MW	150 kV, 500 MW
300	2	1+1	1	1+1	1+1
500	3	2+2	1	2+2	1+1
900	5	4+4	2	3+3	2+2
1200	6	5+5	2	4+4	3+3

The power loss is often used as the main parameter to tell when switch to DC transmission. Figure 48 shows the power loss against the cable length, for HVAC, LCC based HVDC and VSC based HVDC.

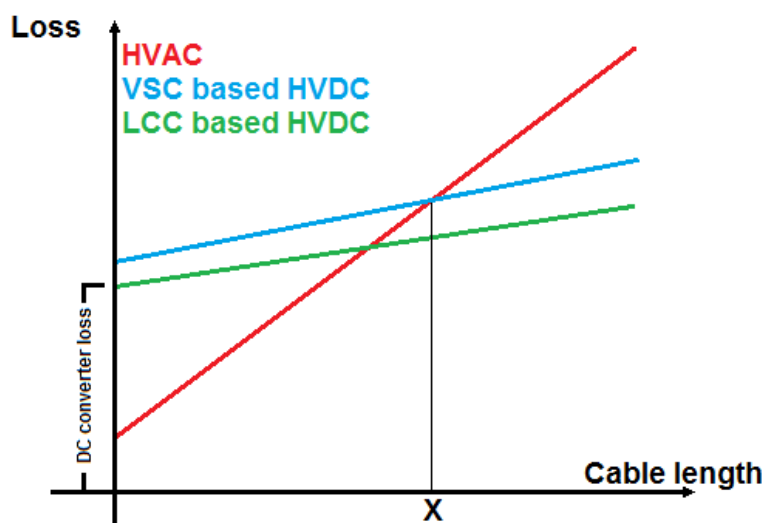


Figure 48 Loss against cable length comparison

For AC configurations, power losses increase significantly with distance, and thus depend on the length and on the cable characteristics. In HVDC transmission, there is a small correlation between the length of the cable and the loss. The main power loss is due to the efficiency of the converter station. As stated previously, VSC based HVDC converter stations are less efficient than LCC based HVDC ones. There is a distance called X on Figure 48 from which HVAC losses become higher than HVDC losses for the same transmission length. The value of X is not fixed and depends on the voltage levels and cable types. For the example of a 200 MW wind farm, X is approximately 100 km. Thus, for a distance over 100 km, the power loss is lower in the case of a VSC based HVDC transmission system than in the case of a HVAC one.

Offshore converter stations are expensive and require expertise to fit as much as possible in the transmission system. Generally, HVAC offshore stations are one third of the size of HVDC offshore stations. Even though LCC based HVDC converter stations have lower power loss than VSC based HVDC stations, their size is a lot larger as explained in Chapter 4.6. However, for power ratings above 300 MW, VSC based HVDC converter stations need to duplicate since 300 MW is their maximum rating. Thus, for 1000 MW wind farms, LCC based HVDC converter stations might take less space compared to multiple VSC converter stations.

The grid impact of the three transmission technologies presented is important regarding the expansion of offshore wind farms in the network. Large offshore wind farms represent a significant amount of energy for a region and it has to be operational at all time. New regulations are proposed, especially in Denmark and Germany where a lot of wind power is installed. The requirements for the onshore network to remain stable during faults is that wind farms will have to be able to reduce their output power to 20% of their rated capacity in 2 seconds in case of a fault. After the fault, the wind farm has to return to the prefault capacity in less than 30 seconds (41). HVDC transmission systems benefit more to the grid than HVAC transmission since they reduce the fault contribution to the onshore network. Upgrades of onshore transformers and switchgears are expensive but may not be necessary when using HVDC transmission. Moreover, VSC based HVDC can provide active and reactive power supply as well as voltage control which benefit to the grid. HVAC and LCC based HVDC can also do so, with the addition of SVC or STATCOM.

Table 5 is the summary of the technical comparison. The total system power losses is higher for LCC based HVDC if offshore ancillary services is required to meet the capability for network support of VSC based HVDC. The HVAC maximum capacity and voltage level for the latest XLPE cables can be up to 1000 MW for 420 kV according to ABB. This could increase the maximum ratings of the cables.

Table 5 Summary of the technical comparison

	HVAC	LCC based HVDC	VSC based HVDC
Maximum capacity	350 MW	1200 MW	500 MW
Maximum voltage level	245 kV	500 kV	150 kV
Transmission capacity depends on distance	Yes	No	No
Total system power losses	Depends on distance	2-3%	4-6%
Black-start capacity	Yes	No	Yes
Capability for network support	Limited	Limited	Wide
Offshore substations in operation	Yes	No	Planned
Space requirement of offshore substations	Small	Large	Medium

4.7.2 ECONOMICAL COMPARISON

This comparison relies on the technological developments at one time and further research in power electronics can change the results. Figure 49 (41) shows the most economical choice for a configuration depending on the transmission distance and the capacity of a wind farm.

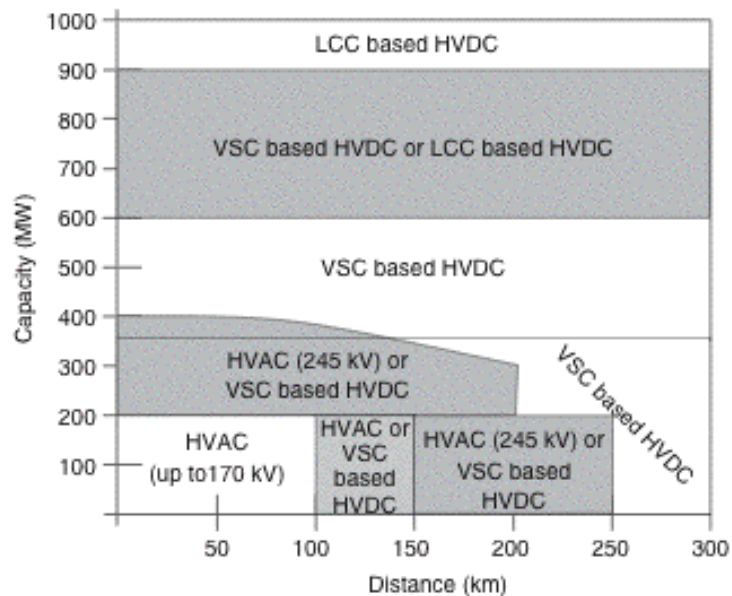


Figure 49 Choice of transmission technology depending on distance and capacity

For wind farms of a capacity less than 200 MW, the cost of three-core XLPE AC cable and the cost of a bipolar DC cable is the same, under 200 km. Though, the converter station for a VSC based HVDC transmission is 10 times higher compared to HVAC. For larger distances, the loss in the cable becomes too high for AC cables and it becomes economically less interesting compared to VSC based HVDC. However, HVAC is still feasible with compensation stations placed on the cable route on offshore platforms.

For wind farms of a capacity between 200 and 350 MW, HVAC transmission is ensured by two 150 kV three-core XLPE cables or one 250 kV three-core XLPE cable. With increasing distance up to 200 km, the use of HVAC is still possible, with a reduced maximum capacity of 300 MW. With such a capacity, it is possible to use VSC based HVDC instead of two AC cables.

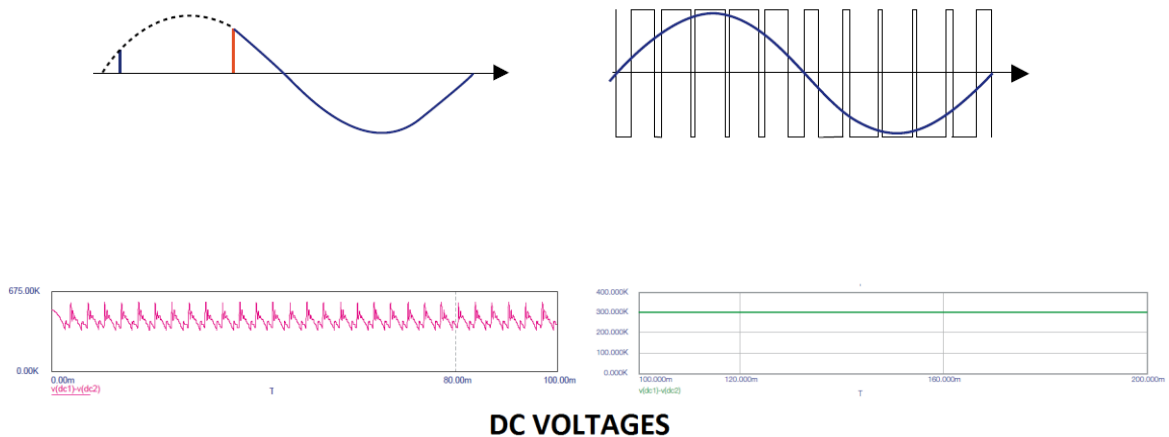
LCC based HVDC becomes interesting above 600 MW compared to VSC based HVDC. At this capacity, LCC based HVDC requires only one cable and one offshore converter station whereas VSC based HVDC needs two cables and at least three converter stations. However, even though is economically preferred, the benefit of having two cables is predominant, since if a fault occurs on the single DC cable of the LCC based HVDC system, then the whole offshore wind farm is disconnected, leading to a huge loss of power for the grid. It is still the case above 900 MW.

4.7.3 COMPARISON BETWEEN VSC AND LCC BASED HVDC

Table 6 shows the differences in the converters between LCC and VSC based HVDC technologies. For VSC based HVDC, the Pulse Width Modulation (PWM) controls both active and reactive power (44).

Table 6 Comparison between VSC and LCC based HVDC

LCC based HVDC	VSC based HVDC
Thyristors	IGBTs
Single silicon wafer	Multi-chip
Forward and reverse blocking capability	Forward blocking capability
Very high surge current capability	Current limiting characteristics
No gate turn-off	Gate turn-off fully controllable
Operate at 50-60 Hz	Operate at 2000 Hz
Power up to 6400 MW	Power up to 1100 MW



5 SIMULATION MODELS

5.1 SIMULATION TOOL

Several simulation tools are being used by the electrical engineering industry and research institutes. The most notable are PSS[®]E (Power System Simulator) from Siemens, PowerFactory from DigSILENT GmbH and SIMPOW from STRI AB. Those three simulation tools are more or less equivalent and provide the user with advanced and proven methods regarding power flow, fault analysis, dynamic simulations and planning of electrical power networks.

SINTEF, the largest independent research organisation in Scandinavia, has a large research centre in NTNU and thus can provide help to master students. The first choice for the simulations was to use PSS[®]E since SINTEF, Statnett (The Norwegian transmission system operator) and Statkraft (The main Norwegian energy producer) are using it. However, it was complicated to get help from the SINTEF department in relation with this subject and thus SIMPOW was chosen.

5.2 GRID MODEL

In order to study large scale integration of offshore wind farms, it is necessary to have a model of the grid to which the wind farms can be connected. As the study is made with Statnett, SINTEF and NTNU, the Scandinavian grid is considered. The Nordic grid model from NORDEL was presented in Chapter 1.4.2 in Figure 7. This model is complex since it is made of more than 2200 busses and it is not necessary for the simulations of this thesis to obtain such a degree of complexity. A simplified grid model was given by SINTEF in PSS[®]E and has been partly translated to SIMPOW thanks to the program PSSE2SIMPOW from STRI AB.

The Nordic grid model used in for the simulations is composed of 35 busses representing Norway and Sweden for the most, but also Finland and Denmark. Thus the entire Scandinavian system is taken into account. 13 geographical regions are considered such as Southern or West regions. There are 22 busses with a voltage level of 420 kV, 12 at 300 kV and one at 135 kV. This last one is the HVDC connection between Sweden and Denmark. Cross-Skagerrak, the connection between Norway and Denmark, and NorNed, the connection between Norway and the Netherlands, were presented in Chapter 1.5.1 but are not computed in the grid model.

Generators and loads that are part of the simple grid model can generate and absorb up to 5000 MW of active power and up to 1500 MVar of reactive power. This is due to aggregation of regions and it should not be considered as real power plants but as an equivalent system. However, the voltage at each bus is within the limits of the grid code. This code states that the voltage should be +/- 10% of the nominal value.

The grid model computed in SIMPOW is fully shown in Figure 50. Each country is represented schematically.

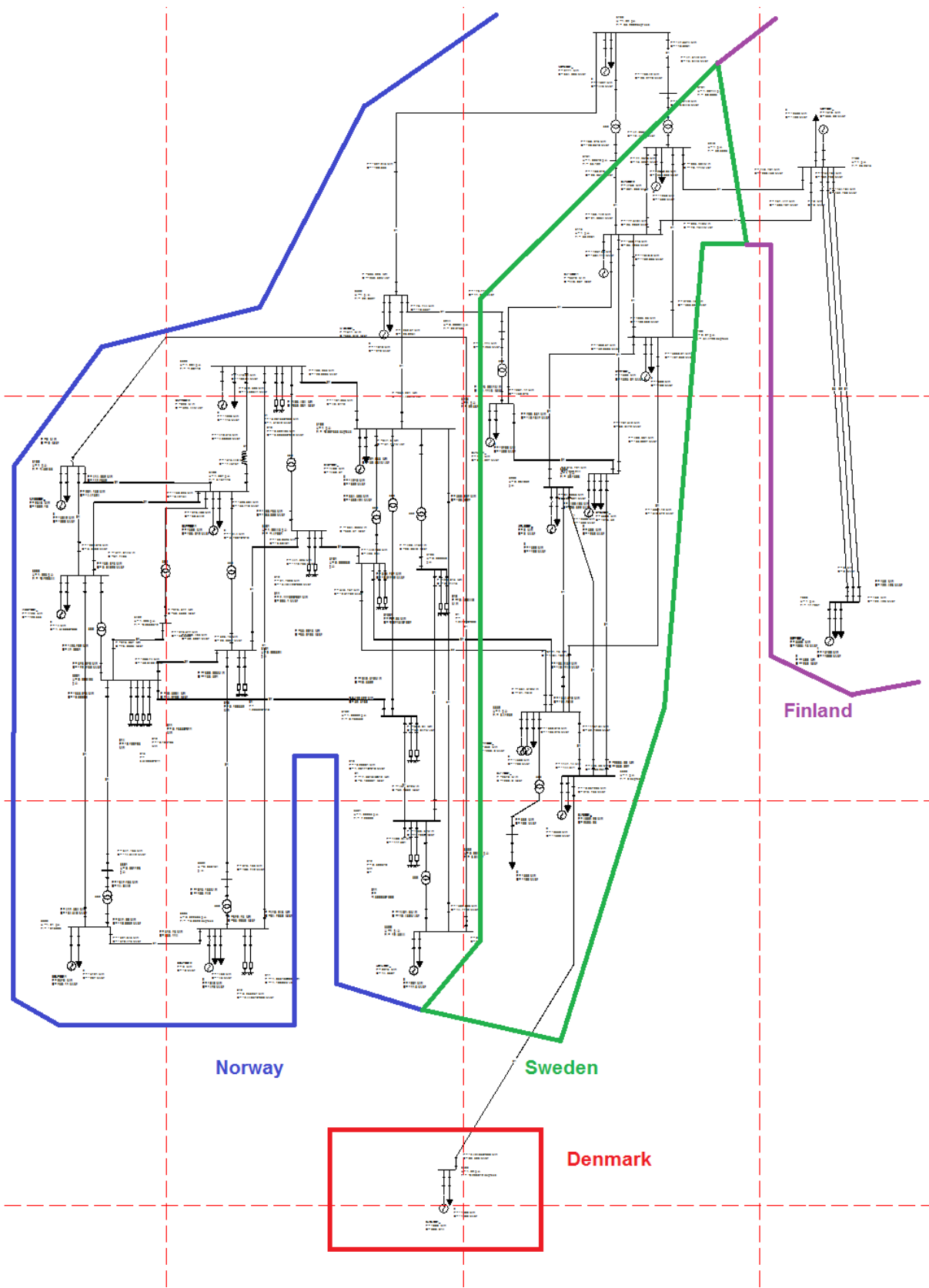


Figure 50 Grid model

The values of exportation and importation in MW and MVar of active and reactive power in the entire grid model are given in Table 7. In this case, Sweden completely exports active power to Denmark and Finland. On the overall, Sweden exports active power to Norway but on the north connection between the two countries, Norway provides active power to the Sweden grid. Denmark creates as much power as it needs but imports little reactive power.

Table 7 Grid model power exchange

Country	Productions and Network generation		Load absorbed and network losses	
	P (MW)	Q (Mvar)	P (MW)	Q (Mvar)
Norway	16306	4897,6	17159,7	4613,7
Sweden	24302,3	11117,4	21699,9	11186,6
Finland	6610	1671,2	8100	1650
Denmark	1000	909,6	1000	1000
Total	48218,3	18595,8	47959,6	18450,3

The total generated and consumed powers are not equal even though the entire system is stationary, because shunts and transmission losses are not accounted in Table 7. Shunt capacitors, shunt reactors and line reactors exchange rates are shown in Table 8.

Table 8 Grid model power exchange

	P (MW)	Q (Mvar)
Productions	48218,3	16411
Shunt capacitors	0	997,7
Network generation	-	3485,4
Total production	48218,3	20894,1
Load absorbed	47407,4	10115,3
Shunt reactors	0	969,1
Line reactors	0,6	0
Network losses	810,3	9809,7
Total load	48218,3	20894,1

The power flow between countries is depicted in Figure 51.

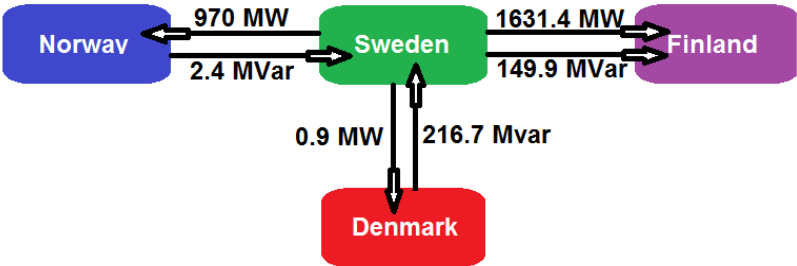


Figure 51 Grid model power flow

The grid model was already constructed in PSS®E but had to be translated into SIMPOW. Table 9 shows the parameters of the generators that are in the original case file. Each generator comprises a generator model, a turbine model, an excitation model and eventually a stabilizer model. The generators are different because they represent different type of generation for each region. Some regions are using thermal power plants and some other, mainly in Norway, incorporate hydro power plants. GENROU generators represent thermal plants and GENSAL hydro turbines.

Table 9 PSS®E generator models

Generator bus	Generator model	Turbine model	Excitation model	Stabilizer model
3300	GENROU	IEESGO	SCRX	STAB2A
3000	GENROU	IEESGO	IEEET2	STAB2A
3100	GENSAL	HYGOV	SCRX	
3115	GENSAL	HYGOV	SCRX	STAB2A
3200	Disconnected			
3245	GENSAL	HYGOV	SCRX	
3249	GENSAL	HYGOV	SCRX	
3359-1	GENSAL	HYGOV	SCRX	
3359-2	GENROU	IEESGO	SCRX	STAB2A
5100	GENSAL	HYGOV	SEXS	
5300	GENSAL	HYGOV	SCRX	STAB2A
5400	GENSAL	HYGOV	SEXS	
5500	GENSAL	HYGOV	SEXS	
5600	GENSAL	HYGOV	SCRX	
5603	Disconnected			
6000	GENSAL	HYGOV	SEXS	
6100	GENSAL	HYGOV	SCRX	STAB2A
6500	GENSAL	HYGOV	SEXS	
6700	GENSAL	HYGOV	SCRX	STAB2A
7000	GENROU	IEESGO	IEEET2	STAB2A
7100	GENSAL	HYGOV	SCRX	STAB2A
8500	GENROU	IEESGO	SCRX	STAB2A

Each of those models has equivalence in SIMPOW which is shown below.

5.2.1 GENROU GENERATOR MODEL

The model for thermal plants used in PSS®E is GENROU, which corresponds to a round-rotor generator model with quadratic saturation. The turbine and governor model is the IEEE Standard Model, called IEESGO in PSS®E. The equivalent in SIMPOW is the general steam turbine model ST2 along with the approximate speed-governing model SG3. Figure 52 (45) shows the turbine model in SIMPOW, Figure 53 (45) shows the governor model in SIMPOW and Figure 54 (46) shows the PSS®E model.

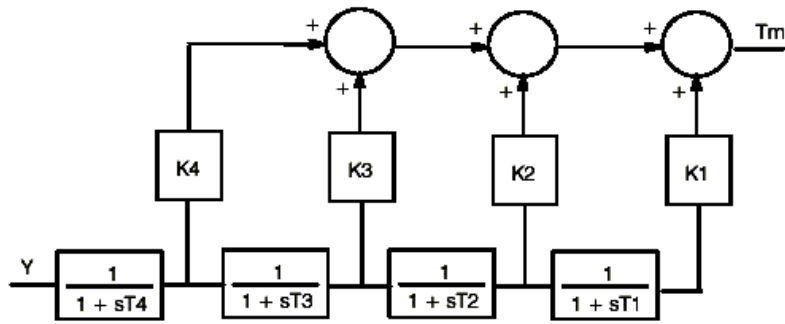


Figure 52 SIMPOW turbine model ST2

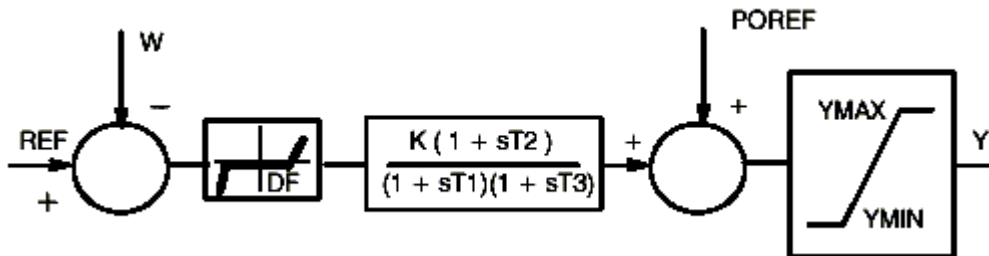


Figure 53 SIMPOW governor model SG3

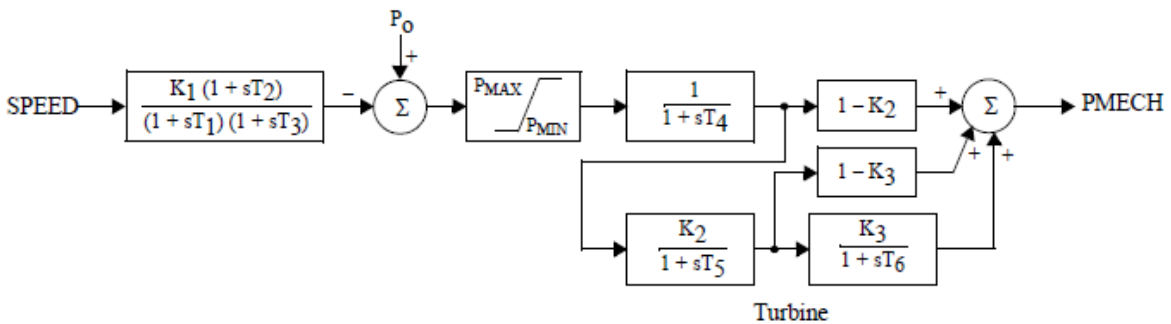


Figure 54 PSS®E turbine and generator model IESGO

Table 10 describes the parameters identification between the SIMPOW turbine model and the PSS®E one.

Table 10 Generator parameters identification

SIMPOW ST2	K1	T1	K2	T2	K3	T3	K4	T4
PSS®E IESGO	$K3 \cdot K2$	$T6$	$K2 \cdot (1 - K3)$	$T5$	$1 - K2$	$T4$	0	0

5.2.2 GENSAI GENERATOR MODEL

The model for hydropower plants used in PSS[®]E is GENSAI, which corresponds to a salient-pole generator model with quadratic saturation on d-axis. The turbine and governor model is the hydro turbine-governor model, called HYGOV in PSS[®]E. The equivalent in SIMPOW is the hydro turbine model HYTUR along with the hydro governor model HYGOV. Figure 55 (45) shows the turbine model in SIMPOW, Figure 56 (45) shows the governor model in SIMPOW and Figure 57 (46) shows the PSS[®]E model.

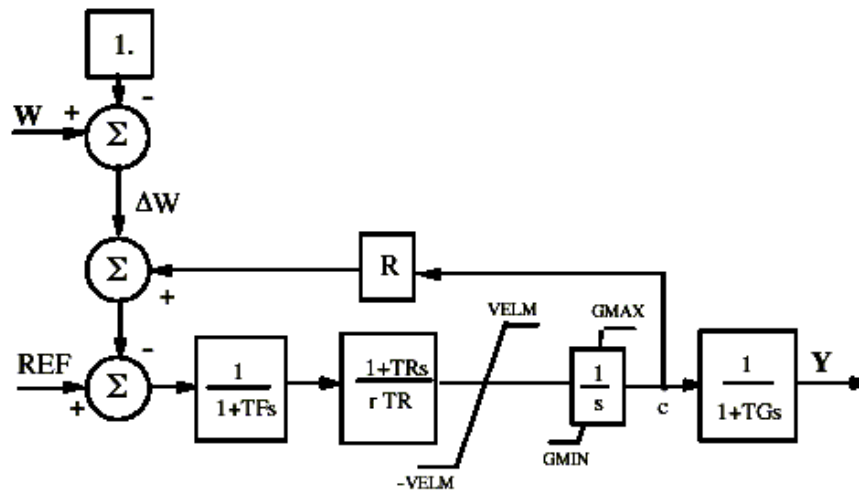


Figure 55 SIMPOW turbine model HYTUR

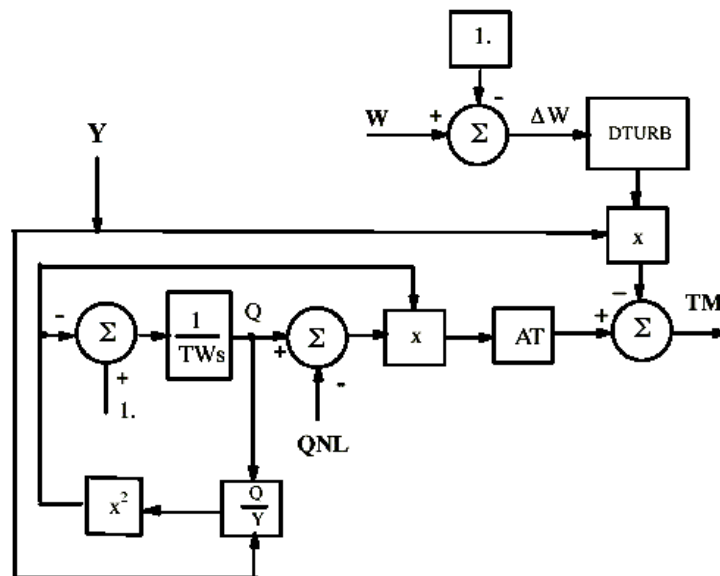


Figure 56 SIMPOW governor model HYGOV

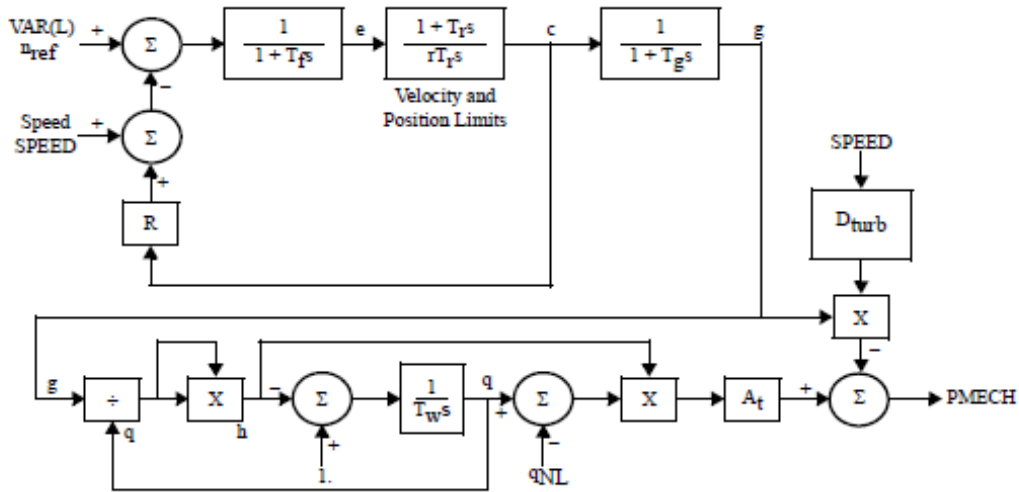


Figure 57 PSS®E turbine and generator model HYG0V

5.2.3 EXCITERS AND STABILIZERS

Three models of exciters are used in PSS®E for the grid model: SCR_X, SEXS and IEET2. Each of them is described below. SCR_X is a bus fed static exciter and corresponds to an excitation system with DC commutator exciter referred as type ST3 in SIMPOW. The SIMPOW model is shown in Figure 58 (45) and the PSS®E model is shown in Figure 59 (46).

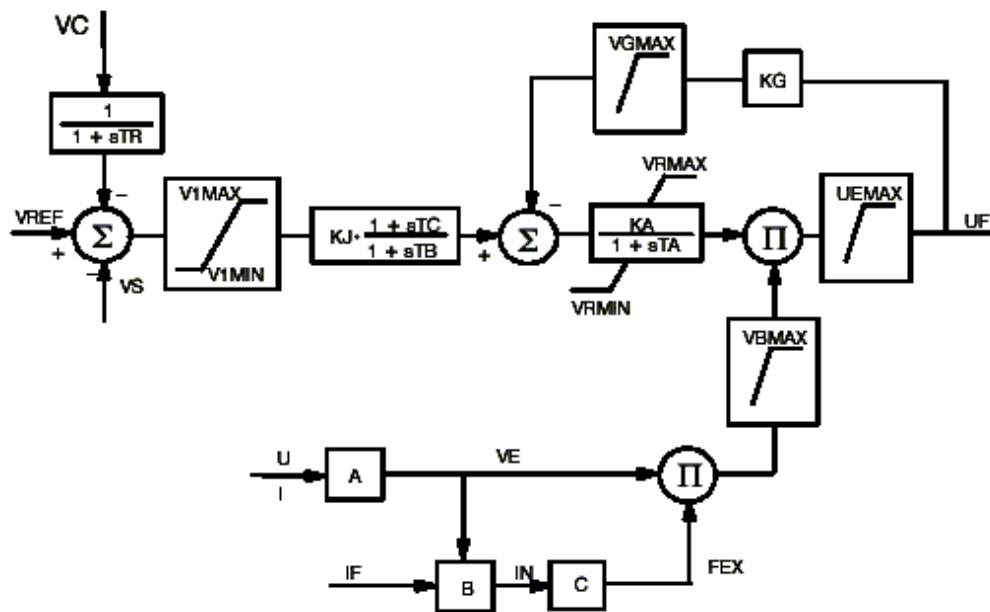


Figure 58 SIMPOW exciter model ST3

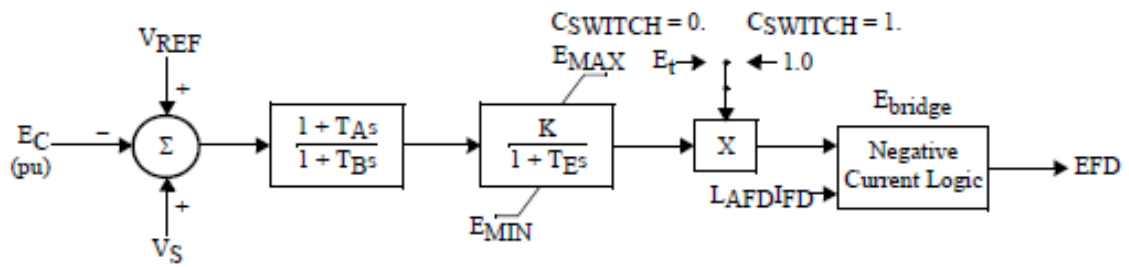


Figure 59 PSS®E exciter model SCRX

SEXS is a simplified excitation system and corresponds to an excitation system with potential source controlled rectifier exciter referred as type BBC1 in SIMPOW. The SIMPOW model is shown in Figure 60 (45) and the PSS®E model is shown in Figure 61 (46).

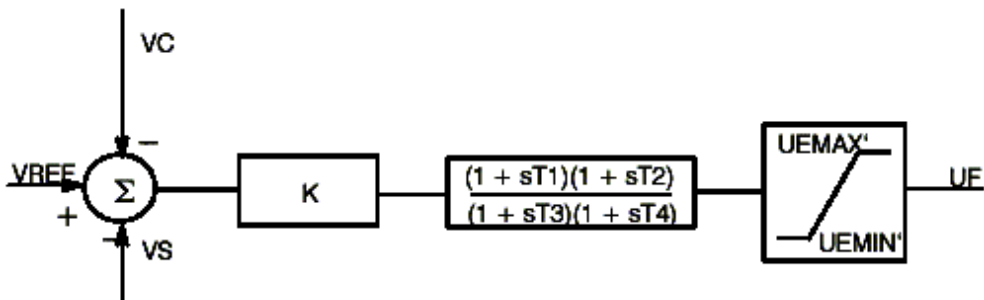


Figure 60 SIMPOW exciter model BBC1

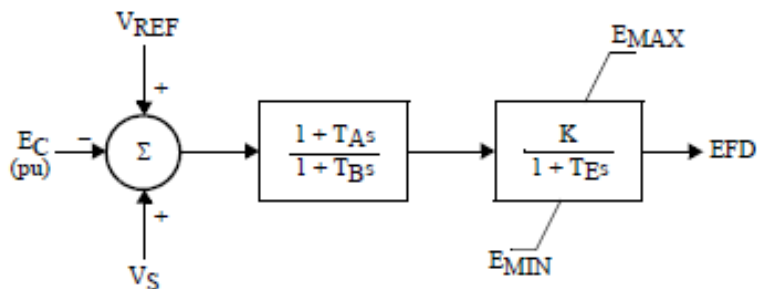


Figure 61 PSS®E exciter model SCRX

IEEET2 is IEEE type 2 excitation system and corresponds to the exact same termination in SIMPOW, as the name IEEEX2 suggests. The SIMPOW model is shown in Figure 62 (45) and the PSS®E model is shown in Figure 63 (46).

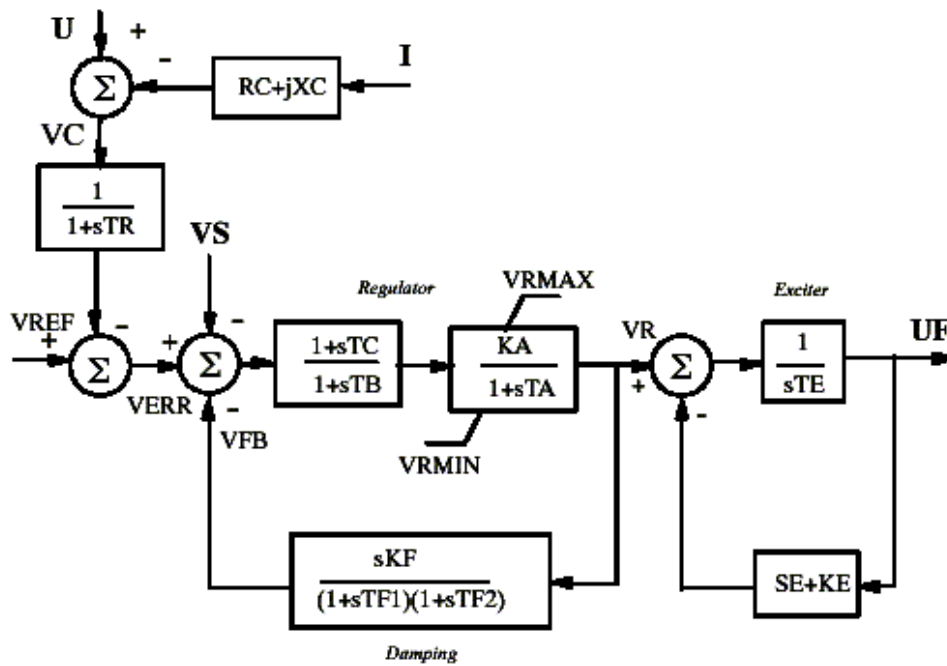


Figure 62 SIMPOW exciter model IEEEX2

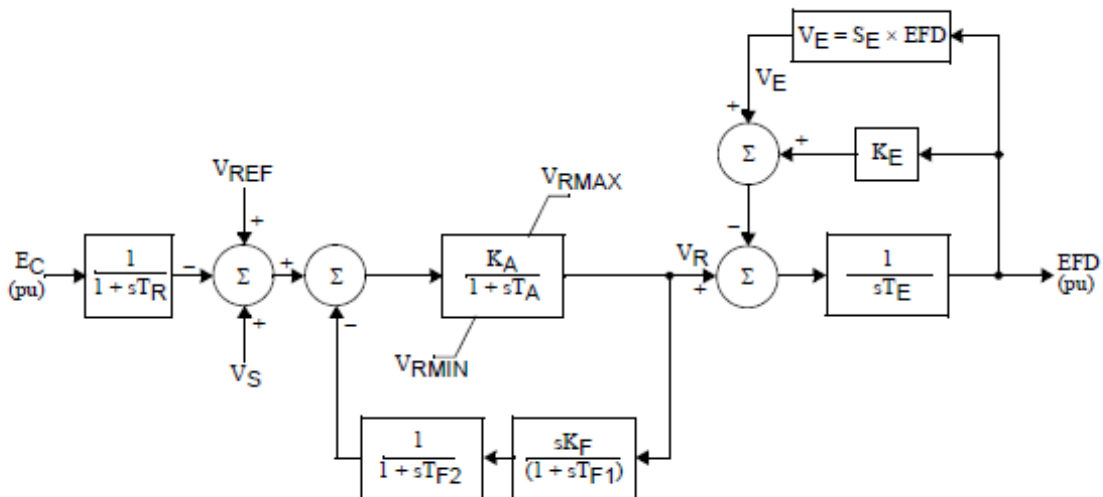


Figure 63 PSS®E exciter model IEEET2

The model used for the stabilizers in PSS[®]E is STAB2A, which corresponds to a power sensitive stabilizing unit (ASEA). The SIMPOW model has the same name. The SIMPOW model is shown in Figure 64 (45) and the PSS[®]E model is shown in Figure 65 (46).

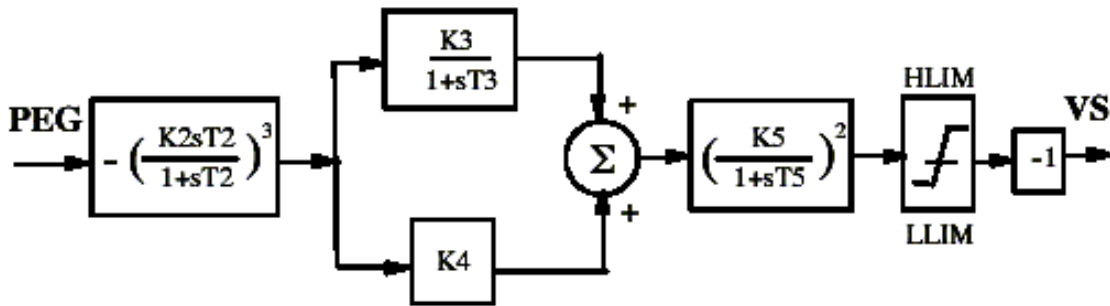


Figure 64 SIMPOW stabilizer model STAB2A

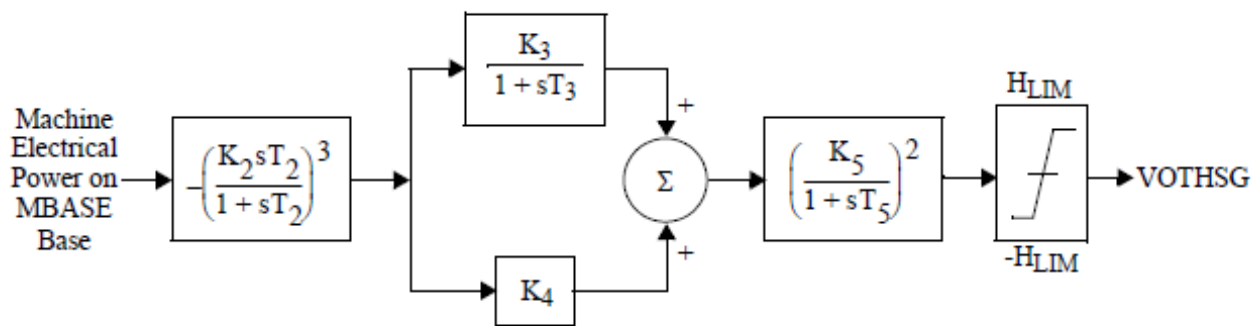


Figure 65 PSS[®]E stabilizer model STAB2A

5.2.4 POWER LINES

Lines in PSS[®]E are not always translated as a single line model in SIMPOW. Line type 13,14 and 15 are translated as lines type 12 in SIMPOW. The schematic representation of these types of lines is shown in Figure 66. As a result, the corresponding G1, B1, G2 and B2 are translated as two shunts impedances at each end of the line. Each shunt is either a pure reactance or a pure resistance. They are thus linked to the busses. Table 11 shows the shunt impedances that were added in order to match the lines in the PSS[®]E file.

At both ends of the line, the reactance value of the shunt capacitor, which symbolizes the susceptance of the line, is equal but the sign is different. Moreover, the resistance value of the shunt capacitor, which symbolizes the conductance of the line, is almost equal at each end of the line, but the sign is also different. Thus, half of shunt impedances have negative value, as if there was production of power. However, SIMPOW only translated what the PSS[®]E contained, and these negative impedances come from the PSS[®]E file. This is due to the PSS[®]E file being an aggregated and reduced model of a very complex one. Thus, in order to meet the production for every region, some lines had to fulfil the power flow and angle direction.

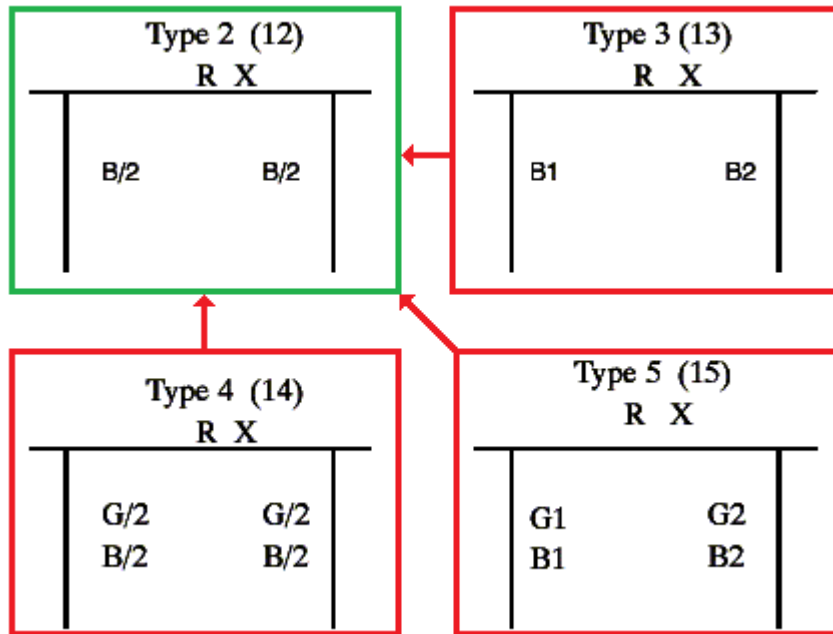


Figure 66 SIMPOW line types

TYPE=12 line is described with R, X and B. TYPE=13 line is described with R, X, B1 and B2. TYPE=14 line is described with R, X, G and B. TYPE=15 line is described with R, X, G1, G2, B1 and B2. R is the resistance, X is the reactance, G is the conductance and B is the susceptance. All values are given in per-unit of the line base power and the node base voltage (45).

Table 11 Shunt impedances

Bus A	R (Ω /phase)	X (Ω /phase)	Bus B	R (Ω /phase)	X (Ω /phase)
5101	0	181.034	5501	0	-181.034
	7910.31	0		-8166.67	0
5102	0	-0.176397E+07	6001	0	0.176397E+07
	882000	0		-882000	0
5103	0	13889.8	5301	0	-13889.8
	441000	0		-588000	0
5401	0	352800	6001	0	-352800
	-882000	0		882000	0
5500	0	-69230.8	5603	0	69230.8
	300000	0		-300000	0

5.3 WIND FARM MODEL

Large scale wind farm of a rated power of 1000 MW require more than 340 turbines for the latest models used on the market (47) and can be up to 500 turbines for regular models. To study such a big farm in an easier but still accurate way, an aggregated model is proposed. Representing each wind generator in the model increases to a high extend the calculation time of dynamic simulations. Thus, the entire offshore wind park is modelled by a single equivalent wind generator.

Among the four classes of wind turbines generators described in Chapter 2.3, the two most widely used nowadays are class C and D. Both models of Doubly-Fed Induction Generators (DFIG) and Full Power Converter Wind Turbines (FPCWT) are available in SIMPOW. In this type of variable-speed generators, the active power is controlled by fast power electronics converters, in order to reduce the impact of wind-fluctuations to the grid. The frequency converters with two PWM-converters of DFIGs and FPCWTs are similar.

In this study, the simulations are considered over a short period of time as it is transient stability analysis. As a result, wind speeds and mechanical speeds are assumed to be almost equal and aggregation of the generators and the mechanical model of variable-speed wind generators are possible (48). Even if full aggregation is easier, a good compromise between accuracy and calculation speed is to aggregate only the electrical system and then to model the mechanical system of each turbine. As the wind farm studied is of 1000 MW, a full aggregation is made and gives sufficient results for the studied cases (48).

Vestas Wind Systems A/S is the largest wind turbine manufacturer in the world and its latest research technology is the V112 (47). Its rated power is 3 MW and it uses a full-scale converter with a permanent magnet generator. In order to study large scale integration of possible future wind farms, such a modern wind turbine is taken into account. Thus, the Full Power Converter Wind Turbine model from SIMPOW is used. The main difference with a DFIG is that the generator is a synchronous machine. The generator terminals are connected to the grid through a frequency converter which consists of a PWM rectifier, an intermediate DC system and a PWM inverter. Figure 67 shows the SIMPOW model.

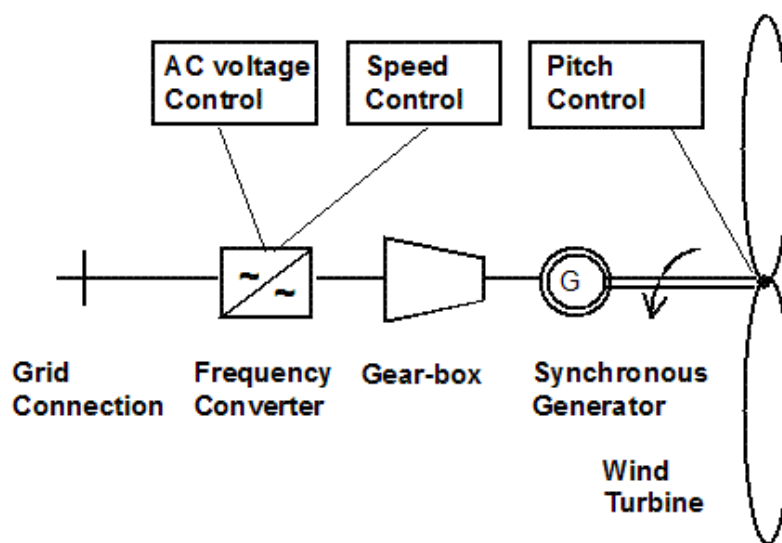


Figure 67 Full Power Converter Wind Turbine model

The values of the parameters used in the 1000 MW (1060 MVA) wind farm aggregated model are computed in Table 12. The aggregation consists of 518 wind turbines.

Table 12 FPCWT data

Wind turbine	
FPCWT rated power (MVA)	2,05
Air density (kg/m ³)	1,2
FPCWT blade length (m)	36
Nominal wind turbine speed (rpm)	23,4
Generator type	One field winding, one damper winding in d-axis, one damper winding in q-axis, saturation excluded
Inertia constant (MVA)	5,5
Stator resistance (p.u.)	0,0025
Stator leakage reactance (p.u.)	0,14
Direct-axis synchronous reactance (p.u.)	1,9
Quadrature-axis synchronous reactance (p.u.)	1,6
Direct-axis transient reactance (p.u.)	0,32
Direct-axis subtransient reactance (p.u.)	0,2
Quadrature-axis subtransient reactance (p.u.)	0,21
Direct-axis transient open-circuit time constant (s)	5
Direct-axis subtransient open-circuit time constant (s)	0,03
Quadrature-axis subtransient open-circuit time constant (s)	0,07
Pitch control	
Gain factor	60
Gain factor in integration	3
Gain factor for speed deviation	20
Gain factor in integration of speed deviation	20
Filter time constant	0,3
Maximum blade angle (deg)	27
Minimum blade angle (deg)	0
Maximum derivative of the blade angle	4
Minimum derivative of the blade angle	-4
Transformer	
Short circuit resistance between winding 1 and 2 (p.u.)	0,0032
Short circuit reactance between winding 1 and 2 (p.u.)	0,0599
DC capacitor	
Time constant (ms)	14,6
Rectifier and inverter	
Series reactance in p.u. of converter base	0,3
No-load losses in p.u. of converter base	0,02
Rectifier Active power (MW)	1000
Inverter DC voltage (kV)	5

In order to perform an aggregation in SIMPOW with the FPCWT model, the parameters listed below are the most relevant and must be taken care of. Most of the data of the wind turbine model is in per-unit and thus, they are taken care automatically by the simulation tool when increasing the rated base power. However, as stated in the help manual (45) under “Modelling of the wind turbine”, in *Full Power Converter Wind Turbine* chapter, the sweep area and the turbine nominal speed have to be correct in order to use the default C_p/λ curves.

OPTPOW parameters (Power flow)

- SN**: base power in MVA
- ORDER**, in the FPCWT_REC (rectifier): set value for the active power in MW

DYNPOW parameters (Dynamic simulations)

- NOM_TURBSPEED**: nominal angular speed of the wind turbine in rpm
- BLADELENGTH**: length of the blades in m

The sweep area is related to the blade length and thus, in order to use the default C_p/λ curves, it is possible to specify that the blade length and the nominal turbine speed are null. As a result, SIMPOW will automatically consider the aggregation, taking the base power and the active power as the only input parameters.

Scaling up the wind farm also implies with the FPCWT available from SIMPOW that the initial wind speed increases. Table 13 shows how the initial speed grows up with an increased value of power.

Table 13 Initial speed

ORDER	SN	NOM_TURBSPEED	Initial speed	BLADELENGTH
0.91	2.05	18	9.044724	36
3	3.2	12.5	10.1955	54.65
5	5.3	14.1	11.396485	59.7
50	53	0	11.56960	0
250	265	0	11.569607	0

This initial speed should not be mixed up with the speed given to the wind curve. It is possible to enter any value of the wind speed but for the 1 ms, the speed is constant and is given a specific value by SIMPOW which can't be changed from now, even by redesigning the parameters.

This phenomenon is depicted in Figure 68. The wind speed is set to be constant during the entire simulation (100 s), to the value of 10 m/s. During the first millisecond, the speed is equal to a value above 11.5 and then drops all of a sudden to 10 m/s. This sudden drop induces a real perturbation on the wind turbine simulation since all the parameters (torque, power, etc.) are calculated in pre-simulation, and thus before the first millisecond. The consequence on the torque is shown in Figure 69. It can be seen that the torque also drops at the beginning and then stabilizes after 40 seconds.

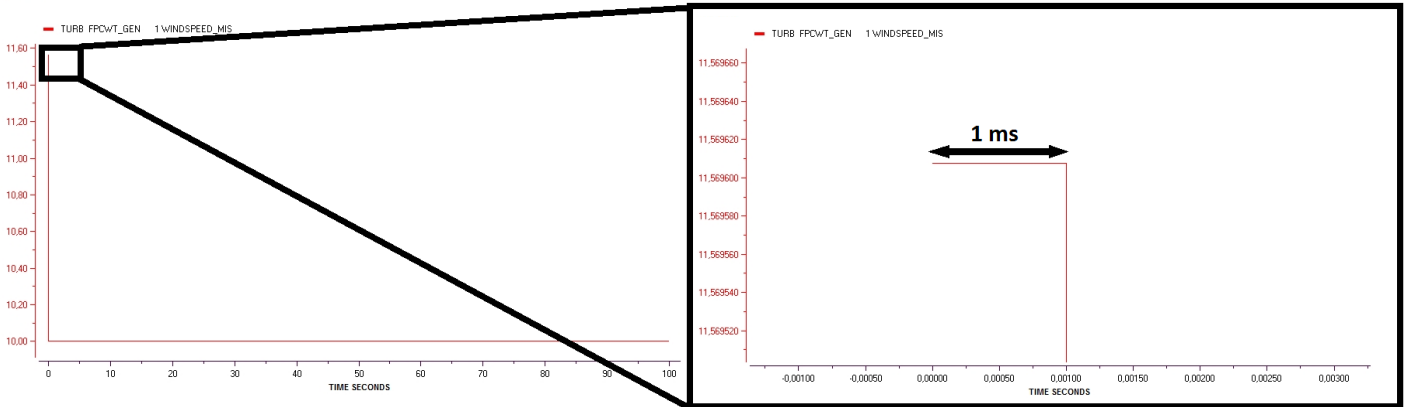


Figure 68 Initial speed drop

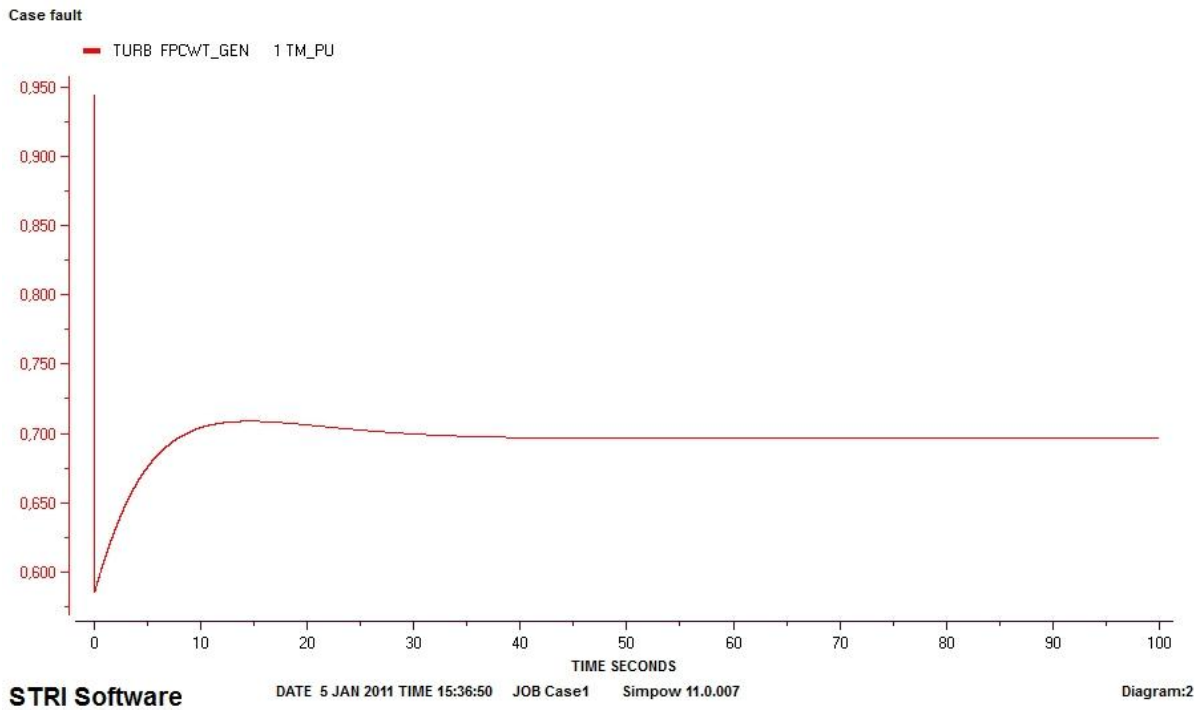
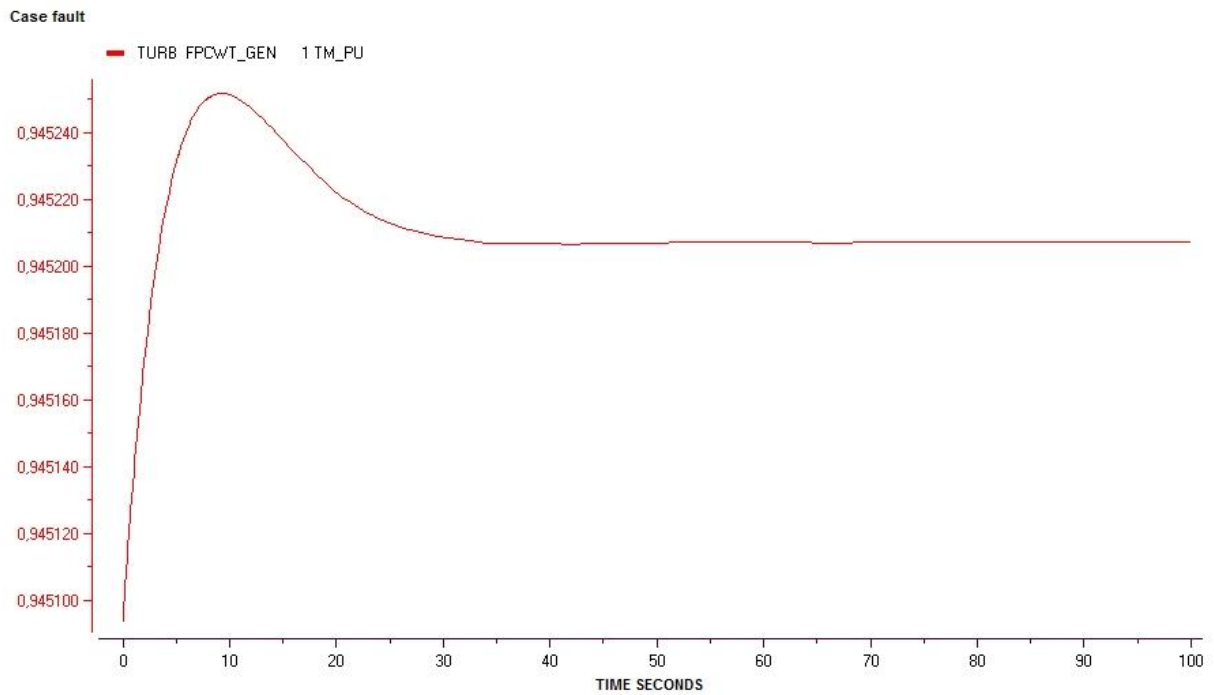


Figure 69 Initial torque drop

The torque is given in per-unit and starts at approximately 0.95 p.u. and drops to 0.7 p.u. This is a huge change that is not desirable for the wind farm simulations. To avoid this phenomenon, the wind curve initial value can be set to the initial value we observe. The maximum precision obtainable with the SIMPOW plotting tool is $1 \cdot 10^{-15}$. As a result the value is 11.569607734680176 m/s.

The torque is again plotted in Figure 70 with the speed given above. There is still a change but it will be neglected compared to the perturbations made in the simulations. The change here is 0.00014 p.u.



STRI Software

DATE 5 JAN 2011 TIME 15:31:09 JOB Case1 Simpov 11.0.007

Diagram:5

Figure 70 Initial torque change

5.4 HVAC CONFIGURATION

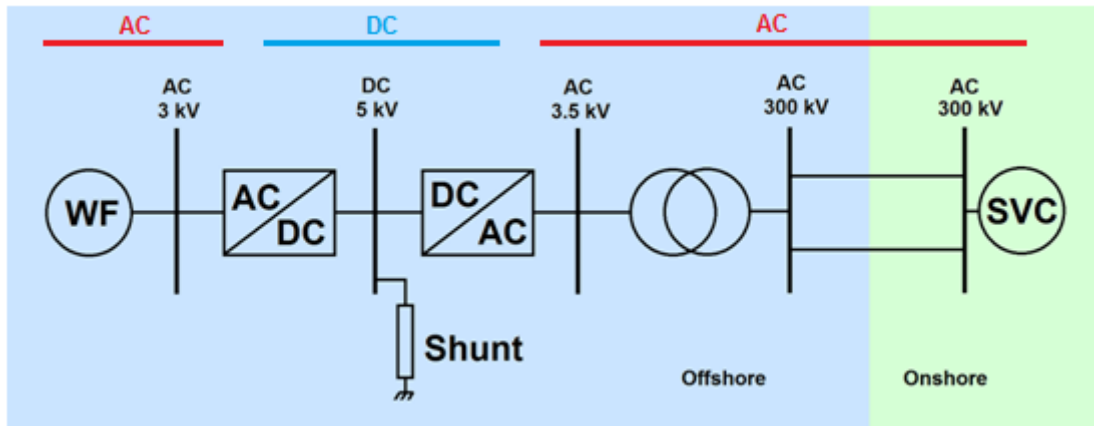


Figure 71 HVAC configuration

HVAC is the simplest and most reliable configuration for short distances. The distance of the wind farm from the shore is considered here to be 50 km which is often the case for offshore wind farms. The wind farm capacity is 1060 MVA, with a production of 1000 MW. The configuration with rectifier, shunt capacitor and inverter is shown in Figure 71.

Exactly one production source acting as a swing bus must be given in each AC network, as the voltage and the phase angle are used as calculation start values (45). As there are two separated AC network, two swing busses are implemented: the wind farm equivalent generator and bus 3300, located far from the onshore connection point. It ensures that there is sufficient influence of the wind farm on the network.

The model used for the cable is a PI-link which corresponds to the connection of two AC nodes with a resistance and a reactance in series and a susceptance at each end of the line. It is the TYPE 2 SIMPOW model and it is shown in Figure 72. Data are given in Ohms and Siemens per kilometre.

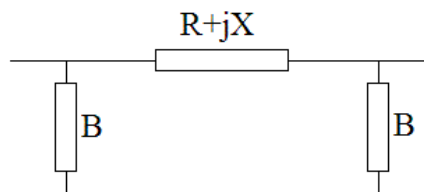


Figure 72 PI-link model

The parameters are chosen according to the manufacturer ABB (49). The cable chosen are three-core XLPE submarine cables with lead sheath. The conductor is made in copper. For a rated power of 1000 MW with 300 kV, the rated current is equal to 1170 A. Copper conductor cross-sections for submarine XLPE cables are limited to 1000 mm² which corresponds to a maximum current of 825 A. Thus, two cables with cross-sections of 500 mm² are able to transmit 655 A each, which is sufficient. For a maximum voltage of 300 kV, the parameters of the chosen cable are shown in Table 14.

Table 14 Chosen XLPE cable data

Cross-section of conductor	Diameter of conductor	Insulation thickness	Diameter over insulation	Lead sheath thickness	Outer diameter of cable	Cable weight (Aluminium)	Cable weight (Copper)	Capacitance	Charging current per phase at 50 Hz	Inductance
mm ²	mm	mm	mm	mm	mm	kg/m	kg/m	µF/km	A/km	mH/km
500	26.2	26.0	81.6	2.9	229.0	75.3	84.7	0.14	6.8	0.44

The resistance R of the cable is calculated with the formula $R = \frac{\rho \cdot L}{S}$ where ρ is copper resistivity, L the cable length and S the cross-section area. The susceptance is calculated using the formula $B = \omega \cdot C$ where ω is the angular frequency at 50 Hz and C is the capacitance. With requested units, the cable data used in SIMPOW are:

$$R= 0.034 [\Omega/\text{km}] \quad X=0.1382 [\Omega/\text{km}] \quad B=0.0000438 [\text{S}/\text{km}] \quad L=50 [\text{km}]$$

As stated previously, it is important for voltage stability and reactive power correction to implement a Static Var Compensator. The inverter of the FPCWT is trying to keep the voltage of the AC node it is connected to as closed to its rated value as possible. By doing so, it sets the required reactive power needed by the wind farm. Moreover, the 50 km HVAC cables also increase the demand for reactive power.

The SVC is connected on the grid bus, as closed as possible to where the reactive power is needed. The equations below are solved in order to calculate the rating of the SVC. The Nordic Grid Code imposes the power factor to be higher than 0.95. The power output of the wind farm is 954.5 MW, after the step-up transformer. Thus, the value of the maximum reactive power compensation Q_{SVC} is calculated.

$$P = UI \cos(\varphi)$$

$$Q = UI \sin(\varphi)$$

$$Q_{SVC \max} = P \cdot \tan(\arccos(\varphi)) = 954.5 * \tan(\arccos(0.95)) = 313.7 \text{ MVar}$$

The maximum value of the SVC is set to 320 MVar but the actual value can be lower if reactive power is already taken into account by the bus generator. The model used in SIMPOW is a Symmetrical SVC with proportional-integral regulator. Its block diagram is shown in Figure 73. The values of the parameters of the SVC are shown in Table 15.

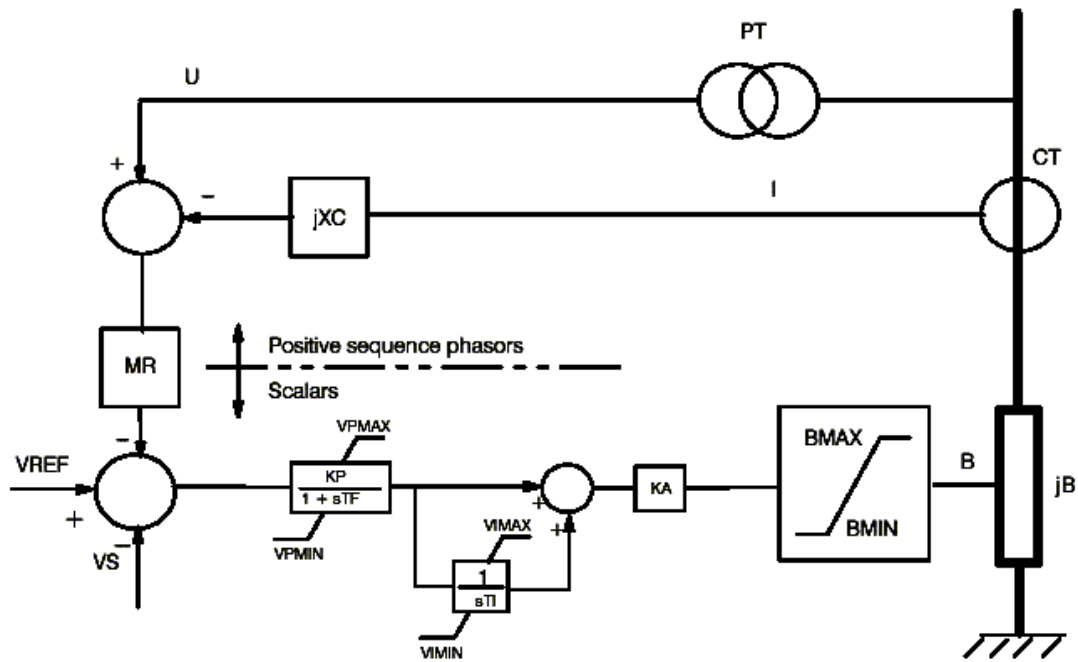


Figure 73 Symmetrical SVC with proportional-integral regulator

Table 15 SVC parameters

Parameter	Value
Proportional gain (p.u.)	15
Filter time constant (s)	0,02
Maximum value of VP	2
Minimum value of VP	-2
Adaptation gain (p.u.)	30
Maximum value of VI	0,1
Minimum value of VI	0
Maximum reactive power absorbed (Mvar)	320
Minimum reactive power absorbed (Mvar)	-320

5.5 HVDC CONFIGURATION

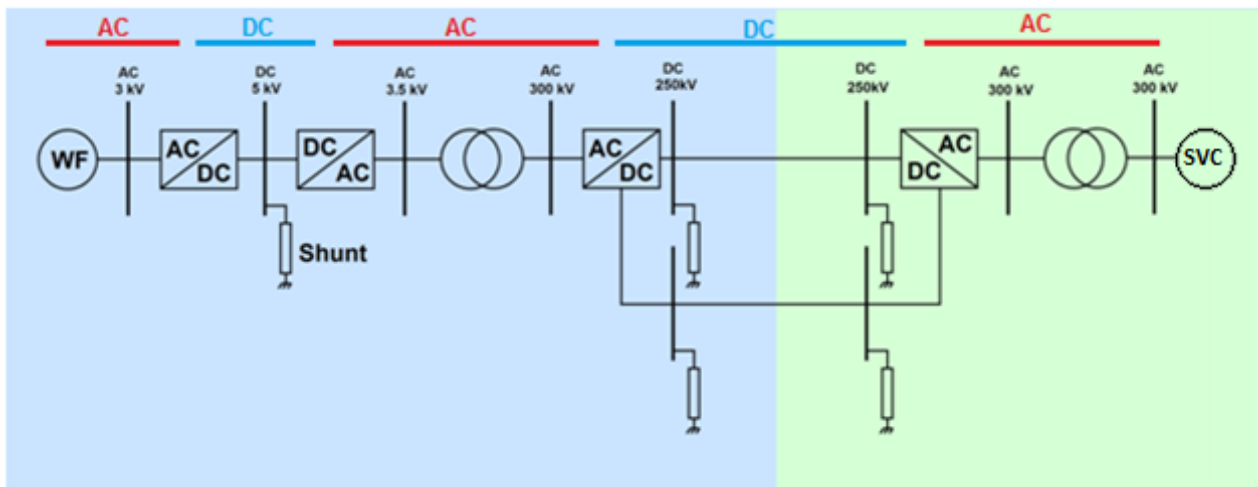


Figure 74 HVDC configuration

HVDC is used for relatively long transmission distances compared to HVAC since losses and total cost become more interesting past a certain distance, based on total capacity. Since VSC-HVDC is a growing field, it may be used for such high power applications for future projects. The choice has been made to use HVDC Light from ABB. The distance of the wind farm from the shore is considered here to be 100 km which is twice the distance considered for the HVAC case. The wind farm capacity is 1060 MVA, with a production of 1000 MW. The configuration with FPCWT and HVDC Light is shown in Figure 74.

Exactly one production source acting as a swing bus must be given in each AC network, as the voltage and the phase angle are used as calculation start values (45). In the HVDC configuration, three AC networks are connected through two DC systems. Thus, it requires three swing busses: the wind farm generator, bus 3300 which is located onshore and a new swing bus.

This new swing bus has to be created in the intermediate AC network where the first transformer operates. Even if in reality such a swing bus does not exist, it has to be created to perform the simulations. It was thus added to the 3.5 kV node via an AC line. It has to be noted that a particular specification needs to be entered for the line linking this swing bus in order to have the system working. The connection specification in the datagroup "LINES" is the parameter NCON. The default value (connected) is NCON=0. Default parameters don't need to be written and are taken care automatically by the software. However, the parameter NCON=0 has to be explicitly written in the code or there won't be any convergence. Another solution is to call the parameter ICPV in datagroup "CONTROL DATA", and to set it to 4.

Figure 75 presents the HVDC Light module from ABB, available in SIMPOW. It consists of four modules: a converter transformer model, a PWM converter model, shunt DC capacitors and DC cables. Each PWM converter consists of an AC filter, a series reactor and a converter. The first PWM converter is the one on the wind farm side and its control strategy is: active power control and reactive power control. The second PWM converter located on the grid side has the following control strategy: DC voltage control and AC voltage control. Converter data is found in Table 17.

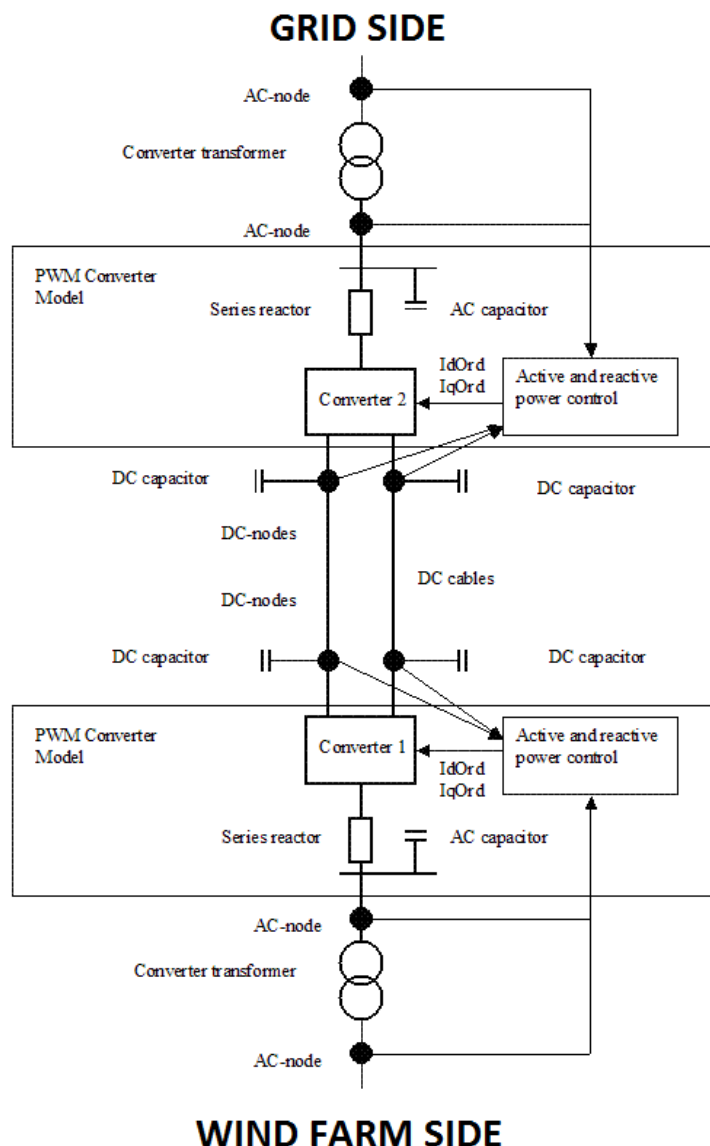


Figure 75 ABB HVDC Light Open Model Version 1.1.6

The line is modelled by a simple DC cable with resistance and inductance. ABB offers three modules depending on the base voltage: 80 kV, 150 kV and 300 kV. Thus, the 300 kV cable bipole in moderate climate is used. The climate influences the amount of power that can be transferred since the soil temperature and thermal resistivity decrease the efficiency. Table 16 shows the cable ratings from ABB (50).

The resistance R of the cable is calculated with the formula $R = \frac{\rho \cdot L}{S}$ where ρ is copper resistivity, L the cable length and S the cross-section area. A 1600 mm² conductor area is chosen.

$$R=0.0105 \text{ } [\Omega/\text{km}] \quad X=0 \text{ } [\Omega/\text{km}] \quad L=100 \text{ } [\text{km}]$$

The DC cable capacitance is merged with the DC capacitors (45). The size of the DC capacitors is obtained with the sum of all the DC capacitances divided by four for symmetrical reasons. It can also be chosen according to the DC time constant.

A reasonable value for the time constant is 15 ms (45). The formula below links the time constant T with the DC capacitance C, the nominal DC voltage U_{DC} and the nominal DC power P_{DC} .

$$T = 4 * \frac{1}{2} * \frac{C * U_{DC}^2}{P_{DC}} \quad \text{and thus} \quad C = \frac{2 * T * P_{DC}}{4 * U_{DC}^2} = 1.2 \times 10^{-4} F$$

The active power reference P_{REF} has to be chosen for the first PWM converter. The no-load losses of the converters of the FPCWT are given by the coefficient 0.02 (Table 12 – FPCWT Data). Thus, for a 1060 MVA aggregated wind turbine, the losses are:

$$P_L = 0.02 * 1060 * 2 \text{ (two converters)} \quad \text{and thus} \quad P_L = 42.4 MW$$

As a result, the output power of the FPCWT is:

$$P = 1000 - 42.4 = 957.6 MW$$

This sets the active power reference in p.u. of the converter base to:

$$P_{REF} = \frac{957.6}{1060} = 0.903396$$

Table 16 HVDC Light cable ratings

Area	Ampacity		150 kV cable bipole				300 kV cable bipole			
	Conductor	Close laying	Spaced laying	Close laying	Spaced laying	Weight per cable	Outer cable diam.	Close laying	Spaced laying	Weight per cable
mm ²	A	A	MW	MW	kg/m	mm	MW	MW	kg/m	mm
1200	1458	1791	437	537	29	100	875	1 075	40	126
1400	1594	1962	478	589	32	103	956	1 177	43	130
1600	1720	2123	516	637	35	107	1 032	1 274	47	133
1800	1830	2265	549	680	38	110	1 098	1 359	50	137
2000	1953	2407	586	722	41	113	1 172	1 444	53	140
2200	2062	2540	619	762	45	118	1 237	1 524	58	145

Table 17 PWM converters data

Parameters	PWM 1	PWM 2
Rated power (MVA)	1060	1060
Rated voltage (kV)	300	300
AC filter (S)	1,50E-03	1,50E-03
Series reactance (p.u.)	0,15	0,15
Nominal total losses (p.u.)	0,0165	0,0165
Part of the losses that are no-load (p.u.)	0,3	0,3
First control	Active power control	DC voltage control
Second control	Reactive power control	AC voltage control
AC voltage reference (p.u.)	1	1
Reactive power reference (p.u.)	0	0
Active power reference (p.u.)	0,903396	-

6 LOAD FLOW

6.1 INITIAL POWER FLOW

Table 18 Initial power flow

BUS	U (p.u.)	U (kV)	Fl(u) (°)	Pgen (MW)	Qgen (MVar)
3000	1	420	30,1386	5300	1276,32
3100	0,97	407,4	34,4729	1500	1323,91
3115	1	420	60,2281	3570	446,937
3200	0,964952	405,28	4,28289	-500	-100
3244	0,99984	299,952	22,2758		
3245	1	420	22,367	780	987,927
3249	1	420	59,3385	4750	901,069
3300	1	420	0	4902,28	2593,95
3359	1	420	6,41252	3500	2419,6
3360	0,99455	134,264	6,04957		
3701	1,00747	302,242	60,6685		
5100	1	300	-0,897533	1480	1408,97
5101	0,989859	415,741	0,255727		
5102	1,00002	420,01	0,760339		
5103	0,998059	419,185	1,56563		
5300	1	300	12,5044	2275	14,9587
5301	1,00063	420,265	7,28899		
5400	1,007	302,1	0,167178	1588	106,812
5401	0,996324	418,456	-2,0789		
5402	1,006	422,519	-0,0659512		
5500	1,004	301,2	-1,80119	828	-523,44
5501	1,00445	421,87	-1,47001		
5600	1,01	303	-9,15986	2378	750,11
5601	0,991126	416,273	-8,8728		
5602	0,956161	401,588	-11,7764		
5603	0,922383	276,715	-13,0629		
6000	1,005	301,5	-0,729344	1129	-129,353
6001	0,999483	419,783	-1,22774		
6100	1	300	-4,58435	2346	1002,18
6500	1	300	22,0527	1511	565,949
6700	1,02	306	63,2992	2771	634,885
6701	1,00678	422,847	63,102		
7000	1	420	17,7937	5300	1005,15
7100	1	420	26,2615	1310	666,08
8500	1,02	428,4	-0,296812	1000	909,614

Table 18 shows the values of voltage in both per-unit and kV, the phase angle and active and reactive powers production at each node. This is the power flow of the initial file before any addition of a wind farm and case faults.

6.2 CONNECTING THE WIND FARM

As the wind farm model has been described in the previous section, it is important to know where to place it. As Norway is the most described area of the grid model, the wind farm will be connected on the shore of this country. The possible connection busses are 5600, 5603, 6000, 6100, 5500, 6500 and 6700. However, connecting 1000 MW to the grid implies the neighbour busses and connections to be able to withstand this amount of power. Moreover, the bus where it is connected must be strong enough to resist faults that could occur.

Every bus is able to integrate the wind farm in this grid model since it is a simplified one. Thus, two places are chosen according to their degree of relevance and their place in the grid. Busses 5600 and 6000 are located respectively in Sørlandet and Vestlandet, the most populated areas in Norway. This is where the power will be needed, and it is also the places in the grid model where most of the connections and details are. Busses 5600 and 6000 are shown in Figure 76.

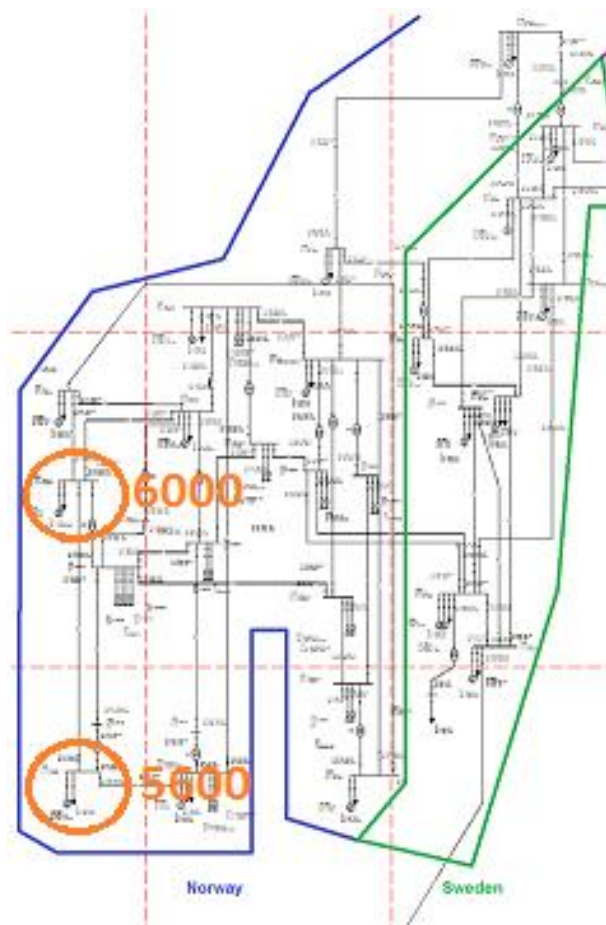


Figure 76 Location of busses 5600 and 6000

6.3 POWER FLOW ON BUS 5600

Figure 77 shows the power flow without a wind farm being connected to Bus 5600. Busses of a 300 kV rated voltage are drawn in green and busses of a 420 kV rated voltage are drawn in blue. The name of the bus is given in the first row, followed by the per-unit value of the voltage and the phase angle in degrees. Closed to the lines, the active and reactive powers are given respectively in MW and MVar. A positive sign stands for production and a negative sign for exportation. Thus, on one line two power pair values appear and are opposite to each other, regardless of the transmission losses, depending on which side they are taken into account.

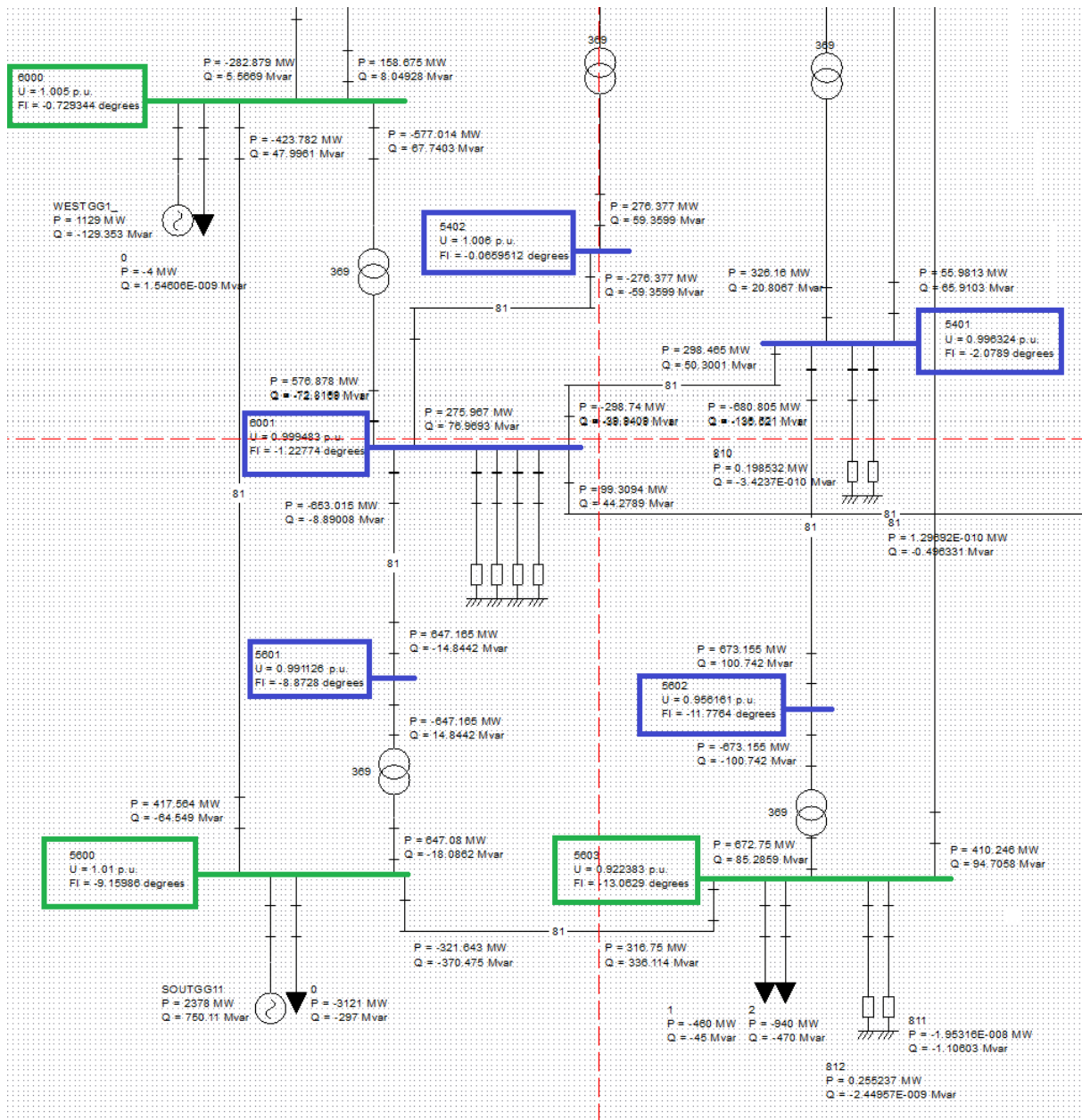


Figure 77 Power flow around bus 5600 without a wind farm connected

The 1000 MW wind farm is now connected to bus 5600. The HVAC configuration is depicted on Figure 78 with two AC lines leaving bus 5600 for bus 1003.

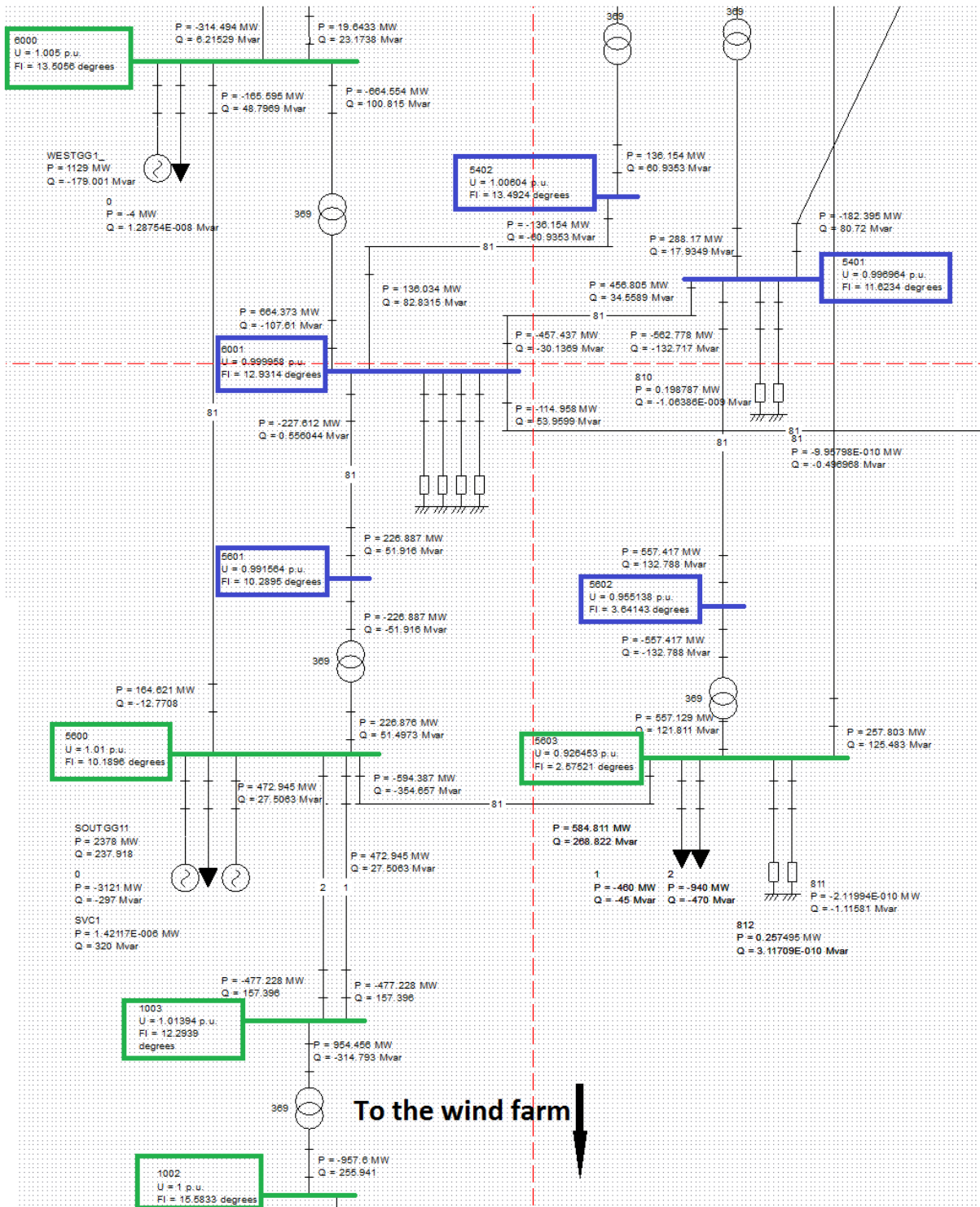


Figure 78 Power flow around bus 5600 with a wind farm connected in HVAC

The wind farm is exporting 954 MW and importing 322 MVar. However, seen from the grid side, bus 5600 is importing 946 MW and 47 MVar from the wind farm. Thus, the rating of the SVC is correct. There is thus roughly 8.58 MW lost in the HVAC connection (0.9% loss) and as the wind farm generator produces 1000 MW, 45 MW are lost in total in the converters, the transformer and the lines. It represents 4.54% loss in active power. According to previous chapters, losses correspond to what we should obtain.

Figure 79 shows the connection of the 1000 MW on bus 5600 with HVDC Light. The wind farm is exporting 941 MW, which is lower than the HVAC case since the first PWM converter consumes energy. Bus 5600 receives 920 MW from the wind farm and exports 357 MVar to the wind farm. The total active power losses represent 7.97% of the generation. According to Table 5, losses should be in the range of 4-6% but the power exchange in the case of a large wind farm is high, and converter stations suffer from too many losses.

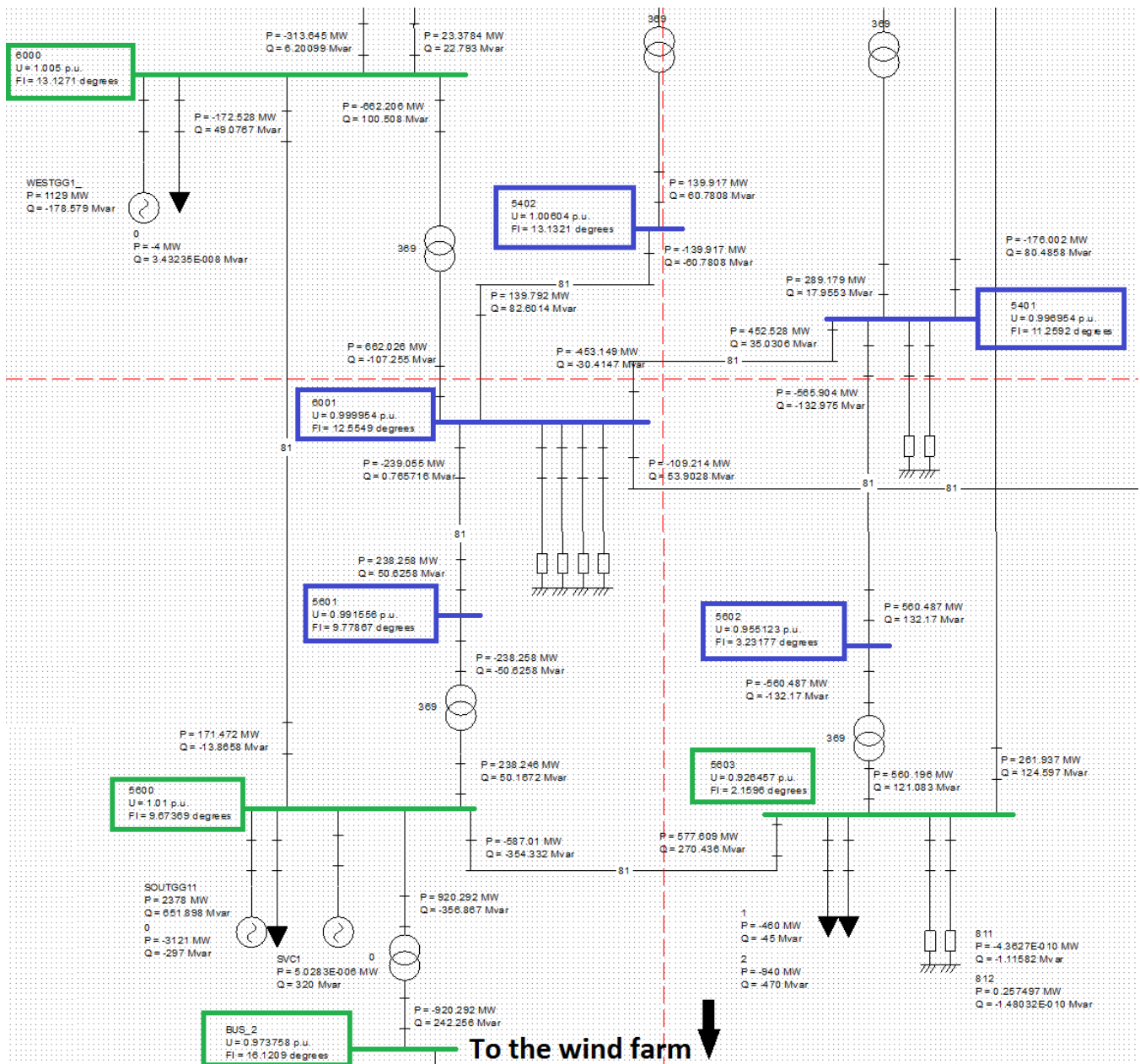


Figure 79 Power flow around bus 5600 with a wind farm connected in HVDC

Table 19 is the summary of the power flow around the connection point (bus 5600) between the wind farm and the grid. A negative sign symbolizes exportation and a positive sign symbolizes importation. The areas are shown on Figure 80. First of all, the addition of a 1000 MW to the grid has almost no effect on the total importation and exportation for each area. The values are roughly equal when no wind farm is connected or when it is connected in HVAC or HVDC. However, the exchange between the areas is completely changed since the power has to flow onto the entire grid to reach the swing bus that will perform the balance of active power. Other generators attached to grid busses are generating the same amount of active power.

Area 56, where the wind farm is connected, imports power from areas 60, 54 and 55. Since the wind farm produces approximately 1000 MW, the amount of power it has to import by has been reduced by the same amount. Most of the reduction was done by a lower exchange with area 60 with HVAC and HVDC connexions. Thus, as area 60 was exporting most of its power to area 56 and as it has to balance, area 60 now exports to all of its neighbour areas. The HVAC- and HVDC-connected cases show the same tendency. Values are poorly changed since the production from the HVDC-connected wind farm is lower by 26 MW compared to the HVAC-connected wind farm.

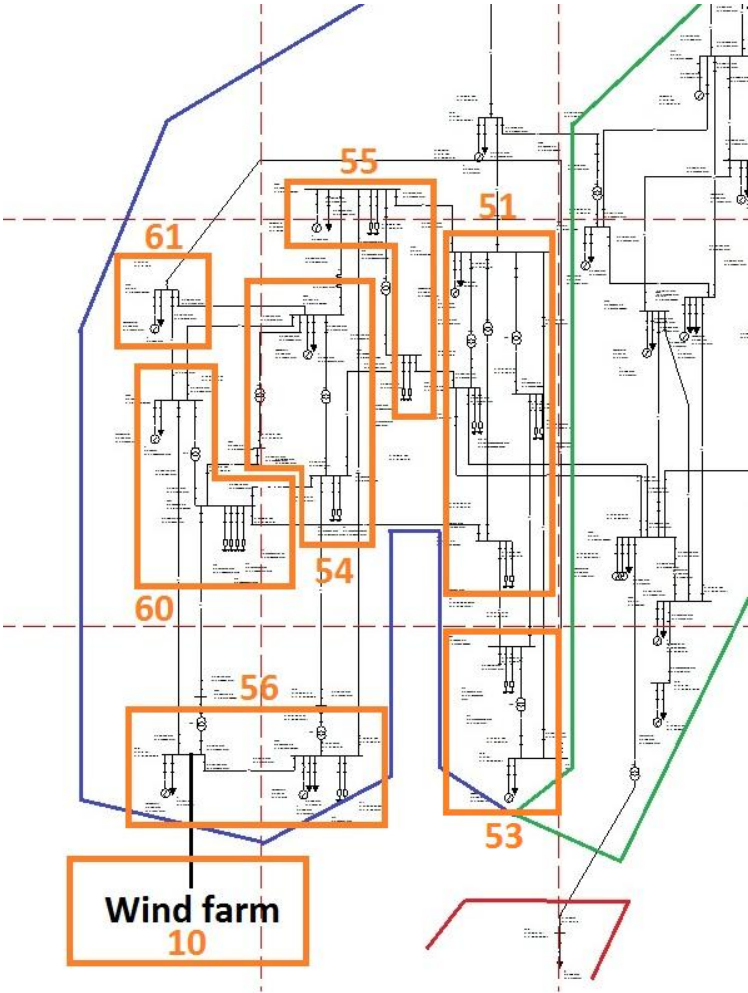


Figure 80 Areas in the Norwegian grid model

Table 19 Inter-area power exchange, connection on bus 5600

Connection on bus 5600 - No Wind Farm							
AREA	FROM AREA	P (MW)	Q (Mvar)	AREA	FROM AREA	P (MW)	Q (Mvar)
54	60	-136.837	-9.48111	54	60	289.224	-38.5073
	61	-418.313	-4.66958		61	-387.457	-5.27993
	55	-257.468	58.4529		55	-829.382	82.1838
	56	-680.805	-136.521		56	-565.904	-132.975
	TOTAL	-1493.42	-92.2185		TOTAL	-1493.52	-94.5782
56	54	673.155	100.742	56	10	920.292	-356.867
	55	410.246	94.7058		54	560.487	132.170
	60	1064.73	-79.3932		55	261.937	124.597
	TOTAL	2148.13	116.054		60	409.730	36.7600
60	51	99.3094	44.2789	60	TOTAL	2152.45	-63.3403
	54	135.902	45.0777		51	-109.214	53.9028
	56	-1076.80	39.1061		54	-289.979	74.9798
	61	-282.879	5.56690		56	-411.583	49.8424
	TOTAL	-1124.46	134.030		61	-313.645	6.20099
Connection on bus 5600 - HVAC Connection				Connection on bus 5600 - HVDC Connection			
AREA	FROM AREA	P (MW)	Q (Mvar)	AREA	FROM AREA	P (MW)	Q (Mvar)
54	60	301.000	-39.4997	54	51	-114.958	53.9599
	61	-386.607	-5.29944		54	-301.759	75.8684
	55	-845.137	82.4899		56	-393.207	49.3530
	56	-562.778	-132.717		61	-314.494	6.21529
	TOTAL	-1493.52	-95.0262		TOTAL	-1124.42	185.397
56	10	945.891	55.0126	56	51	-114.958	53.9599
	54	557.417	132.788		54	-301.759	75.8684
	55	257.803	125.483		56	-393.207	49.3530
	60	391.508	39.1452		61	-314.494	6.21529
	TOTAL	2152.62	352.429		TOTAL	-1124.42	185.397
60	51	-114.958	53.9599	60	51	-114.958	53.9599
	54	-301.759	75.8684		54	-301.759	75.8684
	56	-393.207	49.3530		56	-393.207	49.3530
	61	-314.494	6.21529		61	-314.494	6.21529
	TOTAL	-1124.42	185.397		TOTAL	-1124.42	185.397

6.4 POWER FLOW ON BUS 6000

Figure 81 shows the power flow without a wind farm being connected to Bus 6000. The colour code is unchanged.

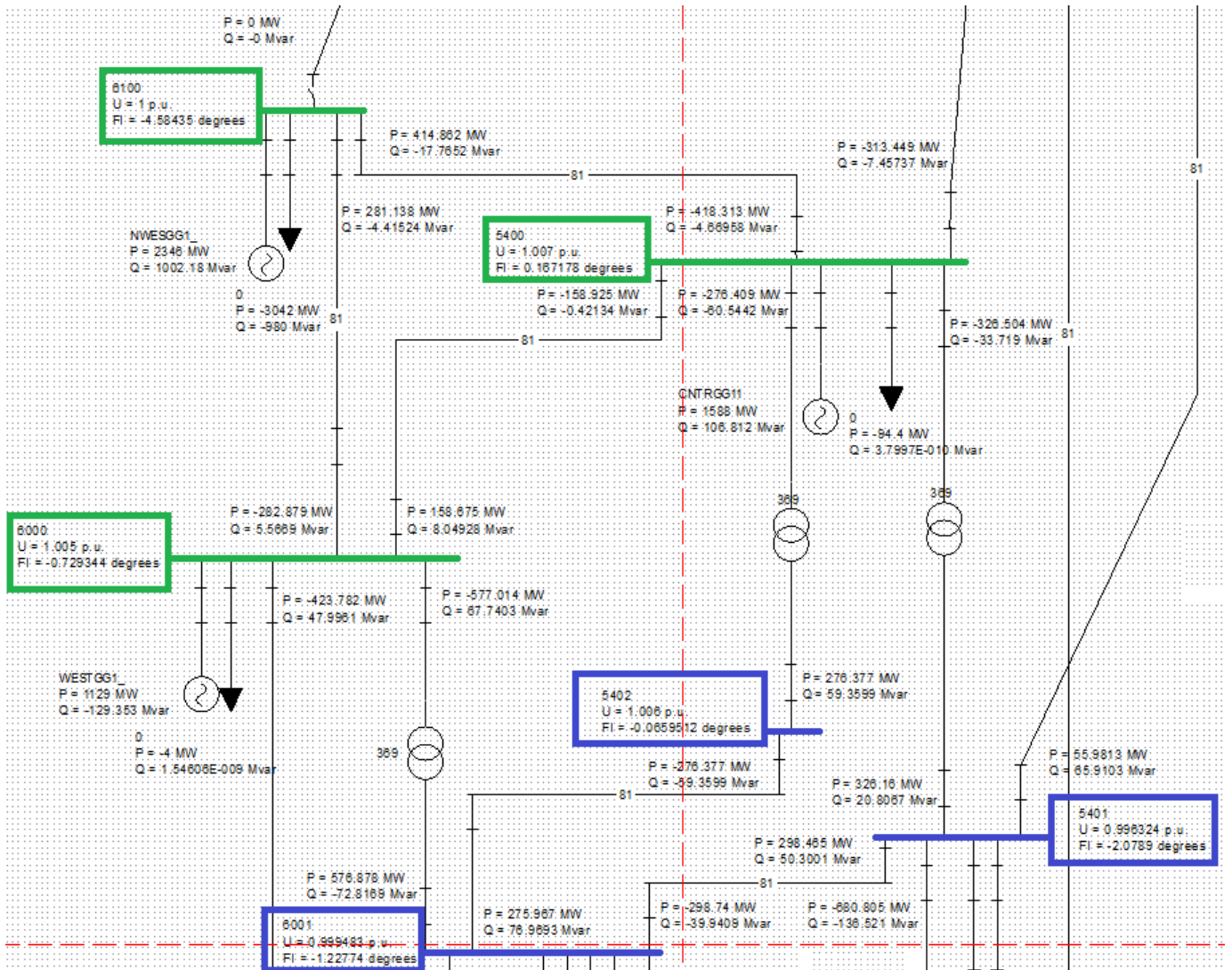


Figure 81 Power flow around bus 6000 without a wind farm connected

The 1000 MW wind farm is now connected to bus 5600. The HVAC configuration is depicted on Figure 82 with two AC lines leaving bus 6000 for bus 1003. Figure 83 shows the connection of the 1000 MW on bus 6000 with HVDC Light. The power output of each wind farm is the same compared to the connection on bus 5600. Voltages are almost unchanged by the addition of a wind farm.

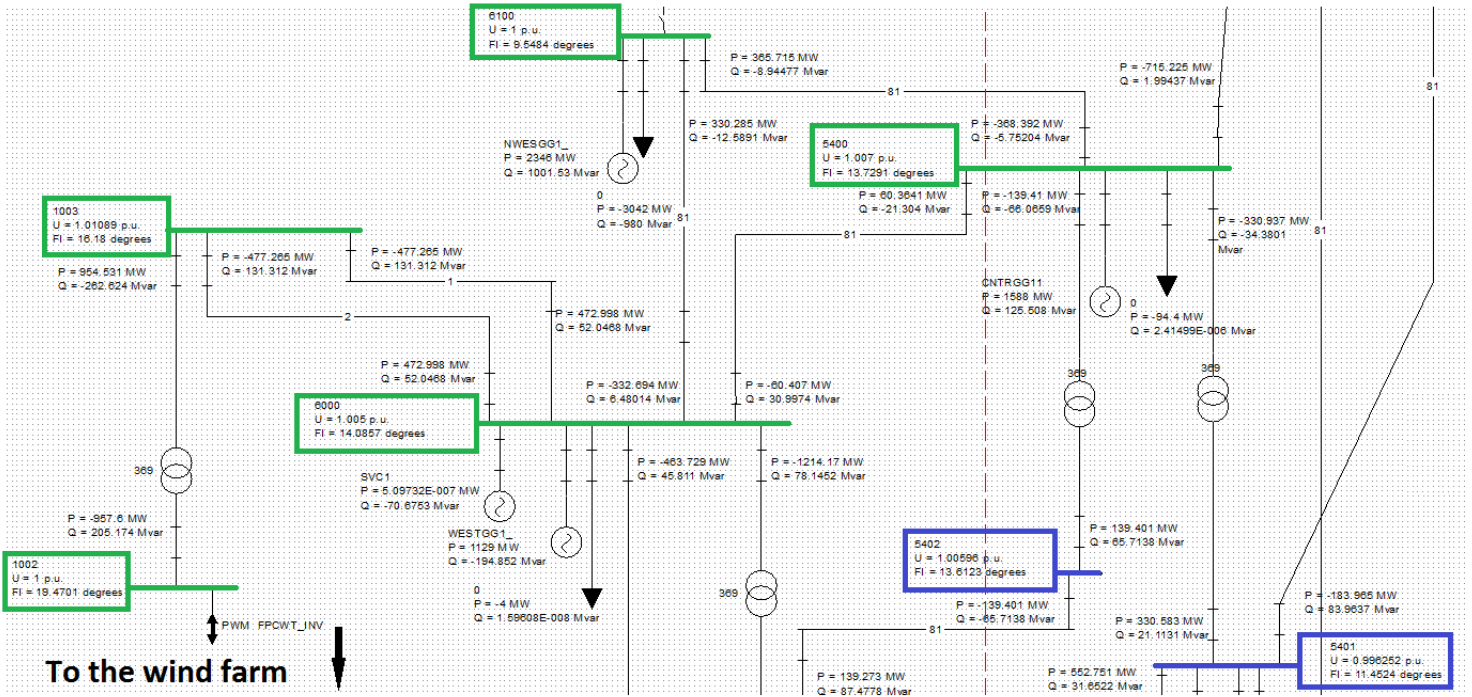


Figure 82 Power flow around bus 6000 with a wind farm connected in HVAC

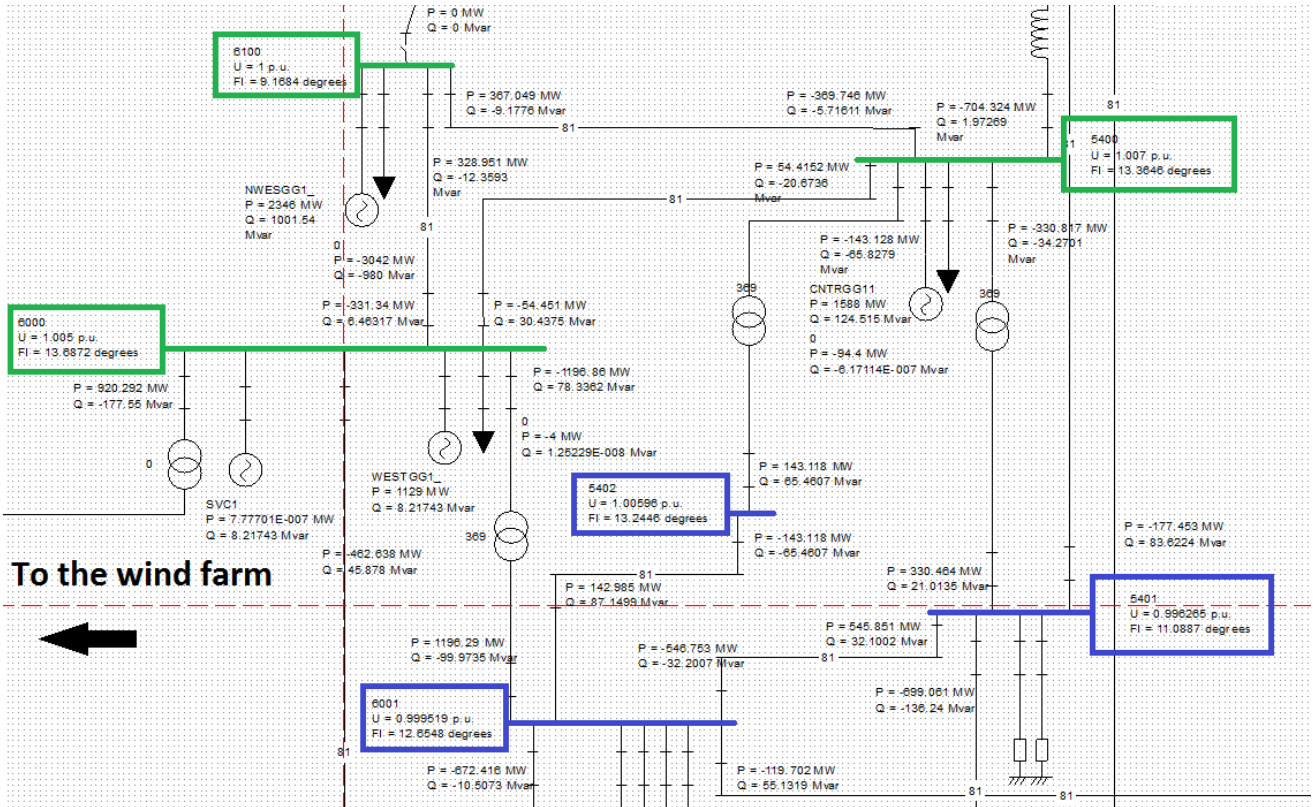


Figure 83 Power flow around bus 6000 with a wind farm connected in HVDC

Table 20 Inter-area power exchange, connection on bus 6000

Connection on bus 6000 - No Wind Farm			
AREA	FROM AREA	P (MW)	Q (Mvar)
54	60	-136.837	-9.48111
	61	-418.313	-4.66958
	55	-257.468	58.4529
	56	-680.805	-136.521
	TOTAL	-1493.42	-92.2185
56	54	673.155	100.742
	55	410.246	94.7058
	60	1064.73	-79.3932
	TOTAL	2148.13	116.054
60	51	99.3094	44.2789
	54	135.902	45.0777
	56	-1076.80	39.1061
	61	-282.879	5.56690
	TOTAL	-1124.46	134.030
61	54	414.862	-17.7652
	60	281.138	-4.41524
	TOTAL	696.000	-22.1804

Connection on bus 6000 - HVAC Connection				Connection on bus 6000 - HVDC Connection			
AREA	FROM AREA	P (MW)	Q (Mvar)	AREA	FROM AREA	P (MW)	Q (Mvar)
54	60	473.811	-55.3734	54	60	457.148	-54.0342
	61	-368.384	-5.75226		61	-369.746	-5.71611
	55	-899.291	85.9601		55	-881.776	85.5951
	56	-699.571	-136.233		56	-699.061	-136.240
	TOTAL	-1493.44	-111.398		TOTAL	-1493.44	-110.395
56	54	691.523	94.2386	56	54	691.023	94.4217
	55	334.328	114.141		55	336.404	113.632
	60	1123.05	-93.1792		60	1121.45	-92.7635
	TOTAL	2148.90	115.201		TOTAL	2148.88	115.290
60	10	946.145	98.3516	60	10	920.292	-177.550
	51	-125.842	55.1923		51	-119.702	55.1319
	54	-474.908	86.3466		54	-458.220	85.3867
	56	-1136.70	35.2847		56	-1135.05	35.3707
	61	-332.701	6.48024		61	-331.340	6.46318
	TOTAL	-1124.01	281.655		TOTAL	-1124.02	4.80279
61	54	365.707	-8.94341	61	54	367.049	-9.17760
	60	330.293	-12.5905		60	328.951	-12.3593
	TOTAL	696.000	-21.5339		TOTAL	696.000	-21.5368

Table 20 describes the inter-area power exchange on the surrounding busses of bus 6000. When the wind farm is not connected to the grid, area 60 imports active power from area 51 and 54 but exports five times more to area 56. However, when a wind farm is connected in HVAC or HVDC to bus 6000, area 60 only exports power since the wind farm provides 946 MW to this area. As a result, area 51 and 54 are not giving power to area 60 and thus import power from it. As a result, area 54 increases its exportation to area 55 by 650 MW. The power flow is reversed as in the wind farm connection to bus 5600, since it tends to reach the swing bus, located in Sweden.

7 DYNAMIC SIMULATIONS

Simulations were made with DYNPOW, which is the tool available in SIMPOW for dynamic simulations of electric power systems. New files have to be done in order to complete initial conditions given by the load flow achieved with OPTPOW.

The aim of these dynamic simulations is to determine the behaviour of the grid and the wind farm when a fault occurs. HVAC and HVDC transmissions have different configurations and thus may have different performance when a problem occurs on the grid. On the contrary, as the wind farm produces a high amount of power, a brutal disconnection of the wind farm from the grid will have a bad influence on the grid.

7.1 THREE-PHASE FAULT AND CRITICAL CLEARING TIME

The three-phase fault is used to explore transient stability in the system. This fault is applied either on a node or on a line. Figure 84 (51) is the schematic representation of a synchronous generator. It is the classical model where E' is the transient e.m.f., X'_d the transient reactance, X_T the transformer reactance, X_L the line reactance, X_s the equivalent reactance of the system and V_s the voltage of the system.

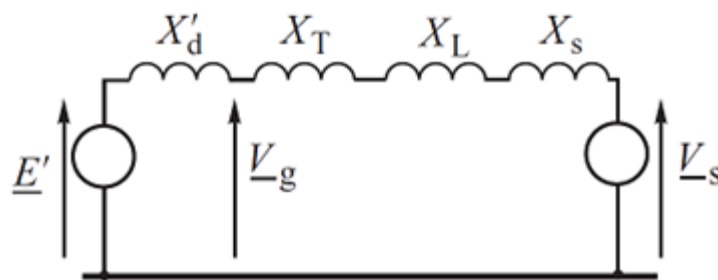


Figure 84 Classical model of a synchronous generator

During a fault, the system can be represented with a fault shunt Δx_f which value is zero in case of a three-phase fault. Figure 85 (51) shows this shunt reactance.

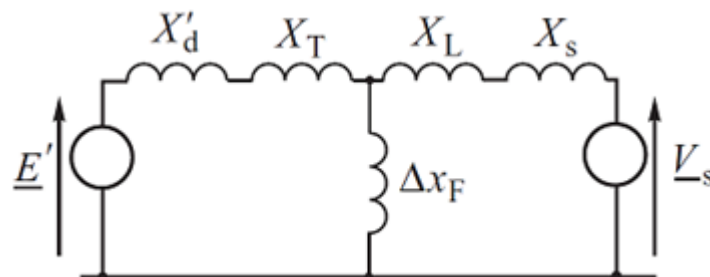


Figure 85 Equivalent circuit during the fault

With a shunt reactance equal to zero, the power transfer from the generator to the rest of the system is impossible. Thus, during the fault, the power drops from the prefault value to zero. It then remains to zero until the fault is cleared when the circuit-breakers are opened. This phenomenon is illustrated in Figure 86, which is the power-angle characteristic. P is the power and δ' is the transient power angle between E' and V_s . Figure 86-a is for a short clearing time and Figure 86-b for a long clearing time. The blue area is the acceleration area and the red area is the deceleration area.

Line 1-2 is when the fault occurs since the power goes down to zero. Before the fault is cleared, the rotor moves which is line 2-3. Then, when the fault is cleared, the rotor of the generator follows the power-angle curve on line 3-4-5. This jump being consequent, the rotor experiences a deceleration but the angle keeps increasing until both areas are equal. If the damping is not sufficient, the cycle starts again on point 1: this is the rotor swing. If the clearing time is too long, as in Figure 86-b, the areas can't be equal and it results in a loss of synchronism from the generator. This method is called the equal-area criterion. It is possible to find a limit from which the generator steps out of phase, and this limit is called the critical clearing time.

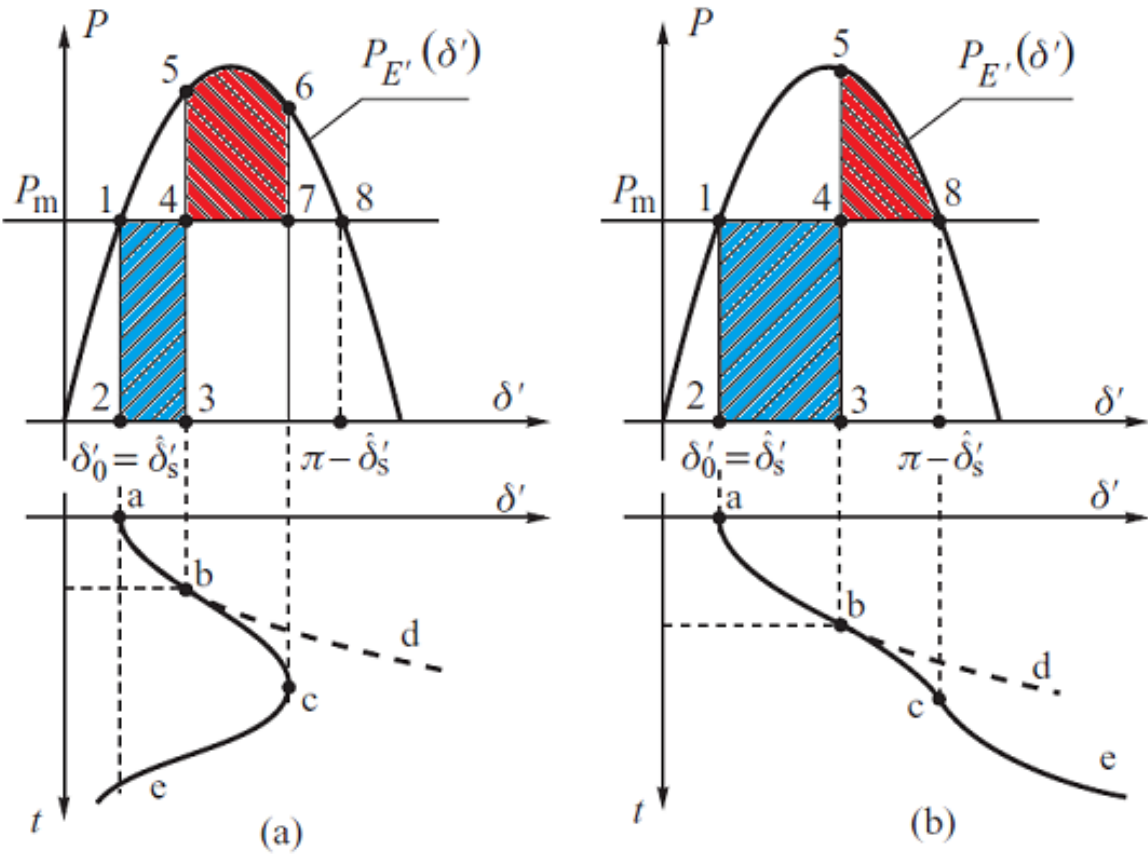


Figure 86 Power-angle characteristics

In order to find the critical clearing time of the system, a three-phase fault to ground is thus applied to the SIMPOW model. The name of the fault is 3PSG and it is applied at exactly $t = 1$ s. The critical clearing time is found to be 185 ms, which means that beyond that point, one of the generators will step out of phase and will not be able to recover from the fault.

7.2 CASE FAULTS

Six HVAC cases and two HVDC cases are studied. The aim of these simulations is to understand the dynamic behaviour of the constructed models. Cases are shown in Table 21. The duration of the simulations is 20 s.

Table 21 Case faults

Case number	Connexion type	Connexion point	Fault type	Fault duration (ms)
1	HVAC	5600	3PSG on connexion point	185
2	HVAC	5600	3PSG on connexion point	50
3	HVAC	5600	3PSG on connexion point	5
4	HVAC	6000	3PSG on connexion point	50
5	HVAC	5600	Stop production on 6100	∞
6	HVAC	5600	Line disconnection	50- ∞
7	HVDC	5600	3PSG on connexion point	185
8	HVDC	5600	Stop production on 6100	∞

3PSG refers to the three-phase fault to ground which is applied directly on one bus. The fault that corresponds to the “stop production” is the disconnection of a generating unit that is between the connexion point and the swing bus. The “line disconnection” means that one of the two lines linking the wind farm to the grid is disconnected after a 50 ms fault is applied on the connection point. Thus, the disconnection is permanent. As the output of making a fault on bus 5600 and 6000 have the same behaviour, this is not looked at for the HVDC connexion.

Faults are coded with the two following data groups. The fault is written in “FAULTS” and then the instruction is run at specific times. The bolded sequences correspond to the parameters that are changed in the nine cases.

```

FAULTS
  F1 TYPE=3PSG NODE 5600
END

RUN INSTRUCTION
  AT 1.000 INST   CONNECT FAULT F1
  AT 1.050 INST DISCONNECT FAULT F1
  AT 1.050 INST DISCONNECT LINE 1003 5600 NO=2
END
  
```

The following figures are the output of the nine cases.

7.3 CASE 1: HVAC - 3PSG ON 5600 FOR 185 ms

This case is a three-phase fault to ground made for a time corresponding to the critical clearing time of our system. Figure 87 is the voltage in p.u. on bus 1000, which is where the synchronous generator of the FPCWT is connected. During the fault, the voltage decreases almost linearly to 0.92 p.u. (-8%) and stops decreasing until the fault is cleared. When the fault is cleared, the voltage increases to 1.08 p.u. (+8%) to try to compensate for the loss that occurred. At $t=1.4$ s, the voltage finally decreases to reach the initial value since the compensation is done. The voltage is stabilized quickly since the value of 1 p.u. is reached in a time of 1 second after the fault is cleared. There is no oscillation on the voltage.

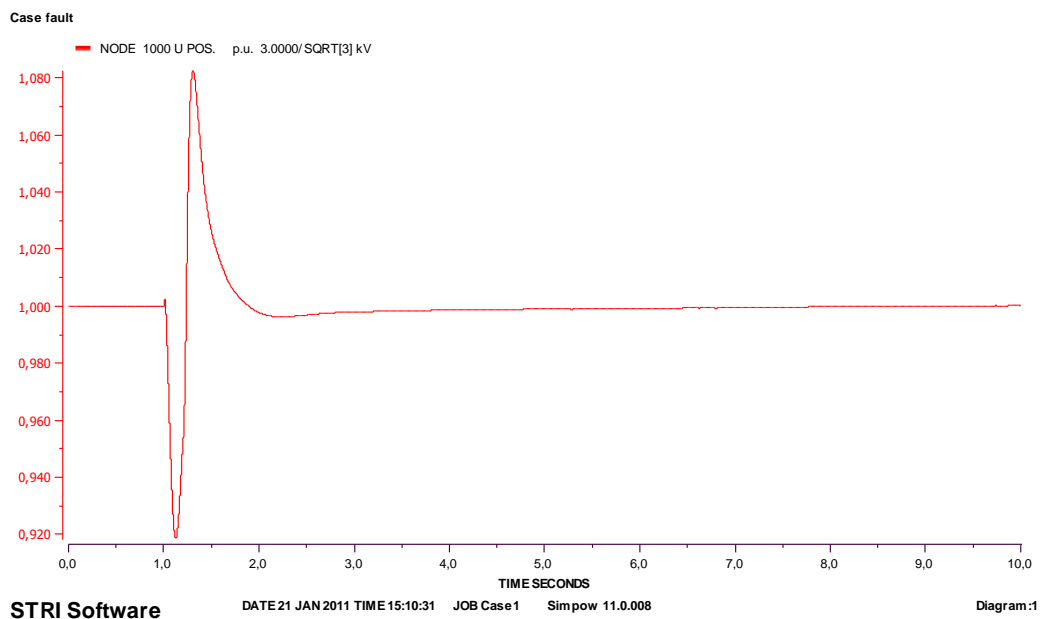


Figure 87 Case1: Voltage on bus 1000

Figure 88 is the voltage onshore (bus 5600) and offshore (bus 1003) in p.u. As the fault occurs on bus 5600, the bus voltage drops immediately to zero until the fault is cleared. The offshore voltage falls to 0.04 p.u. because of the contribution of the FPCWT and because of the losses in the lines. If the lines were perfect, the voltages would have been equal. However, the same behaviour for both voltages is observed after the fault is cleared. The voltage values jump to over 0.8 p.u. and then there is a stabilization that takes 2 s. At $t=5$ s, there is small perturbation because the entire system is not yet stable.

This is shown in Figure 89 with the SVC reactive power. The production of reactive power drops to zero during the fault since the voltage is null. When the fault is cleared, the aim of the SVC is to stabilize the voltage to its previous value. The first oscillations until $t=1.5$ s are the same than those of the voltage. As the time chosen for the fault is the critical clearing time, the system struggles to balance and the SVC has to make too many changes to try to match the reactive power absorption and production.

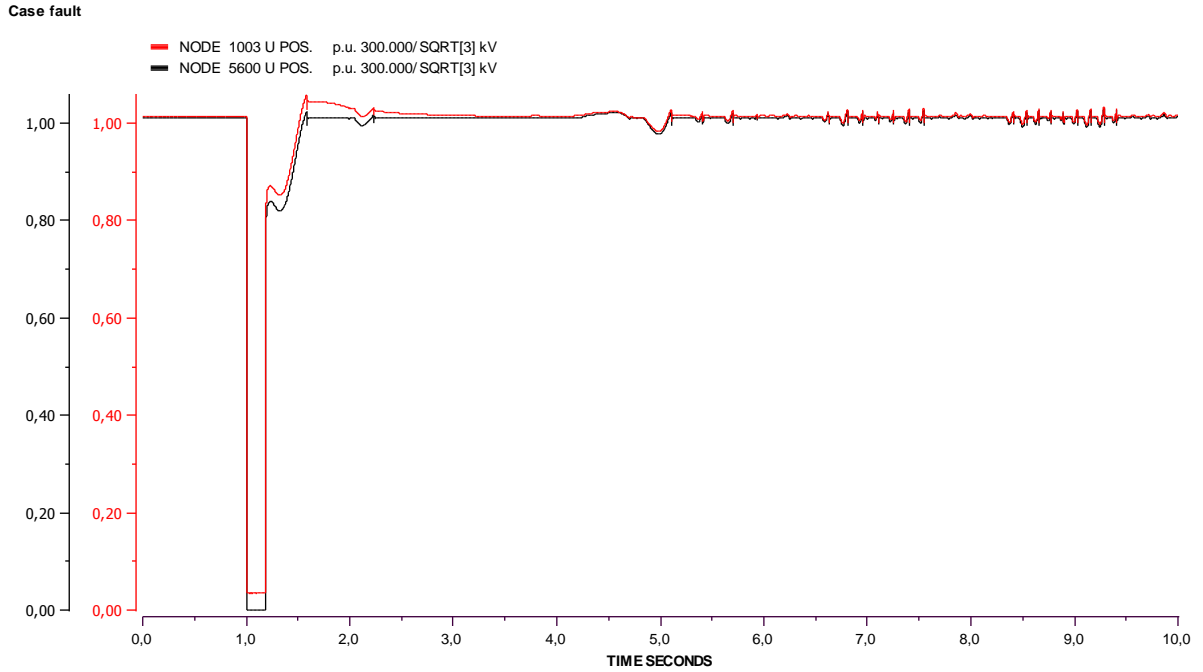


Figure 88 Case 1: Voltages on busses 1003 and 5600

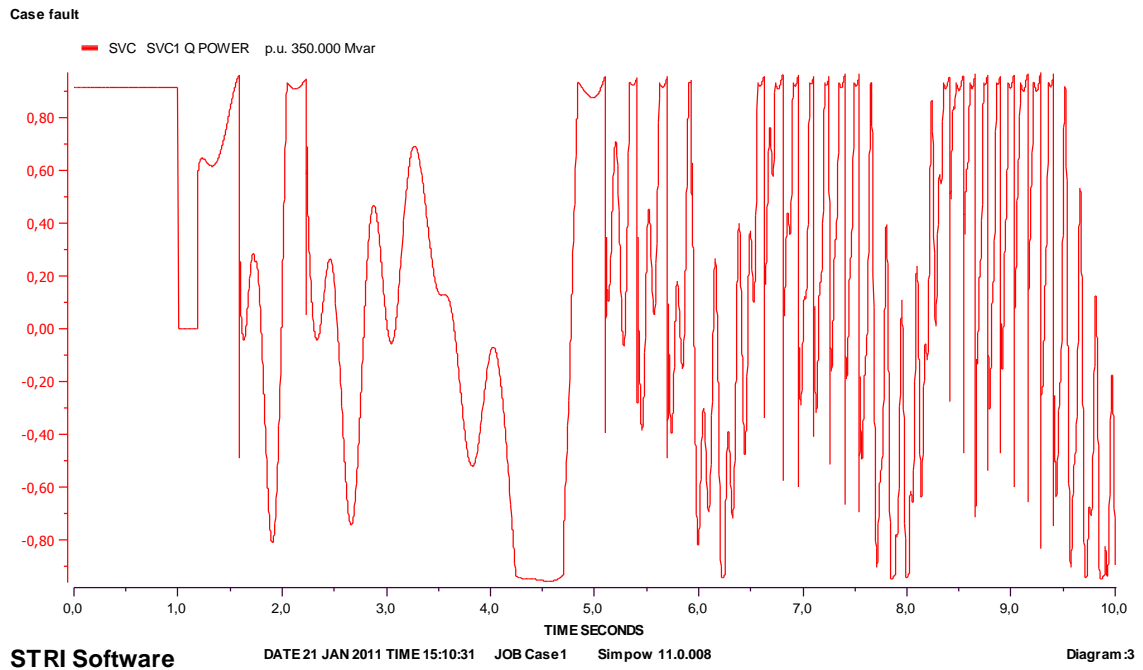


Figure 89 Case 1: Reactive power of the SVC

Figure 90 is the wind turbine mechanical power in p.u. The power is decreasing like the voltage on bus 1000 during the fault. After the fault is cleared, it keeps on decreasing until the voltage is stabilizing. In the FPCWT, there is a frequency converter at the generator terminal that reduces the output power to the grid until this frequency converter is safe from too high currents generated by the fault. The increase in voltage helps the decrease in current and thus, when the voltage is high enough and then decreases, the power can start increasing again.

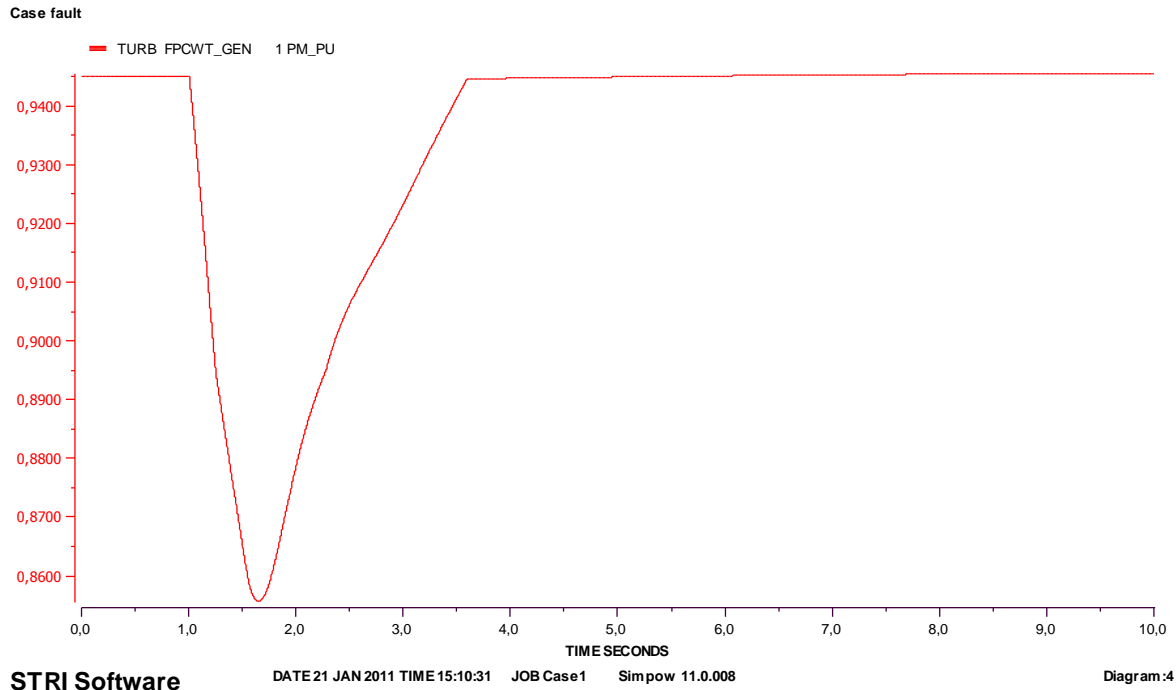


Figure 90 Case 1: Mechanical power of the FPCWT

Figure 91 is the speed of the wind turbine generator. The speed barely changes during the fault, because even if the power is lowered, it is due to the converters and not because the speed is changed. However, the increase of power passed $t=1.60$ s is made by the increase of the speed. When the speed reaches the maximum value of 1.02 p.u., the power has reached its pre-fault value. Thus, the speed can start decreasing to match its own pre-fault value. The stability is long to operate because the speed control is not fast enough.

Figure 92 shows the power transfer from offshore to onshore by the two HVAC transmission lines. During the fault, the transfer is null since the fault is made on the bus to which it is connected. Then, the power transfer stabilizes after 1.5s like the voltage. The post-fault value of the power is 2% higher than the pre-fault one. The pre-fault value is only reached after 10 s.

The reactive power transfer is shown in Figure 93. The reactive power drops to zero during the fault and then increases to a value ten times higher than the pre-fault one. The maximum is reached at $t=1.8$ s at a value of 450 MVar per cable which is huge. In Figure 89 where the SVC reactive power is shown, there is absorption of 290 Mvar at $t=1.8$ s. Thus, the SVC tries to balance for the reactive power contribution from the FPCWT along with the contribution from the rest of the grid.

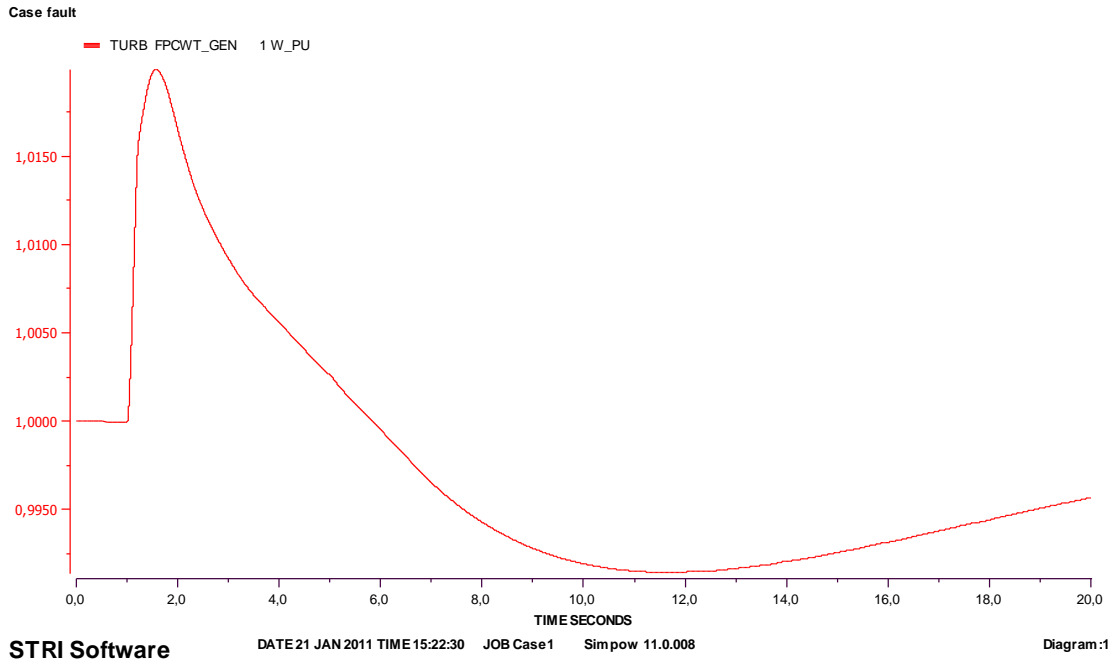


Figure 91 Case 1: Speed of the FPCWT

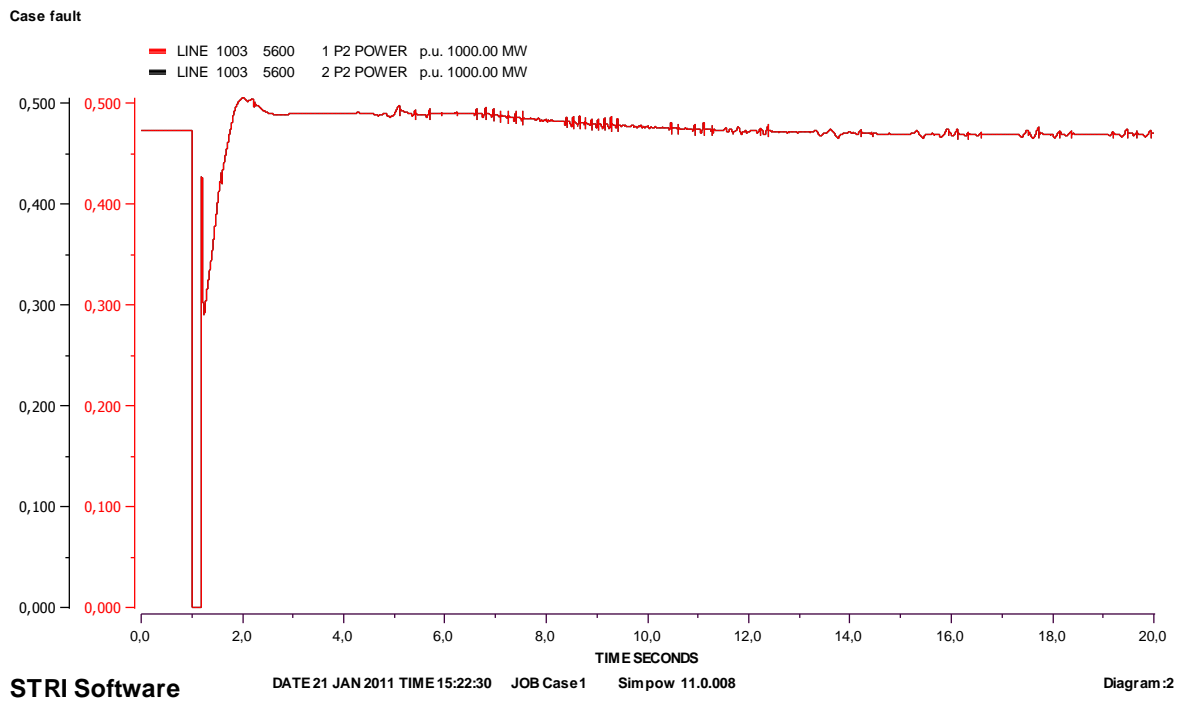
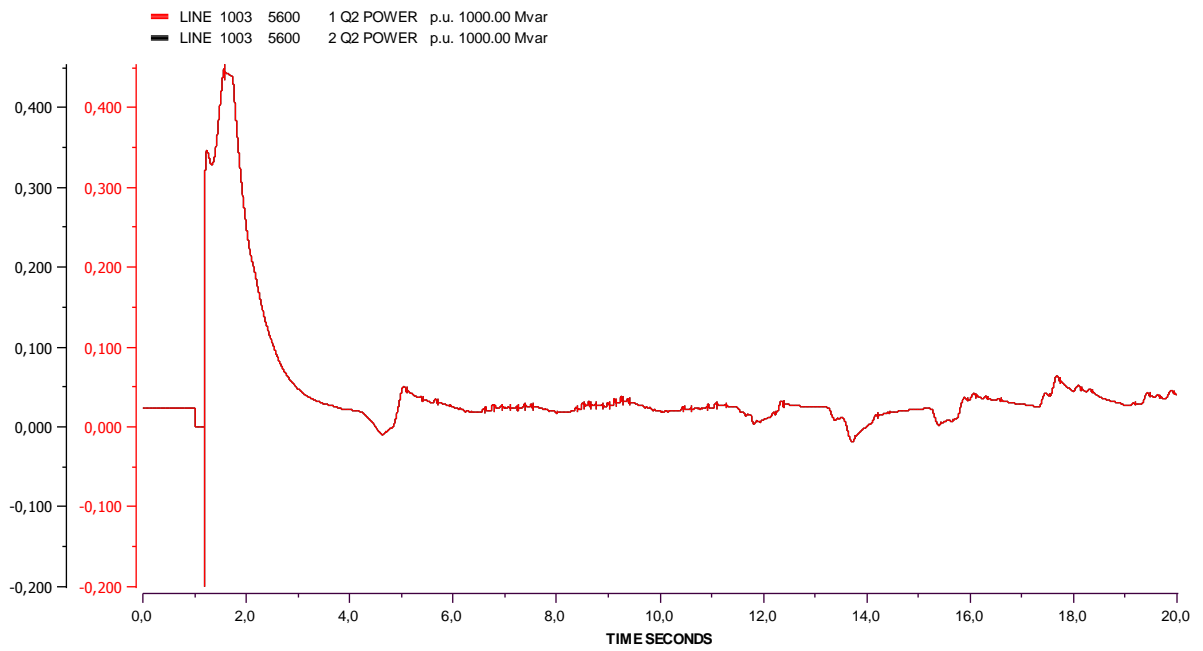


Figure 92 Case 1: Active power transfer from offshore to onshore

Case fault



STRI Software

DATE 22 JAN 2011 TIME 18:25:10 JOB Case1 Simpow 11.0.008

Diagram:3

Figure 93 Case 1: Reactive power transfer from offshore to onshore

7.4 CASE 2: HVAC - 3PSG ON 5600 FOR 50 ms

A fault that lasts shorter than the previous one is applied on the same bus. Figure 94 is the voltage on the FPCWT bus. As the fault is shorter, the voltage drop is lower, and equal to -4% instead of -8%. The behaviour is unchanged but the voltage reaches its pre-fault value in 0.5 s instead of 2 s. Figure 95 shows the voltages of the onshore and offshore busses. The onshore bus voltage stabilizes very fast, in 0.1 s. The offshore bus reaches the 5% response time in 0.5 s and then reaches its pre-fault value in 2.7 s. The system is much more stable since the fault duration is far from the critical clearing time.

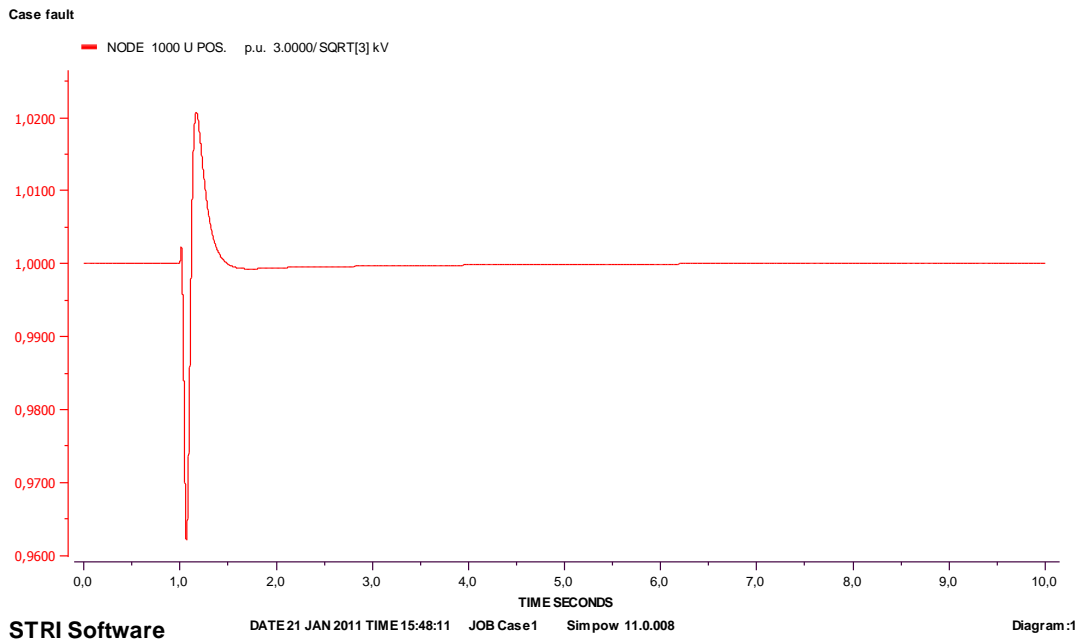


Figure 94 Case 2: Voltage on bus 1000

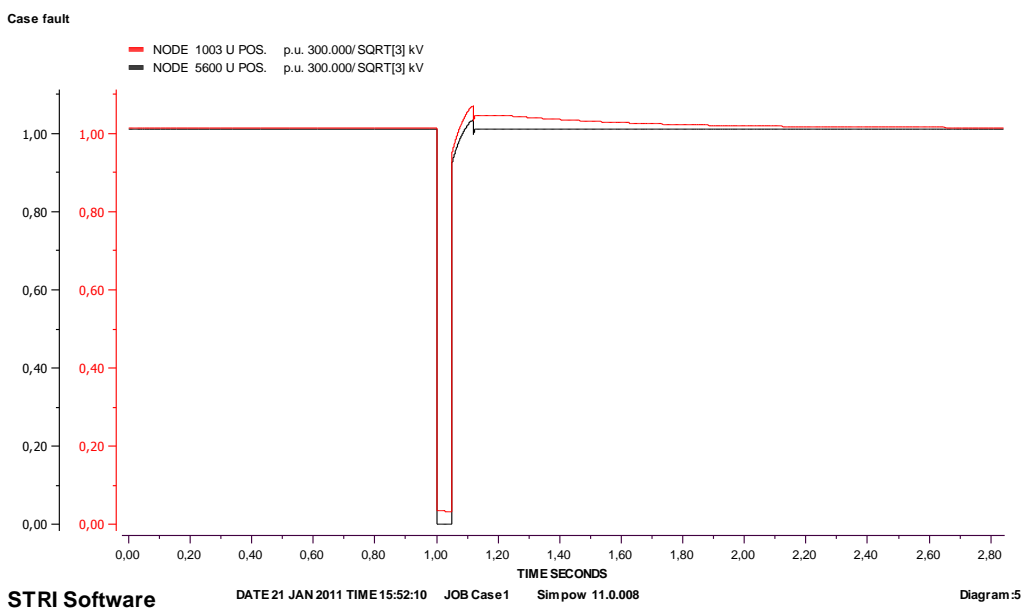


Figure 95 Case 2: Voltages on busses 1003 and 5600

Figure 96 shows the reactive power of the SVC. As the fault is relatively short, the main changes of the SVC reactive power are due to the wind farm and not to the neighbour onshore busses. Thus, the drop of -0.9 p.u. (-315 Mvar) is due to the reactive power exchange with the wind farm. The wind farm is only connected to bus 5600 whereas the neighbour busses of 5600 are connected to other areas which can then provide enough reactive power for this short time. The reactive power of the SVC fluctuates less than in the previous case but it does not stabilize to the pre-fault value. As the other busses had to compensate for the reactive power change, a change of 200 Mvar is observable at the SVC.

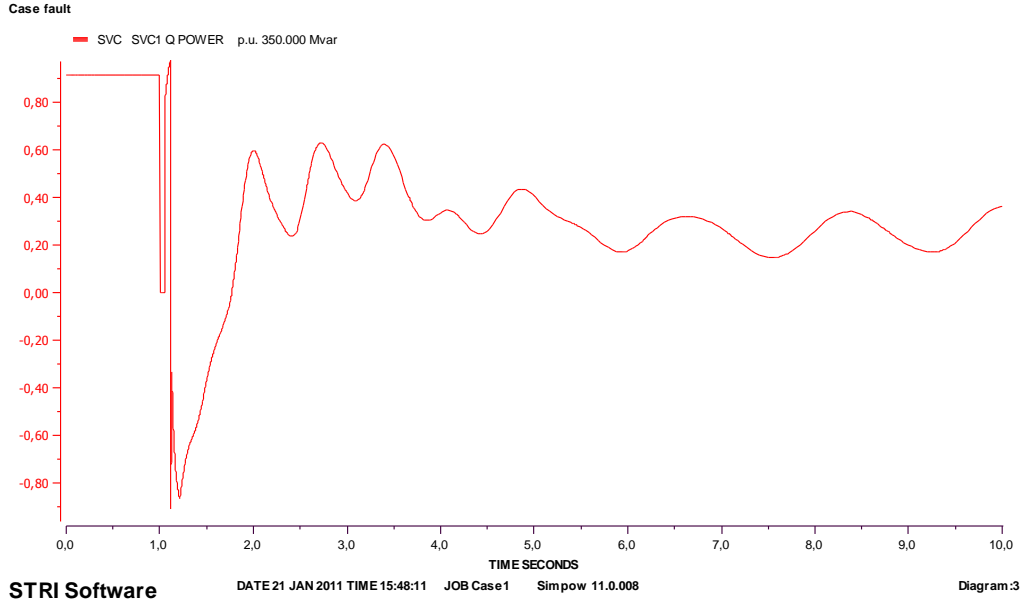


Figure 96 Case 2: Reactive power at the SVC

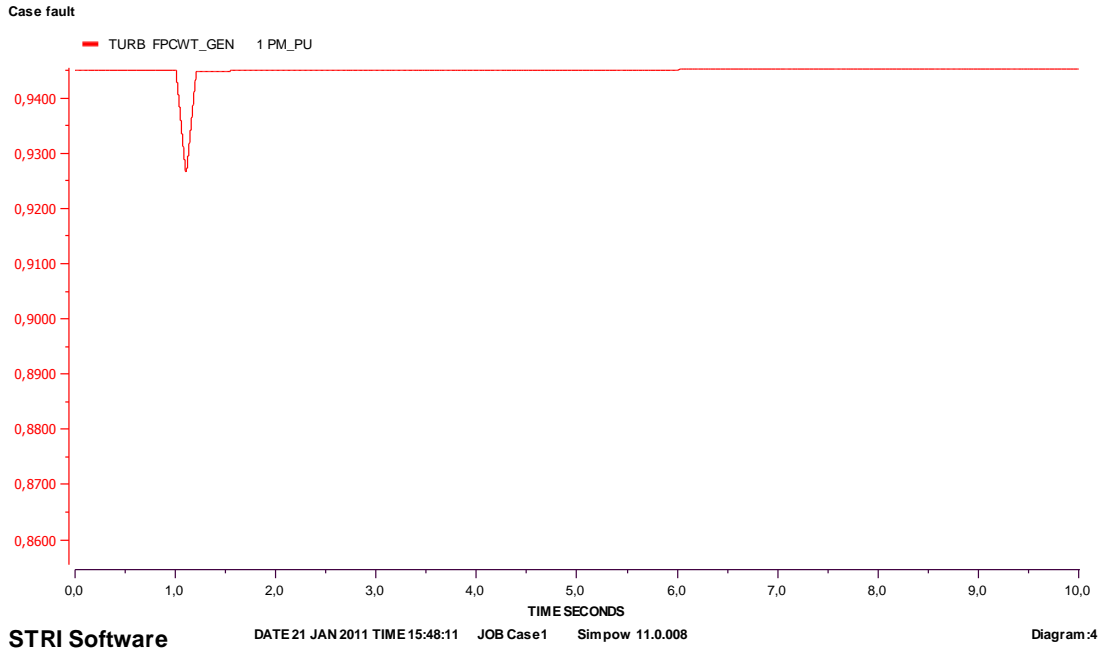


Figure 97 Case 2: Mechanical power of the FPCWT

Figure 97 is the mechanical power of the FPCWT. There is a 1.5% drop in the power for twice the duration of the fault. As the currents at the frequency converter are not high for a long time, the power does not need to be reduced for too long.

The power transfer between the offshore and onshore busses is shown in Figure 98. The power is still zero during the fault but the stabilization is done much faster than in the previous case. After 0.5 s, the post-fault value of the power equals to pre-fault one. The overshoot that appears after the clearing of the fault is a bit higher than in case 1.

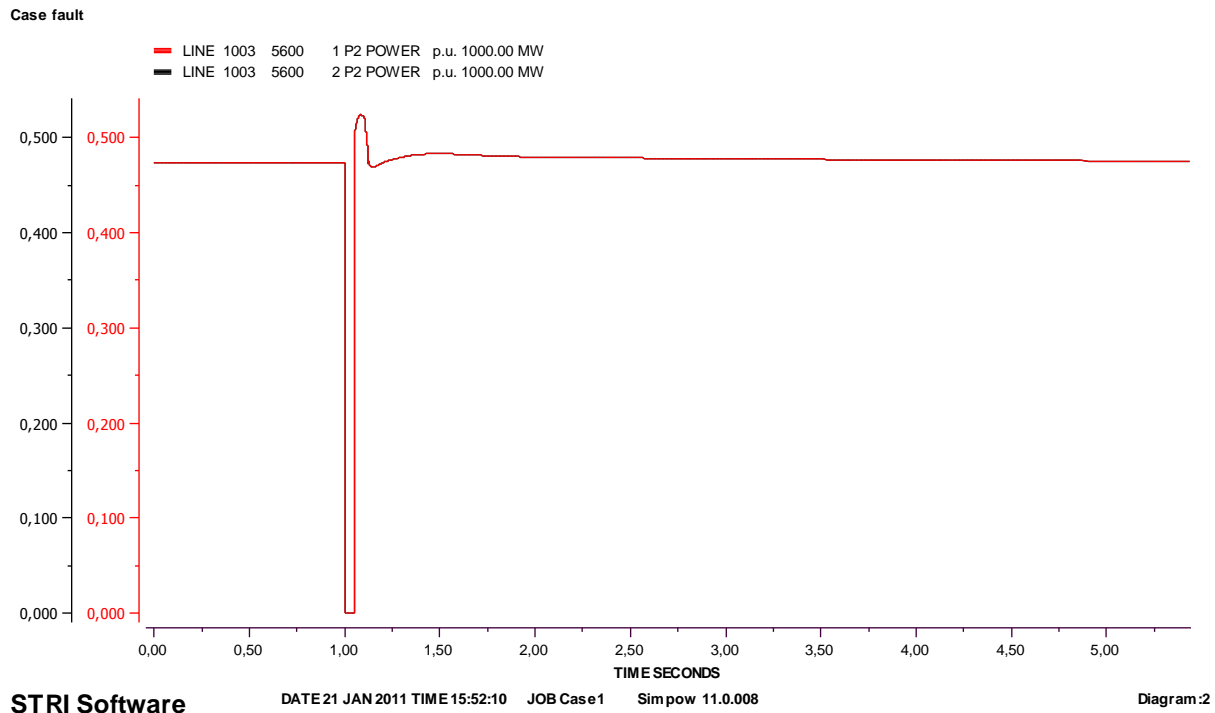
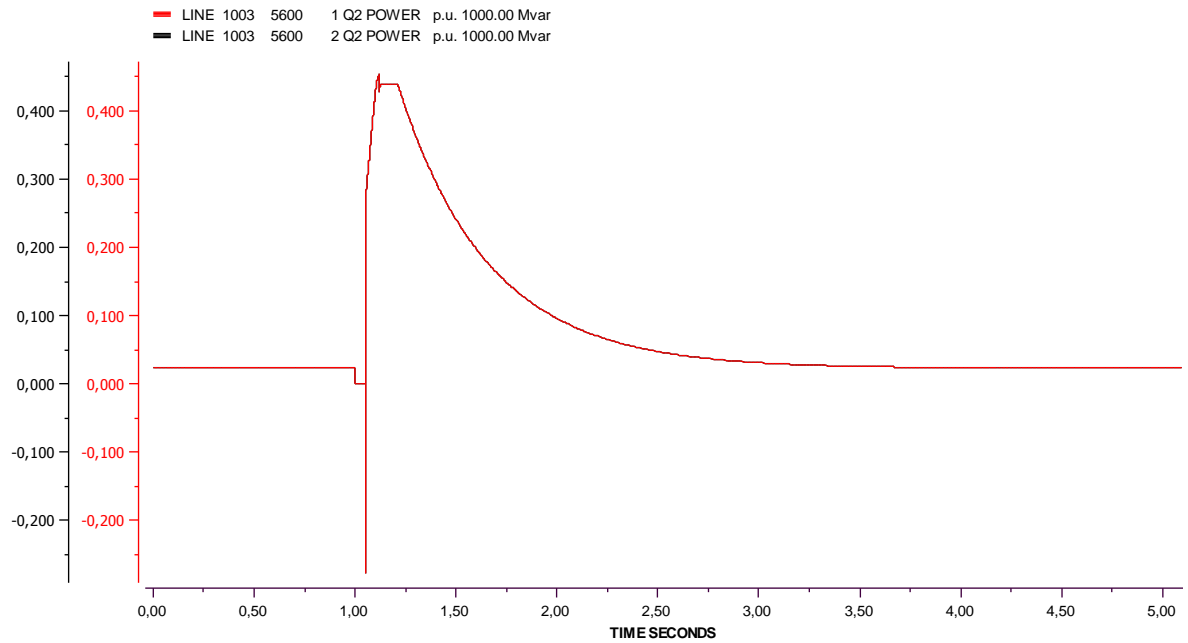


Figure 98 Case 2: Active power transfer from offshore to onshore

Figure 99 shows the reactive power exchange from the offshore bus to the onshore bus. The curve is similar to the one obtained in case 1 since the maximum of reactive power is the same and there is the same decreasing transfer after the maximum. However, as the overall system stabilizes much faster, the curve is a lot smoother and the pre-fault value is obtained after 2.5 s and there are no oscillations.

Figure 100 is the speed of the FPCWT. In case one, the maximum was 1.02 p.u. and it is now 1.003. Moreover, the speed stabilizes much faster, in 8 s instead of more than 20 s in the previous case. Thus, the change in speed of the FPCWT is almost negligible for the system.

Case fault



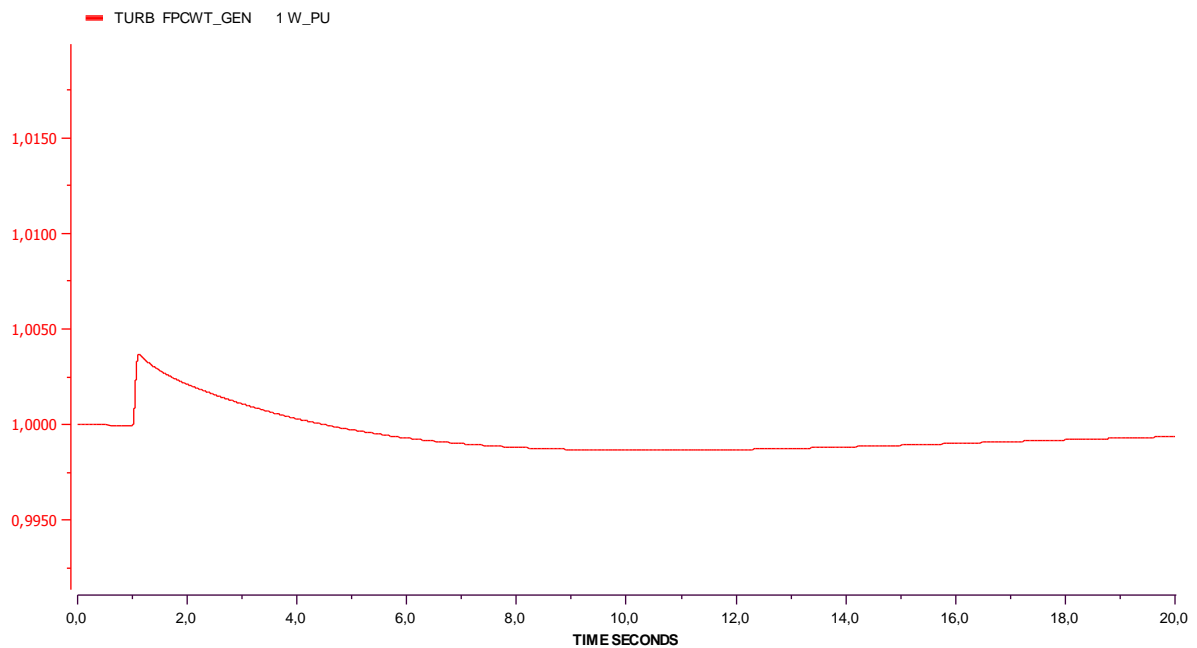
STRI Software

DATE 21 JAN 2011 TIME 15:52:10 JOB Case1 Simpov 11.0.008

Diagram:3

Figure 99 Case 2: Reactive power transfer from offshore to onshore

Case fault



STRI Software

DATE 21 JAN 2011 TIME 15:52:10 JOB Case1 Simpov 11.0.008

Diagram:1

Figure 100 Case 2: Speed of the FPCWT

7.5 CASE 3: HVAC - 3PSG ON 5600 FOR 5 ms

The aim of this case is to study a small fault that could occur at any time from a generating unit. The voltage at the FPCWT is shown in Figure 101. The maximum and minimum due to the fault are up to +/- 0.15%. The voltage now stabilizes in 0.4 s. The mechanical power is not changing during and after the fault since the change in voltage is insignificant. The same behaviour occurs to the speed of the FPCWT.

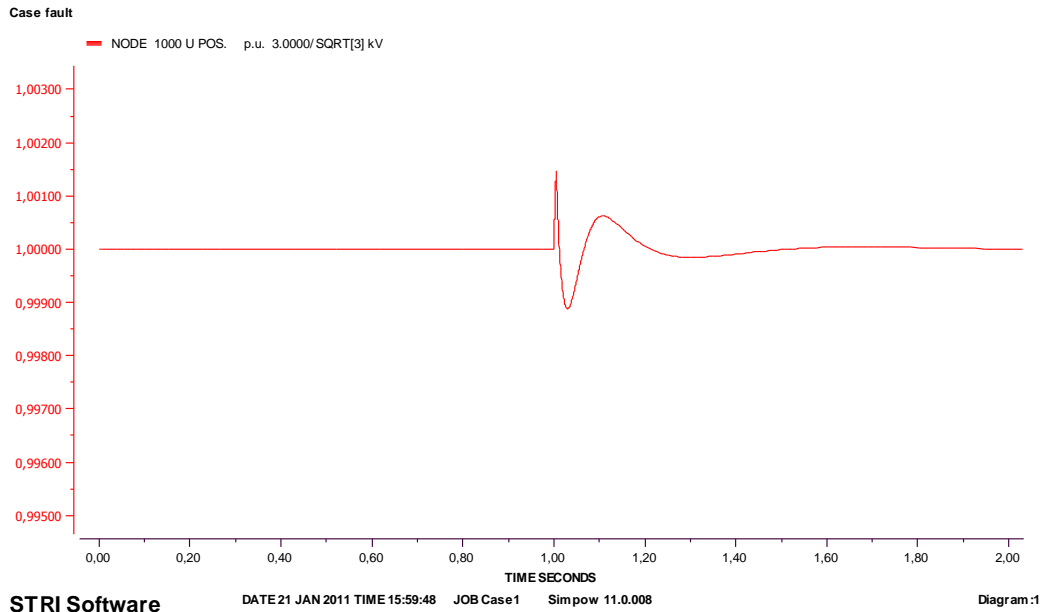


Figure 101 Case 3: Voltage on bus 1000

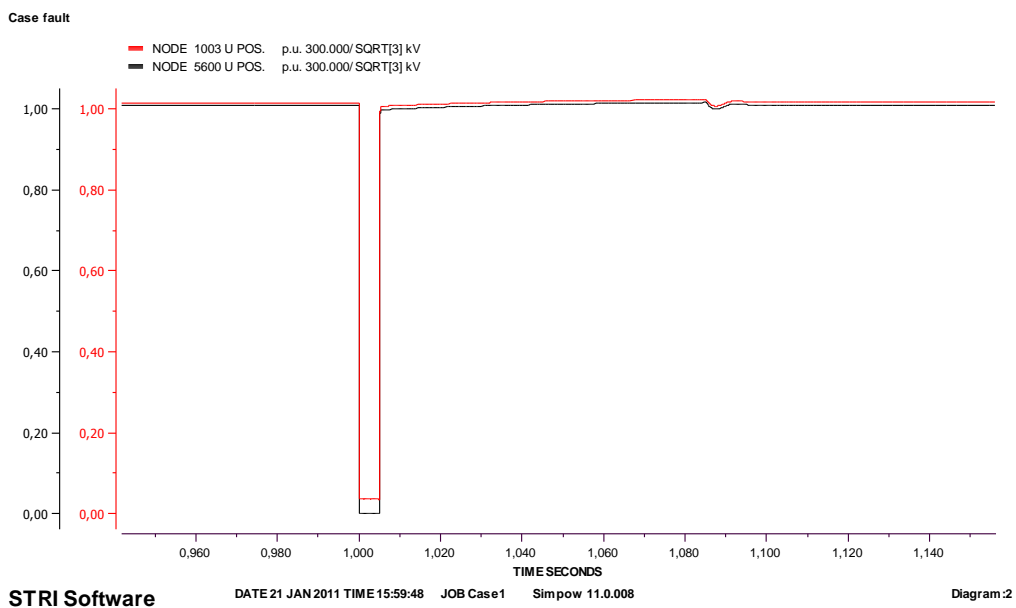
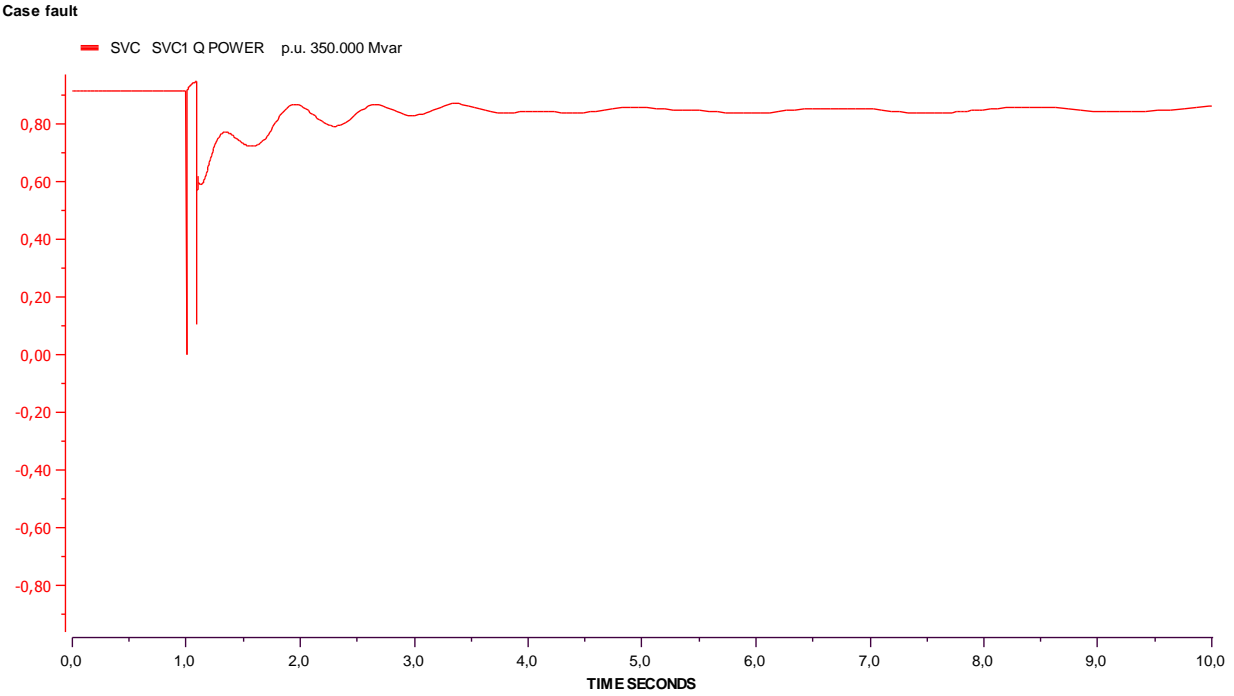


Figure 102 Case 3: Voltages on busses 1003 and 5600

The voltages on busses 1003 and 5600 are shown in Figure 102. They are equal almost to the pre-fault state values after the fault is cleared. Thus the voltage is stable for such a small fault.

Figure 103 is the SVC reactive power. It succeeds to stabilize after 3.5 s to a value lower by 0.1 p.u. compared to the pre-fault one.



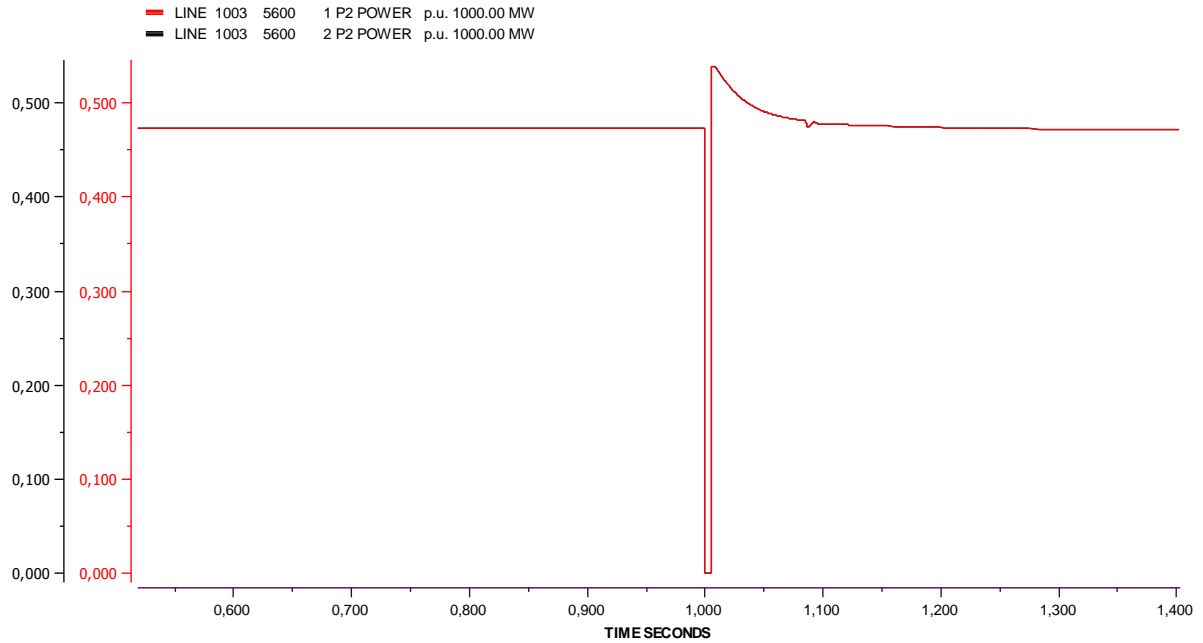
STRI Software DATE 21 JAN 2011 TIME 15:59:48 JOB Case1 Simpov 11.0.008 Diagram:3

Figure 103 Case 3: Reactive power at the SVC

The active power transfer between the offshore and onshore busses is shown in Figure 104. The same overshoot is observed after the fault is disconnected but the system becomes stable after only 0.1 s.

The reactive power transfer is shown in Figure 105. In cases 1 and 2, the overshoot was equal but in case 3, as the fault is short, the overshoot is ten times smaller. Moreover, the system stabilizes faster, in 1.5 s.

Case fault



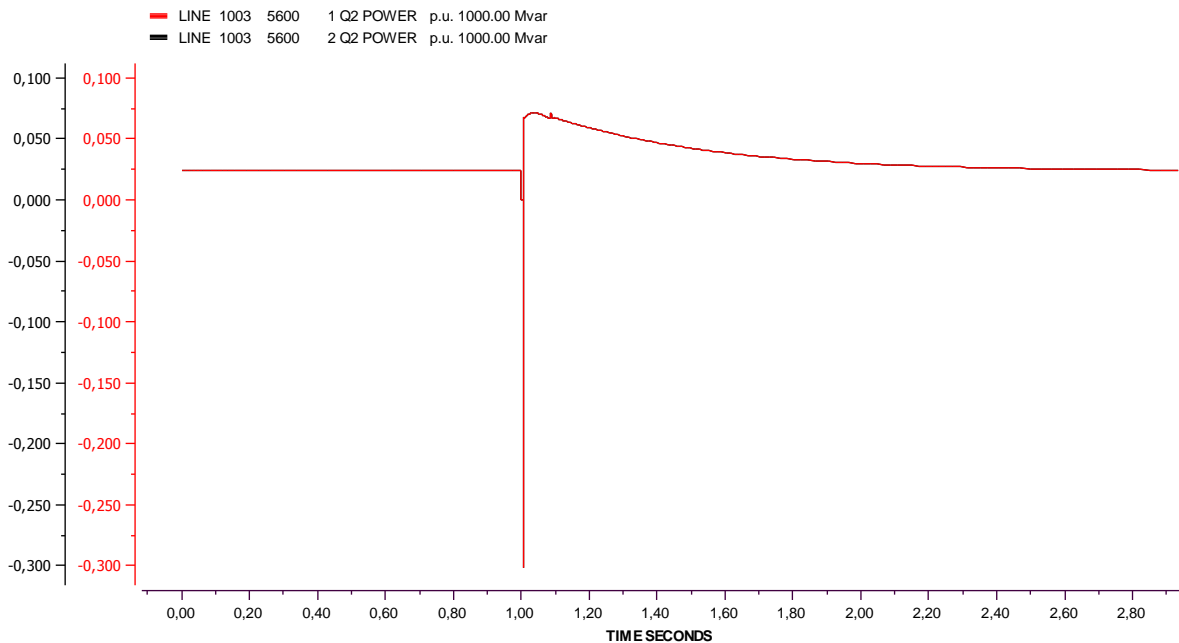
STRI Software

DATE 21 JAN 2011 TIME 15:59:48 JOB Case1 Simpow 11.0.008

Diagram:6

Figure 104 Case 3: Active power transfer between the offshore and onshore busses

Case fault



STRI Software

DATE 21 JAN 2011 TIME 15:59:48 JOB Case1 Simpow 11.0.008

Diagram:7

Figure 105 Case 3: Reactive power transfer between the offshore and onshore busses

7.6 CASE 4: HVAC - 3PSG ON 6000 FOR 50 ms

In this case, the wind farm is connected in HVAC to bus 6000 located in the West of Norway instead of the South. The fault applied on bus 6000 is the same than the one applied on bus 5600 in case 2. Thus, it is possible to compare cases 2 and 4.

Figure 106 is the voltage on the FPCWT bus. The minimum and maximum values of the voltage are the same for both cases since this is the same fault and this is the same wind farm. The time taken to reach the pre-fault value after the fault is also unchanged.

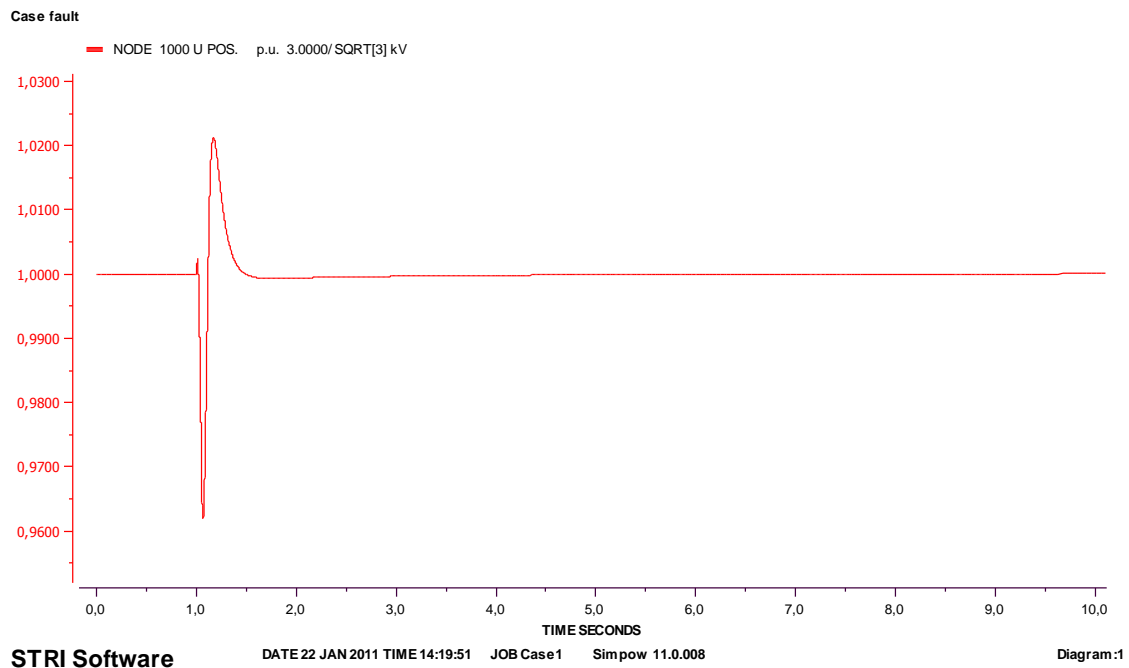


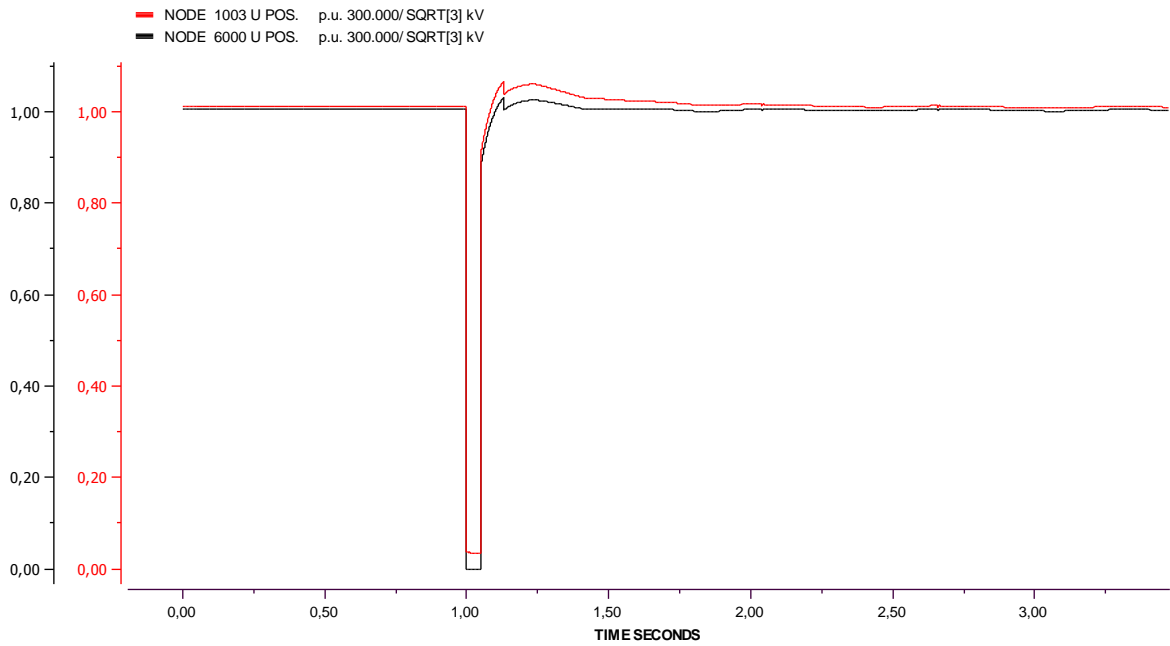
Figure 106 Case 4: Voltage on bus 1000

Figure 107 is the voltage on the offshore bus and the onshore bus. The maxima are the same than in case 2. However, the onshore voltage is less stable, there are some oscillations. Though, the 5% time response is the same since oscillations are small.

In case 2, the reactive power from the SVC was oscillating around a 30 p.u. after the fault but in case 4, reactive power is needed during the first five seconds after the fault is cleared. This is shown in Figure 108. Before the fault, the SVC was absorbing reactive power and during the fault it is delivering reactive power to the system. In case 2, the SVC was delivering reactive power before the fault and it is then equal to zero during the fault.

The mechanical power is exactly the same than in case 2 and so is the speed of the FPCWT.

Case fault



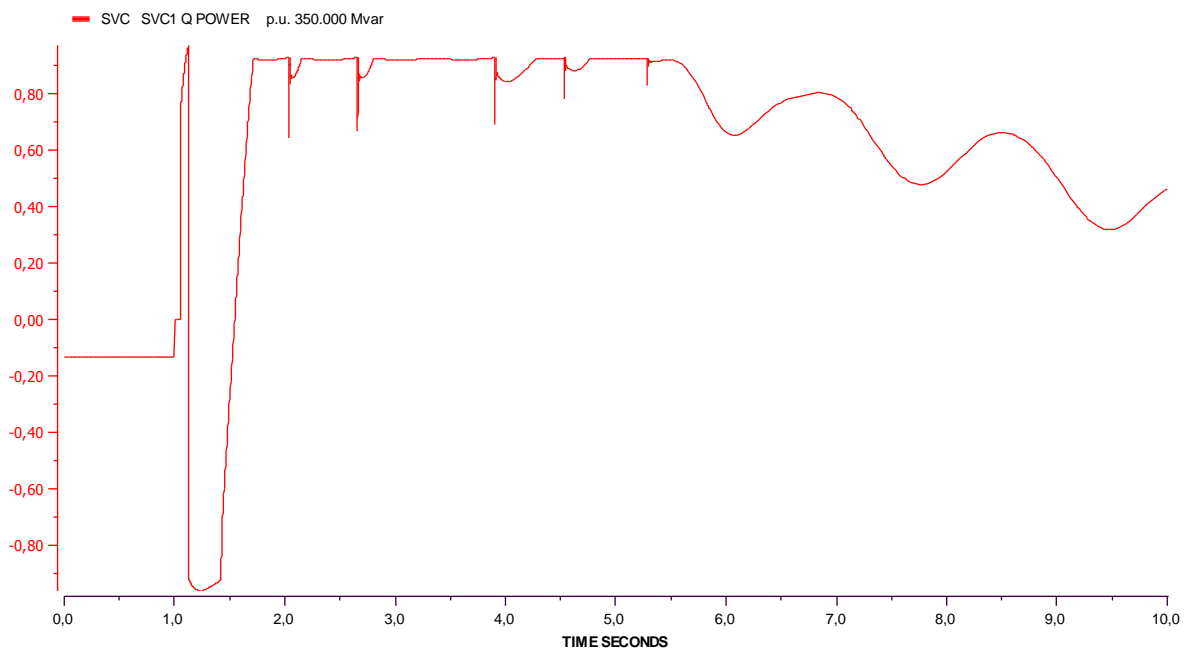
STR Software

DATE 24 JAN 2011 TIME 09:58:46 JOB Case1 Simpov 11.0.008

Diagram:1

Figure 107 Case 4: Voltages on busses 1003 and 6000

Case fault



STR Software

DATE 22 JAN 2011 TIME 14:19:51 JOB Case1 Simpov 11.0.008

Diagram:3

Figure 108 Case 4: Reactive power at the SVC

Figure 109 is the active power exchange between the offshore and onshore busses. The overshoot is similar to case 2 but the system is a bit less stable, even though the 5% time response is the same.

The reactive power exchange is shown in Figure 110. The plot is exactly the same than the one found in case 2. Thus, the change in the two plots of the reactive power in the SVC is mainly due to the neighbour onshore busses.

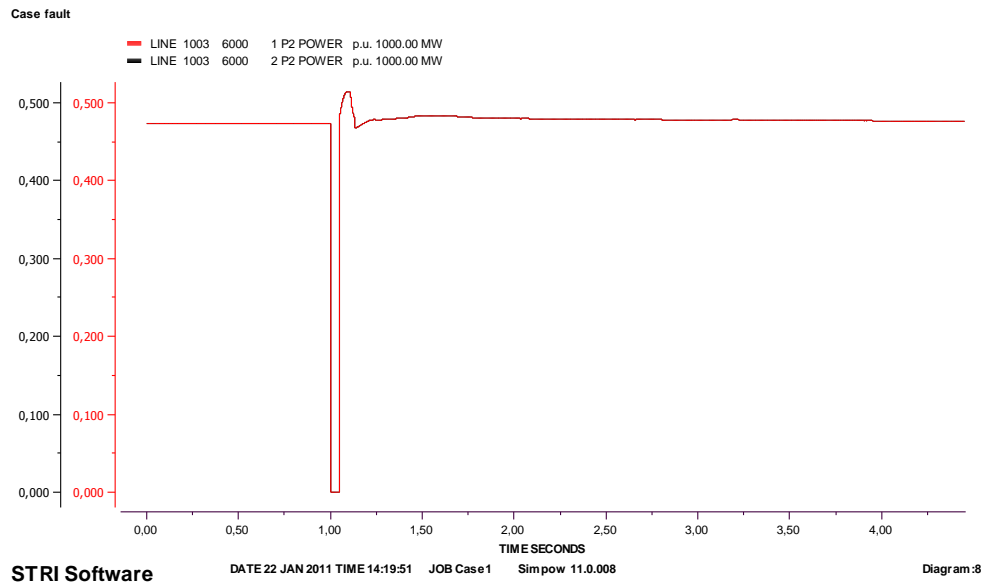


Figure 109 Case 4: Active power transfer between offshore and onshore

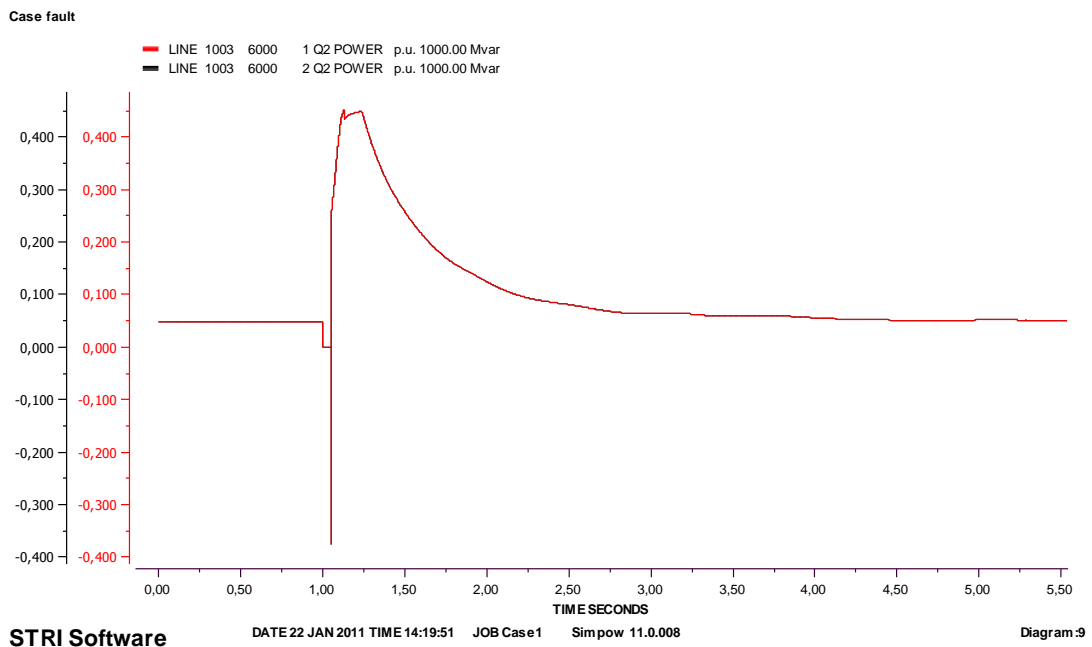


Figure 110 Case 4: Reactive power transfer between offshore and onshore

7.6 CASE 5: HVAC – STOP OF PRODUCTION OF 6100

In this case, the production of bus 6100 is stopped. Bus 6100 is located in Vestlandet and connected to bus 6000. Thus, the main link between bus 5600, where the wind farm is connected, and bus 6100 is bus 6000. The generator on bus 6100 was producing 2346 MW which is approximately the same amount than bus 5600 but twice the production on bus 6000.

The voltage at the FPCWT bus is shown in Figure 111. As soon as the generator is disconnect, the FPCWT experiences oscillations up to 0.00065 p.u. which is less than 2 Volts. Then, the system tends to stabilize after five seconds but oscillates again since the overall system fails to stabilize.

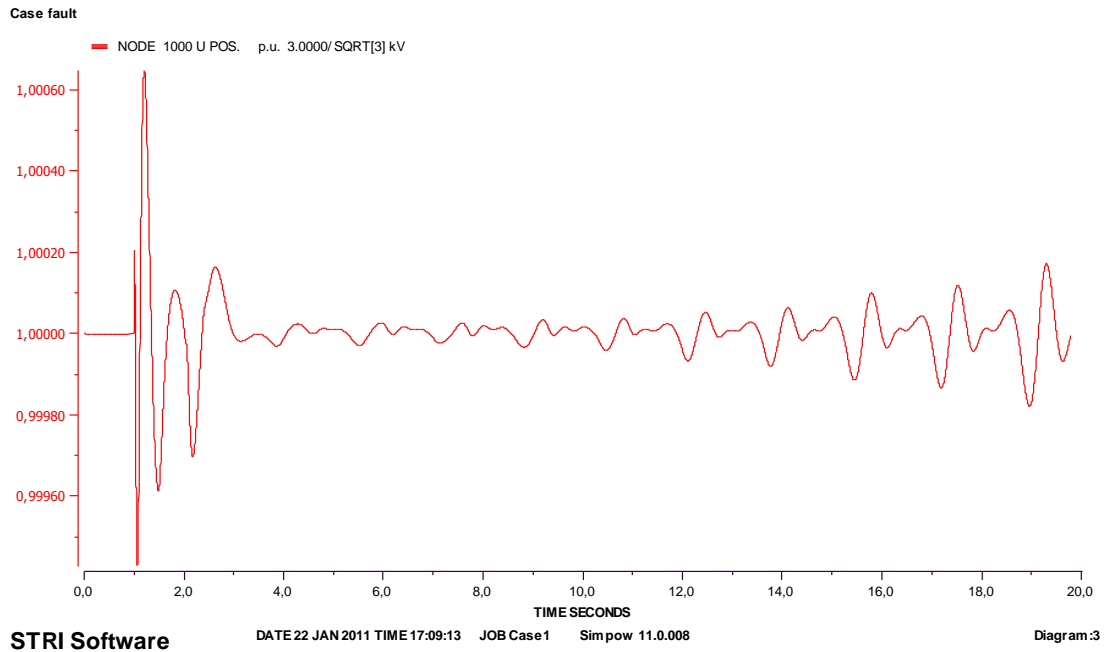


Figure 111 Case 5: Voltage on bus 1000

Figure 112 is the voltage on busses 1003 and 5600. Right after the fault, the voltages drop to 0.88 p.u. before the voltage control starts to act. The difference in voltage between both voltages is enlightened after the fault is applied due to oscillations. The voltages fail to stabilize.

Figure 113 is the voltage on the swing bus of the grid. The oscillations that increase constantly on magnitude prove that the system is totally unstable.

Case fault

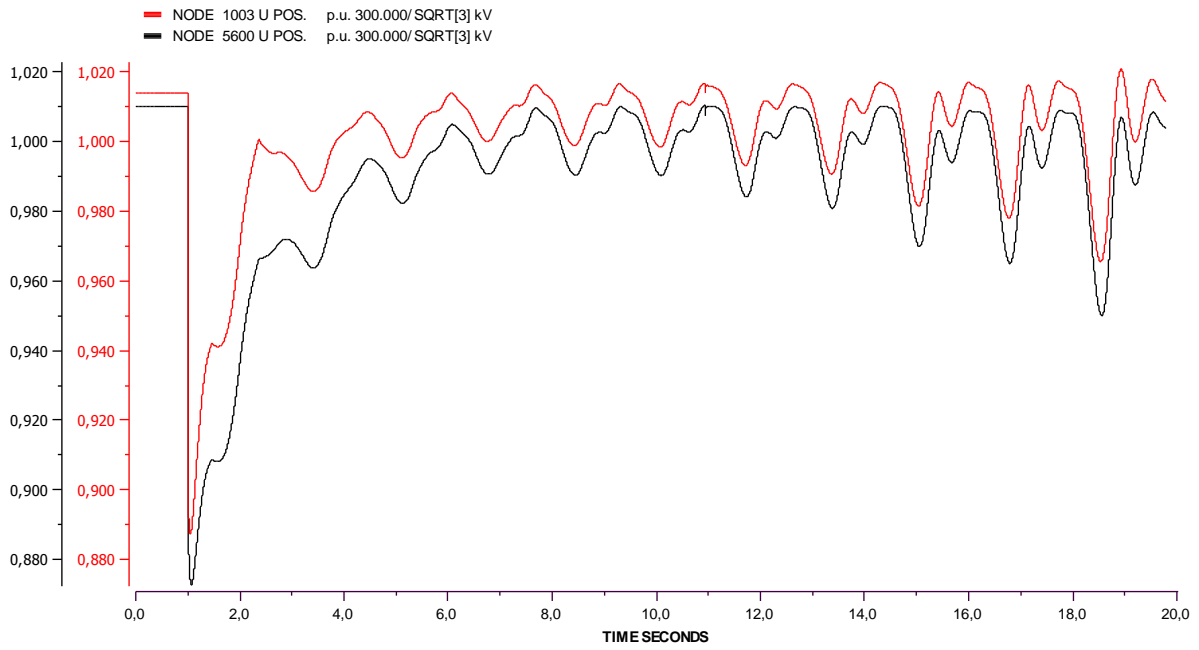


Figure 113 Case 5: Voltage on busses 1003 and 5600

Case fault

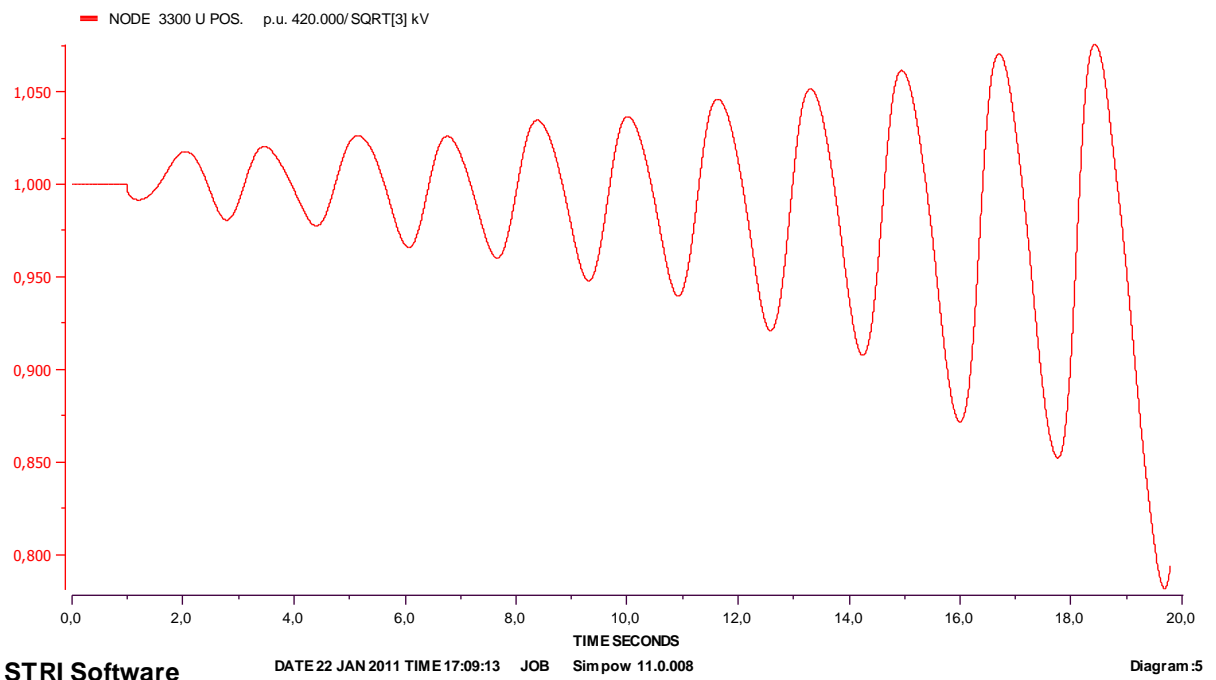


Figure 112 Case 5: Voltage on bus 3300

Figure 114 is the mechanical power of the FPCWT. It doesn't stabilize after the fault is connected but the changes during the first twenty seconds of the simulation are small, up to 0.00005 p.u.

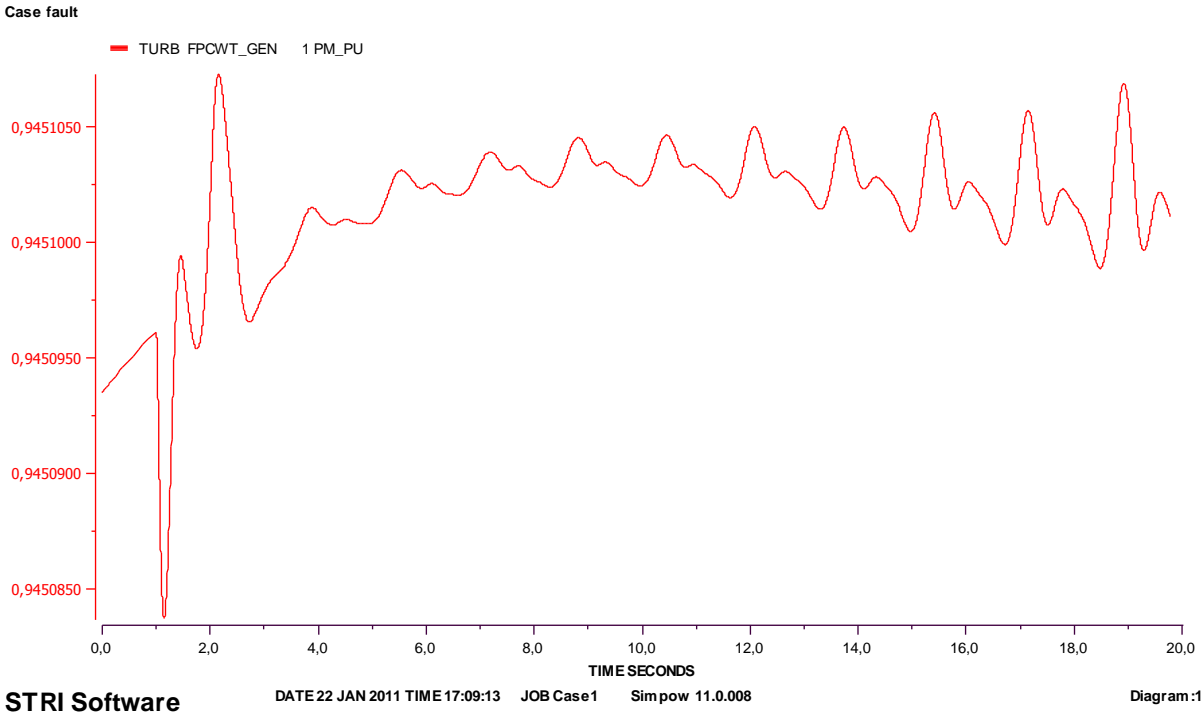
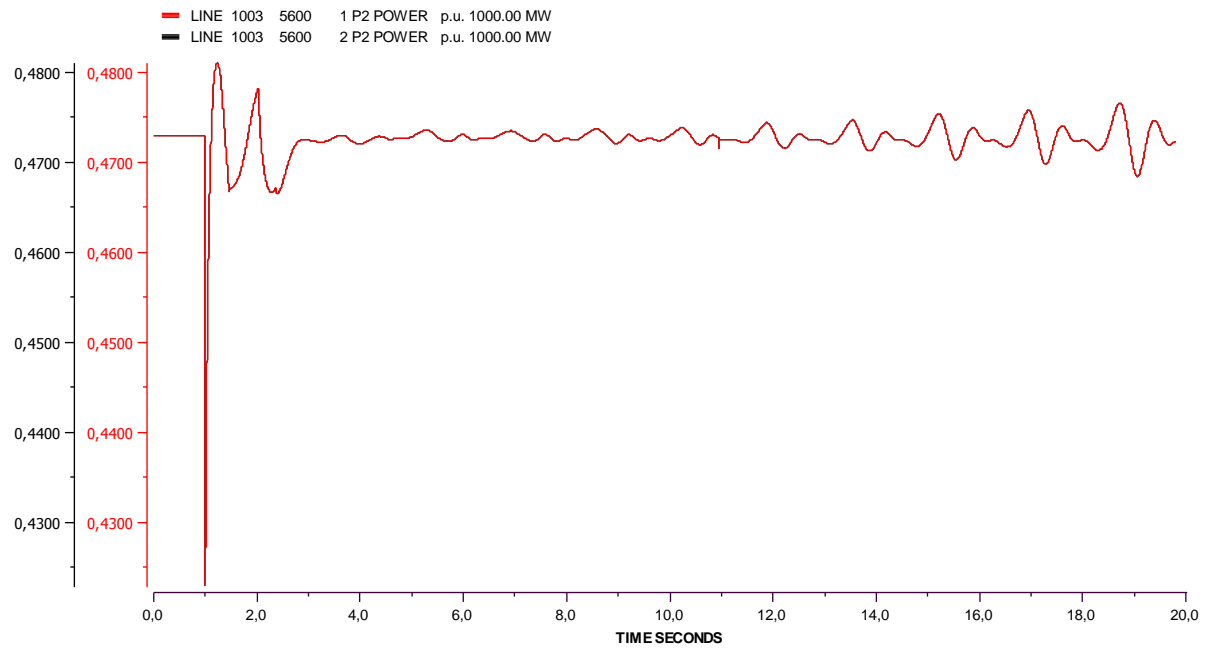


Figure 114 Case 5: Mechanical power of the FPCWT

Figure 115 shows the active power exchange between the offshore and onshore busses. There is drop of 0.05 p.u. after the fault is connected. The overshoot is not as high as in previous examples but the active power does not succeed to stabilize even if after two seconds, the 5% time response was achieved.

The reactive power transfer is shown in Figure 116. Maximum values obtained right after the fault, when the system tries to react as fast as possible, are equal to the one found in previous cases. However, instead of being able to stabilize right after the first overshoot, the reactive power exchange oscillates and fails to remain stable.

Case fault



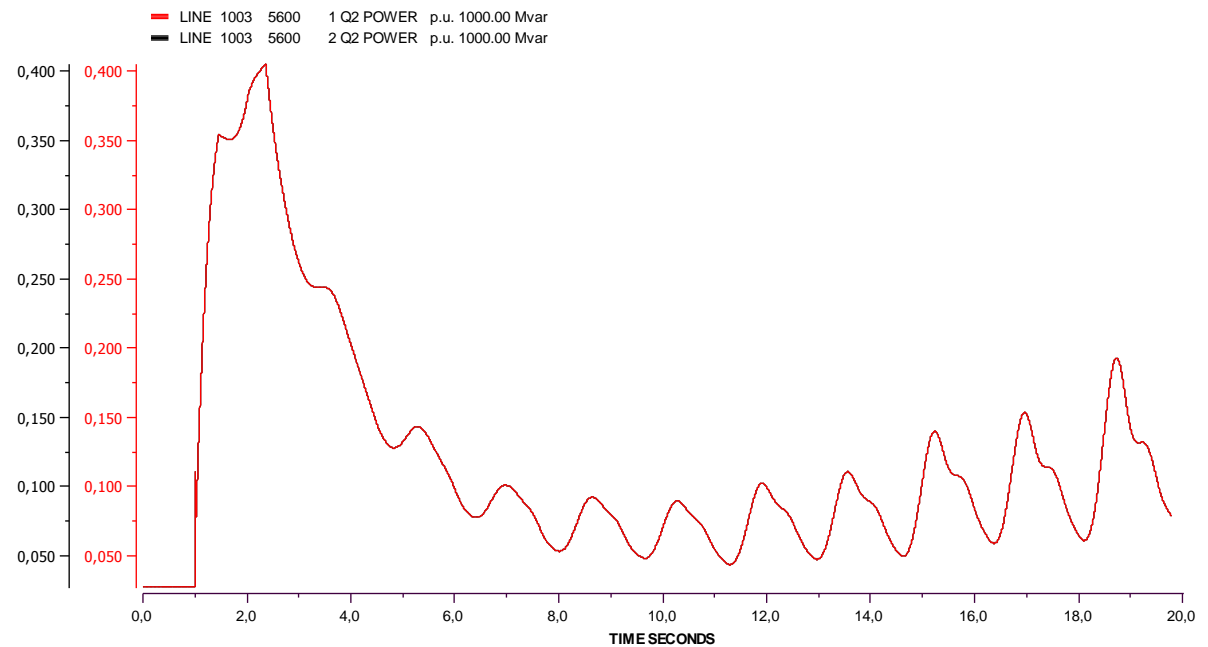
STRI Software

DATE 22 JAN 2011 TIME 17:09:13 JOB Simpow 11.0.008

Diagram:6

Figure 115 Case 5: Active power transfer between the offshore and onshore busses

Case fault



STRI Software

DATE 22 JAN 2011 TIME 17:09:13 JOB Simpow 11.0.008

Diagram:7

Figure 116 Case 5: Reactive power transfer between the offshore and onshore busses

7.7 CASE 6: HVAC – DISCONNECTION OF A LINE

In this case, the wind farm is connected to bus 5600. A 50 ms 3PSG is performed as in case 2 but line 2 between busses 1003 and 5600 is disconnected after the fault is cleared. The FPCWT voltage, mechanical power and speed are similar to the ones found in case 2.

The voltages of the offshore and onshore busses are shown in Figure 117. They are similar to the one found in case 2 but there is a small oscillation at $t=1.95$ s but it is negligible and disappears after.

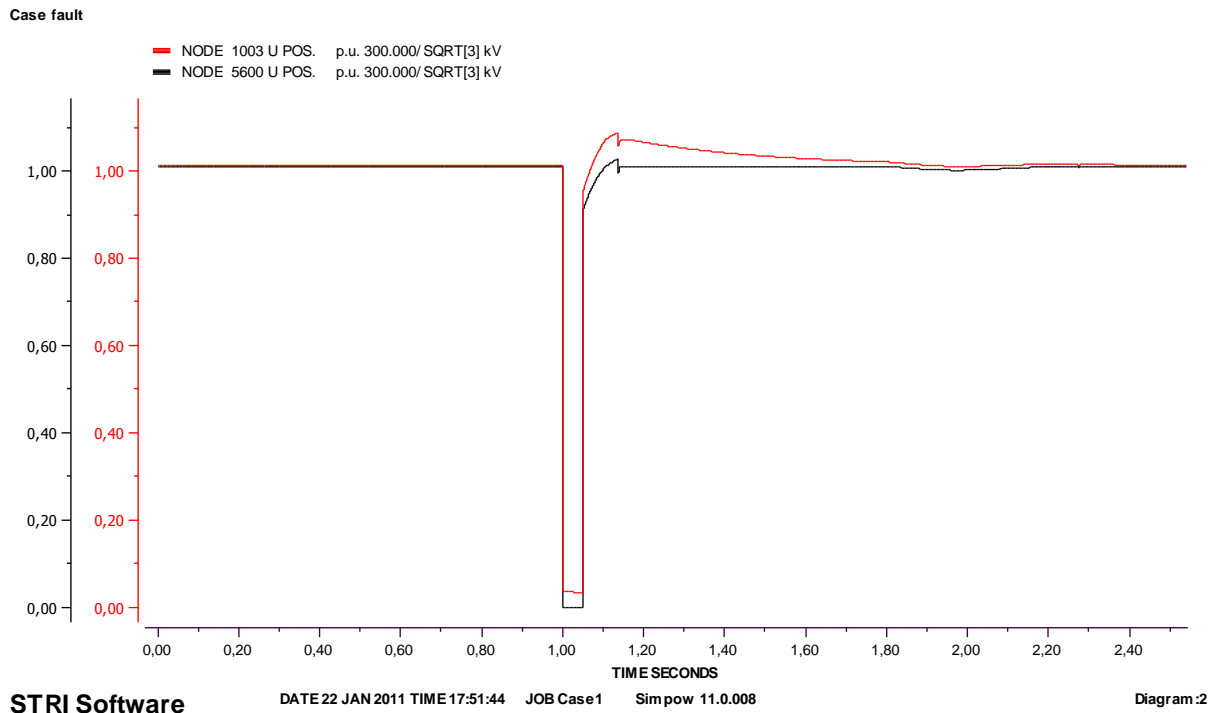
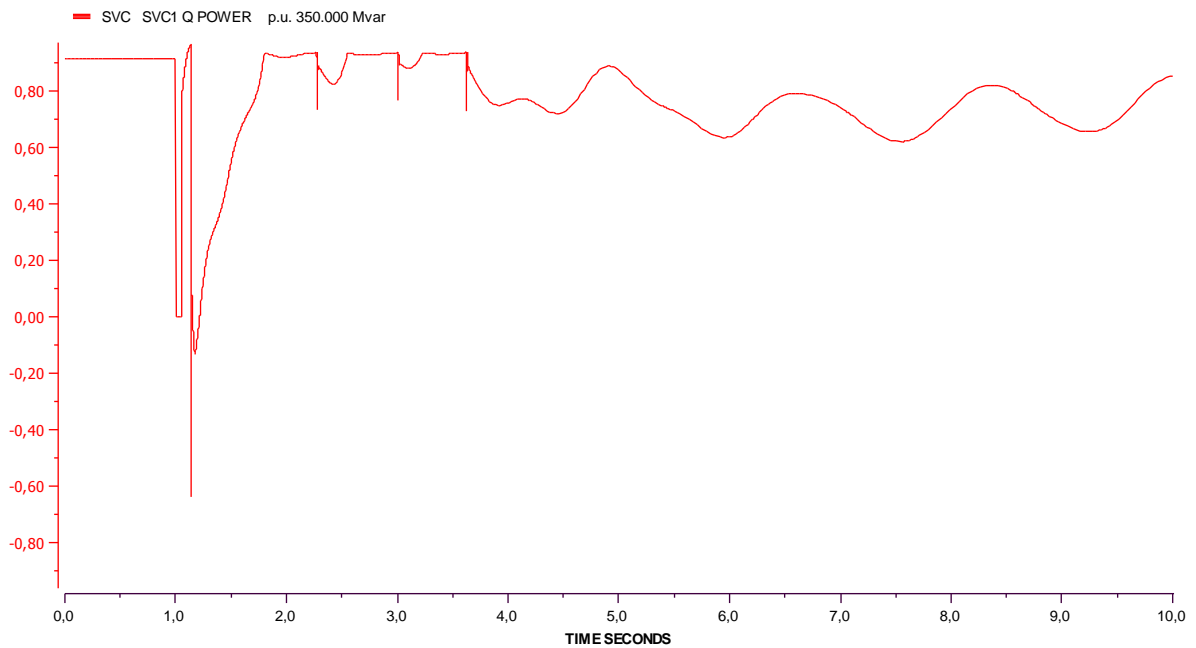


Figure 117 Case 6: Voltages on busses 1003 and 5600

Figure 118 shows the reactive power of the SVC. As one line is disconnected, the amount of reactive power the SVC has to absorb is lower than in case 2. It is here -0.1 p.u. but it is -0.8 p.u. in case 2 just after the fault. However, the amount of reactive power injected to the grid by the SVC oscillates around 0.8 p.u. instead of 0.3 p.u. in case 2. Thus, more reactive power is injected into the grid and to the wind farm as it will be seen on the line that is connected.

Figure 119 is the active power exchange between the offshore and onshore busses. As line 2 is disconnected after the fault is cleared, it can't transfer any power. The amount of power line 1 has to transmit is thus doubled and has exactly the same behaviour than in case 2.

Case fault



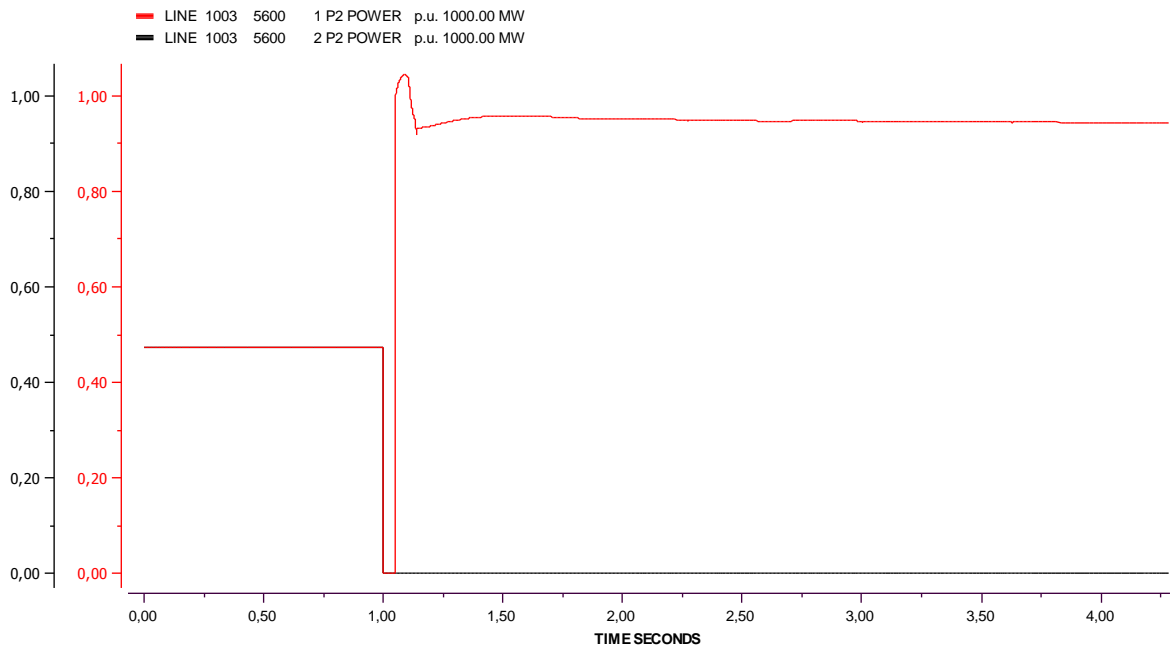
STRI Software

DATE 22 JAN 2011 TIME 17:51:44 JOB Case1 Simpow 11.0.008

Diagram :3

Figure 118 Case 6: Reactive power at the SVC

Case fault



STRI Software

DATE 22 JAN 2011 TIME 17:51:44 JOB Case1 Simpow 11.0.008

Diagram :6

Figure 119 Case 6: Active power exchange between the offshore and onshore busses

The reactive power exchange between the offshore and onshore busses is shown in Figure 120. The maximum of reactive power after the fault is cleared is obtained at the same time than in case 2 but it is higher by 0.2 p.u. since line 2 is disconnected. However, after the stabilization at time $t=3.5$ s, the reactive power flow is reversed and the wind farm consumes reactive power instead of producing. This is because line 1 takes all the power.

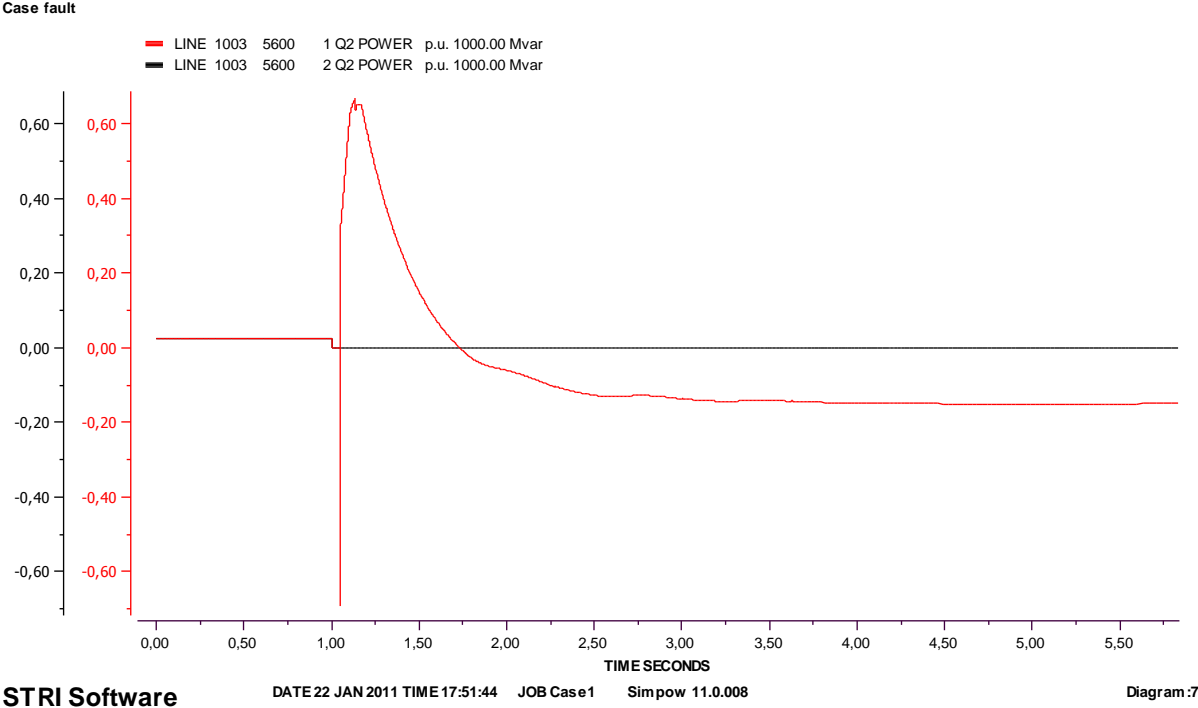


Figure 120 Case 6: Reactive power exchange between the offshore and onshore busses

7.8 CASE 7: HVDC – 3PSG ON 5600 FOR 185 ms

This case is the same than case 1 but the connexion of the wind farm is achieved with HVDC Light, over a longer distance, instead of HVAC.

Figure 121 shows the voltage on the FPCWT. It is not changed during the time of the simulation and so is the mechanical power and the speed. Figure 122 is the AC voltages on the onshore and offshore side. The onshore voltage is the same than in case 1, it is not influenced by the fact that the FPCWT is connected in HVAC or HVDC. However, the offshore voltage is dropping by 0.05 p.u. for a very limited time during the fault and then remains stable. This phenomenon along with the constant voltage on Figure 121 tends to prove that the PWM converters of the HVDC Light module are interfering considerably on voltage regulation.

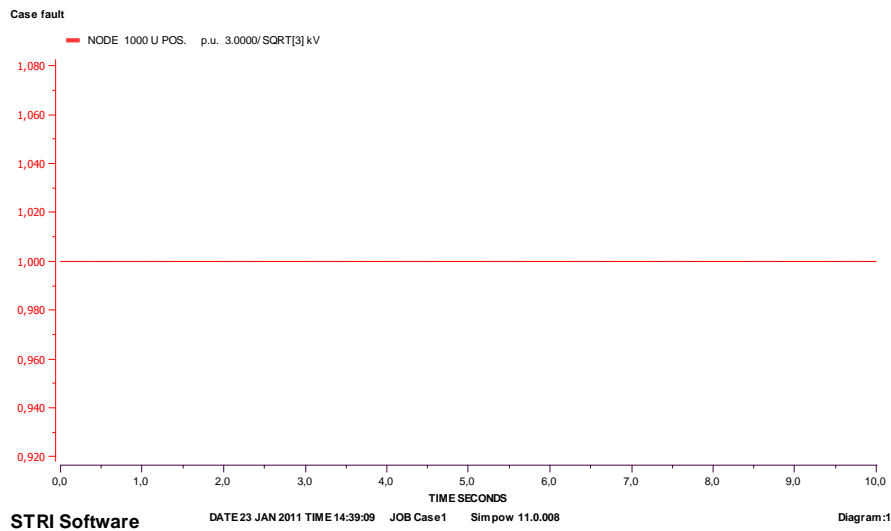


Figure 121 Case 7: Voltage on the FPCWT bus

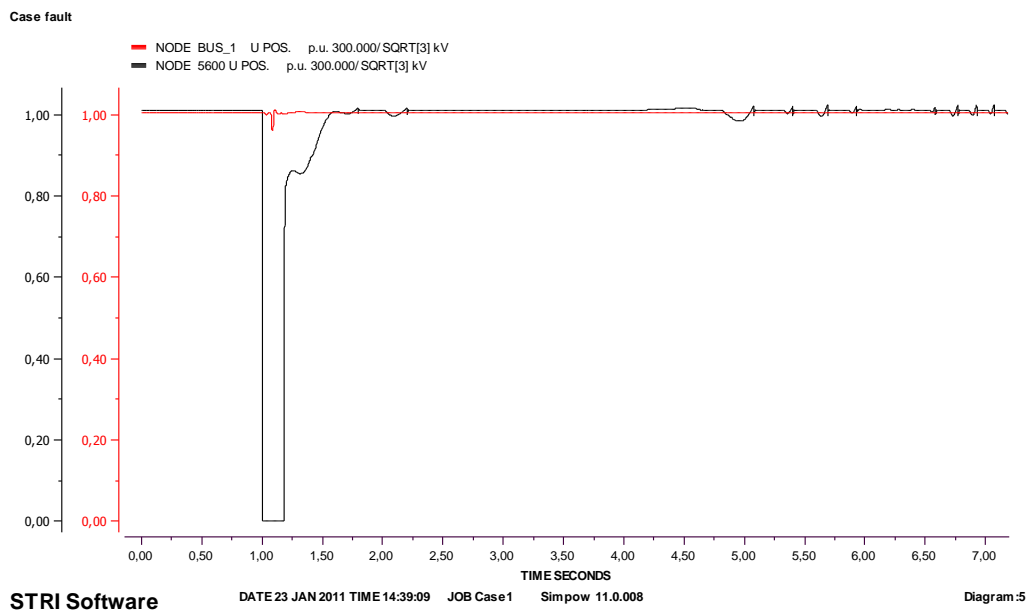


Figure 122 Case 7: Voltage on busses 1003 and 5600

Figure 123 is the SVC reactive power. It shows the same behaviour than in case 1. The same oscillations are observed. In case 1 and 7, the wind farm is exporting between 250 and 300 Mvar of reactive power. Thus, the reactive power seen from bus 5600 and from the SVC is not different.

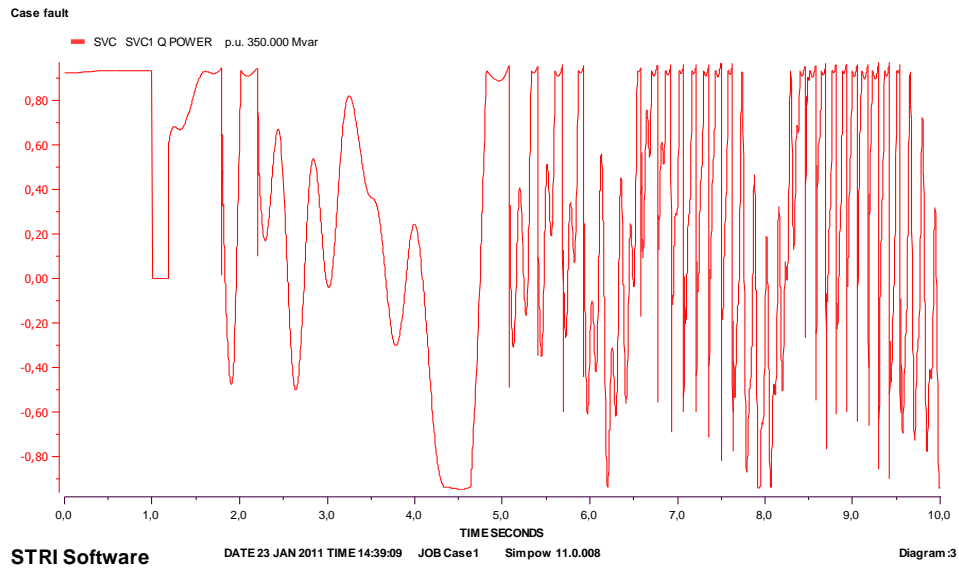


Figure 123 Case 7: Reactive power at the SVC

Figure 124 is the active power exchange in the DC lines. A strange behaviour occurs since during the fault, the power flow reverses to -0.1 p.u. The converter in DC voltage control mode is the one located on the grid side. It is controlling the active power into or out of the AC grid in such a way that the DC system voltage is kept to a constant level. Thus the voltage seen in Figure 122 is kept constant by shortly reversing the power flow. Then the power stabilizes in 0.3 s. However, there is a small increase in power passed 10 s that is explained in case 8. There is no reactive power in the cables; it is taken care by the PWM converter who tried to maintain the AC voltage level.

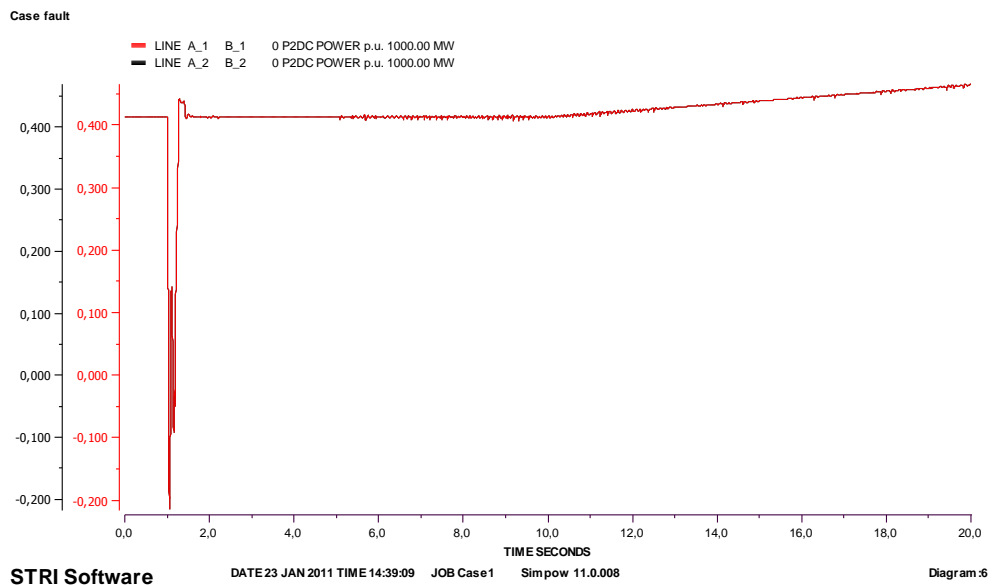


Figure 124 Case 7: Active power transfer in the DC lines

7.9 CASE 8: HVDC – STOP OF PRODUCTION OF 6100

This case is similar to case 5, except that the connexion of the wind farm to the grid is performed in HVDC. As in case 7, the voltage, speed and power of the FPCWT are constant.

Figure 125 is the DC power of the HVDC Light PWM converter on the grid side. When the production is stopped on bus 6100, oscillations are noticeable until $t=1.6$ s. Then, the DC power seems to be stabilized and the disconnection seems to have no effect on the load flow between the wind farm and bus 5600. However, at $t=10$ s, a magnitude increase of the power can be noticed. In the PWM converter on the wind farm side, a reference number of the set-values of the active power control curve are given in the dynamic file. At $t=20$ s, the reference value of the power is slightly changed to 0.9 instead of the previous 0.8 registered at $t=10$ s. Thus, there is a 0.1 p.u. change from $t=10$ s to $t=20$ s that can be seen in Figure 126. As a result, the other converter observed in Figure 125 registers the same change.

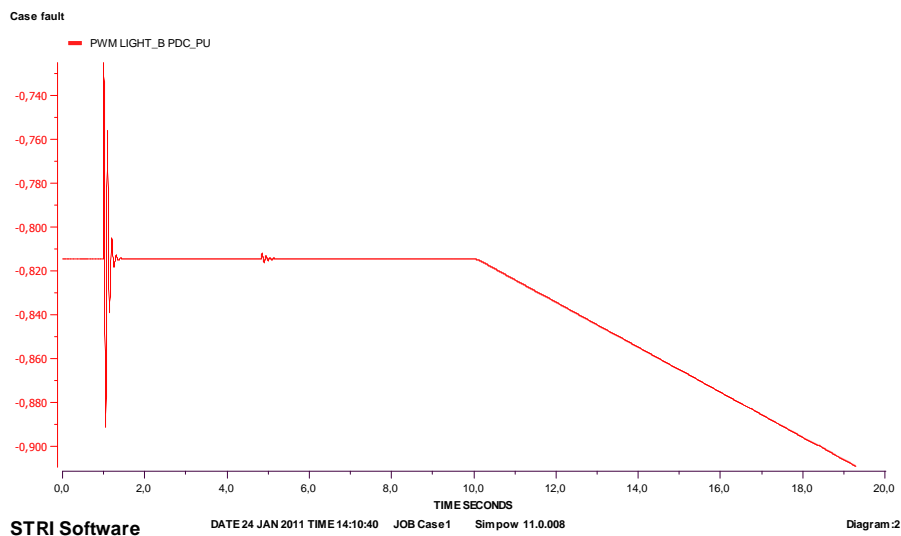


Figure 125 Case 8: DC power on grid-side PWM converter

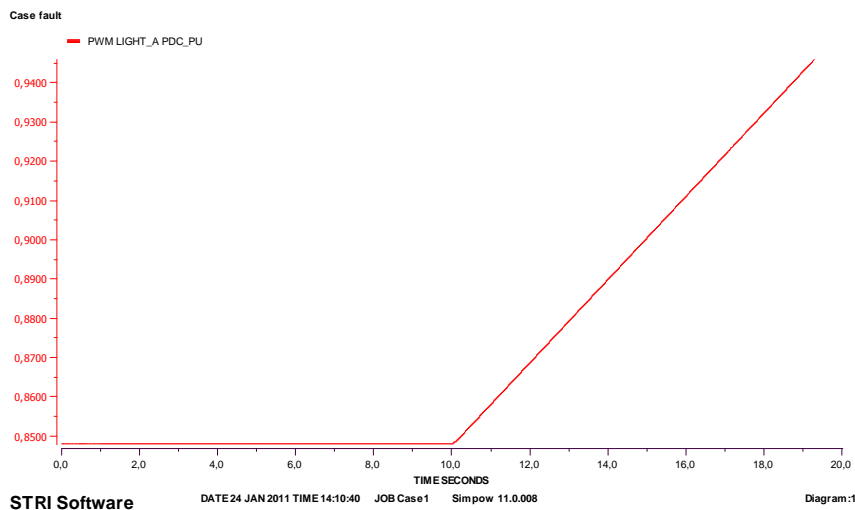


Figure 126 Case 8: DC power on FPCWT-side PWM converter

Figure 127 is the AC voltages on offshore and onshore busses. The onshore bus has the same behaviour than in case 5 except that the oscillations passed $t=4s$ are of a lesser magnitude. The voltage on the AC offshore bus is not perturbed by the disconnection. It is the consequence of the power observed in Figure 126, there is no perturbation observed in the PWM converter to which the AC bus is connected.

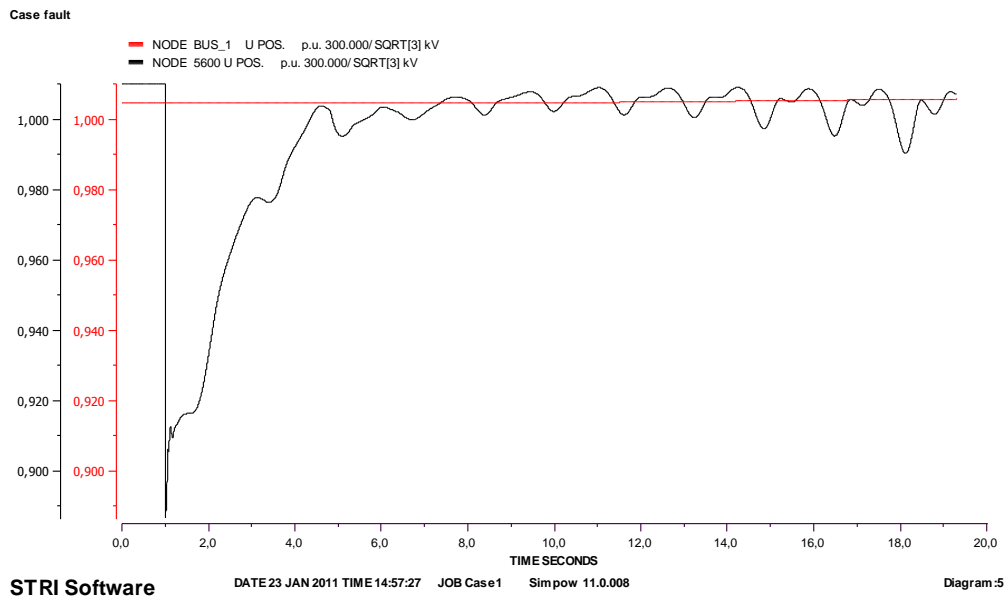


Figure 127 Case 8: Voltages on the offshore and onshore busses

Figure 128 is the reactive power at the SVC. After the disconnection, there is a drop of 0.1 p.u. The 5% time response is equal to 2.3 s and the SVC stabilizes totally to the pre-fault value.

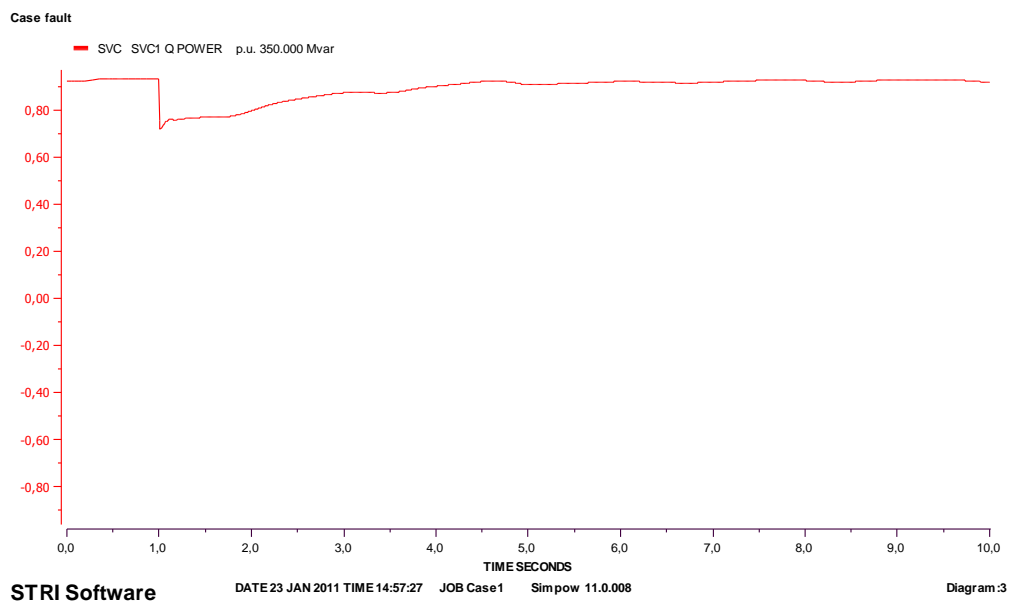


Figure 128 Case 8: Reactive power at the SVC

8 DISCUSSION

HVAC and Voltage Sourced Converters based HVDC transmissions have been implemented on a simplified grid model to connect a large offshore wind farm. The grid should be represented in reality by thousands of nodes. Moreover, the wind farm should not be an aggregated model but about 300 to 500 wind turbines interconnected with different offshore platforms with detailed converters and transformers. This lack of precision is mainly due to a lack of time for the duration of this thesis but also due to ease the work of simulations. However, the model and the simulations can serve as a basis for future works regarding integration of a large scale offshore wind farm to the Norwegian grid.

The HVAC connection in Sørlandet (bus 5600) served as a basis to compare to the other cases. In case 2, for a 50 ms three-phase fault to ground, the low voltage ride through requirements of Statnett's grid code were respected. The wind turbine is not disconnected and supports the grid with reactive power instead.

The 185 ms fault corresponds to the critical clearing time. Thus, beyond this point, a generator of the grid will automatically step out of phase because it will not have enough time to recover from the fault. The results on the SVC are relevant and show that the system is unstable by the end of the twenty seconds simulation. The voltage is regulated but not cleaned and the speed of the wind turbine has not reached a stable state. The results were awaited by implementing such a long fault.

The 5 ms fault shows that the system is stable and does not suffer at all from small faults. The post-fault values are reached in a very short time compared to the 50 ms or the 185 ms fault. Moreover, the post-fault values are equal to the pre-fault values, as if nothing had happened.

The HVAC connection in Vestlandet (bus 6000) shows a similar behaviour to faults compared to the connection in Sørlandet since the wind farm and the connexion are the same. However, it can be observed that the results are smoother in the case in Sørlandet. As the generation is two times bigger on bus 5600 than on bus 6000, it seems that the system is more stable when connected to bus 5600. Bus 5600 is less dependent on the wind farm.

The VSC-HVDC connection shows similar results from the grid side than the HVAC connection. On the offshore wind farm bus, some differences can be noticed: the wind farm voltage is much more stable and seems to be totally protected from variations on the grid thanks to the PWM converters. A disconnection of a line on the HVDC link is not possible since both lines are required to operate the PWM converters. Thus, this case has not been studied. Moreover, the connexion in HVDC to Vestlandet has not been computed in this thesis since it gave similar results to the HVAC connexion.

9 CONCLUSION AND FUTURE WORK

Norway mainly exports electricity, especially during the summer because most of it comes from hydro power and dams are often full in this season. During the winter a high increase in power demand is registered, which is due to its location in Northern Europe. Last winter, in 2009-2010, was rough and thus Norway had to import up to 3000 MWh/h peak at certain time. Thus, new generation units are necessary for the growth of Norway.

Onshore wind power sites are fully exploited nowadays and it leads to implementations of wind farm off the shores, in shallow regions. Where the depth does not exceed 20 meters, the estimated potential for offshore wind generation is 6 000 to 30 000 MW with distances from 1 to 10 km. If large scale offshore wind power farms have to be made, they should be implemented further away from the coast, where the wind is even more stable and where the areas are larger. However, it requires foundations for depth of more than 50 km and further developments are needed in this field.

Improvements have been made regarding generators and converters in the wind turbine and as large wind turbines could be very efficient if placed offshore. Improvements have also been made regarding HVDC connexion because converter stations are not easily installed offshore, they are expansive and bulky. Improvements are made to increase their rating and thus reduce the number of cables and platforms needed. The capacity of HVAC and VSC based HVDC transmission technologies are low compared to LCC based HVDC but research is on the way to improve the ratings. For now, LCC based HVDC is the most economical way to connect a wind farm of 1000 MW to the grid but VSC based HVDC is being constantly improved and should replace LCC based HVDC.

The integration of a 1000 MW offshore wind farm to the grid has been studied. Four configurations were simulated: a 50 km HVAC connexion in Sørlandet and Vestlandet and a 100 km VSC based HVDC connexion in Sørlandet and Vestlandet. First the grid model had to be made in order to fit the simulation software. Then, the aggregated wind farm model had to be created. Finally, the connexions with converters, cables and transformers had to be made according to the ratings of the system and the grid code requirements.

The HVAC configuration showed 4.54% losses between the aggregated wind turbine and the connection bus on the grid. The HVDC configuration showed 7.97% losses. However, line losses are accounted and the HVDC configuration has two more PWM converters compared to the HVAC configuration.

Dynamic simulations have proven that the models were acting correctly regarding the grid code requirements. Voltages are automatically regulated and reactive power is taken care. The HVAC cases have shown that reactive power is important and even more compensating equipments should be installed on the model. The wind farm connected with VSC based HVDC cases have shown the independence created by the HVDC link so that if a problem occurs on the grid side, the wind farm is poorly impacted. The converters are very important in this configuration since the onshore converter is contributing to the stabilization of the grid after the fault.

The results of the simulation show that it is possible to install a large offshore wind farm in Norway in the two areas that were tested. The grid code can be respected but reactive power compensation has to be taken care of.

A more detailed wind farm should be implemented instead of such a big aggregation. Five platforms of 200 MW each at different distances would be more realistic. Moreover, the VSC based HVDC model is too basic and suffers from imprecision. A LCC based HVDC model is available in SIMPOW and could be tested instead. Thus, a comparison between both HVDC models could be developed. The grid model could be made more precise also, especially in Norway, in order to see the influence of the wind farm on more specific regions. Implementing a wind farm on a strong bus as in the cases of this thesis is not the same than on smaller busses.

REFERENCES

1. **European Patent Office.** The Story Behind: Offshore Wind Energy. [Online] 18 August 2008. <http://www.epo.org/topics/innovation-and-economy/european-inventor/inventions/2008/wind-energy.html>.
2. **Syndicat des énergies renouvelables.** L'énergie éolienne en mer. [Online] May 2010. www.enr.fr.
3. **European Wind Energy Association.** The European Offshore Wind Industry -key, trends and statistics 2009. [Online] January 2010. www.ewea.org.
4. **Magnus Korpås, Thomas Trötcher, John Olav Giæver Tande.** *Integration of large-scale offshore wind power in the Norwegian power system.* s.l. : SINTEF Energy Research, 2007.
5. **U.S. Department of Energy.** Wind Power Today. [Online] 2010. www.nrel.gov.
6. **OWEC Tower AS.** [Online] 2010. www.owectower.no.
7. **P. Schaumann, P. Kleineidam and F. Wilke.** *Fatigue Design bei Offshore-Windenergie-anlagen.* s.l. : Ernst & Sohn, 2004.
8. **Danish Wind Industry Association.** Offshore Foundations: Mono Pile. [Online] 10 May 2003. www.windpower.org.
9. **European Network of Transmission System Operators for Electricity.** *Impact of increased amounts of renewable energy on Nordic power system operation.* 2010.
10. —. *Annual report of Nordel.* 2008.
11. **Bonneville Power Administration.** The Skagerrak HVDC Scheme. [Online] <http://web.archive.org/web/20050802085143/www.transmission.bpa.gov/cigresc14/Compendium/SKAGERR.htm>.
12. **Nordel.** *Nordic Grid Code (Nordic collection of rules).* 2007.
13. **Kjeller Vindteknikk.** Vindkart for Norge. [Online] 2010. <http://www.vindteknikk.no/>.
14. **Statkraft.** Wind power. [Online] 2010. www.statkraft.no.
15. **Norges vassdrags- og energidirektorat.** Energistatus av vindkraft. [Online] 22 03 2009. www.nve.no.
16. **K. Hofstad and L. Tallhaug.** *Vindkraftpotensialet utenfor norskekysten (offshore).* s.l. : Norges vassdrags- og energidirektorat, 2009.
17. **J.F. Manwell, J.G. McGowan and A.L. Rogers.** *Wind Energy Explained: Theory, Design and Application.* s.l. : Wiley, 2002.
18. **Siemens AG.** Siemens Wind Turbine SWT-2.3-82 VS. [Online] 2009. www.energy.siemens.com.

19. **Danish Wind Industry Association.** Proof of Betz' Law. [Online] 2003. www.windpower.org.
20. **REUK.** Wind Turbine Tip Speed Ratio. [Online] 6 March 2007. www.REUK.co.uk.
21. **The European Wind Energy Association.** *Large Scale Integration of Wind Energy in the European Power Supply: Analysis, Issues and Recommendations.* 2005.
22. **Kjetil Uhlen.** *Wind Power: Technology Control, System Integration (Basic Dynamic Modelling).* s.l. : SINTEF Energy Research, 2009.
23. **IEEE/CIGRE Joint Task Force.** *Definition and Classification of Power System Stability.* s.l. : IEEE Transactions On Power Systems, 2004.
24. **Global Wind Energy Council.** Global wind capacity to reach close to 200 GW this year. [Online] 23 September 2010. www.gwec.net.
25. **C. Eping, J. Stenzel, M. Pöller and H. Müller.** *Impact of Large Scale Wind Power on Power System Stability.* s.l. : DigSILENT GmbH, 2005.
26. **G. Di Marzio, O. Fosso, K. Uhlen and M. Pålsson.** *Large-scale wind power integration, voltage stability limits and modal analysis.* Liege : PSCC, 2005.
27. **Dunsheath, P.** *A History of Electrical Power Engineering.* Cambridge, MA : The M.I.T. Press, 1962.
28. **Public Broadcasting Service.** Tesla, Life and Legacy - War of the Currents. [Online] www.pbs.org.
29. **Black, R. M.** *The History of Electric Wires and Cables.* London : Peter Peregrinus Ltd, 1983.
30. **Lundberg, S.** *Configuration study of large wind parks.* Göteborg : Department of Electric Power Engineering, Chalmers University of Technology, 2003.
31. **T. Toftevaag.** *Grid Connection of Wind Farms.* s.l. : SINTEF Energiforskning AS, 2009.
32. **McAllister, E. W. G. Bungay and D.** *Electric cables handbook.* s.l. : Oxford, 1990.
33. **F. Kiessling, P. Nefzger, J.F. Nolasco and U. Kaintzyk.** *Overhead Power Lines: Planning, Desing, Construction.* s.l. : Springer, 2003.
34. **ABB.** *Submarine Power Cables.*
35. **Worzyk, T.** *Submarine Power Cables: Design, Installation, Repair, Environmental Aspects.* s.l. : Springer, 2009.
36. **Fujikura America Inc.** High & Low Pressure Fluid Filled Extra High Voltage Cables. [Online] www.fujikura.com.
37. **Shanklin, G .B.** *Low-, Medium-, and High-Pressure Gas-Filled Cable.* s.l. : AIEE, 1942.
38. **Pabla, A. S.** *Electric Power Distribution.* s.l. : Tata McGraw-Hill, 2004.
39. **US Army Corps of Engineers.** *Environmental Impact Statements, Environmental Impact Review and Development of Regional Impact for Cape Wind Project.* s.l. : New England District, 2004.

40. **K. Eriksson, P. Halvarsson, D. Wensky and M. Häusler.** *System Approach on Designing an Offshore Windpower Grid Connection.* s.l. : J. Matevosyan and T. Ackermann, 2003.
41. **Ackermann, T.** *Wind Power in Power Systems.* s.l. : J. Wiley and Sons, 2005.
42. **I. M. De Alegria, J. L. Martin, I. Kortabarria, J. Andreu and P. I. Ereno.** *Transmission Alternatives for Offshore Electrical Power. Renewable and Sustainable Energy Reviews.* Elsevier, 2009.
43. **Bahrman, M. P.** *HVDC Transmission Overview.* s.l. : IEEE, 2008.
44. **ABB.** *Technical Description of HVDC Light (R) Technology.* 2008.
45. **SIMPOW.** *User Manual.* s.l. : STRI AB, 2006.
46. **Siemens Energy Inc.** *PSS[®]E Model Library.* s.l. : Siemens, 2009.
47. **Vestas.** V112-3.0 MW Offshore. [Online] www.vestas.com.
48. **Achilles, M. Pöller and S.** *Aggregated Wind Park Models for Analyzing Power System Dynamics.* s.l. : DlgSILENT GmbH, 2003.
49. **ABB.** *XLPE Submarine Cable Systems.*
50. —. *HVDC Light Cables.* 2006.
51. **J. Machowski, J. W. Bialek and J. R. Bumby.** *Power System Dynamics: Stability and Control.* s.l. : Wiley, 2008.

APPENDIX

APPENDIX A: DEFAULT CP CURVES OF THE FPCWT

$\beta=0$ deg.

λ [p.u.]	Cp[p.u.]
0.	0.00
1.	0.01
2.	0.05
3.	0.08
4.	0.28
5.	0.42
6.	0.48
6.5	0.49
7.	0.50
7.5	0.504
8.	0.50
8.5	0. 9
9.	0.48
10.	0.47
11.	0.45
12.	0.42
13.	0.39
14.	0.35
15.	0.30
16.	0.25
17.	0.19
18.	0.11
19.	0.06
20.	0 00

Table 1. Default values of the Cp/ λ -curve at $\beta=0$ deg.

$\beta=1$ deg.

λ [p.u.]	Cp[p.u.]
0.	0.00
1.	0.01
2.	0.03

3.	0.08
4.	0.26
5.	0. 0
6.	0.44
6.5	0.46
7.	0.47
7.5	0.48
8.	0.47
8.5	0.46
9.	0.45
10.	0.44
11.	0.43
12.	0.40
13.	0.37
14.	0 33
15.	0.28
16.	0.23
17.	0.18
18.	0.11
19.	0.05
19.5.	0.00

Table 2. Default values of the C_p/λ -curve at $\beta=1$ deg.

$\beta=3$ deg.

λ [p.u.]	C_p [p.u.]
0.	0.00
1.	0.01
2.	0.04
3.	0.10
4.	0.25
5.	0.37
6.	0.42
6.5	0.43
7.	0.44
7.5	0.45
8.	0.44
8.	0.43

9.	0.42
10.	0.41
11.	0.40
12.	0.39
13.	0.36
14.	0.32
15.	0.27
16.	0.22
17.	0.15
18.	0.08
19.	0.00

Table 3. Default values of the C_p/λ -curve at $\beta=3$ deg.

$\beta=5$ deg.

λ [p.u.]	C_p [p.u.]
0.	0.00
1.	0.02
2.	0.05
3.	0.15
4.	0.26
5.	0.34
.	0.37
6.5	0.38
7.	0.38
7.5	0.38
8.	0.37
8.5	0.36
9.	0.35
10.	0.32
11.	0.29
12.	0.25
13.	0.18
14.	0.11
15.	0.03
15.5	0.00

Table 4. Default values of the C_p/λ -curve at $\beta=5$ deg.

$\beta=7$ deg.

λ [p.u.]	C_p [p.u.]
0.	0.00
1.	0.02
2.	0.05
3.	0.
4.	0.26
5.	0.30
6.	0.31
6.5	0.31
7.	0.30
7.5	0.28
8.	0.26
8.5	0.24
9.	0.22
10.	0.16
11.	0.08
12.	0.00

Table 5. Default values of the C_p/λ -curve at $\beta=7$ deg.

$\beta=9$ deg.

λ [p.u.]	C_p [p.u.]
0.	0.00
1.	0.02
2.	0.05
3.	0.16
4.	0.23
5.	0.25
6.	0.24
6.5	0.22
7.	0.20
7.5	0.17
8.	0.14

8.5	0.10
9.	0.05
9.5	0.00

Table 6. Default values of the C_p/λ -curve at $\beta=9$ deg.

$\beta=11$ deg.

λ [p.u.]	C_p [p.u.]
0.	0.00
1.	0.03
2.	0.06
3.	0.17
4.	0.21
5.	0.20
6.	0.15
6.5	0.12
7.	0.10
7.5	0.05
.	0.00

Table 7. Default values of the C_p/λ -curve at $\beta=11$ deg.

$\beta=13$ deg.

λ [p.u.]	C_p [p.u.]
0.	0.00
1.	0.03
2.	0.06
3.	0.17
3.5	0.1
4.	0.18
5	0.13
6.	0.08
7.	0.00

Table 8. Default values of the C_p/λ -curve at $\beta=13$ deg.

$\beta=19$ deg.

λ [p.u.]	C_p [p.u.]
0.	0.00
1.	0.03
2.	0.07
3.	0.11
3.5	0.08
4.	0.01
4.5	0.00

Table 9. Default values of the C_p/λ -curve at $\beta=19$ deg.

$\beta=27$ deg.

λ [p.u.]	C_p [p.u.]
0.	0.00
1.	0.03
2.	0.07
2.5	0.07
3.	0.05
3.5	0.00

Table 10. Default values of the C_p/λ -curve at $\beta=27$ deg.

APPENDIX B: HVAC OPTPOW FILE

```
SYSTEM BASE = 1000.000 MVA.
Reduced NORDEL power system model
V 3.2, 12.08.97
**
CONTROL DATA
UBCHECK=NO
NSEP=NO
END
GENERAL
SN=1000.000
END
NODES
!
! PSS NAME
!
! Nodes within the wind farm area 10
!
1000  UB= 3.000  TYPE=AC  AREA= 10
1001  UB= 5.000  TYPE=DC  AREA= 10
1002  UB= 3.500  TYPE=AC  AREA= 10
1003  UB= 300.000 TYPE=AC  AREA= 10
!
! Nodes within area 40
!
3000  UB= 420.000 TYPE=AC  AREA= 40 ! STCKH !
3100  UB= 420.000 TYPE=AC  AREA= 40 ! STRFN !
3115  UB= 420.000 TYPE=AC  AREA= 40 ! SV-N1 !
3200  UB= 420.000 TYPE=AC  AREA= 40 ! KRLSK !
3244  UB= 300.000 TYPE=AC  AREA= 40 ! SV-M2 !
3245  UB= 420.000 TYPE=AC  AREA= 40 ! SV-M1 !
3249  UB= 420.000 TYPE=AC  AREA= 40 ! SV-N2 !
3300  UB= 420.000 TYPE=AC  AREA= 40 ! SV-SW !
3359  UB= 420.000 TYPE=AC  AREA= 40 ! SV-W !
3360  UB= 135.000 TYPE=AC  AREA= 40 ! KONT_135 !
3701  UB= 300.000 TYPE=AC  AREA= 40 ! SV-N2B !
!
! Nodes within area 51
!
5100  UB= 300.000 TYPE=AC  AREA= 51 ! EAST3 !
5101  UB= 420.000 TYPE=AC  AREA= 51 ! EAST4-A !
5102  UB= 420.000 TYPE=AC  AREA= 51 ! EAST4-B !
5103  UB= 420.000 TYPE=AC  AREA= 51 ! EAST4-C !
!
! Nodes within area 53
!
5300  UB= 300.000 TYPE=AC  AREA= 53 ! HDAL3 !
5301  UB= 420.000 TYPE=AC  AREA= 53 ! HDAL4 !
!
! Nodes within area 54
!
```

```

5400    UB= 300.000  TYPE=AC  AREA= 54 ! CNTR3-A !
5401    UB= 420.000  TYPE=AC  AREA= 54 ! CNTR4-A !
5402    UB= 420.000  TYPE=AC  AREA= 54 ! CNTR4-B !
!
! Nodes within area  55
!
5500    UB= 300.000  TYPE=AC  AREA= 55 ! CNTR3-B !
5501    UB= 420.000  TYPE=AC  AREA= 55 ! CNTR4-C !
!
! Nodes within area  56
!
5600    UB= 300.000  TYPE=AC  AREA= 56 ! SOUTH3A !
5601    UB= 420.000  TYPE=AC  AREA= 56 ! SOUTH4A !
5602    UB= 420.000  TYPE=AC  AREA= 56 ! SOUTH4B !
5603    UB= 300.000  TYPE=AC  AREA= 56 ! SOUTH3B !
!
! Nodes within area  60
!
6000    UB= 300.000  TYPE=AC  AREA= 60 ! WEST300 !
6001    UB= 420.000  TYPE=AC  AREA= 60 ! WEST400 !
!
! Nodes within area  61
!
6100    UB= 300.000  TYPE=AC  AREA= 61 ! NWEST3 !
!
! Nodes within area  65
!
6500    UB= 300.000  TYPE=AC  AREA= 65 ! MID300 !
!
! Nodes within area  67
!
6700    UB= 300.000  TYPE=AC  AREA= 67 ! NOR300 !
6701    UB= 420.000  TYPE=AC  AREA= 67 ! NOR400 !
!
! Nodes within area  70
!
7000    UB= 420.000  TYPE=AC  AREA= 70 ! SO-FIN !
!
! Nodes within area  71
!
7100    UB= 420.000  TYPE=AC  AREA= 71 ! NO-FIN !
!
! Nodes within area  90
!
8500    UB= 420.000  TYPE=AC  AREA= 90 ! SJOLLAND !
END

SREACTORS
5400  5500  NO= 81 TYPE=11 R= 0.890000E-02 X= 0.111000
END

```

PWM CONVERTERS

FPCWT_REC 1000 1001 AC2=1000
TYPE=DSL/SL/FPCWT_PWM_OPT/ SN=1060.0
UN=3.0 X=0.3 PL=0.02 MODE=1 ORDER=1000.0

FPCWT_INV 1002 1001 AC2=1002
TYPE=DSL/SL/FPCWT_PWM_OPT/ SN=1060.0
UN=3.5 X=0.3 PL=0.02 MODE=2 ORDER=5

END

SHUNT IMPEDANCES ! Line type 13,14 and 15 are translated as lines type 12.

! Corresponding GI,BI,GJ,BJ are translated as shunts !

1001 NO= 81 R= 1E6 C= 1.2381 !2.4E-3
5101 NO= 81 R= 0.00000 X= 181.034
5101 NO=810 R= 7910.31 X= 0.00000
5501 NO=811 R= 0.00000 X= -181.034
5501 NO=812 R= -8166.67 X= 0.00000
5102 NO= 81 R= 0.00000 X=-0.176397E+07
5102 NO=810 R= 882000. X= 0.00000
6001 NO=811 R= 0.00000 X= 0.176397E+07
6001 NO=812 R= 882000. X= 0.00000
5103 NO= 81 R= 0.00000 X= 13889.8
5103 NO=810 R= 441000. X= 0.00000
5301 NO=811 R= 0.00000 X= -13889.8
5301 NO=812 R= -588000. X= 0.00000
5401 NO= 81 R= 0.00000 X= 352800.
5401 NO=810 R= -882000. X= 0.00000
6001 NO=813 R= 0.00000 X= -352800.
6001 NO=814 R= 882000. X= 0.00000
5500 NO= 81 R= 0.00000 X= -69230.8
5500 NO=810 R= 300000. X= 0.00000
5603 NO=811 R= 0.00000 X= 69230.8
5603 NO=812 R= -300000. X= 0.00000

END

LINES

! See also the second LINES-chapter further below,

! containing all lines of TYPE=11.

1003 5600 NO= 1 TYPE=2 R= 0.034 X=0.1382
B=0.0000438 L= 50

1003 5600 NO= 2 TYPE=2 R= 0.034 X=0.1382
B=0.0000438 L= 50

3000 3115 NO= 81 TYPE=12 R= 0.140000E-01 X= 0.100000
B= 0.300000E-01 L= 10.00

3000 3245 NO= 81 TYPE=12 R= 0.125000E-02 X= 0.170100E-01
B= 0.127460E-01 L= 10.00

3000 3300 NO= 81 TYPE=12 R= 0.113000E-02 X= 0.170100E-01
B= 0.116380E-01 L= 10.00

3100 3115 NO= 81 TYPE=12 R= 0.301000E-02 X= 0.413800E-01
B= 0.775800E-02 L= 10.00

3100 3200 NO= 81 TYPE=12 R= 0.686000E-02 X= 0.561200E-01
B= 0.171790E-01 L= 10.00

3100 3249 NO= 81 TYPE=12 R= 0.108000E-02 X= 0.147400E-01
B= 0.105290E-01 L= 10.00

3100 3359 NO= 81 TYPE=12 R= 0.910000E-03 X= 0.119000E-01
B= 0.221700E-02 L= 10.00

3115 3245 NO= 81 TYPE=12 R= 0.300000E-02 X= 0.500000E-01
B= 0.900000E-02 L= 10.00

3115 3249 NO= 81 TYPE=12 R= 0.150000E-02 X= 0.200000E-01
B= 0.400000E-02 L= 10.00

3115 6701 NO= 81 TYPE=12 R= 0.400000E-02 X= 0.300000E-01
B= 0.500000E-02 L= 10.00

3115 7100 NO= 81 TYPE=12 R= 0.100000E-01 X= 0.700000E-01
B= 0.100000E-01 L= 10.00

3200 3300 NO= 81 TYPE=12 R= 0.125000E-02 X= 0.170100E-01
B= 0.332500E-02 L= 10.00

3200 3359 NO= 81 TYPE=12 R= 0.357000E-02 X= 0.408200E-01
B= 0.775800E-02 L= 10.00

3244 6500 NO= 81 TYPE=12 R= 0.500000E-03 X= 0.500000E-02
B= 0.100000E-03 L= 10.00

3249 7100 NO= 81 TYPE=12 R= 0.100000E-01 X= 0.700000E-01
B= 0.100000E-01 L= 10.00

3300 3359 NO= 81 TYPE=12 R= 0.740000E-03 X= 0.964000E-02
B= 0.166300E-02 L= 10.00

3300 8500 NO= 81 TYPE=12 R= 0.800000E-02 X= 0.310000E-01
B= 0.300000E-01 L= 10.00

3359 5101 NO= 81 TYPE=12 R= 0.148000E-02 X= 0.192800E-01
B= 0.360200E-02 L= 10.00

3701 6700 NO= 81 TYPE=12 R= 0.100000E-02 X= 0.100000
B= 0.500000E-03 L= 10.00

5100 5300 NO= 81 TYPE=12 R= 0.400000E-02 X= 0.400000E-01
B= 0.500000E-02 L= 10.00

5100 5500 NO= 81 TYPE=12 R= 0.180000E-02 X= 0.150000E-01
B= 0.212800E-02 L= 10.00

5100 6500 NO= 81 TYPE=12 R= 0.150000E-01 X= 0.150000
B= 0.100000E-03 L= 10.00

5101 5501 NO= 81 TYPE=12 R= 0.610000E-03 X= 0.643000E-02
B= 0.325920E-01 L= 10.00
RNO1= 810 RNO2= 812

5102 5301 NO= 81 TYPE=12 R= 0.750000E-03 X= 0.107900E-01
B= 0.128600E-01 L= 10.00

5102 6001 NO= 81 TYPE=12 R= 0.200000E-02 X= 0.350000E-01
B= 0.100000E-01 L= 10.00
RNO1= 810 RNO2= 812

5103 5301 NO= 81 TYPE=12 R= 0.170000E-02 X= 0.231200E-01
B= 0.675500E-02 L= 10.00
RNO1= 810 RNO2= 812

5400 6000 NO= 81 TYPE=12 R= 0.100000E-02 X= 0.100000E-01
B= 0.100000E-02 L= 10.00

5400 6100 NO= 81 TYPE=12 R= 0.200000E-02 X= 0.200000E-01
B= 0.120000E-02 L= 10.00

5401 5501 NO= 81 TYPE=12 R= 0.150000E-02 X= 0.200000E-01
B= 0.600000E-02 L= 10.00

5401 5602 NO= 81 TYPE=12 R= 0.154000E-02 X= 0.240600E-01
B= 0.879600E-02 L= 10.00

5401 6001 NO= 81 TYPE=12 R= 0.300000E-03 X= 0.500000E-02
B= 0.150000E-02 L= 10.00
RNO1= 810 RNO2= 814

5402 6001 NO= 81 TYPE=12 R= 0.510000E-03 X= 0.751000E-02
B= 0.235200E-02 L= 10.00

5500 5603 NO= 81 TYPE=12 R= 0.400000E-02 X= 0.450000E-01
B= 0.800000E-03 L= 10.00
RNO1= 810 RNO2= 812

5600 5603 NO= 81 TYPE=12 R= 0.201000E-02 X= 0.221100E-01
B= 0.208400E-02 L= 10.00

5600 6000 NO= 81 TYPE=12 R= 0.350000E-02 X= 0.350000E-01
B= 0.450000E-02 L= 10.00

```

5601  6001  NO= 81 TYPE=12  R= 0.137000E-02 X= 0.203100E-01
          B= 0.636400E-02 L= 10.00

6000  6100  NO= 81 TYPE=12  R= 0.220000E-02 X= 0.239400E-01
          B= 0.200000E-02 L= 10.00

6500  6700  NO= 81 TYPE=12  R= 0.800000E-02 X= 0.110000
          B= 0.100000E-02 L= 10.00

7000  7100  NO= 81 TYPE=12  R= 0.140000E-01 X= 0.100000
          B= 0.300000E-01 L= 10.00

7000  7100  NO= 82 TYPE=12  R= 0.140000E-01 X= 0.100000
          B= 0.300000E-01 L= 10.00

3359  5101  NO= 82 TYPE=12  R= 0.148000E-02 X= 0.192800E-01
          B= 0.360200E-02 L= 10.00

5300  6100  NO= 81 TYPE=12  R= 0.359000E-02 X= 0.382500E-01
          B= 0.115200E-02 L= 10.00
      NCON=1
7000  7100  NO= 83 TYPE=12  R= 0.140000E-01 X= 0.100000
          B= 0.300000E-01 L= 10.00
      NCON=1
END
TRANSFORMERS
! Transformers with TCR, i.e. with STEP, -NSTEP!
1002  1003  NO=369 SN=1060.0 UN1=3.5  UN2=300.0
          ER12=0.0032 EX12=0.0599
          STEP=0.025 +NSTEP=2 -NSTEP=2
3244  3245  NO=369 SN=1000.000 UN1= 300.000 UN2= 420.000
          ER12= 0.00500 EX12= 0.02000 FI= 0.00  TAPSIDE=1
          STEP= 0.63492E-02 +NSTEP= 63 -NSTEP= 63
3701  3249  NO=369 SN=1000.000 UN1= 300.000 UN2= 420.000
          ER12= 0.02000 EX12= 0.50000 FI= 0.00  TAPSIDE=1
          STEP= 0.63492E-02 +NSTEP= 63 -NSTEP= 63
3359  3360  NO=369 SN=1000.000 UN1= 420.000 UN2= 135.000
          ER12= 0.00500 EX12= 0.02000 FI= 0.00  TAPSIDE=1
          STEP= 0.63492E-02 +NSTEP= 63 -NSTEP= 63
5101  5100  NO=369 SN=1000.000 UN1= 420.000 UN2= 300.000
          ER12= 0.00080 EX12= 0.03050 FI= 0.00  TAPSIDE=1
          STEP= 0.63492E-02 +NSTEP= 63 -NSTEP= 63
5102  5100  NO=369 SN=1000.000 UN1= 420.000 UN2= 300.000
          ER12= 0.00080 EX12= 0.03050 FI= 0.00  TAPSIDE=1
          STEP= 0.63492E-02 +NSTEP= 63 -NSTEP= 63
5103  5100  NO=369 SN=1000.000 UN1= 420.000 UN2= 300.000
          ER12= 0.00250 EX12= 0.10000 FI= 0.00  TAPSIDE=1
          STEP= 0.63492E-02 +NSTEP= 63 -NSTEP= 63
5300  5301  NO=369 SN=1000.000 UN1= 300.000 UN2= 420.000
          ER12= 0.00160 EX12= 0.06100 FI= 0.00  TAPSIDE=1
          STEP= 0.63492E-02 +NSTEP= 63 -NSTEP= 63

```

```

5400  5401  NO=369  SN=1000.000  UN1= 300.000  UN2= 420.000
        ER12= 0.00320  EX12= 0.12000  FI= 0.00    TAPSIDE=1
        STEP= 0.63492E-02  +NSTEP= 63  -NSTEP= 63
5400  5402  NO=369  SN=1000.000  UN1= 300.000  UN2= 420.000
        ER12= 0.00040  EX12= 0.01500  FI= 0.00    TAPSIDE=1
        STEP= 0.63492E-02  +NSTEP= 63  -NSTEP= 63
5500  5501  NO=369  SN=1000.000  UN1= 300.000  UN2= 420.000
        ER12= 0.00040  EX12= 0.01500  FI= 0.00    TAPSIDE=1
        STEP= 0.63492E-02  +NSTEP= 63  -NSTEP= 63
5600  5601  NO=369  SN=1000.000  UN1= 300.000  UN2= 420.000
        ER12= 0.00020  EX12= 0.00760  FI= 0.00    TAPSIDE=1
        STEP= 0.63492E-02  +NSTEP= 63  -NSTEP= 63
5603  5602  NO=369  SN=1000.000  UN1= 300.000  UN2= 420.000
        ER12= 0.00080  EX12= 0.03050  FI= 0.00    TAPSIDE=1
        STEP= 0.63492E-02  +NSTEP= 63  -NSTEP= 63
6000  6001  NO=369  SN=1000.000  UN1= 300.000  UN2= 420.000
        ER12= 0.00040  EX12= 0.01500  FI= 0.00    TAPSIDE=1
        STEP= 0.63492E-02  +NSTEP= 63  -NSTEP= 63
6700  6701  NO=369  SN=1000.000  UN1= 300.000  UN2= 420.000
        ER12= 0.00500  EX12= 0.02000  FI= 0.00    TAPSIDE=1
        STEP= 0.63492E-02  +NSTEP= 63  -NSTEP= 63

```

END

TRANSFORMERS

! 3-WINDING TRANSFORMERS

END

LOADS

! PSS/E load data is translated as follows:

! Constant loads PSS/E PL,QL defined with exponents MP=0 MQ=0 !

! Constant current PSS/E IP, IQ defined with exponents MP=1, MQ=1 !

! Constant admittance PSS/E YP,YQ defined with exponents MP=2, MQ=2 !

```
3000  NO= 1  P= 2500.000  Q= 500.000  MP=0  MQ=0
```

```
3000  NO= 2  P= -500.000  Q= 250.000  MP=0  MQ=0
```

```
3100      P= 500.000  Q= 100.000  MP=0  MQ=0
```

```
3200      P= 500.000  Q= 100.000  MP=0  MQ=0
```

```
3245      P= 2700.000  Q= 500.000  MP=0  MQ=0
```

```
3249      P= 1250.000  Q= 300.000  MP=0  MQ=0
```

```
3300      P= 9350.000  Q= 1500.000  MP=0  MQ=0
```

```
3359      P= 4500.000  Q= 700.000  MP=0  MQ=0
```

```
3360      P= 360.000  Q= 180.000  MP=0  MQ=0
```

```
5100      P= 4210.000  Q= 692.000  MP=0  MQ=0
```

```
5300      P= 201.000  Q= 11.300  MP=0  MQ=0
```

```
5400      P= 94.400  Q= 0.000  MP=0  MQ=0
```

```
5500      P= 1229.000  Q= 115.000  MP=0  MQ=0
```

```
5600      P= 3121.000  Q= 297.000  MP=0  MQ=0
```

```
5603  NO= 1  P= 460.000  Q= 45.000  MP=0  MQ=0
```

```
5603  NO= 2  P= 940.000  Q= 470.000  MP=0  MQ=0
```

```
6000      P= 4.000  Q= 0.000  MP=0  MQ=0
```

```
6100      P= 3042.000  Q= 980.000  MP=0  MQ=0
```

```
6500      P= 1919.000  Q= 279.000  MP=0  MQ=0
```

```
6700      P= 1927.000  Q= 446.000  MP=0  MQ=0
```

```
7000  NO= 1  P= 5100.000  Q= 1000.000  MP=0  MQ=0
```

```
7000  NO= 2  P= 500.000  Q= 250.000  MP=0  MQ=0
```

```

7100      P= 2500.000 Q= 400.000 MP=0 MQ=0
8500      P= 1000.000 Q= 1000.000 MP=0 MQ=0
END
POWER CONTROL
1000  TYPE=NODE NAME=FPCWT_GEN  RTYP=SW U= 3.0      FI=0.0
      QMIN=-49995.00  QMAX= 49995.00
5600  TYPE=NODE NAME=SVC1      RTYP=UP U=303 P=0
      QMIN=-320 QMAX=320
3300  TYPE=NODE NAME=SV-SGG1_  RTYP=SW U= 420.000000  FI= 0.0000  !
      QMIN=-49995.00  QMAX= 49995.00
3000  TYPE=NODE NAME=STCKGG1_  RTYP=UP U= 420.0000  P= 5300.000
      QMIN=-49995.00  QMAX= 49995.00
3100  TYPE=NODE NAME=STRFGG1_  RTYP=UP U= 407.4000  P= 1500.000
      QMIN=-49995.00  QMAX= 49995.00
3115  TYPE=NODE NAME=SV-NGG11  RTYP=UP U= 420.0000  P= 3570.000
      QMIN=-49995.00  QMAX= 49995.00
!3200  TYPE=NODE NAME=KRLSGG1_  RTYP=UP U= 420.0000  P= 0.000
!      QMIN=-49995.00  QMAX= 49995.00  NCON=1
3245  TYPE=NODE NAME=SV-MGG1_  RTYP=UP U= 420.0000  P= 780.000
      QMIN=-49995.00  QMAX= 49995.00
3249  TYPE=NODE NAME=SV-NGG12  RTYP=UP U= 420.0000  P= 4750.000
      QMIN=-49995.00  QMAX= 49995.00
3359  TYPE=NODE NAME=SV-WGG1_  RTYP=UP U= 420.0000  P= 2670.000
      QMIN=-49995.00  QMAX= 49995.00
3359  TYPE=NODE NAME=SV-WGG2_  RTYP=UP U= 420.0000  P= 830.000
      QMIN=-9999.000  QMAX= 9999.000
5100  TYPE=NODE NAME=EASTGG1_  RTYP=UP U= 300.0000  P= 1480.000
      QMIN=-49995.00  QMAX= 49995.00
5300  TYPE=NODE NAME=HDALGG1_  RTYP=UP U= 300.0000  P= 2275.000
      QMIN=-49995.00  QMAX= 49995.00
5400  TYPE=NODE NAME=CNTRGG11  RTYP=UP U= 302.1000  P= 1588.000
      QMIN=-49995.00  QMAX= 49995.00
5500  TYPE=NODE NAME=CNTRGG12  RTYP=UP U= 301.2000  P= 828.000
      QMIN=-49995.00  QMAX= 49995.00
5600  TYPE=NODE NAME=SOUTGG11  RTYP=UP U= 303.0000  P= 2378.000
!5603  TYPE=NODE NAME=SOUTGG12  RTYP=UP U= 300.0000  P= 100.000
!      QMIN=-9999.000  QMAX= 9999.000  NCON=1
6000  TYPE=NODE NAME=WESTGG1_  RTYP=UP U= 301.5000  P= 1129.000
      QMIN=-1000.000  QMAX= 1000.000
6100  TYPE=NODE NAME=NWESGG1_  RTYP=UP U= 300.0000  P= 2346.000
      QMIN=-49995.00  QMAX= 49995.00
6500  TYPE=NODE NAME=MID3GG1_  RTYP=UP U= 300.0000  P= 1511.000
      QMIN=-49995.00  QMAX= 49995.00
6700  TYPE=NODE NAME=NOR3GG1_  RTYP=UP U= 306.0000  P= 2771.000
      QMIN=-49995.00  QMAX= 49995.00
7000  TYPE=NODE NAME=SO-FGG1_  RTYP=UP U= 420.0000  P= 5300.000
      QMIN=-49995.00  QMAX= 49995.00
7100  TYPE=NODE NAME=NO-FGG1_  RTYP=UP U= 420.0000  P= 1310.000
      QMIN=-49995.00  QMAX= 49995.00
8500  TYPE=NODE NAME=SJOLGG1_  RTYP=UP U= 428.4000  P= 1000.000
      QMIN=-49995.00  QMAX= 49995.00

```

```

! Transformers RTYP=UFI:
3244  3245  NO=369 TYPE=TREG RTYP=UFI U=420.0000 FI= 0.000
      UMIN= 180.0000 UMAX=420.0000
3359  3360  NO=369 TYPE=TREG RTYP=UFI U=134.2913 FI= 0.000
! UMIN= 252.0000 UMAX=588.0000
5300  5301  NO=369 TYPE=TREG RTYP=UFI U=420.2604 FI= 0.000
! UMIN= 180.0000 UMAX=420.0000
5400  5401  NO=369 TYPE=TREG RTYP=UFI U=418.4880 FI= 0.000
      UMIN= 180.0000 UMAX=420.0000
5400  5402  NO=369 TYPE=TREG RTYP=UFI U=422.5284 FI= 0.000
! UMIN= 180.0000 UMAX=420.0000
5500  5501  NO=369 TYPE=TREG RTYP=UFI U=421.9068 FI= 0.000
! UMIN= 180.0000 UMAX=420.0000
5600  5601  NO=369 TYPE=TREG RTYP=UFI U=416.6610 FI= 0.000
      UMIN= 180.0000 UMAX=420.0000
5603  5602  NO=369 TYPE=TREG RTYP=UFI U=401.5368 FI= 0.000
      UMIN= 180.0000 UMAX=420.0000
6000  6001  NO=369 TYPE=TREG RTYP=UFI U=419.8320 FI= 0.000
      UMIN= 180.0000 UMAX=420.0000
6700  6701  NO=369 TYPE=TREG RTYP=UFI U=422.9316 FI= 0.000
! UMIN= 180.0000 UMAX=420.0000

```

! Transformers defined with RTYP=UFI. CNODE bus voltage is set fixed.

! The CNODE is set as the first node name in order in the data list

```

3701  3249  NO=369 TYPE=TREG RTYP=UFI TAU= 1.00000 FI= 0.000
      UMIN= 180.0000 UMAX=420.0000 CNODE=3701  U=302.22897
5101  5100  NO=369 TYPE=TREG RTYP=UFI TAU= 1.00635 FI= 0.000
      UMIN= 252.0000 UMAX=588.0000 CNODE=5101  U=415.74121
5102  5100  NO=369 TYPE=TREG RTYP=UFI TAU= 1.00000 FI= 0.000
      UMIN= 252.0000 UMAX=588.0000 CNODE=5102  U=420.00842
5103  5100  NO=369 TYPE=TREG RTYP=UFI TAU= 1.00000 FI= 0.000
      UMIN= 252.0000 UMAX=588.0000 CNODE=5103  U=419.17682

```

END

END

APPENDIX C: HVAC DYNPOW FILE

Case fault

**

CONTROL DATA

TEND=20

SPL=1.7

NPRD=3000

DEND=0.1

N7=40

GAM5=0.01

TETL=100000

END

GENERAL

NREF=2

FN 50.0 50.0

REF= FPCWT_GEN SV-SGG1_

END

GLOBALS

FPCWT_REC_IQORD TYPE=REAL

FPCWT_REC_IQORD0 TYPE=REAL

FPCWT_REC_DW TYPE=REAL

FPCWT_INV_IQORD TYPE=REAL

FPCWT_INV_IQORD0 TYPE=REAL

FPCWT_REC_PORD TYPE=REAL

END

SVC

SVC1 5600 SN=350 REG=100

END

SYNCHRONOUS MACHINES

FPCWT_GEN 1000 SN = 1060.0 UN = 3.0 TYPE = 2A H = 5.5

RA= 0.0025 XD= 1.9 XQ = 1.6 XDP = 0.32 XDB = 0.2

XQB = 0.21 XA = 0.14 TDOP = 5.0 TDOB = 0.03 TQOB = 0.07

TURB=1

SV-SGG1_ 3300 TYPE=1 XD=2.42 XQ=2.00 XA=0.1481 XDP=0.23 XQP=0.4108

XDB=0.16 XQB=0.16 RA=0.0 TDOP=10.8 TQOP=1
 TDOB=0.05 TQOB=0.05 V1=1 V2=1.2 SE1=0.1089 SE2=0.378
 TURB=40 H=6.0 SN=5000 UN=420 D=0 VREG=24

STCKGG1_ 3000 TYPE=1 XD=2.22 XQ=2.13 XA=0.1688 XDP=0.36 XQP=0.468
 XDB=0.225 XQB=0.225 RA=0.0 TDOP=5.0 TQOP=1
 TDOB=0.05 TQOB=0.05 V1=1 V2=1.2 SE1=0.1089 SE2=0.378
 TURB=40 H=5.97 SN=5579 UN=420 D=0 VREG=10

STRFGG1_ 3100 TYPE=2 XD=0.65 XQ=0.39 XA=0.0877 XDP=0.19
 XDB=0.1169 XQB=0.1169 RA=0.0 TDOP=4.0
 TDOB=0.06 TQOB=0.1 V1=1 V2=1.2 SE1=0.1024 SE2=0.2742
 TURB=20 H=5.04 SN=1579 UN=420 D=0 VREG=20

SV-NGG11 3115 TYPE=2 XD=0.946 XQ=0.565 XA=0.1108 XDP=0.29
 XDB=0.23 XQB=0.23 RA=0.0 TDOP=7.57
 TDOB=0.045 TQOB=0.1 V1=1 V2=1.2 SE1=0.1024 SE2=0.2742
 TURB=21 H=4.741 SN=3758 UN=420 D=0 VREG=23

!KRLSGG1_ 3200 TYPE=1 XD=1.8 XQ=1.7 XA=0.2 XDP=0.3 XQP=0.55
 ! XDB=0.25 XQB=0.25 RA=0.0025 TDOP=8.0 TQOP=0.4
 ! TDOB=0.03 TQOB=0.05 TAB=1 TURB=3
 ! H=6.5 SN=1 UN=420 D=0 VREG=2

SV-MGG1_ 3245 TYPE=2 XD=0.75 XQ=0.50 XA=0.1154 XDP=0.25
 XDB=0.1538 XQB=0.1538 RA=0.0 TDOP=5.0
 TDOB=0.06 TQOB=0.1 V1=1 V2=1.2 SE1=0.1024 SE2=0.2742
 TURB=22 H=3.3 SN=822 UN=420 D=0 VREG=20

SV-NGG12 3249 TYPE=2 XD=1.036 XQ=0.63 XA=0.1154 XDP=0.28
 XDB=0.21 XQB=0.21 RA=0.0 TDOP=10.13
 TDOB=0.06 TQOB=0.1 V1=1 V2=1.2 SE1=0.1024 SE2=0.2742
 TURB=23 H=4.543 SN=5000 UN=420 D=0 VREG=20

SV-WGG1_ 3359 TYPE=2 XD=0.75 XQ=0.50 XA=0.1154 XDP=0.25
 XDB=0.1938 XQB=0.1938 RA=0.0 TDOP=5.0
 TDOB=0.06 TQOB=0.1 V1=1 V2=1.2 SE1=0.1024 SE2=0.2742
 TURB=22 H=3.3 SN=2811 UN=420 D=0 VREG=25

SV-WGG2_ 3359 TYPE=1 XD=2.13 XQ=2.03 XA=0.1453 XDP=0.31 XQP=0.403
 XDB=0.1937 XQB=0.1937 RA=0.0 TDOP=4.75 TQOP=1
 TDOB=0.05 TQOB=0.05 V1=1 V2=1.2 SE1=0.1089 SE2=0.378
 TURB=40 H=4.82 SN=874 UN=420 D=0 VREG=22

EASTGG1_ 5100 TYPE=2 XD=1.1332 XQ=0.6832 XA=0.1341 XDP=0.243
 XDB=0.1514 XQB=0.1514 RA=0.0 TDOP=4.9629
 TDOB=0.05 TQOB=0.15 V1=1 V2=1.2 SE1=0.10 SE2=0.30
 TURB=25 H=3.9871 SN=1558 UN=300 D=0 VREG=30

HDALGG1_ 5300 TYPE=2 XD=1.14 XQ=0.84 XA=0.2 XDP=0.34
 XDB=0.26 XQB=0.26 RA=0.0 TDOP=6.4
 TDOB=0.05 TQOB=0.15 V1=1 V2=1.2 SE1=0.10 SE2=0.30

TURB=25 H=3.5 SN=2395 UN=300 D=0 VREG=27

CNTRGG11 5400 TYPE=2 XD=1.02 XQ=0.63 XA=0.13 XDP=0.25
XDB=0.16 XQB=0.16 RA=0.0 TDOP=6.5
TD0B=0.05 TQ0B=0.15 V1=1 V2=1.2 SE1=0.10 SE2=0.30
TURB=25 H=4.1 SN=1672 UN=300 D=0 VREG=30

CNTRGG12 5500 TYPE=2 XD=1.2364 XQ=0.6557 XA=0.1619 XDP=0.3741
XDB=0.2283 XQB=0.2283 RA=0.0 TDOP=7.198
TD0B=0.05 TQ0B=0.15 V1=1 V2=1.2 SE1=0.10 SE2=0.30
TURB=25 H=3.0 SN=872 UN=300 D=0 VREG=30

SOUTGG11 5600 TYPE=2 XD=1.0 XQ=0.5132 XA=0.21 XDP=0.38
XDB=0.28 XQB=0.28 RA=0.0 TDOP=7.85
TD0B=0.05 TQ0B=0.15 V1=1 V2=1.2 SE1=0.10 SE2=0.30
TURB=24 H=3.5 SN=2504 UN=300 D=0 VREG=26

!SOUTGG12 5603 TYPE=1 XD=1.8 XQ=1.7 XA=0.2 XDP=0.3 XQP=0.55
! XDB=0.25 XQB=0.25 RA=0.0025 TDOP=8.0 TQ0P=0.4
! TD0B=0.03 TQ0B=0.05 TAB=1 TURB=3
! H=6.5 SN=106 UN=300 D=0 VREG=2

WESTGG1_ 6000 TYPE=2 XD=1.28 XQ=0.94 XA=0.2 XDP=0.37
XDB=0.28 XQB=0.28 RA=0.0 TDOP=9.7
TD0B=0.05 TQ0B=0.15 V1=1 V2=1.2 SE1=0.10 SE2=0.30
TURB=24 H=3.5 SN=1189 UN=300 D=0 VREG=31

NWESGG1_ 6100 TYPE=2 XD=1.2 XQ=0.73 XA=0.15 XDP=0.37
XDB=0.18 XQB=0.18 RA=0.0 TDOP=9.9
TD0B=0.05 TQ0B=0.15 V1=1 V2=1.2 SE1=0.10 SE2=0.30
TURB=25 H=3.0 SN=2470 UN=300 D=0 VREG=27

MID3GG1_ 6500 TYPE=2 XD=1.0679 XQ=0.6420 XA=0.1351 XDP=0.2387
XDB=0.158 XQB=0.158 RA=0.0 TDOP=5.4855
TD0B=0.05 TQ0B=0.15 V1=1 V2=1.2 SE1=0.10 SE2=0.30
TURB=25 H=3.558 SN=1591 UN=300 D=0 VREG=30

NOR3GG1_ 6700 TYPE=2 XD=1.1044 XQ=0.6619 XA=0.1474 XDP=0.2548
XDB=0.1706 XQB=0.1706 RA=0.0 TDOP=5.24
TD0B=0.05 TQ0B=0.15 V1=1 V2=1.2 SE1=0.10 SE2=0.30
TURB=25 H=3.5920 SN=2917 UN=300 D=0 VREG=27

SO-FGG1_ 7000 TYPE=1 XD=2.22 XQ=2.13 XA=0.1688 XDP=0.36 XQP=0.468
XDB=0.225 XQB=0.225 RA=0.0 TDOP=10.0 TQ0P=1
TD0B=0.05 TQ0B=0.05 V1=1 V2=1.2 SE1=0.1089 SE2=0.378
TURB=40 H=5.5 SN=5579 UN=420 D=0 VREG=11

NO-FGG1_ 7100 TYPE=2 XD=0.75 XQ=0.50 XA=0.1154 XDP=0.25
XDB=0.1538 XQB=0.1538 RA=0.0 TDOP=5.0
TD0B=0.06 TQ0B=0.10 V1=1 V2=1.2 SE1=0.1024 SE2=0.2742
TURB=22 H=3.20 SN=1379 UN=420 D=0 VREG=27

SJOLGG1_ 8500 TYPE=1 XD=2.42 XQ=2.00 XA=0.1481 XDP=0.23 XQP=0.4108
XDB=0.1706 XQB=0.1706 RA=0.0 TDOP=10.0 TQOP=1
TDOB=0.05 TQOB=0.05 V1=1 V2=1.2 SE1=0.1089 SE2=0.378
TURB=40 H=7.0 SN=1056 UN=420 D=0 VREG=28

END

REGULATORS

- 10 TYPE=DSLS/IEEEX2/
TR=0 KA=729 TA=0.04 VRMAX=5.32 VRMIN=-4.05
KE=1.0 TE=0.44 KF=0.0667 TF1=2.0 TF2=0.44
E1=6.5 SE1=0.054 E2=8 SE2=0.2020 TB=0 TC=0 SWS=40
- 11 TYPE=DSLS/IEEEX2/
TR=0 KA=800 TA=0.04 VRMAX=5.32 VRMIN=-4.05
KE=1.0 TE=0.44 KF=0.0667 TF1=2.0 TF2=0.44
E1=6.5 SE1=0.054 E2=8 SE2=0.2020 TB=0 TC=0 SWS=44
- 20 TYPE=BBC1
T1=3.3 T3=13 K=31 T4=0.05 T2=0
UEMIN=0 UEMAX=4
- 21 TYPE=BBC1
T1=0 T3=0.04 K=10 T4=0.04 T2=0
UEMIN=0 UEMAX=5
- 22 TYPE=BBC1
T1=2 T3=10 K=165 T4=0.04 T2=0
UEMIN=0 UEMAX=5
- 23 TYPE=BBC1
T1=3.3 T3=13 K=31 T4=0.05 T2=0
UEMIN=0 UEMAX=4 SWS=41
- 24 TYPE=BBC1
T1=0 T3=0.04 K=10 T4=0.04 T2=0
UEMIN=0 UEMAX=5 SWS=42
- 25 TYPE=BBC1
T1=3.3 T3=13 K=31 T4=0.05 T2=0
UEMIN=0 UEMAX=4 SWS=43
- 26 TYPE=BBC1
T1=3.3 T3=13 K=61 T4=0.05 T2=0
UEMIN=0 UEMAX=4
- 27 TYPE=BBC1

T1=3.3 T3=13 K=61 T4=0.05 T2=0
UEMIN=0 UEMAX=4 SWS=42

28 TYPE=BBC1

T1=0 T3=0.04 K=10 T4=0.04 T2=0
UEMIN=0 UEMAX=5 SWS=42

30 TYPE=BBC1

T1=0.00005 T2=0 T3=100 T4=0.5 K=200
UEMIN=0 UEMAX=4

31 TYPE=BBC1

T1=10 T2=0 T3=0.1 T4=0.1 K=20
UEMIN=-4 UEMAX=4

40 TYPE=DSLS/STAB2A/

K2=1 T2=2 K3=0 T3=2 K4=0.55 K5=1 T5=0.01 HLIM=0.03

41 TYPE=DSLS/STAB2A/

K2=1 T2=4.5 K3=0.87 T3=2 K4=0.087 K5=1 T5=0.01 HLIM=0.04

42 TYPE=DSLS/STAB2A/

K2=1 T2=4.5 K3=0 T3=2 K4=0.55 K5=1 T5=0.01 HLIM=0.03

43 TYPE=DSLS/STAB2A/

K2=1 T2=4.5 K3=0 T3=2 K4=0.68 K5=1 T5=0.01 HLIM=0.03

44 TYPE=DSLS/STAB2A/

K2=1 T2=1.0 K3=0 T3=2 K4=0.55 K5=1 T5=0.01 HLIM=0.03

100 TYPE=SVS

RTYP=2 KP=15 TF=0.02 VPMAX=2 VPMIN=-2 KA=30
VIMIN=0 VIMAX=0.1 QMIN=-320 QMAX=320

END

TURBINES

1 TYPE=DSLS/FPCWT_WINDTURB/ NOM_POWER=1060.0 AIRDENS=1.2
NOM_TURBSPEED=0
BLADELENGTH=0 LOWCUTOUT=2.0
GOV=2 WINDCURVE=81

2 TYPE=DSLS/FPCWT_PICON/ KPP=60 KPC=3 KIP=20 KIC=20
TP=0.3 BMAX=27 BMIN=0
DBDTMAX=4.0 DBDTMIN=-4.0 BLOCK=0
DW=FPCWT_REC_DW
PORD=FPCWT_REC_PORD

!!!HYDRO TURBINES

20 TYPE=DSLS/HYTUR/
GOV=29 TW=1 AT=1.0022 DTURB=0.5 QNL=0.1

21 TYPE=DSLS/HYTUR/
GOV=29 TW=1 AT=1.0577 DTURB=0.5 QNL=0.1

22 TYPE=DSLS/HYTUR/
GOV=29 TW=1 AT=1.01 DTURB=0.5 QNL=0.1

23 TYPE=DSLS/HYTUR/
GOV=29 TW=1 AT=1.1 DTURB=0.5 QNL=0.1

24 TYPE=DSLS/HYTUR/
GOV=28 TW=1 AT=1.1 DTURB=0.5 QNL=0.1

25 TYPE=DSLS/HYTUR/
GOV=27 TW=1 AT=1.1 DTURB=0.5 QNL=0.1

27 TYPE=DSLS/HYGOV/
RBIG=0.06 RSMALL=0.4
TR=5.0 TF=0.05 TG=0.2
VELM=0.2 GMIN=0 GMAX=1

28 TYPE=DSLS/HYGOV/
RBIG=0.06 RSMALL=0.3
TR=5.0 TF=0.05 TG=0.2
VELM=0.2 GMIN=0 GMAX=1.5

29 TYPE=DSLS/HYGOV/
RBIG=0.06 RSMALL=0.4
TR=5.0 TF=0.05 TG=0.2
VELM=0.1 GMIN=0 GMAX=1.5

!!!STEAM TURBINES

40 TYPE=ST2
GOV=49 K1=0.301 T1=0.4 K2=0.399 T2=8.0
K3=0.3 T3=0.3 K4=0 T4=0

49 TYPE=SG3
T1=0.01 T2=0.0 T3=0.15 K=0
YMIN=0 YMAX=1

END

LOADS

3000 NO= 1 MP=1 MQ=2

```

3000 NO= 2 MP=1 MQ=2
3100 MP=1 MQ=2
3200 MP=1 MQ=2
3245 MP=1 MQ=2
3249 MP=1 MQ=2
3300 MP=1 MQ=2
3359 MP=1 MQ=2
3360 MP=1 MQ=2
5100 MP=1 MQ=2
5300 MP=1 MQ=2
5400 MP=1 MQ=2
5500 MP=1 MQ=2
5600 MP=1 MQ=2
5603 NO= 1 MP=1 MQ=2
5603 NO= 2 MP=1 MQ=2
6000 MP=1 MQ=2
6100 MP=1 MQ=2
6500 MP=1 MQ=2
6700 MP=1 MQ=2
7000 NO= 1 MP=1 MQ=2
7000 NO= 2 MP=1 MQ=2
7100 MP=1 MQ=2
8500 MP=1 MQ=2
END

```

PWM CONVERTERS

FPCWT_REC

```

TYPE=DSLS/FPCWT_PWM_DYN/ SN=1060.0
UN=3.0 X=0.3 PL=0.02
MODE=1 UDCORD=5.0 IMAX=1.04

```

```
PORD=FPCWT_REC_PORD
```

```
IQORD=FPCWT_REC_IQORD
```

```
IQORD0=FPCWT_REC_IQORD0
```

FPCWT_INV

```

TYPE=DSLS/FPCWT_PWM_DYN/ SN=1060.0
UN=3.5 X=0.3 PL=0.02
MODE=2 UDCORD=5.0 IMAX=1.04
PORD=0.0

```

```
IQORD=FPCWT_INV_IQORD
```

IQORD0=FPCWT_INV_IQORD0
END

MISC

SPC1 TYPE=DSLS/FPCWT_SPCON/ KS=0.6 KP=3.0 TPC=0.05
PMAx=0.976 PMIN=0.0 DPMAX=0.1 DPMIN=-0.1 !PMAx=0.976
WMAx=1.20 WMIN=0.40 WLOW=0.60
!A2=-0.4625 A1=1.0902 A0=0.3764 BLOCK=0
DW=FPCWT_REC_DW
PORD=FPCWT_REC_PORD
SYNC=FPCWT_GEN

VACR 1000 TYPE=DSLS/FPCWT_VACCON/ N=1
INTMAX=1.0 INTMIN=-1.0

UACORD=3.0

IQMAX=0.5 IQMIN=-0.5
K=1.2 TI=0.05 BLOCK=0

IQORD=FPCWT_REC_IQORD

IQORD0=FPCWT_REC_IQORD0

VACI 1002 TYPE=DSLS/FPCWT_VACCON/ N=1
INTMAX=1.0 INTMIN=-1.0

UACORD=3.5

IQMAX=0.5 IQMIN=-0.5
K=1.2 TI=0.05
IQORD=FPCWT_INV_IQORD
IQORD0=FPCWT_INV_IQORD0

END

TABLES

! 1 TYPE=1 F 0.000 0.00 0.700 0.70
! 0.800 0.80 0.830 0.83
! 0.860 0.86 0.962 0.94
! 0.974 0.95 1.039 1.00
! 1.113 1.05 1.202 1.10
! 1.315 1.15 1.467 1.20
! 1.682 1.25 1.998 1.30
! 2.478 1.35

! Cp/lambda curve for beta=0 deg.

11 TYPE=0 F 0.0 0.00

1.0 0.10
2.0 0.20
3.0 0.30
4.0 0.38
5.0 0.42
6.0 0.48
6.5 0.49
7.0 0.50
7.5 0.504
8.0 0.50
8.5 0.49
9.0 0.48
10.0 0.47
11.0 0.45
12.0 0.42
13.0 0.39
14.0 0.35
15.0 0.30
16.0 0.25
17.0 0.19
18.0 0.11
19.0 0.04
20.0 0.00

! Cp/lambda curve for beta=7 deg.

12 TYPE=0 F 0.0 0.00
1.0 0.02
2.0 0.05
3.0 0.16
4.0 0.26
5.0 0.30
6.0 0.31
6.5 0.31
7.0 0.30
7.5 0.28
8.0 0.26
8.5 0.24
9.0 0.22
10.0 0.16
11.0 0.08
12.0 0.00

! Cp/lambda curve for beta=27 deg.

13 TYPE=0 F 0.0 0.00
1.0 0.01
2.0 0.04
3.0 0.16
4.0 0.20
5.0 0.25
6.0 0.26
6.5 0.26
7.0 0.22
7.5 0.20
8.0 0.19

```

      8.5 0.16
      9.0 0.10
     10.0 0.05
     11.0 0.00
! Voltage fluctuations in the grid
51 TYPE=0 F      0.00 1.0
      10.0 1.0
      10.0 0.94
      10.1 0.94
      10.1 1.0
      100.0 1.0
! Wind profile
81 TYPE=0 F 0.0 11.569607734680176
      100.0 11.569607734680176

```

! or from separate file as

```
!!! $INCLUDE TEST-FPCWT.TXT
```

! This text file must look the same as a table given in the Dynpow file.
! It is possible to create a text file from MS Excel if the wind profile is
! stored there, but after export to a text file in the text file, strings edit
! by TABS must be replaced and edit by SPACE

END

FAULTS

```
F1 TYPE=3PSG NODE 5600
END
```

RUN INSTRUCTION

```
AT 1.000 INST CONNECT FAULT F1
AT 1.185 INST DISCONNECT FAULT F1
END
```

END

APPENDIX D: HVDC OPTPOW FILE

```

SYSTEM BASE = 1000.000 MVA.
Reduced NORDEL power system model
V 3.2, 12.08.97
**
CONTROL DATA
  UBCHECK=NO
  NSEP=NO
  ICPV=4
END
GENERAL
  SN=1000.000
END
NODES
! PSS NAME
!
! Nodes within the wind farm area    10
!
1000      UB= 3.000      TYPE=AC      AREA= 10
1001      UB= 5.000      TYPE=DC      AREA= 10
BUS_1     UB= 300        TYPE=AC      AREA= 10
BUS_2     UB= 300        TYPE=AC      AREA= 10
BUS_11    UB= 3.5        TYPE=AC      AREA= 10
A_1       UB= 300        TYPE=DC      AREA= 10
A_2       UB= 300        TYPE=DC      UI=-1      AREA= 10
B_1       UB= 300        TYPE=DC      AREA= 10
B_2       UB= 300        TYPE=DC      UI=-1      AREA= 10
B_SW      UB= 3.5        TYPE=AC      AREA= 10

!
! Nodes within area    40
!
3000      UB= 420.000    TYPE=AC      AREA= 40 ! STCKH    !
3100      UB= 420.000    TYPE=AC      AREA= 40 ! STRFN    !
3115      UB= 420.000    TYPE=AC      AREA= 40 ! SV-N1    !
3200      UB= 420.000    TYPE=AC      AREA= 40 ! KRLSK    !
3244      UB= 300.000    TYPE=AC      AREA= 40 ! SV-M2    !
3245      UB= 420.000    TYPE=AC      AREA= 40 ! SV-M1    !
3249      UB= 420.000    TYPE=AC      AREA= 40 ! SV-N2    !
3300      UB= 420.000    TYPE=AC      AREA= 40 ! SV-SW    !
3359      UB= 420.000    TYPE=AC      AREA= 40 ! SV-W     !
3360      UB= 135.000    TYPE=AC      AREA= 40 ! KONT_135 !
3701      UB= 300.000    TYPE=AC      AREA= 40 ! SV-N2B   !

!
! Nodes within area    51
!
5100      UB= 300.000    TYPE=AC      AREA= 51 ! EAST3    !
5101      UB= 420.000    TYPE=AC      AREA= 51 ! EAST4-A  !
5102      UB= 420.000    TYPE=AC      AREA= 51 ! EAST4-B  !
5103      UB= 420.000    TYPE=AC      AREA= 51 ! EAST4-C  !

!
! Nodes within area    53
!
5300      UB= 300.000    TYPE=AC      AREA= 53 ! HDAL3    !
5301      UB= 420.000    TYPE=AC      AREA= 53 ! HDAL4    !

!
! Nodes within area    54
!
5400      UB= 300.000    TYPE=AC      AREA= 54 ! CNTR3-A  !
5401      UB= 420.000    TYPE=AC      AREA= 54 ! CNTR4-A  !
5402      UB= 420.000    TYPE=AC      AREA= 54 ! CNTR4-B  !

!
! Nodes within area    55
!
5500      UB= 300.000    TYPE=AC      AREA= 55 ! CNTR3-B  !
5501      UB= 420.000    TYPE=AC      AREA= 55 ! CNTR4-C  !

!
! Nodes within area    56

```

```

!
5600      UB= 300.000      TYPE=AC      AREA= 56 ! SOUTH3A !
5601      UB= 420.000      TYPE=AC      AREA= 56 ! SOUTH4A !
5602      UB= 420.000      TYPE=AC      AREA= 56 ! SOUTH4B !
5603      UB= 300.000      TYPE=AC      AREA= 56 ! SOUTH3B !
!
! Nodes within area      60
!
6000      UB= 300.000      TYPE=AC      AREA= 60 ! WEST300 !
6001      UB= 420.000      TYPE=AC      AREA= 60 ! WEST400 !
!
! Nodes within area      61
!
6100      UB= 300.000      TYPE=AC      AREA= 61 ! NWEST3 !
!
! Nodes within area      65
!
6500      UB= 300.000      TYPE=AC      AREA= 65 ! MID300 !
!
! Nodes within area      67
!
6700      UB= 300.000      TYPE=AC      AREA= 67 ! NOR300 !
6701      UB= 420.000      TYPE=AC      AREA= 67 ! NOR400 !
!
! Nodes within area      70
!
7000      UB= 420.000      TYPE=AC      AREA= 70 ! SO-FIN !
!
! Nodes within area      71
!
7100      UB= 420.000      TYPE=AC      AREA= 71 ! NO-FIN !
!
! Nodes within area      90
!
8500      UB= 420.000      TYPE=AC      AREA= 90 ! SJOLLAND !
END

```

```

SREACTORS
5400      5500      NO= 81 TYPE=11 R= 0.890000E-02 X= 0.111000
END

```

PWM CONVERTERS

```

FPCWT_REC      1000      1001      AC2=1000
                TYPE=DSL/ FPCWT_PWM_OPT/ SN=1060.0
                UN=3.0      X=0.3      PL=0.02      MODE=1      ORDER=1000.0

FPCWT_INV      BUS_11      1001      AC2=BUS_11      !BUS_11
                TYPE=DSL/ FPCWT_PWM_OPT/ SN=1060.0
                UN=3.5      X=0.3      PL=0.02      MODE=2      ORDER=5      !UN=
3.5

LIGHT_A      BUS_1      A_1      DC1=A_2
                TYPE=DSL/HVDC_LIGHT_OPEN_MODEL_V116_OPT/ SN=1060.0
                UN=300 BSH=1.5E-3 XL=0.15 PLOSSNOM=0.0165 PLOSSNOLOADPART=0.3
                PCTRL=1 UACCTRL=0 UACREF=1.0 QREF=0.0 PREF=0.903396

LIGHT_B      BUS_2      B_1      DC1=B_2
                TYPE=DSL/HVDC_LIGHT_OPEN_MODEL_V116_OPT/ SN=1060.0
                UN=300 BSH=1.5E-3 XL=0.15 PLOSSNOM=0.0165 PLOSSNOLOADPART=0.3
                PCTRL=0 UACCTRL=1 UACREF=1.0 QREF=0.0
END

```

SHUNT IMPEDANCES ! Line type 13,14 and 15 are translated as lines type 12.

```

! Corresponding GI,BI,GJ,BJ are translated as shunts !
1001      NO= 81 R= 1E6      C= 1.2381 !2.4E-3
A_1      R= 1.0E9      C= 1.2E-4 !70.0E-6
A_2      R= 1.0E9      C= 1.2E-4
B_1      R= 1.0E9      C= 1.2E-4
B_2      R= 1.0E9      C= 1.2E-4

```

```

5101      NO= 81 R=  0.00000      X=  181.034
5101      NO=810 R=  7910.31      X=  0.00000
5501      NO=811 R=  0.00000      X= -181.034
5501      NO=812 R= -8166.67      X=  0.00000
5102      NO= 81 R=  0.00000      X=-0.176397E+07
5102      NO=810 R=  882000.      X=  0.00000
6001      NO=811 R=  0.00000      X=  0.176397E+07
6001      NO=812 R=  882000.      X=  0.00000
5103      NO= 81 R=  0.00000      X=  13889.8
5103      NO=810 R=  441000.      X=  0.00000
5301      NO=811 R=  0.00000      X= -13889.8
5301      NO=812 R= -588000.      X=  0.00000
5401      NO= 81 R=  0.00000      X=  352800.
5401      NO=810 R= -882000.      X=  0.00000
6001      NO=813 R=  0.00000      X= -352800.
6001      NO=814 R=  882000.      X=  0.00000
5500      NO= 81 R=  0.00000      X= -69230.8
5500      NO=810 R=  300000.      X=  0.00000
5603      NO=811 R=  0.00000      X=  69230.8
5603      NO=812 R= -300000.      X=  0.00000

```

END

LINES

! See also the second LINES-chapter further below,
! containing all lines of TYPE=11.

```

A_1      B_1              TYPE=6   R=0.0105   LL=0  L=100
A_2      B_2              TYPE=6   R=0.0105   LL=0  L=100
BUS_11   B_SW            TYPE=0   NCON=0
3000     3115      NO= 81  TYPE=12   R= 0.140000E-01  X= 0.100000
                    B= 0.300000E-01  L= 10.00
3000     3245      NO= 81  TYPE=12   R= 0.125000E-02  X= 0.170100E-01
                    B= 0.127460E-01  L= 10.00
3000     3300      NO= 81  TYPE=12   R= 0.113000E-02  X= 0.170100E-01
                    B= 0.116380E-01  L= 10.00
3100     3115      NO= 81  TYPE=12   R= 0.301000E-02  X= 0.413800E-01
                    B= 0.775800E-02  L= 10.00
3100     3200      NO= 81  TYPE=12   R= 0.686000E-02  X= 0.561200E-01
                    B= 0.171790E-01  L= 10.00
3100     3249      NO= 81  TYPE=12   R= 0.108000E-02  X= 0.147400E-01
                    B= 0.105290E-01  L= 10.00
3100     3359      NO= 81  TYPE=12   R= 0.910000E-03  X= 0.119000E-01
                    B= 0.221700E-02  L= 10.00
3115     3245      NO= 81  TYPE=12   R= 0.300000E-02  X= 0.500000E-01
                    B= 0.900000E-02  L= 10.00
3115     3249      NO= 81  TYPE=12   R= 0.150000E-02  X= 0.200000E-01
                    B= 0.400000E-02  L= 10.00
3115     6701      NO= 81  TYPE=12   R= 0.400000E-02  X= 0.300000E-01
                    B= 0.500000E-02  L= 10.00
3115     7100      NO= 81  TYPE=12   R= 0.100000E-01  X= 0.700000E-01
                    B= 0.100000E-01  L= 10.00
3200     3300      NO= 81  TYPE=12   R= 0.125000E-02  X= 0.170100E-01
                    B= 0.332500E-02  L= 10.00
3200     3359      NO= 81  TYPE=12   R= 0.357000E-02  X= 0.408200E-01
                    B= 0.775800E-02  L= 10.00
3244     6500      NO= 81  TYPE=12   R= 0.500000E-03  X= 0.500000E-02

```

B= 0.100000E-03 L= 10.00

3249	7100	NO= 81	TYPE=12	R= 0.100000E-01	X= 0.700000E-01	B= 0.100000E-01	L= 10.00
3300	3359	NO= 81	TYPE=12	R= 0.740000E-03	X= 0.964000E-02	B= 0.166300E-02	L= 10.00
3300	8500	NO= 81	TYPE=12	R= 0.800000E-02	X= 0.310000E-01	B= 0.300000E-01	L= 10.00
3359	5101	NO= 81	TYPE=12	R= 0.148000E-02	X= 0.192800E-01	B= 0.360200E-02	L= 10.00
3701	6700	NO= 81	TYPE=12	R= 0.100000E-02	X= 0.100000	B= 0.500000E-03	L= 10.00
5100	5300	NO= 81	TYPE=12	R= 0.400000E-02	X= 0.400000E-01	B= 0.500000E-02	L= 10.00
5100	5500	NO= 81	TYPE=12	R= 0.180000E-02	X= 0.150000E-01	B= 0.212800E-02	L= 10.00
5100	6500	NO= 81	TYPE=12	R= 0.150000E-01	X= 0.150000	B= 0.100000E-03	L= 10.00
5101	5501	NO= 81	TYPE=12	R= 0.610000E-03	X= 0.643000E-02	B= 0.325920E-01	L= 10.00
		RNO1= 810	RNO2= 812				
5102	5301	NO= 81	TYPE=12	R= 0.750000E-03	X= 0.107900E-01	B= 0.128600E-01	L= 10.00
5102	6001	NO= 81	TYPE=12	R= 0.200000E-02	X= 0.350000E-01	B= 0.100000E-01	L= 10.00
		RNO1= 810	RNO2= 812				
5103	5301	NO= 81	TYPE=12	R= 0.170000E-02	X= 0.231200E-01	B= 0.675500E-02	L= 10.00
		RNO1= 810	RNO2= 812				
5400	6000	NO= 81	TYPE=12	R= 0.100000E-02	X= 0.100000E-01	B= 0.100000E-02	L= 10.00
5400	6100	NO= 81	TYPE=12	R= 0.200000E-02	X= 0.200000E-01	B= 0.120000E-02	L= 10.00
5401	5501	NO= 81	TYPE=12	R= 0.150000E-02	X= 0.200000E-01	B= 0.600000E-02	L= 10.00
5401	5602	NO= 81	TYPE=12	R= 0.154000E-02	X= 0.240600E-01	B= 0.879600E-02	L= 10.00
5401	6001	NO= 81	TYPE=12	R= 0.300000E-03	X= 0.500000E-02	B= 0.150000E-02	L= 10.00
		RNO1= 810	RNO2= 814				
5402	6001	NO= 81	TYPE=12	R= 0.510000E-03	X= 0.751000E-02	B= 0.235200E-02	L= 10.00
5500	5603	NO= 81	TYPE=12	R= 0.400000E-02	X= 0.450000E-01	B= 0.800000E-03	L= 10.00
		RNO1= 810	RNO2= 812				
5600	5603	NO= 81	TYPE=12	R= 0.201000E-02	X= 0.221100E-01	B= 0.208400E-02	L= 10.00
5600	6000	NO= 81	TYPE=12	R= 0.350000E-02	X= 0.350000E-01	B= 0.450000E-02	L= 10.00
5601	6001	NO= 81	TYPE=12	R= 0.137000E-02	X= 0.203100E-01	B= 0.636400E-02	L= 10.00

```

6000      6100      NO= 81  TYPE=12      R= 0.220000E-02  X= 0.239400E-01
                                         B= 0.200000E-02  L= 10.00

6500      6700      NO= 81  TYPE=12      R= 0.800000E-02  X= 0.110000
                                         B= 0.100000E-02  L= 10.00

7000      7100      NO= 81  TYPE=12      R= 0.140000E-01  X= 0.100000
                                         B= 0.300000E-01  L= 10.00

7000      7100      NO= 82  TYPE=12      R= 0.140000E-01  X= 0.100000
                                         B= 0.300000E-01  L= 10.00

3359      5101      NO= 82  TYPE=12      R= 0.148000E-02  X= 0.192800E-01
                                         B= 0.360200E-02  L= 10.00

5300      6100      NO= 81  TYPE=12      R= 0.359000E-02  X= 0.382500E-01
                                         B= 0.115200E-02  L= 10.00
      NCON=1
7000      7100      NO= 83  TYPE=12      R= 0.140000E-01  X= 0.100000
                                         B= 0.300000E-01  L= 10.00
      NCON=1
END
TRANSFORMERS
! Transformers with TCR, i.e. with STEP, -NSTEP!

BUS_1     BUS_11  SN=1060.0  UN1=300  UN2=3.5
ER12=0.00  EX12=0.12
STEP=0.025  +NSTEP=2  -NSTEP=2
BUS_2     5600    SN=1060.0  UN1=300  UN2=300
ER12=0.00  EX12=0.12
STEP=0.025  +NSTEP=2  -NSTEP=2
3244      3245    NO=369    SN=1000.000  UN1= 300.000  UN2= 420.000
ER12= 0.00500  EX12= 0.02000  FI= 0.00      TAPSIDE=1
STEP= 0.63492E-02  +NSTEP= 63  -NSTEP= 63
3701      3249    NO=369    SN=1000.000  UN1= 300.000  UN2= 420.000
ER12= 0.02000  EX12= 0.50000  FI= 0.00      TAPSIDE=1
STEP= 0.63492E-02  +NSTEP= 63  -NSTEP= 63
3359      3360    NO=369    SN=1000.000  UN1= 420.000  UN2= 135.000
ER12= 0.00500  EX12= 0.02000  FI= 0.00      TAPSIDE=1
STEP= 0.63492E-02  +NSTEP= 63  -NSTEP= 63
5101      5100    NO=369    SN=1000.000  UN1= 420.000  UN2= 300.000
ER12= 0.00080  EX12= 0.03050  FI= 0.00      TAPSIDE=1
STEP= 0.63492E-02  +NSTEP= 63  -NSTEP= 63
5102      5100    NO=369    SN=1000.000  UN1= 420.000  UN2= 300.000
ER12= 0.00080  EX12= 0.03050  FI= 0.00      TAPSIDE=1
STEP= 0.63492E-02  +NSTEP= 63  -NSTEP= 63
5103      5100    NO=369    SN=1000.000  UN1= 420.000  UN2= 300.000
ER12= 0.00250  EX12= 0.10000  FI= 0.00      TAPSIDE=1
STEP= 0.63492E-02  +NSTEP= 63  -NSTEP= 63
5300      5301    NO=369    SN=1000.000  UN1= 300.000  UN2= 420.000
ER12= 0.00160  EX12= 0.06100  FI= 0.00      TAPSIDE=1
STEP= 0.63492E-02  +NSTEP= 63  -NSTEP= 63
5400      5401    NO=369    SN=1000.000  UN1= 300.000  UN2= 420.000
ER12= 0.00320  EX12= 0.12000  FI= 0.00      TAPSIDE=1
STEP= 0.63492E-02  +NSTEP= 63  -NSTEP= 63
5400      5402    NO=369    SN=1000.000  UN1= 300.000  UN2= 420.000
ER12= 0.00040  EX12= 0.01500  FI= 0.00      TAPSIDE=1
STEP= 0.63492E-02  +NSTEP= 63  -NSTEP= 63
5500      5501    NO=369    SN=1000.000  UN1= 300.000  UN2= 420.000
ER12= 0.00040  EX12= 0.01500  FI= 0.00      TAPSIDE=1
STEP= 0.63492E-02  +NSTEP= 63  -NSTEP= 63
5600      5601    NO=369    SN=1000.000  UN1= 300.000  UN2= 420.000
ER12= 0.00020  EX12= 0.00760  FI= 0.00      TAPSIDE=1
STEP= 0.63492E-02  +NSTEP= 63  -NSTEP= 63
5603      5602    NO=369    SN=1000.000  UN1= 300.000  UN2= 420.000
ER12= 0.00080  EX12= 0.03050  FI= 0.00      TAPSIDE=1
STEP= 0.63492E-02  +NSTEP= 63  -NSTEP= 63
6000      6001    NO=369    SN=1000.000  UN1= 300.000  UN2= 420.000
ER12= 0.00040  EX12= 0.01500  FI= 0.00      TAPSIDE=1
STEP= 0.63492E-02  +NSTEP= 63  -NSTEP= 63
6700      6701    NO=369    SN=1000.000  UN1= 300.000  UN2= 420.000

```

```

ER12= 0.00500 EX12= 0.02000 FI= 0.00 TAPSIDE=1
STEP= 0.63492E-02 +NSTEP= 63 -NSTEP= 63
END
TRANSFORMERS
! 3-WINDING TRANSFORMERS
END
LOADS
! PSS/E load data is translated as follows:
! Constant loads PSS/E PL,QL defined with exponents MP=0 MQ=0 !
! Constant current PSS/E IP, IQ defined with exponents MP=1, MQ=1 !
! Constant admittance PSS/E YP,YQ defined with exponents MP=2, MQ=2 !
3000 NO= 1 P= 2500.000 Q= 500.000 MP=0 MQ=0
3000 NO= 2 P= -500.000 Q= 250.000 MP=0 MQ=0
3100 P= 500.000 Q= 100.000 MP=0 MQ=0
3200 P= 500.000 Q= 100.000 MP=0 MQ=0
3245 P= 2700.000 Q= 500.000 MP=0 MQ=0
3249 P= 1250.000 Q= 300.000 MP=0 MQ=0
3300 P= 9350.000 Q= 1500.000 MP=0 MQ=0
3359 P= 4500.000 Q= 700.000 MP=0 MQ=0
3360 P= 360.000 Q= 180.000 MP=0 MQ=0
5100 P= 4210.000 Q= 692.000 MP=0 MQ=0
5300 P= 201.000 Q= 11.300 MP=0 MQ=0
5400 P= 94.400 Q= 0.000 MP=0 MQ=0
5500 P= 1229.000 Q= 115.000 MP=0 MQ=0
5600 P= 3121.000 Q= 297.000 MP=0 MQ=0
5603 NO= 1 P= 460.000 Q= 45.000 MP=0 MQ=0
5603 NO= 2 P= 940.000 Q= 470.000 MP=0 MQ=0
6000 P= 4.000 Q= 0.000 MP=0 MQ=0
6100 P= 3042.000 Q= 980.000 MP=0 MQ=0
6500 P= 1919.000 Q= 279.000 MP=0 MQ=0
6700 P= 1927.000 Q= 446.000 MP=0 MQ=0
7000 NO= 1 P= 5100.000 Q= 1000.000 MP=0 MQ=0
7000 NO= 2 P= 500.000 Q= 250.000 MP=0 MQ=0
7100 P= 2500.000 Q= 400.000 MP=0 MQ=0
8500 P= 1000.000 Q= 1000.000 MP=0 MQ=0
END
POWER CONTROL
1000 TYPE=NODE NAME=FPCWT_GEN RTYP=SW U= 3.0 FI=0.0
QMIN= -49995.00 QMAX= 49995.00
5600 TYPE=NODE NAME=SVC1 RTYP=UP U= 303 P=0
QMIN=-320 QMAX=320
B_SW TYPE=NODE NAME=SWING RTYP=SW U= 3.5 FI=0.0
3300 TYPE=NODE NAME=SV-SGG1 RTYP=SW U= 420.000000 FI= 0.0000
QMIN= -49995.00 QMAX= 49995.00
3000 TYPE=NODE NAME=STCKGG1 RTYP=UP U= 420.0000 P= 5300.000
QMIN= -49995.00 QMAX= 49995.00
3100 TYPE=NODE NAME=STRFGG1 RTYP=UP U= 407.4000 P= 1500.000
QMIN= -49995.00 QMAX= 49995.00
3115 TYPE=NODE NAME=SV-NGG11 RTYP=UP U= 420.0000 P= 3570.000
QMIN= -49995.00 QMAX= 49995.00
!3200 TYPE=NODE NAME=KRLSGG1 RTYP=UP U= 420.0000 P= 0.000
! QMIN= -49995.00 QMAX= 49995.00 NCON=1
3245 TYPE=NODE NAME=SV-MGG1 RTYP=UP U= 420.0000 P= 780.000
QMIN= -49995.00 QMAX= 49995.00
3249 TYPE=NODE NAME=SV-NGG12 RTYP=UP U= 420.0000 P= 4750.000
QMIN= -49995.00 QMAX= 49995.00
3359 TYPE=NODE NAME=SV-WGG1 RTYP=UP U= 420.0000 P= 2670.000
QMIN= -49995.00 QMAX= 49995.00
3359 TYPE=NODE NAME=SV-WGG2 RTYP=UP U= 420.0000 P= 830.000
QMIN= -9999.000 QMAX= 9999.000
5100 TYPE=NODE NAME=EASTGG1 RTYP=UP U= 300.0000 P= 1480.000
QMIN= -49995.00 QMAX= 49995.00
5300 TYPE=NODE NAME=HDALGG1 RTYP=UP U= 300.0000 P= 2275.000
QMIN= -49995.00 QMAX= 49995.00
5400 TYPE=NODE NAME=CNTRGG11 RTYP=UP U= 302.1000 P= 1588.000
QMIN= -49995.00 QMAX= 49995.00
5500 TYPE=NODE NAME=CNTRGG12 RTYP=UP U= 301.2000 P= 828.000
QMIN= -49995.00 QMAX= 49995.00
5600 TYPE=NODE NAME=SOUTGG11 RTYP=UP U= 303.0000 P= 2378.000
!5603 TYPE=NODE NAME=SOUTGG12 RTYP=UP U= 300.0000 P= 100.000
! QMIN= -9999.000 QMAX= 9999.000 NCON=1
6000 TYPE=NODE NAME=WESTGG1 RTYP=UP U= 301.5000 P= 1129.000

```

```

        QMIN= -1000.000      QMAX= 1000.000
6100   TYPE=NODE  NAME=NWESGG1_  RTYP=UP  U= 300.0000      P= 2346.000
        QMIN= -49995.00     QMAX= 49995.00
6500   TYPE=NODE  NAME=MID3GG1_  RTYP=UP  U= 300.0000      P= 1511.000
        QMIN= -49995.00     QMAX= 49995.00
6700   TYPE=NODE  NAME=NOR3GG1_  RTYP=UP  U= 306.0000      P= 2771.000
        QMIN= -49995.00     QMAX= 49995.00
7000   TYPE=NODE  NAME=SO-FGG1_  RTYP=UP  U= 420.0000      P= 5300.000
        QMIN= -49995.00     QMAX= 49995.00
7100   TYPE=NODE  NAME=NO-FGG1_  RTYP=UP  U= 420.0000      P= 1310.000
        QMIN= -49995.00     QMAX= 49995.00
8500   TYPE=NODE  NAME=SJOLGG1_  RTYP=UP  U= 428.4000      P= 1000.000
        QMIN= -49995.00     QMAX= 49995.00

```

! Transformers RTYP=UFI:

```

3244   3245      NO=369  TYPE=TREG  RTYP=UFI  U=420.0000  FI= 0.000
        UMIN= 180.0000  UMAX=420.0000
3359   3360      NO=369  TYPE=TREG  RTYP=UFI  U=134.2913  FI= 0.000
! UMIN= 252.0000  UMAX=588.0000
5300   5301      NO=369  TYPE=TREG  RTYP=UFI  U=420.2604  FI= 0.000
! UMIN= 180.0000  UMAX=420.0000
5400   5401      NO=369  TYPE=TREG  RTYP=UFI  U=418.4880  FI= 0.000
        UMIN= 180.0000  UMAX=420.0000
5400   5402      NO=369  TYPE=TREG  RTYP=UFI  U=422.5284  FI= 0.000
! UMIN= 180.0000  UMAX=420.0000
5500   5501      NO=369  TYPE=TREG  RTYP=UFI  U=421.9068  FI= 0.000
! UMIN= 180.0000  UMAX=420.0000
5600   5601      NO=369  TYPE=TREG  RTYP=UFI  U=416.6610  FI= 0.000
        UMIN= 180.0000  UMAX=420.0000
5603   5602      NO=369  TYPE=TREG  RTYP=UFI  U=401.5368  FI= 0.000
        UMIN= 180.0000  UMAX=420.0000
6000   6001      NO=369  TYPE=TREG  RTYP=UFI  U=419.8320  FI= 0.000
        UMIN= 180.0000  UMAX=420.0000
6700   6701      NO=369  TYPE=TREG  RTYP=UFI  U=422.9316  FI= 0.000
! UMIN= 180.0000  UMAX=420.0000

```

! Transformers defined with RTYP=UFI. CNODE bus voltage is set fixed.

```

! The CNODE is set as the first node name in order in the data list
3701   3249      NO=369  TYPE=TREG  RTYP=UFI  TAU= 1.00000  FI= 0.000
        UMIN= 180.0000  UMAX=420.0000  CNODE=3701  U=302.22897
5101   5100      NO=369  TYPE=TREG  RTYP=UFI  TAU= 1.00635  FI= 0.000
        UMIN= 252.0000  UMAX=588.0000  CNODE=5101  U=415.74121
5102   5100      NO=369  TYPE=TREG  RTYP=UFI  TAU= 1.00000  FI= 0.000
        UMIN= 252.0000  UMAX=588.0000  CNODE=5102  U=420.00842
5103   5100      NO=369  TYPE=TREG  RTYP=UFI  TAU= 1.00000  FI= 0.000
        UMIN= 252.0000  UMAX=588.0000  CNODE=5103  U=419.17682

```

END
END

APPENDIX E: HVDC DYNPOW FILE

Case fault
**

CONTROL DATA
TEND=20
SPL=1.7
NPRD=3000
DEND=0.1
N7=40
GAM5=0.01
TETL=100000
END

GENERAL
NREF=3
FN 50.0 50.0 50.0
REF= FPCWT_GEN SV-SGG1_ B_SW
END

GLOBALS

FPCWT_REC_IQORD TYPE=REAL
FPCWT_REC_IQORD0 TYPE=REAL
FPCWT_REC_DW TYPE=REAL
FPCWT_INV_IQORD TYPE=REAL
FPCWT_INV_IQORD0 TYPE=REAL
FPCWT_REC_PORD TYPE=REAL

END

NODES
B_SW TYPE=1
END

SVC
SVC1 5600 SN=350 REG=100
END

SYNCHRONOUS MACHINES

FPCWT_GEN	1000	SN = 1060.0 UN = 3.0 TYPE = 2A H = 5.5 RA= 0.0025 XD= 1.9 XQ = 1.6 XDP = 0.32 XDB = 0.2 XQB = 0.21 XA = 0.14 TD0P = 5.0 TD0B = 0.03 TQ0B = 0.07 TURB=1
SV-SGG1_	3300	TYPE=1 XD=2.42 XQ=2.00 XA=0.1481 XDP=0.23 XQP=0.4108 XDB=0.16 XQB=0.16 RA=0.0 TD0P=10.8 TQ0P=1 TD0B=0.05 TQ0B=0.05 V1=1 V2=1.2 SE1=0.1089 SE2=0.378 TURB=40 H=6.0 SN=5000 UN=420 D=0 VREG=24
STCKGG1_	3000	TYPE=1 XD=2.22 XQ=2.13 XA=0.1688 XDP=0.36 XQP=0.468 XDB=0.225 XQB=0.225 RA=0.0 TD0P=5.0 TQ0P=1 TD0B=0.05 TQ0B=0.05 V1=1 V2=1.2 SE1=0.1089 SE2=0.378 TURB=40 H=5.97 SN=5579 UN=420 D=0 VREG=10
STRFGG1_	3100	TYPE=2 XD=0.65 XQ=0.39 XA=0.0877 XDP=0.19 XDB=0.1169 XQB=0.1169 RA=0.0 TD0P=4.0 TD0B=0.06 TQ0B=0.1 V1=1 V2=1.2 SE1=0.1024 SE2=0.2742 TURB=20 H=5.04 SN=1579 UN=420 D=0 VREG=20
SV-NGG11	3115	TYPE=2 XD=0.946 XQ=0.565 XA=0.1108 XDP=0.29

		XDB=0.23	XQB=0.23	RA=0.0	TD0P=7.57				
		TD0B=0.045	TQ0B=0.1	V1=1	V2=1.2	SE1=0.1024	SE2=0.2742		
		TURB=21	H=4.741	SN=3758	UN=420	D=0	VREG=23		
!KRLSGG1_	3200	TYPE=1	XD=1.8	XQ=1.7	XA=0.2	XDP=0.3	XQP=0.55		
!		XDB=0.25	XQB=0.25	RA=0.0025	TD0P=8.0	TQ0P=0.4			
!		TD0B=0.03	TQ0B=0.05	TAB=1	TURB=3				
!		H=6.5	SN=1	UN=420	D=0	VREG=2			
SV-MGG1_	3245	TYPE=2	XD=0.75	XQ=0.50	XA=0.1154	XDP=0.25			
		XDB=0.1538	XQB=0.1538	RA=0.0	TD0P=5.0				
		TD0B=0.06	TQ0B=0.1	V1=1	V2=1.2	SE1=0.1024	SE2=0.2742		
		TURB=22	H=3.3	SN=822	UN=420	D=0	VREG=20		
SV-NGG12	3249	TYPE=2	XD=1.036	XQ=0.63	XA=0.1154	XDP=0.28			
		XDB=0.21	XQB=0.21	RA=0.0	TD0P=10.13				
		TD0B=0.06	TQ0B=0.1	V1=1	V2=1.2	SE1=0.1024	SE2=0.2742		
		TURB=23	H=4.543	SN=5000	UN=420	D=0	VREG=20		
SV-WGG1_	3359	TYPE=2	XD=0.75	XQ=0.50	XA=0.1154	XDP=0.25			
		XDB=0.1938	XQB=0.1938	RA=0.0	TD0P=5.0				
		TD0B=0.06	TQ0B=0.1	V1=1	V2=1.2	SE1=0.1024	SE2=0.2742		
		TURB=22	H=3.3	SN=2811	UN=420	D=0	VREG=25		
SV-WGG2_	3359	TYPE=1	XD=2.13	XQ=2.03	XA=0.1453	XDP=0.31	XQP=0.403		
		XDB=0.1937	XQB=0.1937	RA=0.0	TD0P=4.75	TQ0P=1			
		TD0B=0.05	TQ0B=0.05	V1=1	V2=1.2	SE1=0.1089	SE2=0.378		
		TURB=40	H=4.82	SN=874	UN=420	D=0	VREG=22		
EASTGG1_	5100	TYPE=2	XD=1.1332	XQ=0.6832	XA=0.1341	XDP=0.243			
		XDB=0.1514	XQB=0.1514	RA=0.0	TD0P=4.9629				
		TD0B=0.05	TQ0B=0.15	V1=1	V2=1.2	SE1=0.10	SE2=0.30		
		TURB=25	H=3.9871	SN=1558	UN=300	D=0	VREG=30		
HDALGG1_	5300	TYPE=2	XD=1.14	XQ=0.84	XA=0.2	XDP=0.34			
		XDB=0.26	XQB=0.26	RA=0.0	TD0P=6.4				
		TD0B=0.05	TQ0B=0.15	V1=1	V2=1.2	SE1=0.10	SE2=0.30		
		TURB=25	H=3.5	SN=2395	UN=300	D=0	VREG=27		
CNTRGG11	5400	TYPE=2	XD=1.02	XQ=0.63	XA=0.13	XDP=0.25			
		XDB=0.16	XQB=0.16	RA=0.0	TD0P=6.5				
		TD0B=0.05	TQ0B=0.15	V1=1	V2=1.2	SE1=0.10	SE2=0.30		
		TURB=25	H=4.1	SN=1672	UN=300	D=0	VREG=30		
CNTRGG12	5500	TYPE=2	XD=1.2364	XQ=0.6557	XA=0.1619	XDP=0.3741			
		XDB=0.2283	XQB=0.2283	RA=0.0	TD0P=7.198				
		TD0B=0.05	TQ0B=0.15	V1=1	V2=1.2	SE1=0.10	SE2=0.30		
		TURB=25	H=3.0	SN=872	UN=300	D=0	VREG=30		
SOUTGG11	5600	TYPE=2	XD=1.0	XQ=0.5132	XA=0.21	XDP=0.38			
		XDB=0.28	XQB=0.28	RA=0.0	TD0P=7.85				
		TD0B=0.05	TQ0B=0.15	V1=1	V2=1.2	SE1=0.10	SE2=0.30		
		TURB=24	H=3.5	SN=2504	UN=300	D=0	VREG=26		
!SOUTGG12	5603	TYPE=1	XD=1.8	XQ=1.7	XA=0.2	XDP=0.3	XQP=0.55		
!		XDB=0.25	XQB=0.25	RA=0.0025	TD0P=8.0	TQ0P=0.4			
!		TD0B=0.03	TQ0B=0.05	TAB=1	TURB=3				
!		H=6.5	SN=106	UN=300	D=0	VREG=2			
WESTGG1_	6000	TYPE=2	XD=1.28	XQ=0.94	XA=0.2	XDP=0.37			
		XDB=0.28	XQB=0.28	RA=0.0	TD0P=9.7				
		TD0B=0.05	TQ0B=0.15	V1=1	V2=1.2	SE1=0.10	SE2=0.30		
		TURB=24	H=3.5	SN=1189	UN=300	D=0	VREG=31		
NWESGG1_	6100	TYPE=2	XD=1.2	XQ=0.73	XA=0.15	XDP=0.37			
		XDB=0.18	XQB=0.18	RA=0.0	TD0P=9.9				
		TD0B=0.05	TQ0B=0.15	V1=1	V2=1.2	SE1=0.10	SE2=0.30		
		TURB=25	H=3.0	SN=2470	UN=300	D=0	VREG=27		
MID3GG1_	6500	TYPE=2	XD=1.0679	XQ=0.6420	XA=0.1351	XDP=0.2387			
		XDB=0.158	XQB=0.158	RA=0.0	TD0P=5.4855				
		TD0B=0.05	TQ0B=0.15	V1=1	V2=1.2	SE1=0.10	SE2=0.30		

		TURB=25	H=3.558	SN=1591	UN=300	D=0	VREG=30	
NOR3GG1_	6700	TYPE=2	XD=1.1044	XQ=0.6619	XA=0.1474	XDP=0.2548		
		XDB=0.1706	XQB=0.1706	RA=0.0	TD0P=5.24			
		TDOB=0.05	TQ0B=0.15	V1=1	V2=1.2	SE1=0.10	SE2=0.30	
		TURB=25	H=3.5920	SN=2917	UN=300	D=0	VREG=27	
SO-FGG1_	7000	TYPE=1	XD=2.22	XQ=2.13	XA=0.1688	XDP=0.36	XQP=0.468	
		XDB=0.225	XQB=0.225	RA=0.0	TD0P=10.0	TQ0P=1		
		TDOB=0.05	TQ0B=0.05	V1=1	V2=1.2	SE1=0.1089	SE2=0.378	
		TURB=40	H=5.5	SN=5579	UN=420	D=0	VREG=11	
NO-FGG1_	7100	TYPE=2	XD=0.75	XQ=0.50	XA=0.1154	XDP=0.25		
		XDB=0.1538	XQB=0.1538	RA=0.0	TD0P=5.0			
		TDOB=0.06	TQ0B=0.10	V1=1	V2=1.2	SE1=0.1024	SE2=0.2742	
		TURB=22	H=3.20	SN=1379	UN=420	D=0	VREG=27	
SJOLGG1_	8500	TYPE=1	XD=2.42	XQ=2.00	XA=0.1481	XDP=0.23	XQP=0.4108	
		XDB=0.1706	XQB=0.1706	RA=0.0	TD0P=10.0	TQ0P=1		
		TDOB=0.05	TQ0B=0.05	V1=1	V2=1.2	SE1=0.1089	SE2=0.378	
		TURB=40	H=7.0	SN=1056	UN=420	D=0	VREG=28	

END

REGULATORS

10	TYPE=DSLS/IEEEX2/							
	TR=0	KA=729	TA=0.04	VRMAX=5.32	VRMIN=-4.05			
	KE=1.0	TE=0.44	KF=0.0667	TF1=2.0	TF2=0.44			
	E1=6.5	SE1=0.054	E2=8	SE2=0.2020	TB=0	TC=0	SWS=40	
11	TYPE=DSLS/IEEEX2/							
	TR=0	KA=800	TA=0.04	VRMAX=5.32	VRMIN=-4.05			
	KE=1.0	TE=0.44	KF=0.0667	TF1=2.0	TF2=0.44			
	E1=6.5	SE1=0.054	E2=8	SE2=0.2020	TB=0	TC=0	SWS=44	
20	TYPE=BBC1							
	T1=3.3	T3=13	K=31	T4=0.05	T2=0			
	UEMIN=0	UEMAX=4						
21	TYPE=BBC1							
	T1=0	T3=0.04	K=10	T4=0.04	T2=0			
	UEMIN=0	UEMAX=5						
22	TYPE=BBC1							
	T1=2	T3=10	K=165	T4=0.04	T2=0			
	UEMIN=0	UEMAX=5						
23	TYPE=BBC1							
	T1=3.3	T3=13	K=31	T4=0.05	T2=0			
	UEMIN=0	UEMAX=4	SWS=41					
24	TYPE=BBC1							
	T1=0	T3=0.04	K=10	T4=0.04	T2=0			
	UEMIN=0	UEMAX=5	SWS=42					
25	TYPE=BBC1							
	T1=3.3	T3=13	K=31	T4=0.05	T2=0			
	UEMIN=0	UEMAX=4	SWS=43					
26	TYPE=BBC1							
	T1=3.3	T3=13	K=61	T4=0.05	T2=0			
	UEMIN=0	UEMAX=4						
27	TYPE=BBC1							
	T1=3.3	T3=13	K=61	T4=0.05	T2=0			
	UEMIN=0	UEMAX=4	SWS=42					

```

28  TYPE=BBC1
    T1=0      T3=0.04   K=10      T4=0.04   T2=0
    UEMIN=0   UEMAX=5    SWS=42

30  TYPE=BBC1
    T1=0.00005 T2=0    T3=100    T4=0.5    K=200
    UEMIN=0   UEMAX=4

31  TYPE=BBC1
    T1=10     T2=0    T3=0.1    T4=0.1    K=20
    UEMIN=-4  UEMAX=4

40  TYPE=DSLS/STAB2A/
    K2=1     T2=2     K3=0     T3=2     K4=0.55  K5=1     T5=0.01  HLIM=0.03

41  TYPE=DSLS/STAB2A/
    K2=1     T2=4.5   K3=0.87  T3=2     K4=0.087 K5=1     T5=0.01  HLIM=0.04

42  TYPE=DSLS/STAB2A/
    K2=1     T2=4.5   K3=0     T3=2     K4=0.55  K5=1     T5=0.01  HLIM=0.03

43  TYPE=DSLS/STAB2A/
    K2=1     T2=4.5   K3=0     T3=2     K4=0.68  K5=1     T5=0.01  HLIM=0.03

44  TYPE=DSLS/STAB2A/
    K2=1     T2=1.0   K3=0     T3=2     K4=0.55  K5=1     T5=0.01  HLIM=0.03

100 TYPE=SVS
    RTYP=2   KP=15   TF=0.02  VPMAX=2   VPMIN=-2  KA=30
    VIMIN=0  VIMAX=0.1  QMIN=-320 QMAX=320

```

END

TURBINES

```

1  TYPE=DSLS/FPCWT_WINDTURB/  NOM_POWER=1060.0  AIRDENS=1.2
    NOM_TURBSPEED=0
    BLADELENGTH=0  LOWCUTOUT=2.0
    GOV=2          WINDCURVE=81

2  TYPE=DSLS/FPCWT_PICON/  KPP=60  KPC=3  KIP=20  KIC=20
    TP=0.3  BMAX=27  BMIN=0
    DBDTMAX=4.0  DBDTMIN=-4.0  BLOCK=0
    DW=FPCWT_REC_DW
    PORD=FPCWT_REC_PORD

```

!!!HYDRO TURBINES

```

20  TYPE=DSLS/HYTUR/
    GOV=29  TW=1  AT=1.0022  DTURB=0.5  QNL=0.1

21  TYPE=DSLS/HYTUR/
    GOV=29  TW=1  AT=1.0577  DTURB=0.5  QNL=0.1

22  TYPE=DSLS/HYTUR/
    GOV=29  TW=1  AT=1.01  DTURB=0.5  QNL=0.1

23  TYPE=DSLS/HYTUR/
    GOV=29  TW=1  AT=1.1  DTURB=0.5  QNL=0.1

24  TYPE=DSLS/HYTUR/
    GOV=28  TW=1  AT=1.1  DTURB=0.5  QNL=0.1

25  TYPE=DSLS/HYTUR/
    GOV=27  TW=1  AT=1.1  DTURB=0.5  QNL=0.1

27  TYPE=DSLS/HYGOV/
    RBIG=0.06  RSMALL=0.4

```

```

TR=5.0          TF=0.05          TG=0.2
VELM=0.2        GMIN=0           GMAX=1

28  TYPE=DSLS/HYGOV/
    RBIG=0.06    RSMALL=0.3
    TR=5.0      TF=0.05          TG=0.2
    VELM=0.2    GMIN=0           GMAX=1.5

29  TYPE=DSLS/HYGOV/
    RBIG=0.06    RSMALL=0.4
    TR=5.0      TF=0.05          TG=0.2
    VELM=0.1    GMIN=0           GMAX=1.5

!!!STEAM TURBINES

40  TYPE=ST2
    GOV=49      K1=0.301    T1=0.4    K2=0.399    T2=8.0
    K3=0.3      T3=0.3      K4=0      T4=0

49  TYPE=SG3
    T1=0.01     T2=0.0      T3=0.15   K=0
    YMIN=0      YMAX=1

```

END

LOADS

```

3000    NO= 1    MP=1 MQ=2
3000    NO= 2    MP=1 MQ=2
3100                    MP=1 MQ=2
3200                    MP=1 MQ=2
3245                    MP=1 MQ=2
3249                    MP=1 MQ=2
3300                    MP=1 MQ=2
3359                    MP=1 MQ=2
3360                    MP=1 MQ=2
5100                    MP=1 MQ=2
5300                    MP=1 MQ=2
5400                    MP=1 MQ=2
5500                    MP=1 MQ=2
5600                    MP=1 MQ=2
5603    NO= 1    MP=1 MQ=2
5603    NO= 2    MP=1 MQ=2
6000                    MP=1 MQ=2
6100                    MP=1 MQ=2
6500                    MP=1 MQ=2
6700                    MP=1 MQ=2
7000    NO= 1    MP=1 MQ=2
7000    NO= 2    MP=1 MQ=2
7100                    MP=1 MQ=2
8500                    MP=1 MQ=2

```

END

PWM CONVERTERS

FPCWT_REC

```

TYPE=DSLS/FPCWT_PWM_DYN/ SN=1060.0
UN=3.0    X=0.3    PL=0.02
MODE=1      UDCORD=5.0    IMAX=1.04

```

PORD=FPCWT_REC_PORD

IQORD=FPCWT_REC_IQORD

IQORD0=FPCWT_REC_IQORD0

FPCWT_INV

```

TYPE=DSLS/FPCWT_PWM_DYN/ SN=1060.0
UN=3.5 X=0.3 PL=0.02
MODE=2 UDCORD=5.0 IMAX=1.04
PORD=0.0

IQORD=FPCWT_INV_IQORD

IQORD0=FPCWT_INV_IQORD0

LIGHT_A TYPE=DSLS/HVDC_LIGHT_OPEN_MODEL_V116_DYN/ DC1=A_2
BLOCKED=0 PTAB=2 QTAB=3 PCTRL=1 UACCTRL=0

LIGHT_B TYPE=DSLS/HVDC_LIGHT_OPEN_MODEL_V116_DYN/ DC1=B_2
BLOCKED=0 UTAB=4 PCTRL=0 UACCTRL=1

END

MISC
SPC1 TYPE=DSLS/FPCWT_SPCON/ KS=0.6 KP=3.0 TPC=0.05
PMAX=0.976 PMIN=0.0 DPMAX=0.1 DPMIN=-0.1
WMAX=1.20 WMIN=0.40 WLOW=0.60
DW=FPCWT_REC_DW
PORD=FPCWT_REC_PORD
SYNC=FPCWT_GEN

VACR 1000 TYPE=DSLS/FPCWT_VACCON/ N=1
INTMAX=1.0 INTMIN=-1.0

UACORD=3.0

IQMAX=0.5 IQMIN=-0.5
K=1.2 TI=0.05 BLOCK=0

IQORD=FPCWT_REC_IQORD

IQORD0=FPCWT_REC_IQORD0

VACI BUS_11 TYPE=DSLS/FPCWT_VACCON/ N=1
INTMAX=1.0 INTMIN=-1.0

UACORD=3.5

IQMAX=0.5 IQMIN=-0.5
K=1.2 TI=0.05
IQORD=FPCWT_INV_IQORD
IQORD0=FPCWT_INV_IQORD0

END

TABLES
! 1 TYPE=1 F 0.000 0.00 0.700 0.70
! 0.800 0.80 0.830 0.83
! 0.860 0.86 0.962 0.94
! 0.974 0.95 1.039 1.00
! 1.113 1.05 1.202 1.10
! 1.315 1.15 1.467 1.20
! 1.682 1.25 1.998 1.30
! 2.478 1.35

2 TYPE 0 F 0.0 0.8
10.0 0.8
20.0 0.9
100.0 0.9

3 TYPE 0 F 0.0 0.0

```

```

40.0  0.0
50.0  0.05
100.0 0.05
4 TYPE 0  F  0.0  1.0
70.0  1.0
80.0  0.95
100.0 0.95

```

! Cp/lambda curve for beta=0 deg.

```

11 TYPE=0  F  0.0  0.00
1.0  0.10
2.0  0.20
3.0  0.30
4.0  0.38
5.0  0.42
6.0  0.48
6.5  0.49
7.0  0.50
7.5  0.504
8.0  0.50
8.5  0.49
9.0  0.48
10.0 0.47
11.0 0.45
12.0 0.42
13.0 0.39
14.0 0.35
15.0 0.30
16.0 0.25
17.0 0.19
18.0 0.11
19.0 0.04
20.0 0.00

```

! Cp/lambda curve for beta=7 deg.

```

12 TYPE=0  F  0.0  0.00
1.0  0.02
2.0  0.05
3.0  0.16
4.0  0.26
5.0  0.30
6.0  0.31
6.5  0.31
7.0  0.30
7.5  0.28
8.0  0.26
8.5  0.24
9.0  0.22
10.0 0.16
11.0 0.08
12.0 0.00

```

! Cp/lambda curve for beta=27 deg.

```

13 TYPE=0  F  0.0  0.00
1.0  0.01
2.0  0.04
3.0  0.16
4.0  0.20
5.0  0.25
6.0  0.26
6.5  0.26
7.0  0.22
7.5  0.20

```

```

      8.0 0.19
      8.5 0.16
      9.0 0.10
          10.0 0.05
          11.0 0.00
! Voltage fluctuations in the grid
51 TYPE=0   F   0.00   1.0
          10.0   1.0
          10.0   0.94
          10.1   0.94
          10.1   1.0
          100.0   1.0
! Wind profile
81 TYPE=0   F   0.0   11.569607734680176
          100.0 11.569607734680176

! or from separate file as

!!! $INCLUDE TEST-FPCWT.TXT

! This text file must look the same as a table given in the Dynpow file.
! It is possible to create a text file from MS Excel if the wind profile is
! stored there, but after export to a text file in the text file, strings edit
! by TABS must be replaced and edit by SPACE

END

FAULTS
F1 TYPE=3PSG NODE 6100
END

RUN INSTRUCTION
AT 1.000 INST   CONNECT FAULT F1
END

END

```

APPENDIX F: INITIAL POWER FLOW

*** BASIC BALANCE REGION 1 AREA 40 ***

3000	(40)	1.00000	p.u.		
		420.000	kV		
		30.1386	DEGREES		
POWER FROM					
LINE 3000	3115	81		MW	Mvar
				498.661	-53.9927
LINE 3000	3245	81		-797.542	68.0472
LINE 3000	3300	81		-3001.12	-540.372
LOAD 3000	1			-2500.00	-500.000
LOAD 3000	2			500.000	-250.000
PROD STCKGG1_				5300.00	1276.32
3100 (40) 0.970000 p.u.					
		407.400	kV		
		34.4729	DEGREES		
POWER FROM					
LINE 3100	3115	81		MW	Mvar
				1006.93	-199.668
LINE 3100	3200	81		-868.370	-52.8393
LINE 3100	3249	81		2729.45	-563.566
LINE 3100	3359	81		-3868.01	-407.839
LOAD 3100	0			-500.000	-100.000
PROD STRFGG1_				1500.00	1323.91
3115 (40) 1.00000 p.u.					
		420.000	kV		
		60.2281	DEGREES		
POWER FROM					
LINE 3000	3115	81		MW	Mvar
				-536.713	83.4253
LINE 3100	3115	81		-1040.80	-192.805
LINE 3115	3245	81		-1257.53	-304.111
LINE 3115	3249	81		-77.3494	25.2032
LINE 3115	6701	81		168.142	21.0854
LINE 3115	7100	81		-825.749	-79.7344
PROD SV-NGG11				3570.00	446.937
3200 (40) 0.964952 p.u.					
		405.280	kV		
		4.28289	DEGREES		
POWER FROM					
LINE 3100	3200	81		MW	Mvar
				813.721	-238.244
LINE 3200	3300	81		-408.405	228.622
LINE 3200	3359	81		94.6833	109.621
LOAD 3200	0			-500.000	-100.000
3244 (40) 0.999840 p.u.					
		299.952	kV		
		22.2758	DEGREES		
POWER FROM					
LINE 3244	6500	81		MW	Mvar
				-76.7740	11.2350
TR2 3244	3245	369		76.7740	-11.2350
3245 (40) 1.00000 p.u.					
		420.000	kV		
		22.3670	DEGREES		
POWER FROM					
LINE 3000	3245	81		MW	Mvar
				789.631	-48.1647
LINE 3115	3245	81		1207.17	-450.876
TR2 3244	3245	369		-76.8041	11.1146
LOAD 3245	0			-2700.00	-500.000
PROD SV-MGG1_				780.000	987.927

3249 (40) 1.00000 p.u.
 420.000 kV
 59.3385 DEGREES

POWER FROM			MW	Mvar
LINE 3100	3249	81	-2818.83	-556.968
LINE 3115	3249	81	77.2575	13.6231
LINE 3249	7100	81	-805.694	-70.1740
TR2 3701	3249	369	47.2664	12.4497
LOAD 3249	0		-1250.00	-300.000
PROD SV-NGG12			4750.00	901.069

3300 (40) 1.00000 p.u. SWING BUS
 420.000 kV
 0.00000 DEGREES

POWER FROM			MW	Mvar
LINE 3000	3300	81	2895.98	-930.827
LINE 3200	3300	81	405.560	-235.234
LINE 3300	3359	81	1147.14	-144.641
LINE 3300	8500	81	-0.957295	216.753
LOAD 3300	0		-9350.00	-1500.00
PROD SV-SGG1_			4902.28	2593.95

3359 (40) 1.00000 p.u.
 420.000 kV
 6.41252 DEGREES

POWER FROM			MW	Mvar
LINE 3100	3359	81	3721.75	-1484.19
LINE 3200	3359	81	-95.2452	-40.7748
LINE 3300	3359	81	-1157.04	32.1969
LINE 3359	5101	81	-554.319	-21.7842
LINE 3359	5101	82	-554.319	-21.7842
TR2 3359	3360	369	-360.819	-183.276
LOAD 3359	0		-4500.00	-700.000
PROD SV-WGG1_			2670.00	1209.80
PROD SV-WGG2_			830.000	1209.80

3360 (40) 0.994550 p.u.
 134.264 kV
 6.04957 DEGREES

POWER FROM			MW	Mvar
TR2 3359	3360	369	360.000	180.000
LOAD 3360	0		-360.000	-180.000

3701 (40) 1.00744 p.u.
 302.232 kV
 60.6685 DEGREES

POWER FROM			MW	Mvar
LINE 3701	6700	81	47.3142	13.6443
TR2 3701	3249	369	-47.3142	-13.6443

 *** SUMMARY OF RESULT AREA 40 ***

IMPORT (+)	EXPORT (-)	MW	Mvar		

		215.456	34.7297	FROM AREA	67
		-1631.44	-149.908	FROM AREA	71
		-76.7740	11.2350	FROM AREA	65
		-0.957295	216.753	FROM AREA	90
		-1108.64	-43.5684	FROM AREA	51

TOTAL		-2602.36	69.2405		

TOTAL PRODUCTION	MW	Mvar

PRODUCTIONS	24302.3	9949.72
NETWORK GENERATION		1167.64

TOTAL	24302.3	11117.4
TOTAL LOAD	MW	Mvar

LOAD ABSORBED	21160.0	4130.00
NETWORK LOSSES	539.926	7056.60

TOTAL	21699.9	11186.6
	MW	Mvar

SWING 3300	4902.28	2593.95
SWING BUS TOTAL	4902.28	2593.95
TRANSMISS. LOSSES	539.029	7052.01

*** BASIC BALANCE REGION 1 AREA 51 ***

5100 (51) 1.00000 p.u.
300.000 kV
-0.897533 DEGREES

POWER FROM			MW	Mvar
LINE 5100	5300	81	568.907	-99.9627
LINE 5100	5500	81	-101.063	48.6119
LINE 5100	6500	81	252.221	-77.4994
TR2 5101	5100	369	634.383	-560.424
TR2 5102	5100	369	947.600	-37.7610
TR2 5103	5100	369	427.953	-39.3340
LOAD 5100	0		-4210.00	-692.000
PROD EASTGG1_			1480.00	1458.37

5101 (51) 0.989859 p.u.
415.741 kV
0.255727 DEGREES

POWER FROM			MW	Mvar
SHUN 5101	81		0.00000	-954.740
LINE-REACTOR 5101	810		-21.8500	0.145519E-07
LINE 3359	5101	81	549.757	-2.01702
LINE 5101	5501	81	-442.709	420.204
LINE 3359	5101	82	549.757	-2.01702
TR2 5101	5100	369	-634.956	538.570

5102 (51) 1.00002 p.u.
420.010 kV
0.760339 DEGREES

POWER FROM			MW	Mvar
SHUN 5102	81		0.00000	0.100007
LINE-REACTOR 5102	810		-0.200010	0.227374E-09
LINE 5102	5301	81	1048.04	-62.9470
LINE 5102	6001	81	-99.5220	52.5168
TR2 5102	5100	369	-948.319	10.3302

5103 (51) 0.998059 p.u.
419.185 kV
1.56563 DEGREES

POWER FROM			MW	Mvar
SHUN 5103	81		0.291038E-07	-12.6507
LINE-REACTOR 5103	810		-0.398448	0.00000
LINE 5103	5301	81	428.813	-8.21415
TR2 5103	5100	369	-428.415	20.8649

*** TRANSFORMERS OFF NOMINAL *** AREA 51

				TAU p.u.	FI DEG.	STEP	MW	Mvar

TR2	5101	5100	369	1.0063	0.000	1	-634.956	538.570

*** SUMMARY OF RESULT AREA 51 ***

IMPORT(+)	EXPORT(-)	MW	Mvar		

		1099.51	-4.03403	FROM AREA	40
		2045.76	-171.124	FROM AREA	53
		-543.772	468.816	FROM AREA	55
		252.221	-77.4994	FROM AREA	65
		-99.5220	52.5168	FROM AREA	60

TOTAL 2754.20 268.675

TOTAL PRODUCTION	MW	Mvar

PRODUCTIONS	1480.00	1458.37
SHUNT CAPACITORS	0.00000	0.100007

TOTAL 1480.00 1458.47

TOTAL LOAD	MW	Mvar

LOAD ABSORBED	4210.00	692.000
SHUNT REACTORS	0.00000	967.391
LINE REACTORS	22.4485	0.00000
NETWORK LOSSES	1.75435	67.7537

TOTAL 4234.20 1727.14

*** BASIC BALANCE REGION 1 AREA 53 ***

5300 (53) 1.00000 p.u.
300.000 kV
12.5044 DEGREES

POWER FROM			MW	Mvar	
LINE 5100	5300	81	-582.396	14.7792	
LINE 5300	6100	81	0.00000	0.00000	
(NOT CONNECTED)					
TR2	5300	5301	369	-1491.60	-18.4380 *
LOAD	5300	0		-201.000	-11.3000
PROD	HDALGG1_			2275.00	14.9587

5301 (53) 1.00063 p.u.
420.265 kV
7.28899 DEGREES

POWER FROM			MW	Mvar	
SHUN	5301	811	0.00000	12.7160	
LINE-REACTOR	5301	812	0.300379	-0.363798E-08	
LINE	5102	5301	81	-1056.37	71.7963
LINE	5103	5301	81	-431.972	32.7882
TR2	5300	5301	369	1488.04	-117.301 *

 *** SUMMARY OF RESULT AREA 53 ***

IMPORT(+)	EXPORT(-)	MW	Mvar		

		-2070.74	119.364	FROM AREA	51
		0.00000	0.00000	FROM AREA	61

TOTAL		-2070.74	119.364		
TOTAL PRODUCTION		MW	Mvar		

PRODUCTIONS		2275.00	14.9587		
SHUNT CAPACITORS		0.00000	12.7160		

TOTAL		2275.00	27.6747		
TOTAL LOAD		MW	Mvar		

LOAD ABSORBED		201.000	11.3000		
LINE REACTORS		-0.300379	0.00000		
NETWORK LOSSES		3.56051	135.738		

TOTAL		204.260	147.038		

 *** TRANSFORMERS OVER LIMITS *** AREA 53
 TR2 5300 5301 369 SIMAX S = 1491.72 MVA DELTA= 491.718 MVA
 1.49 p.u.

 *** BASIC BALANCE REGION 1 AREA 54 ***

5400	(54)	1.00700	p.u.			
		302.100	kV			
		0.167178	DEGREES			
		POWER FROM		MW	Mvar	
		LINE 5400	6000	81	-158.925	-0.421340
		LINE 5400	6100	81	-418.313	-4.66958
		SREA 5400	5500	81	-313.449	-7.45737
		TR2 5400	5401	369	-326.504	-33.7190
		TR2 5400	5402	369	-276.409	-60.5442
		LOAD 5400	0		-94.4000	0.00000
		PROD CNTRGG11			1588.00	106.812
5401	(54)	0.996324	p.u.			
		418.456	kV			
		-2.07890	DEGREES			
		POWER FROM		MW	Mvar	
		SHUN 5401	81		0.00000	-0.496331
		LINE-REACTOR 5401	810		0.198532	-0.454747E-09
		LINE 5401	5501	81	55.9813	65.9103
		LINE 5401	5602	81	-680.805	-136.521
		LINE 5401	6001	81	298.465	50.3001
		TR2 5400	5401	369	326.160	20.8067
5402	(54)	1.00600	p.u.			
		422.519	kV			
		-0.659512E-01	DEGREES			

POWER FROM				MW	Mvar
LINE	5402	6001	81	-276.377	-59.3599
TR2	5400	5402	369	276.377	59.3599

*** TRANSFORMERS OFF NOMINAL *** AREA 54

			TAU p.u.	FI DEG.	STEP	MW	Mvar	
TR2	5400	5401	369	1.0063	0.000	1	-326.504	-33.7190

*** SUMMARY OF RESULT AREA 54 ***

IMPORT(+)	EXPORT(-)	MW	Mvar		
		-136.837	-9.48111	FROM AREA	60
		-418.313	-4.66958	FROM AREA	61
		-257.468	58.4529	FROM AREA	55
		-680.805	-136.521	FROM AREA	56

TOTAL		-1493.42	-92.2185		
-------	--	----------	----------	--	--

TOTAL PRODUCTION	MW	Mvar
PRODUCTIONS	1588.00	106.812
TOTAL	1588.00	106.812

TOTAL LOAD	MW	Mvar
LOAD ABSORBED	94.4000	0.00000
SHUNT REACTORS	0.00000	0.496331
LINE REACTORS	-0.198532	0.00000
NETWORK LOSSES	0.376035	14.0967
TOTAL	94.5775	14.5930

*** BASIC BALANCE REGION 1 AREA 55 ***

5500	(55)	1.00400	p.u.
		301.200	kV
		-1.80119	DEGREES

POWER FROM				MW	Mvar
SHUN	5500	81		-0.363798E-08	1.31042
LINE-REACTOR	5500	810		-0.302405	0.00000
LINE	5100	5500	81	100.853	-28.9883
LINE	5500	5603	81	-418.540	-180.640
SREA	5400	5500	81	312.586	-3.30341
TR2	5500	5501	369	406.404	850.061
LOAD	5500	0		-1229.00	-115.000
PROD	CNTRGG12			828.000	-523.440

5501	(55)	1.00445	p.u.
		421.870	kV
		-1.47001	DEGREES

POWER FROM				MW	Mvar
SHUN	5501	811		0.00000	983.100
LINE-REACTOR	5501	812		21.7928	-0.582077E-07

LINE 5101	5501	81	441.025	-112.796
LINE 5401	5501	81	-56.0525	-6.69481
TR2 5500	5501	369	-406.765	-863.609

*** TRANSFORMERS OFF NOMINAL *** AREA 55

			TAU p.u.	FI DEG.	STEP	MW	Mvar
TR2 5500	5501	369	1.0127	0.000	2	406.404	850.061

*** SUMMARY OF RESULT AREA 55 ***

IMPORT (+)	EXPORT (-)	MW	Mvar		
		541.878	-141.784	FROM AREA	51
		256.534	-9.99822	FROM AREA	54
		-418.540	-180.640	FROM AREA	56

TOTAL		379.871	-332.422		
-------	--	---------	----------	--	--

TOTAL PRODUCTION	MW	Mvar
PRODUCTIONS	828.000	-523.440
SHUNT CAPACITORS	0.00000	984.410
TOTAL	828.000	460.971

TOTAL LOAD	MW	Mvar
LOAD ABSORBED	1229.00	115.000
LINE REACTORS	-21.4904	0.00000
NETWORK LOSSES	0.361189	13.5482
TOTAL	1207.87	128.548

*** BASIC BALANCE REGION 1 AREA 56 ***

5600	(56)	1.01000	p.u.
		303.000	kV
		-9.15986	DEGREES

				MW	Mvar
POWER FROM					
LINE 5600	5603	81		-321.643	-370.475
LINE 5600	6000	81		417.564	-64.5490
TR2 5600	5601	369		647.080	-18.0862
LOAD 5600	0			-3121.00	-297.000
PROD SOUTGG11				2378.00	750.110

5601	(56)	0.991126	p.u.
		416.273	kV
		-8.87280	DEGREES

				MW	Mvar
POWER FROM					
LINE 5601	6001	81		647.165	-14.8442
TR2 5600	5601	369		-647.165	14.8442

5602	(56)	0.956161	p.u.
		401.588	kV
		-11.7764	DEGREES

POWER FROM				MW	Mvar
LINE	5401	5602	81	673.155	100.742
TR2	5603	5602	369	-673.155	-100.742

5603 (56) 0.922383 p.u. ** LOW **
 276.715 kV
 -13.0629 DEGREES

POWER FROM				MW	Mvar
SHUN	5603	811		-0.145519E-07	-1.10603
LINE-REACTOR	5603	812		0.255237	0.00000
LINE	5500	5603	81	410.246	94.7058
LINE	5600	5603	81	316.750	336.114
TR2	5603	5602	369	672.750	85.2859
LOAD	5603	1		-460.000	-45.0000
LOAD	5603	2		-940.000	-470.000

*** TRANSFORMERS OFF NOMINAL *** AREA 56

				TAU p.u.	FI DEG.	STEP	MW	Mvar

TR2	5600	5601	369	1.0190	0.000	3	647.080	-18.0862
TR2	5603	5602	369	0.9683	0.000	-5	672.750	85.2859

*** LOW VOLTAGE NODES *** AREA 56

5603 0.922383 p.u.

*** SUMMARY OF RESULT AREA 56 ***

IMPORT (+)	EXPORT (-)	MW	Mvar		

		673.155	100.742	FROM AREA	54
		410.246	94.7058	FROM AREA	55
		1064.73	-79.3932	FROM AREA	60

 TOTAL 2148.13 116.054

TOTAL PRODUCTION	MW	Mvar

PRODUCTIONS	2378.00	750.110
NETWORK GENERATION		19.5022

 TOTAL 2378.00 769.612

TOTAL LOAD	MW	Mvar

LOAD ABSORBED	4521.00	812.000
SHUNT REACTORS	0.00000	1.10603
LINE REACTORS	-0.255237	0.00000
NETWORK LOSSES	5.38457	72.5602

 TOTAL 4526.13 885.666

		MW	Mvar

TRANSMISS. LOSSES	4.89368	53.8625	

*** BASIC BALANCE REGION 1 AREA 60 ***

6000 (60) 1.00500 p.u.
 301.500 kV
 -0.729344 DEGREES

POWER FROM				MW	Mvar
LINE	5400	6000	81	158.675	8.04928
LINE	5600	6000	81	-423.782	47.9961
LINE	6000	6100	81	-282.879	5.56690
TR2	6000	6001	369	-577.014	67.7403
LOAD	6000	0		-4.00000	0.00000
PROD	WESTGG1_			1129.00	-129.353

6001 (60) 0.999483 p.u.
 419.783 kV
 -1.22774 DEGREES

POWER FROM				MW	Mvar
SHUN	6001	811		0.227374E-09	-0.998984E-01
LINE-REACTOR	6001	812		-0.199793	0.00000
SHUN	6001	813		0.00000	0.499484
LINE-REACTOR	6001	814		-0.199793	0.00000
LINE	5102	6001	81	99.3094	44.2789
LINE	5401	6001	81	-298.740	-39.9409
LINE	5402	6001	81	275.967	76.9693
LINE	5601	6001	81	-653.015	-8.89008
TR2	6000	6001	369	576.878	-72.8169

*** TRANSFORMERS OFF NOMINAL *** AREA 60

			TAU p.u.	FI DEG.	STEP	MW	Mvar

TR2	6000	6001	369	1.0063	0.000	1	-577.014 67.7403

*** SUMMARY OF RESULT AREA 60 ***

IMPORT (+)	EXPORT (-)	MW	Mvar	

		99.3094	44.2789	FROM AREA 51
		135.902	45.0777	FROM AREA 54
		-1076.80	39.1061	FROM AREA 56
		-282.879	5.56690	FROM AREA 61

 TOTAL -1124.46 134.030

TOTAL PRODUCTION	MW	Mvar

PRODUCTIONS	1129.00	-129.353
SHUNT CAPACITORS	0.00000	0.499484
TOTAL	1129.00	-128.853

TOTAL LOAD	MW	Mvar

LOAD ABSORBED	4.00000	0.00000
SHUNT REACTORS	0.00000	0.998984E-01
LINE REACTORS	0.399587	0.00000
NETWORK LOSSES	0.135424	5.07660
TOTAL	4.53501	5.17650

*** BASIC BALANCE REGION 1 AREA 61 ***

6100 (61) 1.00000 p.u.
 300.000 kV
 -4.58435 DEGREES

POWER FROM			MW	Mvar
LINE 5400	6100	81	414.862	-17.7652
LINE 6000	6100	81	281.138	-4.41524
LINE 5300	6100	81	0.00000	0.00000
(NOT CONNECTED)				
LOAD 6100	0		-3042.00	-980.000
PROD NWESGG1_			2346.00	1002.18

*** SUMMARY OF RESULT AREA 61 ***

IMPORT(+)	EXPORT(-)	MW	Mvar		

		414.862	-17.7652	FROM AREA	54
		281.138	-4.41524	FROM AREA	60
		0.00000	0.00000	FROM AREA	53

TOTAL 696.000 -22.1804

TOTAL PRODUCTION MW Mvar

PRODUCTIONS 2346.00 1002.18

TOTAL 2346.00 1002.18

TOTAL LOAD MW Mvar

LOAD ABSORBED 3042.00 980.000

NETWORK LOSSES -0.238419E-03 0.800937E-04

TOTAL 3042.00 980.000

*** BASIC BALANCE REGION 1 AREA 65 ***

6500 (65) 1.00000 p.u.
 300.000 kV
 22.0527 DEGREES

POWER FROM			MW	Mvar
LINE 3244	6500	81	76.7440	-10.5357
LINE 5100	6500	81	-262.670	-26.0234
LINE 6500	6700	81	593.926	-250.390
LOAD 6500	0		-1919.00	-279.000
PROD MID3GG1_			1511.00	565.949

*** SUMMARY OF RESULT AREA 65 ***

IMPORT(+)	EXPORT(-)	MW	Mvar		

		76.7440	-10.5357	FROM AREA	40
		-262.670	-26.0234	FROM AREA	51
		593.926	-250.390	FROM AREA	67

TOTAL 408.000 -286.949

TOTAL PRODUCTION	MW	Mvar

PRODUCTIONS	1511.00	565.949

TOTAL	1511.00	565.949
TOTAL LOAD	MW	Mvar

LOAD ABSORBED	1919.00	279.000
NETWORK LOSSES	0.00000	0.00000

TOTAL	1919.00	279.000

*** BASIC BALANCE REGION 1 AREA 67 ***

6700	(67)	1.02000	p.u.
		306.000	kV
		63.2992	DEGREES

	POWER FROM			MW	Mvar
	LINE 3701	6700	81	-47.3374	-10.8291
	LINE 6500	6700	81	-627.243	-198.333
	TR2 6700	6701	369	-169.420	20.2779
	LOAD 6700	0		-1927.00	-446.000
	PROD NOR3GG1_			2771.00	634.885

6701	(67)	1.00678	p.u.
		422.847	kV
		63.1020	DEGREES

	POWER FROM			MW	Mvar
	LINE 3115	6701	81	-169.276	20.8518
	TR2 6700	6701	369	169.276	-20.8518

*** TRANSFORMERS OFF NOMINAL *** AREA 67

				TAU p.u.	FI DEG.	STEP	MW	Mvar

TR2	6700	6701	369	1.0127	0.000	2	-169.420	20.2779

*** SUMMARY OF RESULT AREA 67 ***

IMPORT(+)	EXPORT(-)	MW	Mvar		

		-216.614	10.0228	FROM AREA	40
		-627.243	-198.333	FROM AREA	65

TOTAL		-843.856	-188.311		

TOTAL PRODUCTION	MW	Mvar

PRODUCTIONS	2771.00	634.885

TOTAL	2771.00	634.885

TOTAL LOAD	MW	Mvar

LOAD ABSORBED	1927.00	446.000
NETWORK LOSSES	0.143528	0.573978

TOTAL 1927.14 446.574

 *** BASIC BALANCE REGION 1 AREA 70 ***

7000 (70) 1.00000 p.u.
 420.000 kV
 17.7937 DEGREES

POWER FROM			MW	Mvar
LINE 7000	7100	81	150.000	122.426
LINE 7000	7100	82	150.000	122.426
LINE 7000	7100	83	0.00000	0.00000
(NOT CONNECTED)				
LOAD 7000	1		-5100.00	-1000.00
LOAD 7000	2		-500.000	-250.000
PROD SO-FGG1_			5300.00	1005.15

 *** SUMMARY OF RESULT AREA 70 ***

IMPORT(+)	EXPORT(-)	MW	Mvar	

		300.000	244.853	FROM AREA 71

 TOTAL 300.000 244.853

TOTAL PRODUCTION	MW	Mvar

PRODUCTIONS	5300.00	1005.15

 TOTAL 5300.00 1005.15

TOTAL LOAD	MW	Mvar

LOAD ABSORBED	5600.00	1250.00
NETWORK LOSSES	-0.476837E-03	-0.596046E-04

 TOTAL 5600.00 1250.00

 *** BASIC BALANCE REGION 1 AREA 71 ***

7100 (71) 1.00000 p.u.
 420.000 kV
 26.2615 DEGREES

POWER FROM			MW	Mvar
LINE 3115	7100	81	757.417	-303.197
LINE 3249	7100	81	740.791	-288.459
LINE 7000	7100	81	-154.104	162.788
LINE 7000	7100	82	-154.104	162.788
LINE 7000	7100	83	0.00000	0.00000
(NOT CONNECTED)				
LOAD 7100	0		-2500.00	-400.000
PROD NO-FGG1_			1310.00	666.080

 *** SUMMARY OF RESULT AREA 71 ***

```

IMPORT (+) EXPORT (-)    MW           Mvar
*****
                1498.21      -591.655   FROM AREA  40
                -308.208      325.576   FROM AREA  70
-----
TOTAL                1190.00      -266.080

TOTAL PRODUCTION        MW           Mvar
*****
PRODUCTIONS            1310.00      666.080
-----
TOTAL                  1310.00      666.080

TOTAL LOAD              MW           Mvar
*****
LOAD ABSORBED          2500.00      400.000
NETWORK LOSSES         0.00000      -0.119209E-03
-----
TOTAL                  2500.00      400.000

```

*** BASIC BALANCE REGION 1 AREA 90 ***

```

8500    ( 90)          1.02000    p.u.
                428.400    kV
                -0.296812    DEGREES

POWER FROM
LINE 3300  8500      81          MW           Mvar
LOAD 8500      0          -1000.00      90.3860
PROD SJOLGG1_          1000.00      -1000.00      909.614

```

*** SUMMARY OF RESULT AREA 90 ***

```

IMPORT (+) EXPORT (-)    MW           Mvar
*****
                0.00000      90.3860   FROM AREA  40
-----
TOTAL                0.00000      90.3860

TOTAL PRODUCTION        MW           Mvar
*****
PRODUCTIONS            1000.00      909.614
-----
TOTAL                  1000.00      909.614

TOTAL LOAD              MW           Mvar
*****
LOAD ABSORBED          1000.00      1000.00
NETWORK LOSSES         0.00000      -0.223517E-04
-----
TOTAL                  1000.00      1000.00

```

*** TOTAL SUMMARY OF RESULT ***

```

IMPORT (+) EXPORT (-)    MW           Mvar
*****
AREA                40      -2602.36      69.2405
AREA                51      2754.20      268.675
AREA                53      -2070.74      119.364
AREA                54      -1493.42      -92.2185

```

AREA	55	379.871	-332.422
AREA	56	2148.13	116.054
AREA	60	-1124.46	134.030
AREA	61	696.000	-22.1804
AREA	65	408.000	-286.949
AREA	67	-843.856	-188.311
AREA	70	300.000	244.853
AREA	71	1190.00	-266.080
AREA	90	0.00000	90.3860
TIE LINE LOSSES	258.637		2443.80
TIE LINE GENERATION			2298.24
TOTAL PRODUCTION	MW		Mvar

PRODUCTIONS	48218.3		16411.0
SHUNT CAPACITORS	0.00000		997.726
NETWORK GENERATION			3485.38

TOTAL	48218.3		20894.1
TOTAL LOAD	MW		Mvar

LOAD ABSORBED	47407.4		10115.3
SHUNT REACTORS	0.00000		969.093
LINE REACTORS	0.603535		0.00000
NETWORK LOSSES	810.278		9809.75

TOTAL	48218.3		20894.1
	MW		Mvar

SWING 3300	4902.28		2593.95
SWING BUS TOTAL	4902.28		2593.95
TRANSMISS. LOSSES	543.922		7105.87